Mathematical modelling, analysis and simulations to improve the control of Miridae, a cocoa pest

Myriam Sonia Djoukwe Tapi

REPUBLIQUE DU CAMEROUN
Paix - Travail - Patrie

UNIVERSITE DE DOUALA

ECOLE DOCTORALE DES SCIENCES FONDAMENTALES ET APPLIQUEES

Unité de Formation Doctorale de Mathématiques, Informatique Appliquée et Physique Fondamentale
---
Laboratoire de Mathématiques
BP 24157 Douala
Email: facsciences.douala@ymail.com

REPUBLIC OF CAMEROON
Peace - Work - Fatherland

THE UNIVERSITY OF DOUALA

POSTGRADUATE SCHOOL FOR PURE AND APPLIED SCIENCE

Postgraduate Training Unit for Mathematics, Applied Computer Science and Pure Physics
---
Laboratory of Mathematics
PO Box 24157 Douala
Email: facsciences.douala@ymail.com

MATHEMATICAL MODELLING, ANALYSIS AND SIMULATIONS TO IMPROVE THE CONTROL OF MIRIDAE, A COCOA PEST

THESIS

defended publicly on June 19, 2020 in fulfillment of the requirements for the award of

DOCTORAT / Ph.D in Applied Mathematics

Specialty

MATHEMATICAL MODELLING

By

DJOUKWE TAPI Myriam Sonia
DEA in Applied Mathematics
Registration number: **08S02819**

Jury:

President:	**OWONO ONANA Charles**	**Professor**	**The University of Douala**
Reporters:	**SALLET Gauthier**	**Professor**	**Université de Lorraine**
	NGWA Gidéon	**Associate Professor**	**University of Buea**
	FONO Louis Aimé	**Associate Professor**	**The University of Douala**
Advisors:	**BOWONG Samuel**	**Professor**	**The University of Douala**
	DUMONT Yves	**Director of Research**	**CIRAD**
	BAGNY BEILHE Leila	**Researcher**	**CIRAD**

Academic Year: 2018-2019

MATHEMATICAL MODELLING, ANALYSIS AND SIMULATIONS TO IMPROVE THE CONTROL OF MIRIDAE, A COCOA PEST

DJOUKWE TAPI Myriam Sonia

Academic Year: 2018/2019

Dedication

To

My late father TAPI Jean Pierre,

Dad, you left early and you did not have the grace to see your daughter shine. Father, I miss you so much and you will always be in my heart.

My mother MANGWA Rosalie,

Mom, Thanks for all your love, all your sacrifices and efforts made during all these years for me.

Remerciements

La préparation de cette thèse a nécessité l'intervention de plusieurs personnes sans lesquelles ce travail n'aurait pas abouti. C'est pourquoi, je tiens à remercier tous ceux qui ont contribué à la préparation de ce travail.

Je remercie Dieu le père tout puissant pour le don de la vie et pour son infinie assistance.

L'immense rôle joué par mes encadrants **Pr Samuel Bowong** (Chef de Département de Mathématiques et Informatique, Université de Douala, Cameroun), **Pr Yves Dumont** (Professeur extraordinaire, Université de Pretoria, CIRAD/AMAP) and **Dr Leila Bagny-Beilhe** (Chargé de la recherche, CIRAD), ne sera en aucun cas quantifié pour façonner mon potentiel de recherche et réaliser mon rêve de devenir Docteur en Mathématiques et œuvrer au développement de la communauté scientifique. Je vous remercie très sincèrement pour votre patience, vos conseils et votre enthousiasme tout au long de ma période d'étude. L'énorme soutien (financier) et vos contributions (nouvelles idées mathématiques et différents séminaires) ont conduit à la concrétisation de ce projet de recherche. Monsieur le Professeur **Samuel Bowong**, vous avez accepté de me faire partager vos activités de recherche en me proposant de réaliser mon mémoire de Master 2, puis ma thèse de doctorat sous votre direction. Vous m'avez toujours honoré de votre confiance durant tout ce temps en me conseillant et en me tenant par la main. Vous m'avez laissé prendre des initiatives, et vous avez constamment été présent pour orienter et corriger mon travail. Nos discussions ainsi que votre vision toute particulière pour aborder les questions scientifiques m'ont beaucoup influencé et ont grandement contribué à développer mon jeune esprit d'apprenti chercheur. Je ne vous remercierai jamais assez pour tout ce que vous m'avez appris. De plus, je remercie tout particulièrement le Professeur **Yves Dumont**. Par votre amour du travail bien fait et par votre rigueur, vous avez développé en moi un intérêt particulier pour la recherche en biologie mathématique. J'ai réellement apprécié travaillé avec vous, nos différents échanges par mails, vos différents séjours ici au Cameroun durant ma thèse et surtout le séjour que j'ai effectué au centre de recherche AMAP, Montpellier n'ont fait qu'apprécier le travail à vos côtés. Vous m'avez fourni durant ces différentes séances de travail de précieux conseils et surtout de la critique en vue de l'amélioration de mon travail. Docteur **Leila Bagny-Beilhe**, vous avez toujours ménagé de votre temps chaque fois que je rencontrais des difficultés. J'apprécie

tous les encouragements à mon égard et toutes les critiques apportées durant ces années de travail. N'étant pas mathématicienne de formation, j'ai sincèrement apprécié tous les efforts consentis pour comprendre toutes les grosses formules mathématiques: ce n'était pas toujours facile de passer d'un langage à l'autre; mais avec nos différentes séances de travail on a toujours réussi à se comprendre. Merci chers encadrants pour le chercheur que je suis devenu.

Mes remerciements vont à l'endroit de tout le staff académique et administratif de l'Université de Douala pour les différentes opportunités et facilités pour la réalisation de ce travail.

Un merci particulier à tous les rapporteurs de cette thèse. Vous avez sacrifié de votre temps pour apporter votre part de contribution à l'amélioration de ce travail à travers vos idées et vos recommandations.

Merci à l'équipe projet EPITAG à travers le laboratoire LIRIMA; à l'équipe projet GRIMCAPAE et UMMISCO, au DP/PCP Agroforesterie Cameroun, au CIRAD, l'IRD et l'INRIA/LIRIMA pour le support logsistique et financier durant la préparation et la finalisation de cette thèse. Je remercie tous les membres de l'UMR AMAP et de l'équipe projet BIOCORE pour leur esprit d'équipe durant mon séjour à leurs côtés. J'ai vraiment appris de vous.

Je remercie tous les enseignants du département de Mathématiques et Informatique de l'Université de Douala et tous les enseignants du département de Mathématiques de l'Université de Yaoundé I pour toute votre aide et vos enseignements. Que cette soutenance soit pour vous l'accomplissement d'un dur labeur. Plus particulièrement Pr Jean Jules Tewa, Pr Louis Aimé Fono, Dr Anatole Temgoua, Dr Ferdinand Ngakeu, Dr Armand Tsimi, Dr Bertrand Mbama, merci pour tous vos conseils et pour la patience que vous avez toujours eu à mon égard.

Dr Roger Tagne Wafo, merci pour votre assistance et votre support inconditionnel. Durant toutes ces années, vous avez été et vous êtes un père pour moi; vous m'avez toujours encouragé à me surpasser et à aller de l'avant. Merci pour tous ces sacrifices consentis à ma juste personne.

Je remercie mes camarades de promotion et mes ainés: Dr Plaire Tchinda, Dr Alexis Tchuinte, Dr Valaire Yatat, Dr Gabriel Kolaye, Dr Yannick Malong, Dr Vidal Kamdem, Dr Janvier Ntahomvukiye, Justin Dzuche, Luther Mann, Yves Fotso. Merci pour votre support et votre collaboration, vous m'avez toujours prêté une oreille attentive.

Je remercie tous les membres du laboratoire de Mathématiques de l'Université de Douala spécialement tous les membres de l'équipe "Team Mathematical Modelling" pour tous vos encouragements et pour votre esprit d'équipe. J'ai vraiment aimé travaillé avec vous. Je pense spécialement à Camelle Kabiwa, Yssel Hyonta, Cédric Hameni et Clotilde Djuikem.

Merci à mes amis, mon autre famille. Je pense particulièrement à Giresse Noubissie, Hermann

Tafo, Boris Njike, Eddy Kowa, Sophie Menkui, Armel Foko, Floriane Fondop, Giresse Essouan, Franc Djapa, Ismael Ngounou, Carole Djokam et Félicité Barth Nkamen. Merci pour votre disponibilité et votre attention à mon égard durant toutes ces années. Merci à vous tous qui avez toujours été là pour moi et qui m'avez toujours soutenu. Je pense particulièrement aux prêtres: les abbés René Ngon, Michel Tchoumbou, Henri-Joel Ndjeyep, Meinrad Hebga, Dimitri Chokouago, le couple Mbolda et mes amis Ulrich Nguemdjo, Yannick Foadjo, Sandra Mbialeu, Corneille Megaptche, Nathalie Matsinkou, Alphonsine Massu, Cabrelle Ndjodo. Merci pour toutes vos prières.

Il n'y a pas un jour qui passe sans que je ne pense avec amour à mes parents précisement à ma maman Mangwa Rosalie. Les valeurs que tu m'as enseigné ne cessent de guider mes pas. Que cette thèse soit le témoignage que tout ceci n'ait pas été vain. Sachez que je t'aime de tout mon coeur. Merci à ma grand mère Nguenang Elise, à vous mes frères et soeurs: Dimitri, Flavien, William, Michelle et Claude; mes oncles Joseph Ledoux Teponou, Calvin Njayong, Etienne Yankou et mon cousin Mohoue Jacques pour votre amour, votre patience, votre support et tous les sacrifices consentis dans la réalisation de projet.

Enfin, nous disons merci à tous ceux qui de près ou de loin ont contribué à la réalisation de ce travail. Recevez l'expression de ma profonde gratitude et de ma sympathie.

Contents

List of Figures

List of Tables

Abstract

Cocoa is an important cash crop in Central and West Africa, especially in Cameroon. In this part of the world, cacao production is impacted by several diseases, like the Cocoa Swollen Shoot Virus (CSSV) and the black pod disease, and several pests, like Miridae, *Distantiella theobroma* and *Sahlbergella singularis*, causing significant damage to pods and vegetative parts of the cocoa tree, and thus impacting the cocoa production. However, the damage and losses associated with this pest remain difficult to estimate due in particular to the bio/ecology of this species (camouflage, low number of individuals, etc) preventing a good estimate of the population dynamics along the year. Statistical models have shown to be ineffective in describing these dynamics. That is why we have developed several Mathematical models to describe the time evolution dynamics of mirids, including the effect of different control methods. After an introductory chapter where we recall the biology and ecology of mirids, we develop, analyze and study a compartmental cooperative periodic and non-periodic model in chapter 2. Then, considering time developments and sexual maturation duration for females, we develop and study a delayed cooperative model (with and without periodic parameters). In this latter model, we consider different control methods, including chemical control (insecticides) and semi-chemical control (sexual confusion and trapping). Through our numerical simulations, we recover recommendation given by mirid control organizations for the use of insecticides and show that chemical treatment can be replaced efficiently by mating disrupting and trapping. We also derive a global sensitivity analysis highlighting the importance of some key parameters. Then, based on the previous results, we develop, in chapter 3, a more complex delay model, modeling mating disrupting and trapping, using the piecewise-smooth system approach. Our analysis shows the existence of two thresholds based on mirid's biological parameters: one under which the control has no effect on established populations, and the second above which control on established populations is feasible. We illustrate our results with various numerical simulations and discuss the results. We conclude our thesis with possible extension of our models and also applications in the field.

Keywords: Cocoa pest, Pest control, *Sahlbergella singularis*, chemical control, Mating disruption, Mathematical models, Delay differential equations, Piecewise smooth system, Cooperative system, Stability analysis, Numerical simulation.

RESUME

Le cacao est la principale culture de rente Afrique Centrale Occidentale, en particulier au Cameroun. Dans cette région du monde, la production est affectée par plusieurs maladies parmi lesquelles, le Cacao Swollen Shoot Virus (CSSV) et la pourriture brune du cacaoyer causée par *Phytophthora sp.*. Elle est aussi affectée par les ravageurs notamment les mirides *Distantiella theobroma* et *Sahlbergella singularis* qui causent d'énormes dégâts sur les cabosses et les parties végétatives du cacaoyer. Au Cameroun, *S. singularis* est décrite comme l'espèce la plus présente dans les cacaoyères et la plus préjudiciable pour la production. Cependant, les dégâts et les pertes associés à ce ravageur restent difficiles à estimer en raison de la bio-écologie de cette espèce (camouflage, faible nombre d'individus) empêchant une bonne estimation in situ de la dynamique des populations. Les modèles statistiques ont jusqu'alors été peu efficaces pour appréhender cette dynamique. Des modèles mathématiques semblent plus adaptées. C'est pourquoi, dans le cadre de nos travaux, nous avons développé plusieurs modèles mathématiques pour décrire la dynamique d'évolution des mirides, mais aussi l'effet des différentes méthodes de contrôle sur les tailles de population de mirides. Après un chapitre introductif où nous rappelons la biologie et l'écologie des mirides, nous développons et analysons un modèle coopératif (en distinguant les cas où les paramètres sont périodiques ou pas) au chapitre 2 et nous obtenons les conditions sur la persistance ou non de la population des mirides. Ensuite, en tenant compte de la durée de développement larvaire et de la période de maturation des femelles, nous développons et étudions un modèle coopératif à retard (avec et sans paramètres périodiques). A ce modèle, nous appliquons les différentes méthodes de lutte: la lutte chimique (insecticides) et la lutte semiochimique (confusions sexuelle et piégeage). A l'aide de nos simulations numériques, nous obtenons des résultats en termes de recommandations pour lutte contre les mirides et montrons que le traitement chimique peut être remplacé efficacement par le traitement semiochimique. Nous faisons une analyse de sensibilité globale du modèle mettant en exergue l'importance de certains paramètres clés. Sur la base des résultats précédents, nous développons au chapitre 3, un modèle à retard plus complexe, modélisant la confusion sexuelle et le piégeage, en utilisant l'approche des systèmes réguliers par morceaux. Notre analyse mathématique montre l'existence de deux seuils basés sur les paramètres biologiques des mirides: un seuil sous lequel le contrôle n'a aucun effet sur les populations établies,

et le second seuil qui permet de contrôler les populations établies. Nous illustrons nos résultats par des simulations numériques. Nous concluons notre thèse avec une extension possible de nos modèles, mais également nous proposons des travaux qui peuvent être menés sur le terrain.

Mots clés: Ravageurs du cacaoyer, *Sahlbergella singularis*, Equations différentielles à retard, Modèles mathématiques, Systèmes monotones, Lutte contre les ravageurs, Confusion sexuelle, Analyse mathématique, Stabilité, Simulations numériques, "Systèmes réguliers par morceaux".

General Introduction

Cacao (*Theobroma cacao*) is originated from wet tropical forest in equatorial America [5]. It is essentially cultivated because of its beans which are destined for the industry of chocolate and also to the pharmaceutical and cosmetic industry [6]. Cacao cultivation began during the Maya era in Central America and Mexico [7]. Towards the end of the 17th century, it was introduced in many other countries like: Curaçao (Pays-Bas), Jamaica, Martinique, Dominicain Republic, Brasil, Guyane, and Grenade (France). In 19^{th} century, global cocoa production has proved insufficient. It was therefore necessary to extend production to other continents like Africa which constitutes nowadays the main producers [6]. In the years 1950, production of beans in Africa represents approximately 70% of the world production estimated to 700 000 tons (ICCO, 2008). Nowadays, world production is evaluated to 4, 552 billions of tons (ICCO, 2017). Cameroon was the third producer in 2017 with 380 000 tons of beans outpaced by Côte d'Ivoire and Ghana (ICCO, 2017). Despite cocoa (*Theobroma cacao*) is essential for the livelihood of millions of small producers in Africa especially in Cameroon [8], Cameroon production is by the damages caused by two pests, *Sahlbegella singularis* and *Distantiella theobroma* known as mirids bug or cacao capsids [9, 10].

Mirids (*Sahlbegella singularis* and *Distantiella theobroma*) which originate from the forests of Central Africa, have very similar life histories and regularly live together in cacao-based systems [11]. In Cameroon *Sahlbegella singularis* is nowadays the most common and the most harmful for the production [1]. Mirids feed on cacao and are responsible to the losses of 25 to 30% of the potential production in West Africa more precisely in Ghana and in Côte d'Ivoire [12]. In Cameroon, the losses of production due to the action of mirids represent 30% to the potential national production [13]. Another species of bugs also feed on cacao; we can cite mirid Helopeltis, bug Pentatomidae, Coreidae and Pyrrhocoridea [14]. Mirids also feed on other plants like *Cola nitida* and *Ceiba pentandra* known to be the alternative hosts when cacao resource is unavailable. Mirids feed on the sap of young semi-lignifed branches, on plant tissues by injecting a digestive saliva, on buds and on fruits [11, 15]. Mirid damage on the pod is relatively superficial since the pods cortex is very thick. In general, the most harmful damage that is also the less obvious to quantify is the damage caused to cocoa vegetative growth parts. Those lesions prevent sap circulation favouring leaves fall and branches

death that is characteristic of mirids attacks. Extensive feeding by mirids on branches results in the degradation of the canopy of discrete groups of trees, which can be up to 100 and are referred as mirid pockets. The impact of mirids on cacao tree is a long term impact as cacao is a perennial plant, which can produce for more than 20 years. Damage of mirid bugs on the cacao are cumulated over time and can lead to premature ageing of plantations and to the rapid death of the most severely damaged trees [16, 17, 18]. Losses due to mirids are difficult to estimate but can reach 30% to 40% of potential production [19, 20] depending on the system management strategy. In fact, mirids attacks are known to be the most harmful in full sun plantations. In multi-strata and highly diversified [21, 22] cacao-based agroforestry system as the one that is widespread in Cameroon, shade management is a relevant option to control mirid population [15]. But shade management is a long-term process that is sometimes difficult to set up for the farmers given antagonistic effects on black pod disease. Whatever the type of system considered, synthetic insecticides of the neonicotinoid family, such as λ-*cyhalothrine* and *imidacloprid* [9]are still themain input used to control these pests [23]. Since 1970, the economic threshold for phytosanitary intervention has been fixed at 0.7 mirids/tree in Cameroon [15] and 0.6 mirids/tree in Ghana [24]. These indicators based on mirid populations are however difficult to evaluate regarding the ecology of the species. In fact, it is challenging to count mirids individuals (immatures and adults) on the field since they used to hide during the day to avoid direct light. It is likely a relatively low level of mirid population can cause important damage in the plantation. Mirids do not pullulate in the plantations even during the peak period. Due to controversial effects of chemical insecticides, alternative cocoa pest control methods have been developed including cultural management, varietal management [25], as well as semio-chemical management, using synthetic sexual pheromone traps [26] or the use of plant extracts as pesticides [9]. Considering the difficulty to estimate mirid population and to obtain long-term data on the field, the mathematical approach appears as the most relevant option to forecast the efficiency of control strategy. In that sense, the aim of this work is to develop some (generic) mathematical models of mirid population to better predict its time evolution in a plot under different management strategies. Several compartmental models, with constant or periodic parameters, are developed based on the mirid life cycle. The work is organised as follows:

- The first chapter presents the context and main motivation of our study. We also present the cocoa mirid and especially *Sahlbergella singularis* species which is predominant in Cameroon. We present the biology and the ecology of this species and the importance to construct a mathematical model. The aim of this literature review is to regroup all the mathematical tools used to solve our different systems

- In Chapter 2, we study the dynamics of this pest. Based on biological and ecological partial knowledge, we built and analyse 2 cooperative mathematical models that aim to describe the time dynamics of the cocoa mirids. We first develop a cooperative stage-structured model, derived some qualitative results, and a sensitivity analysis study in order to determine the most important parameters. Assuming that all parameters are or not periodic, we obtain conditions that allow the persistence or not of the population. We highlight the influence of cocoa pods variation along the year on the time evolution of the population. Then, we derive a 2-stage cooperative time-delay model, with 2 delays, that takes into account the egg's development time and the female's maturation time. We illustrate our theoretical results with some simulations and show that the delayed system provides the best results compared with real observations. Finally, we focus on chemical control that is commonly used in Cameroon and compare it to a new biological control, mixing mating disrupting and trapping. We discuss the results and provide future perspectives based on this work.

- In Chapter 3, we consider a biological control method, based on mating disrupting, using artificial sex pheromones, and trapping, to limit the impact of mirids in plots. We develop and study a piece-wise smooth delayed dynamical system. A theoretical analysis is provided in order to derive all possible dynamics of the system. We show that two main threshold parameters exist that will be useful for practical applications, and also to derive successful control strategies. We illustrate and discuss our results when cacao pods are either constant along the year or periodic. To conclude, we will provide future perspectives based on this work.

1

Literature review and Mathematical tools

In this chapter, we provide a non exhaustive literature review on Mirids and the importance of Cocoa in Africa. We also summarize important results related to the mathematical theories that we will use throughout the manuscript, namely, the theory of monotone systems, the theory of delay differential equations and also the theory of Piecewise smooth systems.

1.1 The cacao tree: *Theobroma cacao*

1.1.1 Origin and importance

Cacao (*Theobroma cacao*) is originated from wet tropical forest in equatorial America [5]. Cacao-culture is an old activity because it was made for a long time by people Maya in Central America and Mexico. These people use cocoa as feeding product and also as change. Since the 19th century, it is cultivated in African countries. Cocoa is considered by these countries as the first cash crop. In West and Central Africa, cacao cultivation require approximately 10% of the yields destined to agriculture. Cacao plantations require respectively 6.88, 6.29, 1.05, and 0.78% of the yield of Côte d'Ivoire, Ghana, Nigeria and Cameroon. Since the 20^{th} century, the world cacao production increases between 2 and 2.5% and reaches 1.5 billion of tons in 1964, and today exceeds 2 billion of tons. The main importers of cacao around the world are United States of America, Germany, France, United Kingdom and Russia (CNUCED, 2007). In cacao year 2015-2016, production is evaluated to 3.965 billion of tons with a prediction of 4.552 billions for the next year (ICCO). Table 1.1 regroups the cacao production for the years 2014-2015; 2015-2016 and a prediction for the year 2016-2017. Cacao cultivation has its high development in Black Africa and countries like Côte d'Ivoire, Ghana, Nigeria and Cameroon which are the main producers in the world with approximately 72% of the world production [ICCO 2016]. Cacao is essential for the livelihood of millions of small producers in Africa especially in Cameroon [8] and the increasing of cocoa production contribute to increase an income of farmers and also to fight against poverty. Despite this production, cacao cultivation

Table 1.1: Production of cocoa beans (thousand tons). *Source: ICCO Quarterly Bulletin of Cocoa Statistics, Vol XLIII, No 1, Cocoa year 2016/17. Published: 28-02-2017*

	2014/2015		Estimates 2015/16		Forecasts 2016/17	
Africa	3074	72,3%	2911	73,4%	3365	73,9%
Cameroon	232		211		250	
Côte d'Ivoire	1796		1581		1900	
Ghana	740		778		850	
Nigeria	195		141		135	
Others	110		141		135	
America	777	18,3%	657	16,6%	766	16,8%
Brazil	230		140		190	
Ecuador	261		232		270	
Others	286		285		306	
Asia and Oceania	400	9,4%	397	10,0%	421	9,2%
Papua New Guinea	36		36		41	
Others	39		41		50	
World total	4251	100,0%	3965	100,0%	4552	100,0%

faced to many factors bugs: this leads to the losses of production of cacao in these countries. Bug control was recommended to increase production of cacao and reinforce the economy of countries producers. Principally in Cameroon, cacao-culture is practised in many regions of the country. It is an old practise. Firstly practised during a long time in the traditional way, the culture of cacao in Cameroon has been ameliorated since the introduction of the news systems of culture: agroforests. Production and marketing of all these cultures associated with cacao in agroforests and also the marketing of cocoa contribute to reinforce the economy of the country: This represent an enormous source of income for farmers and increase yielding of the country. So, cacao cultivation contributes to the increasing of the economy of the country. Cacao and coffee production represents approximately 2% of national PIB, 6% of primary PIB and approximately 1/3 of PIB of sub-sector of agricultural products destined to exportation and transformation. Cacao and coffee producers have a great rule to the equilibrium oh commercial balance of Cameroon and in the elaboration of income of populations of areas of production.

Cacao is a tree which can have a mean higher of 25 meters in the case of it has been cultivated in the savannah area. Generally, farmers limit his higher growth between 5 and 7 meters. The high of cacao is on the average 1.5 meters when the crown appears but this high can change according to variety of trees, conditions of culture and environment. The crown is most high in the shady plantations than sunny plantations [6]. Cacao tree is represented by figure 1.1.1.

Figure 1.1: Cacao tree

1.1.2 Characteristics of agroforests in Cameroon

There exists two types of culture in Cameroon: mono-farming systems and agroforestery systems.

Mono-farming designate the whole agricultural or forestries practices in which it is only one plant or a very limited species which are cultivated on a big area. Mono-farming systems based on cacao culture come from massive and complete clearing of the forest. This apparent mono-farming is shaded by the presence of the annual cultures associated during the first three years of plantation corresponding this time exactly to the delay of entry in production of cacao tree in "full sun" situation or by the presence of tuft of banana tree surviving in adults plantation. Cacao culture begins after the third year.

In 2000, Torquebiau define agroforestery as an simultaneous or sequentially association of trees, annuals cultures or animals productions in order to obtain goods and courses useful for humans [27]. These systems of culture are called agroforests. There exists several types of agroforests in the world (culture under arboreous cover, systems in linear disposition, sequentially agorforesteries technical,...).

The main agroforests are the ones which belong to the category of simultaneous associated trees because of their ecological asset such that biodiversity, protection of the ground and recycling of nutriments [28]. Then, agroforests are generally typical by a dominant culture, main source of revenues or utilization (hevea, coffee tree, cacao), they are also invested of other components (trees, creepers, shrubs), organized in multi strata [29]. There exists two types of agroforests: agroforests based on culture of "canopy" and culture based on culture of sub-stage. We will principally interest to agroforests based on cacao culture in Cameroon. In Cameroon, precisely in the regions of centre and southern of Cameroon, agroforests based on cacao culture are association of two different cultures: cacao which is the main culture and other species associated pluri-specific and multi-functional, more difficult to characterize and to evaluate with the agronomic tools.

In Cameroon, agroforests are also organised in three strata of high: the higher strata, intermediary strata and strata of cacao. Cocoa production in Cameroon is primarily affected by mirid bug *Sahlbergella singularis*, and Black Pod (BP) disease, caused by *Phytophthora megakarya*, whose host range is currently not well known.

In Cameroon, the mean yield is small (evaluated between 100 to 1200 kg/ha). This small production is due to diseases, pests and also to the ageing of plantations. After extracting beans, pods of cacao should be use as fertilisers (organic fertiliser) and also to the feeding of animals. In the same plot, cacao may be cultivated in association with several other culture like banana. Cacao can also be associated with fruit trees such that plum tree (*Dacryodes edulis*), avocado tree (*Persea americana*), coconut palm or palm tree (*Elacis guincensis*). A plot can be exploited for 20 years. This time depends on the care of the plantation. After 25 years, production reduces considerably because of difficulties linked to the care of trees which became very high. The areas of production of cacao in Cameroon are the regions of Centre, South, East, South-West and Littoral.

Schematically, we can identify 4 layers of vegetation in the Cocoa agroforests in Cameroon: the upper stratum composed of forest trees about 15 to 30 meters high, the intermediate stratum mostly composed of fruit trees about 5 to 15 m high, the low stratum mostly composed of cocoa trees and Musaceae between 2 and 5 m high and the lower strata consisting mainly of young plants and Herbaceae less than 2 meters high. Despite its schematic character, all or part of this classification in four strata has been used in the vast majority of vertical structure studies of cocoa agroforests in Cameroon ([30], [6]).

Trees which assure shade on cacao tree present a high diversity. Forest native species are associated to the fruit species which participate to the daily feeding and susceptible to be commercialise (avocado tree, citrus fruit, mango tree, plum tree). Generally, native trees are highly favoured and represent

Figure 1.2: Cacao tree in association with coconut palm

a high part of arboreous population. These species give medicinal, feeding resources and many other domestic uses. Cocoa cultivation in agroforests in Cameroon give the yield plus or less consequent to the Cameroon economy. In fact, the yield varies to 2 to 3 tons per hectare. In Cameroon, in the areas ecologically favourable to the culture of cacao tree, there exists an equatorial climate. There is a climate favourable to the culture of cacao. The main regions where high practice of cacao cultivation are regions of Centre, South and West. In the "Centre" region, the culture of cacao is doing in the districts of Ntui, Bokito, Bafia, Talba and Ngomedzap and approximately. In this area, cocoa cultivation is strongly practised. The South region has a land favourable to the cocoa cultivation: the most cacao plantation area are Lolodorf, the district of Ntem, of Dja and Lobo. In the West region, the culture of cacao is practised in "Bamiléké" countries especially in the districts of Kekem and Bana. However, we also have the big cacao plantations in Kumba, Manfé, Mbongue, Tombel and Limbé.

Cameroon is a country which has several agricultural resources such as banana and cacao. In fact, since 2005 Cameroon is the fifth world producer on cocoa with annual production evaluated at $242,600$ tons of beans per year [31]. According to the International Cocoa Organization (ICCO), Cameroon is ranked third in the world with 380,000 tonnes in 2017, compared to 882,175 tonnes for Ghana and 2.01 million tonnes for Côte d'Ivoire. This increase in production is due to the fact that in 2012, Cameroon set up a "New Generation" program to boost cocoa production. Since then, this program has created 15,333 hectares of cocoa plantations in the country. Specifically, this program, which stems from a study revealing that the average age of producers in particular production areas,

is based on the recruitment of young people interested in cocoa farming, for a training spread over 3 years.In central Cameroon, the cocoa growing model appears to be different from the one prevailing in many cocoa producing countries such as Côte d'Ivoire. In this part of Cameroon, we found that cocoa stands were more than 40 years earlier, corresponding to the age of cocoa tree senescence.

For cocoa cultivation, annual precipitations on the average are variable between 1400 and 1600 mm per year and are principally separated in two periods: the small rainy season between Mars and May and the big rainy season between September and November.

1.1.3 Phenology and physioloygy of cacao tree *Theobroma cacao*

The genus Theobroma originated millions of years ago in South America, to the east of the Andes. Theobroma has been divided into twenty-two species of which textit T. cacao is the most known. It was the Maya who provided tangible evidence of cocoa as a domesticated crop. Archaeological evidence in Costa Rica says cocoa was drunk by Maya traders. The first to drink chocolate was Christopher Columbus, who reached Nicaragua in 1502 searching for a road to the spices of the East. But it was Hernan Cortès, leader of an expedition in 1519 to the Aztec empire, who returned to Spain in 1528 bearing the Aztec recipe for cocktail (chocolate drink) with him. The drink was originally received unenthusiastically and it was not until it became a popular drink in the Spanish courts. Strong demand for chocolate has boosted cocoa cultivation worldwide. Amelonado cacao from Brazil was planted in Principe in 1822, Sao Tomé in 1830 and Fernando Po in 1854, then in Nigeria in 1874 and Ghana in 1879. In Cameroon, cocoa was introduced during the colonial period of 1925 to 1939.

Cacao (*T. cacao*) is a plant of the family of Sterculiaceae and originated from the wet tropical forests of Central America [7]. The firsts exportations of cacao towards Europa are been done in 1 585. In 17^{e} century, there are many plantations of cacao around the world and it was through Fernando Pô island (actually Malabo), Sao Tome and Principe, which cacao is introduced in Africa. Cacao will be introduced in Cameroon in 1892 by Germans ([32], [33], [34]).

Table 1.2 recapitulate the taxonomy of cacao tree. The growth of leaves and stems is done by successively thrusts separated by rest period. During these periods, the final buds take back their "dormancy" [35]. Several factors influence the growth of leaves and stems in particular temperature, daylight, tenor of hydrate of carbon and regulators of growth.

Production needs several stage: flowering, fruition, harvesting and marketing of beans. Cacao tree is able to flower all the year. Cocoa is raised from seed. Seeds will germinate and produce good plants when taken from pods not more than 15 days under-ripe. A bud is cut from a tree and placed under a flap of bark on another tree. The budding patch is then bound with raffia and waxed tape of clear

Table 1.2: Systematic of *Theobroma cacao*.

Reign	Vegetative
Branch	Spermaphytes
Sub-branch	Angiospermes
Class	Dicotyledon
Sub-class	Dilleniidae
Order	Malvales
Family	Malvaceae
Gender	Theobroma
Specie	*Theobroma cacao*

plastic to prevent moisture loss. When the bud is growing, the old tree above it is cut off. A strip of bark is removed from a branch and the area covered in sawdust and a polyethylene sheet. The area will produce roots and the branch can then be chopped off and planted. The flowering of cacao has the particularity to appear on branch and trunk. There exists a large flowers which succeed all the year. On mature cacao, flowering is cyclic so to speak that the high growing period alternate to the small growing period [36]. The next period after flowering is fruiting. The number of fruits present on cacao tree depends on the genotype of cacao. There is function of fertility of land, availability of water and daylight. Maturity of fruits can be affect by temperature: we remark that during the warm months, pods needs approximately 140 to 175 days for its total development whereas during the cold period, pods need approximately 167 to 207 days for its total development.

Cacao produces yearly several thousand of flowers but only less than 5% of these flowers develop to young fruits. This small percent is mainly due to the phenomenon of drying pf young fruits. this phenomenon appears about 50 to 60 days after pollination and influence the production by affecting 20 to 90% of young fruits (cherelle) produced. The fruit of cacao is called pod and the eatable part of the pod is called beans. When a pod has a height less than 10 centimetres, it is called "cherelle". There are supported by a peduncle which proceeds from the development of thickness of the peduncle of flowers. Cacao fruit needs tree or four months or even five or six months for their total development. This time depends on the variety of cacao tree and it is necessary for the full development of fruits. After this, pod will ripen during one or two months, to undergo interior transformations and to change colours. The high of a pod varies between 10 and 35 centimetres. On the average, its length varies between 15 and 20 centimetres and its width varies between 10 and 15 centimetres. The weight of a pod varies between 200 g and 1 Kg (on the average 400 and 500g). A pod contain approximately

30 to 40 beans. The weight of a bean after elimination of the pulp and husk varies between 1.3g and 2.3g; after drying, the weight of the bean varies between 0.9g and 1.5g. fermentation and drying of the beans of the pods lead to obtaining of commercial cacao. This commercial cacao is be useful to the production of chocolate and obtaining a cocoa butter. Different stages of evolution of the pod are represented in figure 1.3.

Figure 1.3: Stage of evolution of cocoa pods: (a) flower; (b) cherelle; (c) young pod; (d) pod.

African continent is the main producer of cocoa. In 2010, its production was evaluated to 2.6 millions of tons for the world production variable of 3.4 to 3.7 millions of tons. In Cameroon, cacao production has an important for the rural populations: it is the main source of income to farmers. Cacao production also contribute to the reinforce of the economy of the country. For the higher produces in commercial cocoa, cacao need to be cultivated in pure culture under shade ([37], [33]). Now, when cacao is cultivated without shade, its optimum production will be obtain if all environmental

factors are favourable: availability in mineral elements in sufficient quantities, regular share in fertilizer, sufficient and well retort pluviometry, protection against bio-agressors [5]. when there is not mineral fertilizers (as it is the case of familial cocoa plantation), produce of cacao plantation is heavy during the first years of exploitation but after 20 to 30 years and even less, cacao plantation break down ([38], [39]).

1.1.4 Diseases and bugs of *T. cacao*

As all plants or vegetative organism, cacao tree faced to several diseases: diseases of fungicidal or viral origins. Cacao also faced to the multiple attacks doing by pests and diseases and principally mirids which lead to many damage observed on the plant. Among fungicidal attacks, the main disease of cacao tree in Cameroon is the black pod diseases caused by *Phytohptora megakarya* which is the main specie observed in Cameroon. This disease on fruits which present one or several brown spot can also be observed on leaves, roots where it leads to the appearance of chancres [6]. In the countries where *P. megakarya* is the dominant, the losses of production can be evaluated to 50%. As fungicidal attacks, we can also cite the moniliose caused by *Moniliophthora roreri* which is only present on the American continent.

As viral disease, we can cite the Cacao Swollen Shoot Virus (CSSV) due to the "*Cocoa Swollen Shoot Virus*". This disease is manifested by the appearance of inflation of the wood of branches and roots [40]

Another factor which influence production of cacao tree is the action of pests. These bugs are responsible of the most damages on cacao and lead to important losses of production. In young plantations, many insects destroy a terminal bud and retard the development of the tree. In Cameroon, there are two main types of mirids *Distantiella theobroma* and *Sahlbergella singularis* which is the dominant specie. The impact of mirids on cocoa production varies between regions and between farmers fields, this is the variability of shading. Heavy shades reduce mirid density but also cocoa vegetative growth. At the same time, shade has negative effects on cocoa trees: the declining cocoa tree abundance and favour the black pod disease.

1.2 Cacao mirids

Mirids constitute the largest family belonging to the order Heroptora. They are the most common insects on cocoa and about 40 mirid species prey on the tree. They are considered most harmful to the tree. Mirids can also feed and grow on other host plants (*Cola nitida, Ceiba pentandra*) and are

divided into two main tribes namely: Odoniellini and Monaloniili. In Cameroon, there are several species of mirids belonging to different tribes. The most common species of the tribe Monaloniini found in Cameroon is *Helopeltis Afropeltis*. The most harmful species found in Cameroon belong to the tribe Odeniellini and are represented by *Distantiella Theobroma* and *Sahlbergella singularis* which predominate in most of the plantations. In this study, we are interested to the *S. singularis* specie.

1.2.1 The cacao mirid: *Sahlbergella singularis*

1.2.1.1 Presentation of *Sahlbergella singularis*

The adult female of *Sahlbergella singularis* is shown in Figure 1.4. The cocoa mirid *Sahlbergella singularis*, like other mirids is a sucking insect. Adults and nymphs feed on cocoa fruit and shoot thanks to the rostrum. Using their ovipositor, females also laid their eggs in the pods and sometimes in the shoots. Systematic of *Sahlbergella singularis* according Delvare and Aberlenc [41] is given by the table 1.3.

Figure 1.4: Female adult of *Sahlbergella singularis*.

1.2.2 Life cycle of *S.singularis*

The life cycle of *S. singularis* is composed of 3 stages: egg stage, nymph stage, and adult stage that develop mainly on pods either on shoots. The eggs are individually inserted into the host plant tissues [42] principally in the cortex of pods and sometimes under the bark of young shoots [43].

Table 1.3: Systematic of *Sahlbergella singularis*

Order	Hemiptera
Sub-order	Heteroptera
Infra-order	Cimicomorpha
Super-family	Incertae sedis
Family	Miridae
Sub-family	Bryocorinae
Tribe	Odoniellini
Genus	*Sahlbergella* Haglund 1895
Specie	*S. singularis* Haglund 1895

The incubation period of eggs is on average 15 days with a minimum of 9 days 25 and a maximum of 21 days [44] before reaching nymph stage. Mirid *S. singularis* has a very long life cycle (eggs to adults). It is on average 40 days with a minimum of 36 days [30] and a maximum of 50 days [11] The percentage of hatching eggs is globally 96.53% as the eggs are protected in the pods cortex.

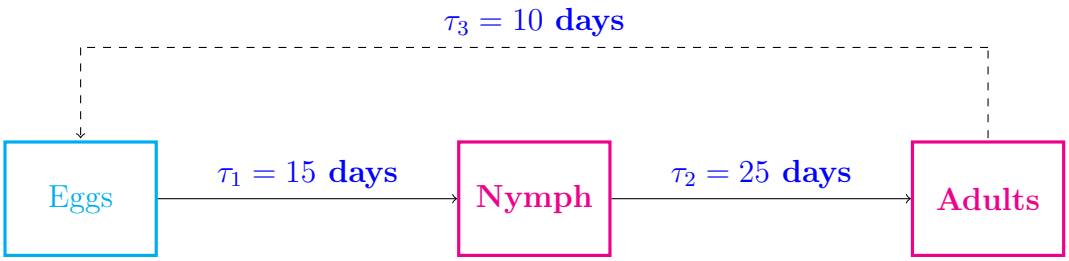

Figure 1.5: Life cycle of *S. singularis*

Adult stage can be subdivided into two stages: females and males. The under stage female can also be subdivided into two classes: immature females and mature females. Immature females are females aged less than 10 days: Indeed, after emergence, female need approximatively 10 days to have mating and begin laying eggs. Females *S. singularis* mate with one male (that is around 4-5 days old) 3 to 7 days after their emergence. The female produce and release pheromones until their death but males older than 19 days are not receptive any more to those pheromones [14]. After emergence, the female leaves the tree from which it originated to migrate to another tree. It is likely the females do not lay all their eggs on the same pod. Eggs are inserted individually and rarely by two in the tissue of the host plant. During a laying phase, the female could lay a maximum of 4 eggs per day [1]. In general, females start to lay eggs after 10 days old. But it has to be noticed that

Table 1.4: Table of values on parameters of the development of *Sahlbergella singularis*.

Longevity of males					37.20
Longevity of female	30-50				38.15
Fecundity (nymphs)	35.35	37.9 ± 3.09	14.6 ± 6.7		50.7
	± 10.42	max: 111.4	max: 79		
Fecundity (eggs)		29-62		65	52.52
Sex-ratio		1:1.03	1:1.5	1:1.17	
Fecundity period					16 days
Number of eggs by a female per day					3.2825
References	Babin et al 2011	Anikwé 2010	Babin et al 2006-2008	Youdeowei 1973	Estimated

some immature females ($<$ 10 days old) could lay eggs but they died without passing from immature stage to mature females. Number of eggs laid by those immature females will be added to the total number of eggs laid during the mature female stage to calculate the average fecundity per female which is around 50.7 nymphs or 52.52 eggs. The mean number of eggs laying by a female per day was calculated like the ratio between the total number of eggs laid by a female and the fecundity period. The fecundity period is the mean time between the first and the last egg-laying. It lasts on average 16 days from the 15^{th} to the 31^{th} day after female emergence. Based on those estimation, the daily fecundity per female is around 3.28 eggs. The daily survival of mirids adult has been evaluated thanks to data collected and the results are respectively 98.14% for immature females, 92.778% for mature females and 93% for males. A proportion 72.1% of immature females becomes mature females. To model the evolution of *S. singularis*, we consider the same survival rate for adult which is the one of mature females; the sex ratio which we consider is $1 : 1.5$ [11]. Longevity of adult female describes the period between emergence and death. Table 1.4 recapitulate all the data about the development of adults *S. singularis*.

1.2.3 Biology of *S. singularis*

1.2.3.1 Development of *S. singularis*

The eggs of *S. singularis* are individually inserted into the host plant tissues [14] principally on the pods and sometimes on the branches of the cocoa tree [43]. The egg is cylindrical and slightly

curved shape with length comprise between 1.6 and 1.9 mm. It is whitish and becomes shortly pink before hatching. The incubation period of eggs is on average 15 days with a minimum of 9 days [45] and a maximum of 21 days [44] and after these days the mirid spends egg stage to nymph stage. The percentage of hatching eggs is globally 96.53% The insertion of eggs *S. singularis* in a host tissue is shown in figure 1.6. After hatching, nymphs evolve from the first to fifth nymph stage.

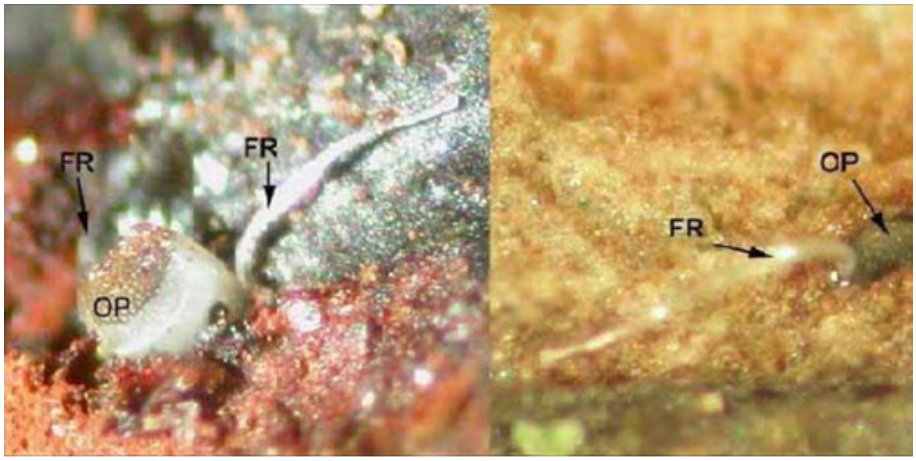

Figure 1.6: Eggs of *Sahlbergella singularis* inserted into the host tissue (cortex pod left and peduncle pod right). FR: Respiratory filament OP: cap [1].

Nymphs *S. singularis* are able to move within a cacao tree to find pods and shoots to ensure their nutrition and development. Nymphs *S. singularis* would take in average 25 days to complete their nymph development. The data used to model the development cycle of *S. singularis* were obtained from different items. For unknown data (at least the one that do not appear in the articles), we made an estimate using the raw data that were collected by Cameroonian colleagues. Published studies conducted in Cameroon ([46], [11], [30]) were realized at constant temperature ($24.7 \pm 0.9°C$). For studies conducted in Nigeria ([45], [2]), the temperature during the experiments ranges from $24°C$ during the day and $22°C$ during the night [2]; and from $15.88°C$ during the day to $36.16°C$ during the night for Youdeowei experiments [45]. These values represent the minimum and maximum temperature values obtained according to the month in which took place the breeding. The data reflecting detailed larval development parameters are recorded in Table 1.5.

1.2.3.2 Mating, reproduction and egg-laying

After emergence, nymphs become adults males or females. Males need 2 days to have their sexual maturity whereas females need approximately 3 to 7 days [1]. Existence of sexual pheromon has been demonstrated for this specie. This sexual pheromon attract males towards females.

Table 1.5: Values of the development (days) of *S. singularis* according to several authors.

Stage	Development Anikwé 2010	Development Babin 2011	Development Babin 2006-2008	Development Youdeowei 1973	Development Wacri, in Lavabre, 1977
Eggs	14.1		*min 16*	13.1	17.4
	11-16			*13-21*	
L1		3.8	2.7		4.5
			2-4		*3-8*
L2		4.0	2.9		4.8
			2-4		*3-7*
L3		4.1	3.5		4.5
			2-5		*3-6*
L4		5.3	2.7		3.7
			2-7		*3-7*
L5		7.6	6.3		5.2
			3-9		*3-8*
Nymphs	27	24.88±0.34	22.7±3.7		
Total	41.1	36.022±3.4	46		
		max 49.225	*40-50*		
Hatching rate	96.53				

1.2.3.3 Feeding behavior of *S. singularis*

Mirid *S. singularis* usually feed on the cacao by sucking the sap. For their development, nymphs extract sap using their stylus. So they bite cocoa via pods, young shoots and twigs. Experiments in the laboratory used to estimate the average number of bites per nymph and according to its stage of development. In this experiment, there was only one larva per box which receive a cherelle about 10 cm for its nutrition. There is no competition with another nymph food for resource. The data obtained were recorded in the table 1.6. The number and diameter of bites for the adult is the same as nymph of the fifth nymph stage. Males and females feed on pods and shoots: the number and diameter of bites for adult is consigned in Table 1.6 (same values for fifth larval stage).

Furthermore, the feeding behaviour of *Sahlbergella singularis* has also been evaluated from efficacy

Table 1.6: Number and diameter of nymphs bites *Sahlbergella singularis* per day

	stage L_1	stage L_2	stage L_3	stage L_4	stage L_5
Number of bites	27.53	28.46	26.72	24.77	26.88
Diameter of bites	1mm	1mm	2-3mm	2-3mm	4-5mm

tests of insecticide. In these tests, the authors compare the number of bites of *S. singularis* in the presence of insecticides and control groups (without insecticide) [47]. The number of bites per mirid was obtained under laboratory condition on different genotypes of cocoa trees to assess the resistance of different genotypes of cocoa trees ([25], [48]); these tests were done on twigs of $6cm$ cocoa long, each corresponding to different genotypes of cocoa. These studies presented a number of bites per mirid, ranges from 2 to 12.1 bites per day: this according to the genotype of the cocoa tree, but also with the stage of development of mirid. Thus, the genotype of the tree determines mirid bites because some trees seem more susceptible to mirid bites than others. For the study of our models, we prefer using the data reported in the table 1.6.

1.2.4 Ecology of *S.singularis*

1.2.4.1 Estimated mirid populations in plots

Several methods are used to assess the number of mirids present in the plots. In some published papers, the authors counted mirids on the trees every week. There is some lack with this method as the visual estimation is not easy due to the size of the insect and its hiding behaviour. With this method, we have to know that most of nymphs are counted twice or sometimes three times. So the estimation of the population in the plot based on this method should take account of these adjustments.

The other method is based on Knock-down method. Once a year, trees are treated with an insecticide (by fumigation). Insects that were present on the trees fall on a white plastic bag on the soil. This method is quite exhaustive to evaluate the density at a precise time and also to evaluate distribution in the plantations but it can't be used to follow a population dynamics and to estimate the level of population during one year.

Parameters such as the number of occupied trees and the tree infestation index have to be considered in order to better estimate the number of mirid present in the plots. The number of occupied trees represents the proportion of trees showing mirids presence or damage depending of the authors and the papers. The tree infestation index represents the average number of mirids present on a

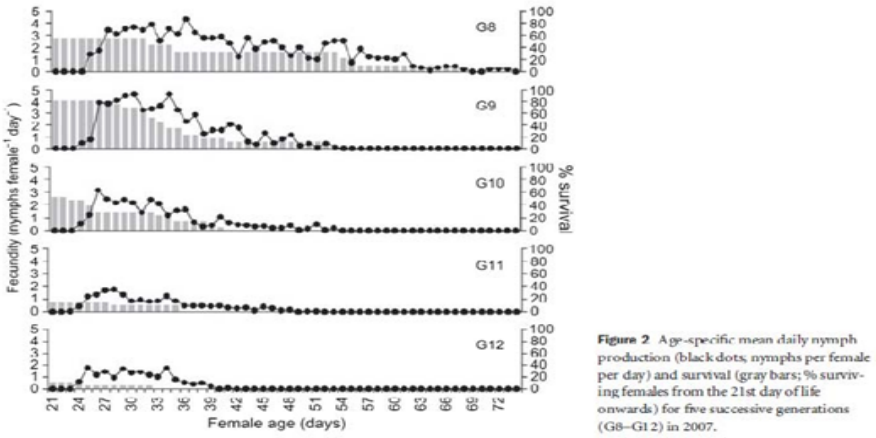

Figure 2 Age-specific mean daily nymph production (black dots, nymphs per female per day) and survival (gray bars; % surviving females from the 21st day of life onwards) for five successive generations (G8–G12) in 2007.

Figure 1.7: Fluctuation in the mean monthly population of *S. singularis* per 100 trees in Ibadan, Nigeria [2].

tree. The number of trees is marked by mirids recorded using sampling reduction method. The number of identified mirids per hectare is quite variable. The maximum densities are about 2500 mirids hectare [16] or approximately 7000 per hectare mirids [49]. In Cameroon, we have on average $2,1$ mirids per tree [15].

Figure 1.7 represents the fluctuation of miridae populations obtained in [2] during the following period: the mean monthly population of *Sahlbergella singularis* per 100 sampled trees in Nigeria over a period of three years (2004, 2005 and 2006). The peak of populations of mirids is obtained in September 2005 with 107 mirids. There was respectively 42 and 59 mirids in October 2004 and 2006. In April and May 2004, from March to July 2005 and May to July 2006, the result of their study showed the absence of *Sahlbergella singularis* in the field. Figure 1.8 represents the mean number of *S. singularis* per tree in tree regions of Côte d'Ivoire. The peak of populations of mirids is obtained in September with a mean of 20 mirids per tree.

1.2.4.2 Seasonal variations of mirids populations

Mirids dynamics varied greatly during the year. Density of population is likely to be influenced by pods availability on the trees. Mirid population is low on cocoa during the period from February to March. From June to July, the populations start to grow more or less rapidly depending on external conditions like weather and fruits production on the trees. The peak of the population appears between September and November when the pods are almost mature ([11]; [50]; [2],[3]). Between January and March, despite the low number of pods present on cacao tree, it is still possible to collect mirids principally on the greedy and branches. Even if the lack of resource (i.e pods) can explain the

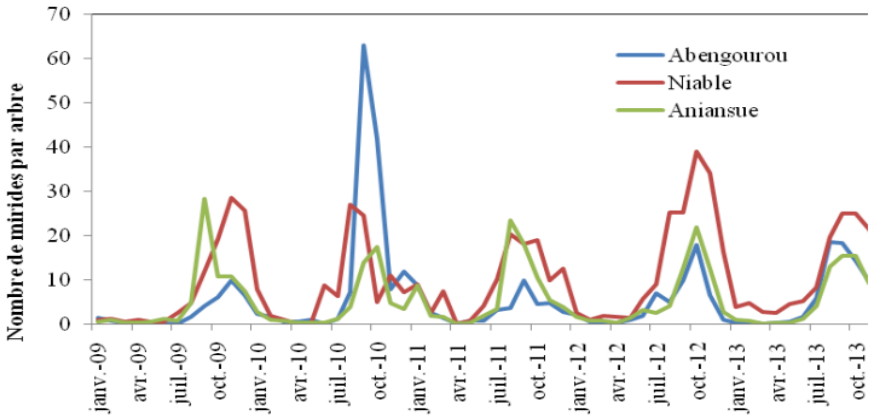

Figure 1.8: Seasonal variations of *Sahlbergella singularis* in Côte d'Ivoire [3].

decrease in mirid population, other hypotheses have been formulated to explain the drastic decline that occurred between February and March. In Babin et al. 2010 [15], it is assumed that lower mirid populations observed in plantations during a certain period of the year (the period from November-December to June) is due to declining fertility of females and increased mortality of individuals 1.5. Thus, it seems that development parameters (longevity, fecundity) of mirids vary depending on season. The G8 and G9 generations obtained in June, July and August (during pods formation on the trees) were the most productive generations with high fecundity and female longevity. On the other hand, generations G11 and G12 obtained in November, December and January showed lowest fecundity and female longevity. In Kouame et al. 2014 [3], it is assumed that the lower mirid population is observed in plantations between February to June. This variation depends on temperature and pluviometry.

Another hypothesis that can explain the drop of the mirid population on the plot is migration. In fact, cacao is cultivated in agroforestery systems in association with several other crops among which potential mirid host plants (*Cola nitida, Ceiba pentandra*). Mirids are originated from African forests therefore before the arrival of cocoa in Cameroon, those insects developed on other forest trees like *D. dewevrei, Ceiba pentandra* in Cameroon. So it could not be excluded that mirids take refuge in those trees when resources from cocoa trees become less suitable for the species development. An experience proved that *S singularis* is able to feed on *D. dewevrei* but its capacity to multiply on this tree remains to be confirm. Then, when development condition become more favourable on the cocoa trees, the mirids can re-infest the plantations.

1.2.4.3 Dispersal availability of *S. singularis*

Moving of *S. singularis* in the plot is an important factor using for evaluate the interaction

between *S. singularis* and cacao. Eggs of *S. singularis* are immobile and wait for hatching to become nymphs. Nymphs of *S. singularis* are very mobile but only in the same tree. Nymphs do not have the ability to fly from one plant to another. They must complete their development and become adults for that; therefore, nymphs usually feed on the same cocoa tree view on the same tree. The dispersal potential of this species is entirely determined by the mirid adult flight capabilities. Concerning adults *S. singularis*, studies in Ghana and Nigeria, according to various methods have demonstrated that adult mirids can fly 24 hours after emergence, but the first long flight occurs only after 3 to 5 days. A fight of mirid can be started by coming of predator and in this case, flight is short and in zigzag or in spiral [51]. He esteem that, on the average the distance travelled by adult of *D. theobroma* is 1.1 km for males and 2.3 km for females, with on the average speed of 3.4 meters per second. Youdeowei distinguish two types of flight of *S. singularis*: the trivial flight and the dispersion flight. A trivial flight only last for some seconds and have for main objective the feeding or researching of partner for mating. A dispersion flight can last more than thirty minutes and allow *S. singularis* to colonize a new habitats [52]. In the same article, he observe that female of *S. singularis* are able to flight more than one hour without any interruption and males more than one hour and thirty minutes.

1.2.5 Interaction between mirids and cacao in agroforests.

Interaction between mirids and cacao is essentially due to the action of mirids on cacao. Mirids use cocoa for their feeding and their development. Mirids feed and lay on cacao tree: this action lead to damages observed on the tree: anecdotal damages on a pod and cumulated damages on the other parts of the tree.

Mirids tend to hide themselves to feed and move quickly. So,it is difficult to establish a link between mirids population and damages observed in the yield because the treatment is based on the estimation of population of mirids and not on the damages observed in the yields. Moreover, several farmers cannot see the insect but they are able to recognize the damages on the pods. The bite on pod are check off on peduncle and according to the cortex size, damages on pods are remain anecdotal. In fact, the harvest remains interesting and the selling of beans continues. The most damages (damages which appears on the other parts of cacao tree) are cumulated over time and can lead to the destruction of the tree ([17], [53], [16], [43]).

1.2.6 Damage caused by mirids

Feeding and egg-laying of *S. singularis* lead to important damages observed on cacao tree. These damages are observed in several parts of the tree especially pods, shoots, branches and leaves. Dam-

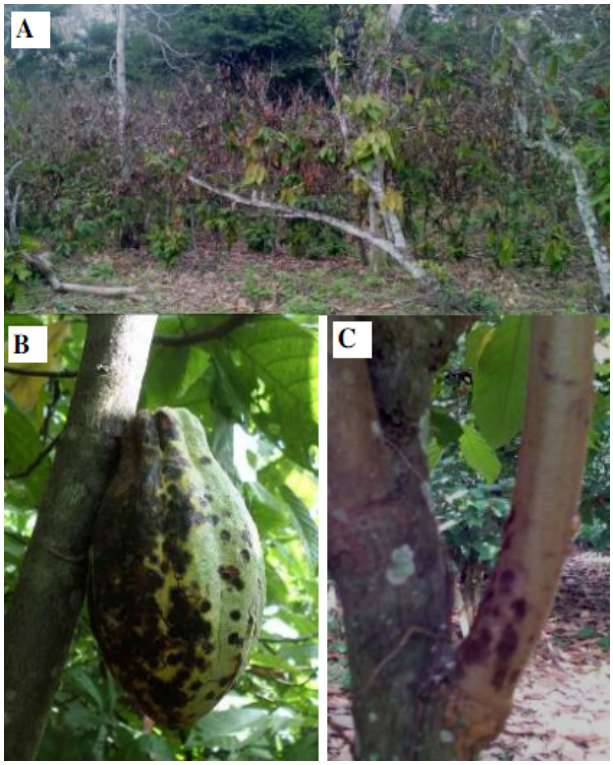

Figure 1.9: Damages observed on cacao due to the action of *S. singularis*

ages observed in the pods are anecdotal: indeed, once the pod has passed cherelle stage it can no longer die under the action of mirids. The death on pods due to *S. singularis* is only in "cherelle" stage: this damages lead to the deformation of the fruit current in growing and even drying of the fruit if peduncle is affected. The bites of *S. singularis* on pods don't prevent harvesting but damages on the rest of part of the tree can lead to the destruction of the tree. When mirids feed on leaves or on branches of cacao, this involves the interruption of the circulation of the sap in this part. We observe the phenomenon of the drying of the leaves and branches. Damage on the pod and leaves is represented by figure 1.9. Several parts of the tree where the attacks of mirids are repetitive are especially damaged. These parts of mirids are called "mirid pocket". They concerns generally any about ten trees which are particularly non productive and present several "gourmands". They are attractive for the mirid for the feeding and egg-laying and generally leads to the death of the tree. The feeding lesions due to the impact of mirids are also infected by a parasitical toadstool *Calonectria rigidiuscula*. These lesions develop in cankers which accumulate and weaken the branches and the trunk of the tree; this lead to the death of the entire branches, all the coronet and even the tree. This phenomenon is currently called "die-back".

1.2.6.1 Effects of the action of mirids on the growth of cacao tree

Mirid aggression cause a losses of leaves due to the fact that they cannot supply in saps. Mirid aggression lead to the death of many plants: in fact, it has been proved in one study that for a total of 14 infected plants, we observe the death of 6 plants. According to treatment, some plants before their death develop "rejects" (death due to the action of toadstool) and others not. Then appearing of new flowers is elevated of infected plants than non infected plants.

1.2.6.2 Impact of the action of mirids on the development of cherelle: Cherelle withered

Mirid aggression lead to the death of several "cherelle". Withered of "cherelle" is either due to mirid aggression, or internal factors of cocoa and environmental factors. Biting "cherelle" tend to be wither instead of to evolve as pods. In mean, 63% of biting "cherelle" whiter. In the plot, there has a small "cherelle" aggression. Mirid which prefer feed on pods are very low in the plot between February and June; this period correspond to the flowering and "cherelle" development. Mirid aggression on "cherelle", even if they are low, they are very harmful for the "cherelle" development.

1.2.7 Natural enemies and control *S. singularis*

Mirid *S. singularis* have many natural enemies: entomopathogenus, parasitoids, parasites and predators. *Leiophron (Euphoros) sahlbergellae* is the only parasite which lives in depend on the larvae of *S. singularis*. A parasitism rate of this specie is evaluated to less than 6 to 20% in Cameroon [14]. Several species of toadstool are identified as harmful for the population of *S. singularis*: we can cite *Hirsutella sp.* and *Beauveria sp.*. More recently, a stock of *Beauveria bassiana* has been isolated in Cameroon [54]. There is not several species of predators of mirids. We can cite species of spider and ants which are predators of *D. theobroma*. In consideration of the morphological similarity between *S. singularis* and *D. theobroma*, these species of predators of *D. theobroma* are probably predators of *S. singularis*.

1.2.8 How to control *S. singularis*?

There exists many strategies to control mirids in generally and *S. singularis* in particularly: agronomic control, biological control, chemical control, varietal control. We also control mirids by using attractive traps or insecticide doing by plants. In Cameroon, farmers develop a way to control mirids using cultivated plants as hemp or tobacco; also using plants which we find in cacao agroforests

like bubinga and tali to make insecticides. These insecticides also have a rule to clean up the plot against diseases and bugs. Another method which can be used to struggle against mirids is to do the pheromone traps. In fact, before mating female *S. singularis* usually broadcast sexual pheromon for attract males. This method is used to capture mirids in order to eradicate mirids population. The trap catches the optimum number of males mirids when it is at $1,8$ metres above ground level when suspended in cacao tree. In Cameroon, by using this method, the densities of mirids are evaluated to approximately $2.5-7$ mirids per tree at the peak of the proliferation period, while the economic threshold level for cocoa mirids in Cameroon has been determined at just 0.7 mirids per tree [15]. The chemical management of mirids is doing by use of insecticide. Agronomic management regroups all the cultural methods which permit to create the non favourable conditions to the development of mirids populations (to rid the "gourmands" which are the part on the tree where mirids lays in absence of pods, to remove all the alternative hosts plants). Varietal control consists to replace the variety of cacao traditionally cultivated by variety more resistant or tolerant of mirids attacks. Biological control is in opposition to chemical control. It consists to use organisms in order to prevent or reduce damages caused by mirids: the use of natural enemies of *S. singularis* in this case.

Despite all these ways of mirid control, the losses of production due to the action of mirids are very important and lead to the important economic losses for the world producers of cacao. Another approach to solve this problem caused by mirids would be to use mathematical approach. By using the life cycle of mirids and its interaction with cacao tree, may be we will develop or ameliorate strategies to control mirids.

1.3 Problematic

The culture of cacao is important for the economy of Cameroon but this activity faced to many diseases and bugs of cocoa. More precisely, cacao bug *S. singularis* are very harmful for the cacao trees. They are responsible of many damages and a small quantities of bugs are able to cause several damages. Damages caused by this bug are approximately 40% of the potential production on the plot: it is enormous. Since cacao is the first cash crop, these losses of production lead to the decrease of the economy of country. Many research works are developed in order to study the bug *S. singularis* and the other diseases of *T. cacao*; but none of the works in our knowledge consider the evolution of damages caused by mirid bug *S. singularis*, the mechanism of destruction of cocoa due to the action of *S. singularis*. The population of mirids constitute an enormous source of problems for the cacao cultivation around the world and especially in Cameroon in particular. There are two types

of damages caused by mirids: anecdotal and cumulated damages. We would want to understand the evolution of these damages caused by mirids in the plots in Cameroon: we would want to know approximately how much time is necessary for a plot deserted to the mercy of mirids to become completely destructed. We would also want to be able to explain to the farmers which will be the indicator to start a treatment. The aims of this study are multiple: to predict how populations of *S. singularis* develop in the plot at time, to apprehend the distribution of damages caused by mirids in the plot, to test the strategies of control mirid population in order to increase cocoa production in Cameroon, to contribute to control mirids in agroforests in Cameroon.

Then, our research question is to estimate the evolution of damages due to mirids especially *S. singularis* in Cameroon using mathematical models. The objectives are to acquire knowledges in order to understand the base of interaction between cacao and *S. singularis*, to integrate all these knowledges in order to formalize this interaction between *S. singularis* and cacao. Our aims are multiple: to predict the appearance and the level of *S. singularis* in the plot, to apprehend the distribution of damages caused by mirids in the plot, to test the strategies of control of mirids population in order to increase cocoa production in Cameroon, to contribute to control against mirids in the agroforests in Cameroon.

Several works have been developed in order to estimate the level of mirids in the plots [15, 24]. The result of this work is: there exists a small number of mirids but this little number of pests lead to enormous damage. It is likely that the approach to estimate the number of this pest was not well done. This is why we have thought of a mathematical approach to predict mirid population levels. In the next section, we will therefore recall all the mathematical tools that will help us in the modelling and resolution of our different models. However, biological works allowed us to have data on the life cycle of the insect and these data will help us to implement our different mathematical models.

1.4 Dynamical systems

Definition 1.1. *Dynamical systems: A dynamical system is a system whose state evolves with time over a state space according to a fixed rule. Especially, in Mathematics, it is a system which a function describes the time dependence of a point in a geometrical space*

At any given time, a dynamical system has a state given by a tuple of real numbers (a vector) that can be represented by a point in an appropriate space (a geometrical manifold). The evolution rule of the dynamical system is a function which describes what future states follow from the current state. Often, the system is deterministic, that is, for a given time interval only a one future state

follows from the current state.

The study of dynamical systems is the focus of dynamical systems theory, which has applications to a wide variety of fields such as Mathematics, Physics, Biology, Chemistry... In applications of mathematics, we have the delayed systems, monotone dynamical systems, piecewise dynamical systems and so on.

1.4.1 Theory of delays differential equations (DDE)

In many applications, the future behaviour of many phenomena are assumed to be described by the solutions of an ordinary differential equation. This implies that the future behaviour is uniquely determined by the present and independent of the past. In order to correct and do the model more realistic, it is better to model a phenomenon by delay differential equations, differential difference equations, or more generally functional differential equations.

1.4.1.1 Generalities

Let the following equation be the delay differential equation:

$$\dot{x}(t) = f(t, x(t), x(t-\tau)) \tag{1.1}$$

where τ is the delay, $x(t)$ is the state of the system and $f : \mathbb{R} \times \mathbb{R}^n \times \mathbb{R}^n \longrightarrow \mathbb{R}^n$ a continuous function in relation to all its arguments. Let $t_0 \in \mathbb{R}^+$ be the initial time. In order to construct the solution $x(t)$, it is not sufficient to know only the value $x(0) = x_0$ as in the case of ordinary differential equations. It is necessary to know the solution on the interval $[-\tau, 0]$.

There exists many types of delays differential equation:

1. Delay differential equation

$$\frac{dx}{dt}(t) = f(t, x(t), x(t-\tau_1), ..., x(t-\tau_n))$$

where $f : \mathbb{R} \times \mathbb{R}^n \times \mathbb{R}^n \longrightarrow \mathbb{R}^n$, $0 \leq \tau_1 < ... < \tau_n$.

Note that the set $\mathbb{R}^n$ can be replaced by a Banach space.

2. Neutral equation: the delay also happens on the derivative

$$\frac{d}{dt}F(t, x\mid_{[t-\tau,t]}) = G(t, x\mid_{[t-\tau,t]})$$

3. Equation with delay depending on the state

$$\frac{d}{dt}x(t) = f(x(t - r(x(t))))$$

with $x(t) \in \mathbb{R}$, $f : \mathbb{R}^n \longrightarrow \mathbb{R}^n$ and $r : \mathbb{R}^n \longrightarrow \mathbb{R}^+$

4. Partial delay differential equations

$$\frac{du}{dt}(t) = Au(t) + F(u(t-\tau))$$

where A is an operator define on a Banach space X.

1.4.1.2 Useful results about delays differential equations

Given $r > 0$, denote $\mathcal{C}([a,b],\mathbb{R}^n)$, the Banach space of continuous mapping from the interval $[a,b]$ into $\mathbb{R}^n$ with the topology of uniform convergence. If $[a,b] = [-\tau, 0]$, we let $\mathcal{C} = \mathcal{C}([-\tau,0],\mathbb{R}^n)$ and define the norm of an element φ in $\mathcal{C}$ by $\mid \varphi \mid = \sup_{-\tau \leq x \leq 0} \mid \varphi(\theta) \mid$.

Let $\sigma \in \mathbb{R}$, $A > 0$ and $x \in \mathcal{C}([\sigma - r, \sigma + A],\mathbb{R}^n)$, then for any $t \in [\sigma, \sigma + A]$, we let $x_t \in \mathcal{C}$, be defined by

$$x_t(\theta) = x(t+\theta), \quad for \quad -\tau \leq \theta \leq 0.$$

Let $f : \mathbb{R} \times \mathcal{C} \longrightarrow \mathbb{R}^n$ be a given function. A functional differential equation is given by the following relation

$$\begin{cases} \frac{dx}{dt} = f(t, x_t), \quad for\ all\ t \geq \sigma, \\ and \ \ x_\sigma = \varphi \end{cases} \tag{1.2}$$

Definition 1.2. *[55] x is said to be solution of (1.1) if there exists $\sigma \in \mathbb{R}, A > 0$ such that $x \in \mathcal{C}([\sigma - r, \sigma + A],\mathbb{R}^n)$ and x satisfies (1.2) for $t \in [\sigma, \sigma + A]$.*

We have the following results about the delays differential equations:

Lemma 1.1. *[56] Let $\sigma \in \mathbb{R}$ and $\varphi \in \mathcal{C}$ be given and f be continuous on the product $\mathbb{R} \times \mathcal{C}$. Then finding a solution of (1.2) through (σ, φ) is equivalent to solving*

$$x(t) = \varphi(0) + \int_\sigma^t f(s, x_s)ds \qquad t \geq \sigma \ \ and \ \ x_\sigma = \varphi$$

Lemma 1.2. *[56] If $x \in \mathcal{C}([\sigma - r, \sigma + \alpha],\mathbb{R}^n)$, then x_t is a continuous function of $t \in [\sigma, \sigma + \alpha]$.*

Theorem 1.1. *(Existence of solutions)[56] Let D be an open subset of $\mathbb{R} \times \mathcal{C}$ and $f : D \longrightarrow \mathbb{R}^n$ be a continuous function. For any $(\sigma, \varphi) \in D$, there exists a solution of equation (1.2) through (σ, φ).*

Theorem 1.2. *(Uniqueness of solutions)[56] Let D be an open subset of $\mathbb{R} \times \mathcal{C}$ and suppose that $f : D \longrightarrow \mathbb{R}^n$ is continuous and $f(t, \varphi)$ be Lipschitz with respect to φ on every compact subset of D. If $(\sigma, \varphi) \in D$, then equation (1.2) has a unique solution passing through (σ, φ)*

Theorem 1.3. *Furthermore on the hypotheses of the precedent theorem, if f is a bounded function, then equation (1.2) has a maximal solution defined on $[-\tau, \beta[$ with*

$$if \ \ \beta < \infty \Longrightarrow \limsup_{t \longrightarrow \beta} \mid x_t(., \varphi) \mid = \infty$$

1.4.2 Theory of monotone dynamical systems

Monotone dynamical systems is systems which preserve some partial order on the state space. Monotonicity has been shown to constrain system behaviour in various ways, for example ruling out attracting nontrivial periodic orbits, under fairly general assumptions. When the system is strongly monotone, behaviour is constrained further: for almost all initial conditions bounded solutions converge to the set of equilibria. Sometimes such generic convergence claims can be strengthened: for instance, convergence of every bounded orbit can be obtained in a variety of special cases.

Mathematical models of biosystems, in general, and in population studies, in particular, are often represented by continuous dynamical systems. The qualitative analysis of such systems regarding the long term behaviour of their solutions is one of the main mathematics involvements is such studies. The aim of our study concerns the properties of global nature like basins of attraction and global asymptotic stability of equilibria. The theory of monotone dynamical systems offers alternative monotonicity-based approach which is to a large extend independent of the dimensionality of the system. There exists two types of monotone systems: Cooperative and competitive systems.

We denote by $F : X \longrightarrow \mathbb{R}^n$ a $\mathcal{C}^1$ vector field generating the (local) flow $\phi = \{\phi_t\}$, in X. Thus the solution to the initial value problem $\dot{u} = F(u)$, $u(0) = x$ is the curve $t \longrightarrow \phi_t\, x$, defined for t in some open interval $I_x = (\sigma_x, \tau_x)$, $-\infty \leq \sigma_x \leq 0 \leq \tau_x \leq +\infty$.
We call F (or ϕ) cooperative if

$$\partial F_i/\partial x_j \geq 0 \quad for\ \ i \neq j.$$

For some results we need the additional assumption that F is irreducible, i.e., the Jacobian matrices $DF(x)$ are irreducible. When this holds and F is cooperative then $D\phi_t(x) > 0$ for $t > 0$, and p-convexity then implies that ϕ is strongly monotone [57]:

$$\phi_t(x) < \phi_t(y)\ \ if\ \ x < y\ \ and\ \ t > 0.$$

A vector field H is competitive if $-H$ is cooperative, that is, if $\partial H_i/\partial x_j \leq 0$ for $i \neq j$. Many propositions about cooperative fields are invariant under time reversal (replacing the field by its negative) and thus are also true for competitive fields [57].

We will give some of the main results in the theory of competitive and cooperative systems. But first, we give some new strong monotonicity results for odes. Let J be a nontrivial open interval, $\mathcal{D} \subseteq \mathbb{R}^n$ be an open set, $f : J \times \mathcal{D} \longrightarrow \mathbb{R}^n$ be a locally Lipschitz function, and consider the ordinary differential equation

$$x'(t) = f(t, x) \tag{1.3}$$

Denote by $x(t, t_0 x_0)$ the non-continuable solution of the initial value problem $x(t_0) = x_0$ for $t_0 \in J$. A cone K in $\mathbb{R}^n$ is a non-empty, closed subset of $\mathbb{R}^n$ satisfying $K + K \subseteq K$, $\mathbb{R}.K \subseteq K$ and $K \cap (-K) = \{\mathbf{0}\}$. We hereafter assume K nonempty interior in $\mathbb{R}^n$.

Definition 1.3. *We say that (1.3) is monotone, or order-preserving, if whenever $x_0; x_1 \in \mathcal{D}$ satisfy $x_0 \leq x_1$ and the solutions $x(t, t_0, x_0)$ and $x(t, t_0, x_1)$ are defined on $[t_0, t_1]$, $t_1 > t_0$,*
then $x(t, t_0, x_0) \leq x(t, t_0, x_1)$ holds for $t \in [t0, t1]$.
The vector field $f : J \times \mathcal{D} \longrightarrow \mathbb{R}^n$ is said to satisfy the quasimonotone condition in $\mathcal{D}$ if for every $(t, x); (t, y) \in J \times \mathcal{D}$,
we have $(Q) : x \leq y$ and $\phi(x) = \phi(y)$ for some $\phi \in K^*$ implies $\phi(f(t, x)) \leq \phi(f(t; y))$. Where K^* is the dual cone and is the set positive linear functionals, i.e., linear functionals
$\lambda \in (\mathbb{R}^n)^*$, the dual space of $\mathbb{R}^n$, such that $\lambda(K) \geq 0$.

In order words, let us consider an n-dimensional autonomous differential system:

$$\dot{x} = f(x), \tag{1.4}$$

Definition 1.4. *System (1.4) is called monotone if*

$$a \leq b \Rightarrow x(t, a) \leq x(t, b)$$

for all $t \geq 0$

In order words, the flow preserves the partial ordering between the initial condition for all time $t \geq 0$.

Definition 1.5. *(Metzler matrix) A matrix $A \in \mathbb{R}^{n \times m}$ is called Metzler if every off-diagonal entry of A is non-negative.*

The condition: $J(x) := \dfrac{\partial f(x)}{\partial x}$ is Metzler means that for any $i \neq j$, $\dfrac{\partial f_i}{\partial x_j}(x) \geq 0$.
Thus, an increase in x_j yields an increase in $\dot{x}_i = f_i$. The state-variables "cooperate" with one another.

Let us consider the dynamical system (1.4) whose trajectories evolve on a compact set $\mathcal{D}$.

Definition 1.6. *The omega limit set $\omega(x_0)$ of a point $x_0 \in \mathcal{D}$ is the set of points p such that: $x(t_k, x_0) \to p$ for some sequence $t_1, t_2, t_3, ... \to \infty$.*

Lemma 1.3. *Let $x_0 \in \mathcal{D}$. If there exists $\tau > 0$ such that $x(\tau, x_0) \geq x_0$, then $\omega(x_0)$ is a closed orbit with period τ.*

Theorem 1.4. *([58]) Almost every compact trajectory of a monotone system converges to the set of equilibria.*

Theorem 1.5. *([59]) Consider the monotone system (1.4) whose trajectories evolve on a compact set $\mathcal{D}$. If $\mathcal{D}$ contains a single equilibrium point e then $\lim_{t\to\infty} x(t,a) = e$ for all $a \in \mathcal{D}$.*

Theorem 1.6. *([60]) Consider the monotone system (1.4) whose trajectories evolve on a compact set $\mathcal{D}$. If $J(x)$ is tridiagonal and strongly Metzler on $\mathcal{D}$ then $x(t,a)$ converges to an equilibrium for all $a \in \mathcal{D}$.*

1.4.2.1 Cooperative systems

Let $K \subseteq \mathbb{R}^n$ be a closed cone with nonempty interior and denote by $int(K)$ the interior of K in $\mathbb{R}^n$. In what follows, K^* will be used to denote the dual cone of K, i.e.,

$$K^* = \{\lambda \in \mathbb{R}^n; \langle \lambda, x\rangle \geq 0 \ for\ all\ x \in K\}$$

in which $\langle ., .\rangle$ is the standard inner product in $\mathbb{R}^n$.

For $x; y \in \mathbb{R}^n$, we denote

(i) $x \leq_K y$ if and only if $(y - x) \in K$;

(ii) $x <_K y$ if and only if $x \leq_K y$ and $x \neq y$;

(iii) $x \ll_K y$ if and only if $(y - x) \in int(K)$.

We say that $U \subseteq \mathbb{R}^n$ is p-convex if $tx + (1-t)y \in U$ for all $t \in [0; 1]$ whenever $x; y \in U$ and $x \leq_K y$. We need the following key definitions:

Definition 1.7. *[61] Let A be an $n \times n$ matrix.*

- *A is said to be cooperative with respect to K if and only if for any $x \in K$ and any $\lambda \in K^*$ with $\langle \lambda, x\rangle = 0$, we have $\langle \lambda, Ax\rangle \geq 0$.*
- *A is said to be irreducible with respect to K if for any $x \in K \setminus \{int(K) \setminus \{0\}\}$, there exists $\lambda \in K^*$ such that $\langle \lambda, x\rangle = 0$ and $\langle \lambda, Ax\rangle \neq 0$ (necessarily $\lambda \in K^* \setminus \{int(K) \setminus \{0\}\}$).*
- *A is said to be totally cooperative with respect to K if $Ax \in int(K)$ for all $x \in K \setminus \{0\}$.*

Let us consider an n-dimensional autonomous differential system:

$$\dot{x} = f(x), \qquad x(0) = x_0 \tag{1.5}$$

where $f : \mathcal{D} \longrightarrow \mathbb{R}^n$, $\mathcal{D} \in \mathbb{R}^n$ is a given vector function, i.e $f = (f)_i$, with $f_i : \mathbb{R}^n \longrightarrow \mathbb{R}$.
We assume thet f is locally Lipschitz so that local existence and uniqueness of solutions is assured. We will use the following notations. Denote

$$x(x_0, t)$$

the solution of 1.5 initiated in x_0. Further, for $x,\ y\ \in \mathbb{R}^n_+$, we have:

$$x \leq y \Longleftrightarrow x_i \leq y_i,\ \forall\, i \in \{1,2,3,...,n\}.$$

Typically, $\mathcal{D}$ is assumed open to avoid complications. However, for several models, we assume only $\mathcal{D} \subset closure(int(\mathcal{D}))$ and that for some $\delta > 0$ the vector fields defined by $f(t,.),\ t \in [0,\delta)$, are all directed inwards at the points of $\partial\mathcal{D}$. This is enough to ensure that for every $a \in \mathcal{D}$, there exists $T_a > 0$ such that the system (1.5) has a solution $x(t,a)$ on the interval $[0,T_a)$ which satisfies $x(a,0) = a$. We further assume that f is such that the solution initiated at a is unique. We assume that $[0,T_a)$ is the maximal (nonnegative) interval of existence of $x(a,t)$.

Definition 1.8. *System (1.5) is said to be cooperative if for every $i,\ j\ \in \{1,2,...,n\}$, such that $i \neq j$ the function $f_i(x_1,...,x_n)$ is monotone increasing with respect to x_j.*

Theorem 1.7. *If f is differentiable on $\mathcal{D}$, system 1.5 is cooperative if and only if*

$$\frac{\partial f_i}{\partial x_j}(x) \geq 0, \qquad i \neq j, \quad x\ \in \mathcal{D}$$

Theorem 1.8. *Let system (1.5) be cooperative. Then for every $a, b \in \mathcal{D}$*

$$a \leq b \Rightarrow x(a,t) \leq x(b,t), \qquad t \in [0, \min(T_a, T_b)]$$

Theorem 1.9. *If system (1.5) is cooperative and irreducible, then for every $a, b \in \mathcal{D}$*

$$a \leq b \Rightarrow x(a,t) \ll x(b,t), \qquad t \in [0, \min(T_a, T_b)]$$

Theorem 1.10. *Let (1.5) be a cooperative system and let $x(x_0,t)$ be a solution of (1.5) on $[0,T)$. If $y(t)$ is a differentiable function on $[0,T)$ satisfying*

$$\frac{dy}{dt} \leq f(y), \qquad y(0) \leq x_0,$$

then

$$y(t) \leq x(x_0,t), \quad t \in [0,T).$$

Theorem 1.11. *Assume system (1.5) is cooperative and let $a, b \in \mathcal{D}$ such that $f(a) \geq 0\,(f(a) \leq 0)$, then the solution $x(a,t)$ is monotone increasing (decreasing) function of $t \in [0,T_a)$.*

Stability of cooperative systems is given by the following theorem:

Theorem 1.12. *[62] Let $a,\ b \in \mathcal{D}$ such that $a < b$, $[a,b] \subset \mathcal{D}$ and $f(b) \leq 0 \leq f(a)$. Then (1.5) defines a (positive) dynamical system on $[a,b]$. Moreover, if $[a,b]$ contains a unique equilibrium p then p is globally asymptotically stable on $[a,b]$.*

1.4.2.2 Cooperative systems with concave nonlinearities

For autonomous systems, Hirsch [63] showed that for systems that are cooperative and irreducible, almost all (with respect to Lebesgue measure) points whose forward orbits are bounded approach the equilibrium set. His result implies a strong tendency of the solutions oh these systems to converge to an equilibrium if system is cooperative and irreducible. For some particular cooperative systems, a stronger conclusion holds: every bounded solution converges to an equilibrium. This type of cooperative systems is called cooperative systems of differential equations with concave nonlinearities.

Definition 1.9. *[64] Let us consider an n-dimensional autonomous differential system:*

$$\dot{x} = F(t, x), \qquad x \in \mathbb{R}^n \tag{1.6}$$

The system of differential equations (1.6) is called cooperative with concave non-linearities if

(i) $\dfrac{\partial F_i}{\partial x_j} \geq 0,\ i \neq j$ *for each* $(t, x) \in \mathbb{R}_+ \times \mathbb{R}^n_+$.

(ii) $x > y > 0$ *implies* $D_x F(t, y) > D_x F(t, x)$.

A special case of this type of systems is periodic cooperative systems of differential equations with concave nonlinearities. System (1.6) with periodic parameters.
In order to study the stability of equilibria in such systems, let us recall useful theorems (Theorem 3.1 in [65] and Theorem 5.5 in [64]).

Theorem 1.13 (Theorem 3.1 [65])**.** *Let F(t, x) be continuous in* $\mathbb{R} \times \mathbb{R}^n_+$*, T-periodic in t for fixed x. and assume* $D_x F(t, x)$ *exists and is continuous in* $\mathbb{R} \times \mathbb{R}^n_+$*. Assume that if* $x \geq 0$*, with* $x_i = 0$*, then* $F_i(t, x) \geq 0$*,* $1 \leq i \leq n$*,* $t \in \mathbb{R}$*. Assume*

$$(M) \quad \frac{\partial F_i}{\partial x_j} \geq 0,\ i \neq j, (t, x) \in \mathbb{R} \times \mathbb{R}^n_+$$

and

$$D_x F(t, x) \text{ is irreducible for each } (t, x)\, \mathbb{R} \times \mathbb{R}^n_+$$

$$(C) \quad \text{if } 0 < x < y, \text{ then } D_x F(t, x) \geq D_x F(t, y).$$

Then every solution of (1.6) with $x(t_0) \geq 0$ *can be continued to* $[t_0, \infty]$ *with* $x(t) \geq 0$ *for* $t \geq t_0$.

If $F(t, 0) \equiv 0$ *and*

$$z' = D_x F(t, 0) z \tag{1.7}$$

is the variational equation about $x \equiv 0$*, them* $\lim_{t\to\infty} x(t) = 0$ *for every solution of (1.6) with* $x(t_0) \geq 0$ *provided all Floquet multipliers of (1.7) lie inside or on the unit circle in the complex plane. If any*

multiplier of (1.7) lies outside the unit circle, then one of the following holds: (a) every solution $x(t)$ of (1.6) with $x(t_0) \geq 0$ satisfies $\lim_{t\to\infty} x(t) = \infty$, or (b) (1.6) possess a unique non zero T-periodic solution $q(t)$. In the latter case $q(t) > 0$ for all t and $\lim_{t\to\infty} x(t) = q(t)$ for every solution of (1.6) with $x(t_0) > 0$.

If $F(t, 0) \equiv 0$, then exactly one of the alternatives (a) or (b) occurs, except that $x(t_0) > 0$ is replaced by $x(t_0) \geq 0$ above.

In general, the determination of Floquet multipliers is not obvious at all. That is why, we will now consider an additional result [64]: this is an algebraic criterion, related to the study of

$$A(t) = D_x F(t, 0)$$

.

Let $A(t)$ be a $n \times n$ continuous matrix in $\mathbb{R}$ τ-periodic in t, denote

$$\overline{a_{ij}} = \max_{0\leq t\leq\tau} a_{ij}(t), \qquad \underline{a}_{ij} = \min_{0\leq t\leq\tau} a_{ij}(t)$$
$$\overline{A} = (\overline{a_{ij}}), \qquad \underline{A} = (\underline{a}_{ij})$$

Thus

$$\underline{A} \leq A(t) \leq \overline{A}, \quad for \quad 0 \leq t \leq \tau.$$

Let p be a positive real number. In order to study system (1.6), we will use the following theorem:

Theorem 1.14. *([64], Theorem 5.5, page 203) Let $F(t, x)$ be continuous in $\mathbb{R} \times \mathbb{R}^n_+$, T-periodic in t for a fixed x and assume $D_x F(t, x)$ exists and is continuous in $\mathbb{R} \times \mathbb{R}^n_+$ Assume that all solutions are bounded in $\mathbb{R}^n_+$ and $F(t, 0) = 0$. Assume*

- $\dfrac{\partial F_i}{\partial x_j} \geq 0, \qquad (t, x) \in \mathbb{R} \times \mathbb{R}^n_+$
- *and $A(t) = D_x F(t, 0)$ is irreducible for any $t \in \mathbb{R}$.*
- *If $0 < x < y$, then $D_x F(t, x) > D_x F(t, y)$.*

Then

1. *If all principal minors of $-\overline{A}$ are non-negative, then $\lim_{t\to+\infty} x(t) = 0$ for every solution of (1.6) in $\mathbb{R}^n_+$*
2. *If $-\underline{A}$ has at least one negative principal minor, then (1.6) possesses a unique positive T-periodic solution which attracts all initial conditions in $\mathbb{R}^n_+$.*

1.4.2.3 Cooperative delayed systems

The aim of the present subsection is to apply the theory of cooperative systems to differential equations containing delayed arguments. Such equations are often referred to as delay differential equations or functional differential equations. Since delay differential equations contain ordinary differential equations as a special case, when all delays are zero, the treatment is quite similar to the ODE equations. The main difference is that a delay differential equation generally can't be solved backward in time and therefore there is not a well-developed theory of competitive systems with delays. The following results come from [66, 67].

If τ denotes the maximum delay appearing in the equation, then the space $\mathcal{C} := C([-\tau; 0]; \mathbb{R}^n)$ is a natural choice of state space. Given a cone K in $\mathbb{R}^n$, C_K contains the cone of functions which map $[-\tau; 0]$ into K. We identify sufficient conditions on the right hand side of the delay differential equation for the semi flow to be monotone with respect to the ordering induced by this cone. This condition called "quasimonotone condition" reduces to the condition for ordinary differential equations when no delays are present.

A natural space of initial conditions is the space of continuous functions on $[-\tau; 0]$, which we denote by $\mathcal{C}$, where $n = 1$ in this case. $\mathcal{C}$ is a Banach space with the usual uniform norm

$$|\phi| = \sup_{\theta \in [-\tau, 0]} \phi(\theta).$$

If $\phi \in \mathcal{C}$ is given, then it is easy to see that the equation has a unique solution $x(t)$ for $t \geq 0$ satisfying

$$x(\theta) = \phi(\theta), \quad -\tau \leq \theta \leq 0.$$

If the state space is $\mathcal{C}$, then we need to construct from the solution $x(t)$, an element of the space $\mathcal{C}$ to call the state of the system at time t. It should have the property that it uniquely determines $x(s)$ for $s \geq t$. The natural choice is $x_t \in \mathcal{C}$, defined by

$$x_t(\theta) = x(t + \theta); \quad -\tau \leq \theta \leq 0.$$

Then, $x_0 = \phi$ and $x_t(0) = x(t)$.

Let (1.8) be a delay differential system:

$$x'(t) = f(x(t), x(t - \tau)) = f(x, Y), \tag{1.8}$$

where $Y = (x(t - \tau)$.

Following [66], If system (1.8) without delays reduces to a irreducible cooperative system, for the time-delayed system, we can show that f verifies the quasi-monotone condition (QMD), defined as

follows in [66, 67]

$$\phi, \psi \in \mathcal{D}, \phi \leq \psi \text{ and } \phi_i(0) = \psi_i(0) \quad \text{implies} \quad f_i(\phi) \leq f_i(\psi).$$

In fact, it suffices to use Theorem 4.5 ([67], page 308), to show that f is cooperative to deduce that (QMD) holds for f, that is

$$\frac{\partial f_i}{\partial x_j}(x, Y) \geq 0, \quad \text{for } i \neq j, \tag{1.9}$$

$$\frac{\partial f_i}{\partial y_j^k}(x, Y) \geq 0, \quad \text{for all } i, j, k. \tag{1.10}$$

When the quasimonotone is verified, if the initial condition is positive (with at most one zero component), then the solution x is still nonnegative, ie, $x(t) \geq 0$. The quasimonotone condition also ensure the boundedness of the solutions.

When the delayed system satisfies the quasimonotone condition, there is no need to study the stability/instability of the equilibria. Indeed, according to Smith [66] (chapter 5), there is a nice property pointed out about cooperative irreducible time delay systems: the asymptotic stability of each equilibrium is preserved for the delay differential system, whatever the values taken by the delays.

In order to study the stability of delayed systems, we can also apply Theorems 2.2 and 2.3 (Lu [68], page 293). Let (1.11) be the delayed differential system

$$\begin{cases} u'(t) = a_1\, u(t) + b_1\, v(t - d_2), \\ v'(t) = a_2\, v(t) + b_2\, u(t - d_1), \end{cases} \tag{1.11}$$

and $G(s) = \det(I\, s - A - B\, e^{-D\, s})$ its characteristic equation,

where

$$e^{-D\, s} = diag(e^{-d_1\, s}, e^{-d_2\, s}), \quad A = \begin{pmatrix} a_1 & \\ & a_2 \end{pmatrix}, \quad B = \begin{pmatrix} & b_1 \\ b_2 & \end{pmatrix}$$

Theorem 1.15. *If A and B satisfy*

$$R_e(a_1),\, R_e(a_2) < 0, \tag{1.12}$$

$$|b_1\, b_2| < R_e(a_1)\, R_e(a_2) < 0, \tag{1.13}$$

then for any delay $d_1,\, d_2 > 0$, all the roots of equation (1.11) have negative real parts.

1.4.3 Theory of piecewise dynamical systems

There are several different formalisms for dealing with continuous time non smooth systems, including hybrid systems, variational inequalities, complementarity problems, and set valued ordinary

differential equations (ODEs); see, e.g., [14, 60] for reviews. The key notion is that of a differential inclusion [32, 5]. Here we allow the right-hand side of an ODE $\dot{x} = f(x)$ to be not strictly a function, but to be set-valued. For example, such set-valued functions arise in Coulomb dry friction laws encountered in mechanics which model objects in contact that slide with velocity v only if their tangential contact force ft exceeds some critical value. There are critical issues surrounding the well-posedness of such systems, and often the smooth existence and uniqueness results for smooth ODEs (see, e.g., [23]) do not apply.

For example, consider the simple system

$$\dot{x}(t) = \alpha sign(x(t)),$$

where $\alpha \in \mathbb{R}$ is a parameter that can vary and the sign function is multivalued at $x = 0$ with $sign(0) = [-1, 1]$. When $\alpha < 0$ for any value $x(0)$, there is a unique solution to this problem and a unique attractor, a stable equilibrium at $x = 0$. For $\alpha = 0$, however, all points $x \in \mathbb{R}$ are equilibria, and when $\alpha > 0$, $x = 0$ is still an equilibrium, but is no longer stable. In the latter case, the equation has three different solutions with initial condition $x(0) = 0$, showing that uniqueness of solution no longer holds. However, from a different point of view, namely, that of bifurcation theory, this example presents no challenge. Instead of focusing on the ill-posedness of the problem in state space, we think instead of the asymptotic behaviour as we vary the parameter. This is a simple example of a non smooth bifurcation. For $\alpha < 0$ there is a unique attractor, and for $\alpha > 0$ almost all trajectories diverge to infinity. The case $\alpha = 0$ is a pathology; therefore we single this out as a bifurcation point. Because of the intricacy of these well-posedness issues, we shall avoid here the technicalities associated with formulating existence and uniqueness results for the classes of system we study. Nevertheless, when introducing various classes of PWS systems below we shall give references to the appropriate research literature dealing with well-posedness and give some indication of the smoothness of the solutions one should expect.

Definition 1.10. *[69] A piecewise-smooth flow is given by a finite set od ODEs $\dot{x}_i(t) = F_i(x, \mu)$, $x \in S_i$; where $\cup_i S_i = \mathcal{D}$ is a domain, each S_i has a non-empty interior and $\mathcal{D}$ is a domain.*

The intersection $\sum_{ij} := S_i \cap S_j$ is either an $\mathbb{R}^{n-1}$-dimensional manifold included in the boundaries ∂S_j and ∂S_i, or is the empty set. Each vector field F_i is smooth in both state x and parameter μ, and defines a smooth flow $\phi_i(x, t)$ within any open set $U \supseteq S_i$. In particular, each flow ϕ_i is well defined on both side of the boundary ∂S_i.

A non-empty border between two regions $\sum_{ij}$ will be called a discontinuity set, discontinuity boundary, or a switching manifold.

When we have a single discontinuity set $\sum = \sum_{12}$ as in this thesis

$$\dot{x}(t) = \begin{cases} f_1(x,\mu) & if \quad x \in S_1 \\ f_2(x,\mu) & if \quad x \in S_2. \end{cases} \tag{1.14}$$

where $S_1 \cup S_2 = \mathcal{D}$, f_1 generates a flow ϕ_1, f_2 a flow ϕ_2. When $f_1(x) = f_2(x)$ at a point $x \in \sum$, but there is a difference in the Jacobian derivatives $f_{1,x} \neq f_{2,x}$ at x, then the degree of smoothness is said to be 2.

Definition 1.11. *Systems with smoothness of degree* 2 *or higher are called piecewise-smooth continuous systems(PWCS).*

Definition 1.12. *([69], Definition 2.1, p. 638) A discontinuity boundary* $\sum$ *is said to be uniformly discontinuous in some domain* $\mathcal{D}$ *if the degree of smoothness of the vector field across* $\sum$ *is the same throughout* $\mathcal{D}$*. Furthermore, we say that the discontinuity is uniform with degree* $m+1$ *if the first* $m-1$ *derivatives* $f_1 - f_2$ *evaluated on* $\sum$ *are zero.*

When the switching manifold $\sum$ is uniform with degree of smoothness 2, let us consider that the system (1.14) rewritten as follows

$$\dot{x}(t) = \begin{cases} f_1(x,\mu) & if \quad H(x,\mu) > 0 \\ f_2(x,\mu) & if \quad H(x,\mu) < 0 \end{cases} \tag{1.15}$$

where H defines the switching manifold $\sum$ by

$$\sum := \{x \in \mathcal{D} : H(x) = 0\}.$$

For PWCS system (1.15), it is possible to identify different types of equilibria, leading to the following definition.

Definition 1.13. *([69], Definition 2.2, p. 640) We term a point* $x \in \mathcal{D}$ *as a regular equilibrium of (1.15) if* x *is such that either*

$$f_1(x,\mu) = 0 \quad and \quad H(x,\mu) > 0 \quad or \quad f_2(x,\mu) = 0 \quad and \quad H(x,\mu) < 0$$

Alternatively, we say that a point $y \in \mathcal{D}$ *is a virtual equilibrium of (1.15) if either*

$$f_1(y,\mu) = 0 \quad and \quad H(y,\mu) < 0 \quad or \quad f_2(x,\mu) = 0 \quad and \quad H(x,\mu) > 0$$

For standard autonomous continuous system, i.e $\dot{x} = f(x)$ with $f : G^* \longrightarrow \mathbb{R}^n$ continuous, and G^* an open set in $\mathbb{R}^n$, according to well known theory, for any given initial conditions $x_0 \in G^*$, we have existence of a unique solution $u(t, x_0)$. Let also V a compact set in $\mathbb{R}^n$. Then to study the local or global asymptotically stability of equilibria, we consider the following general definitions.

Definition 1.14. *([70], Definition 7.1, p. 32). A compact set $V \subseteq G^*$ is said to be stable, if given a neighbourhood U of V, there is a neighbourhood W of V such that $x \in W$ implies $u(t,x) \in U$ for all $t \geq 0$.*

Definition 1.15. *([70], Definition 7.5, p. 32). A compact set $V \subseteq G^*$ is said to be an attractor if there is a neighbourhood U of V such that $x \in U$ implies $u(t,x) \to V$ as $t \to \infty$. If $u(t,x) \to V$ for each $x \in G*$, V is called a global attractor. If V is both stable and an attractor, V is said to be asymptotically stable. V is said to be globally asymptotically stable if it is stable and a global attractor.*

Definition 1.16. *[71] Let $\dot{x}(t) = f(x(t), x(t-\tau))$ be a delay dynamical system. A simple example of a PWS-DDE composed of two smooth vector fields is*

$$\dot{x}(t) = \begin{cases} f_1(x(t), x(t-\tau)) & if \quad f(x(t), x(t-\tau)) \leq 0 \\ f_2(x(t), x(t-\tau)) & if \quad f(x(t), x(t-\tau)) \geq 0. \end{cases} \tag{1.16}$$

where $x(t) \in \mathbb{R}^n$, and f_1, f_2, f are sufficiently smooth functions. Transitions between the different vector fields occur on the switching surface defined by $f = 0$.

Definition 1.17. *[71] We define a PWS-DDE to be a collection of smooth vector fields*

$$\dot{x}(t) = f_m(x^t) \tag{1.17}$$

indexed by a mode variable $m \in \mathcal{M}$ where $x^t \in C([-\tau, 0], \mathbb{R}^n)$ is the solution segment $x(t+s)$ for $-\tau \leq s \leq 0$ and $\mathcal{M}$ is a finite set. (Equation 1.17 encompasses distributed delays as well as discrete delays; however, we deal here with discrete delays only.) Associated with this is a collection of events $e \in \mathcal{E}$ where $\mathcal{E}$ is a finite set and e consists of a pair $\pi_e = (m_{in}, m_{out})$, a smooth event function $h_e(x^t) : \mathcal{C}([-\tau, 0], \mathbb{R}^n) \longrightarrow \mathbb{R}$ and a smooth jump function $g_e(x^t) : \mathcal{C}([-\tau, 0], \mathbb{R}^n) \longrightarrow \mathcal{C}([-\tau, 0], \mathbb{R}^n)$.

The event function $h_e = 0$ implicitly defines a switching manifold marking the transition point between the (potentially) different vector fields $(f_{m_{in}}, f_{m_{out}})$ and the jump function g_e determines the instantaneous change of state that occurs upon impact with the switching manifold. The minimal state needed to uniquely identify a particular trajectory of the system starting at time t_0 is thus x^{t^0} along with the mode m at time t_0.

A system with a single discontinuity is a system defined as:

$$\dot{x}(t) = \begin{cases} f_1(x(t), x(t-\tau_1), x(t-\tau_2)) & if \quad x \in S_1 \\ f_2(x(t), x(t-\tau_1), x(t-\tau_2)) & if \quad x \in S_2. \end{cases} \tag{1.18}$$

where $S_1 \cup S_2 = \mathcal{D}$, f_1 generates the flow ϕ_1, f_2 generates the flow ϕ_2.

Definition 1.18. *Following [72], the degree of smoothness at a point x_0 in a switching $\sum_{ij}$ set of a piecewise-smooth ODE is the highest order r such the Taylor series expansions of $\varphi(x_0, t)$ and $\varphi_j(x_0, t)$ with respect to t, evaluated at $t = 0$, agree up to terms of $\mathcal{O}(t^{r-1})$. That is, the first non-zero partial derivative with respect to t of the difference $[\varphi_i(x_0, t)\varphi_j(x_0, t)]|t = 0$ is of order r.*

2

Mathematical modelling of the time evolution of *Sahlbergella singularis*: Application to control's improvement

The focus of this chapter is to study the time evolution of cacao mirid *S. singularis*. We will formulate several mathematical models based on the life cycle of *S. singularis* described in Chapter 1. Firstly, we build an ODEs model and derive some theoretical results as well as a sensitivity analysis and some numerical simulations. We consider two cases: the resource pods is available along the year and the case of resource is not available along the year; in this case it is modeled by a periodic function. Then, we derive a model with two taking into account the delays in the maturation processes at the different stages of the life-cycle of the mirid. After a brief study, we provide some numerical simulations and compare with the previous non-delayed model. This chapter has been published at "*Mathematical Methods in the Applied Sciences*

2.1 The ODE model with constant parameters

2.1.1 Formulation of the model

In order to build the models, we recall here what we know about the biology and ecology of Mirids. The life cycle of *S. singularis* is composed of three stages: egg stage, nymph stage and adult stage that develop mainly on pods either on shoots. The eggs are individually inserted into the host plant tissues [14] principally in the cortex of pods and sometimes under the bark of young shoots [18]. The incubation period of eggs is on average 15 days with a minimum of 9 days [45] and a maximum of 21 days [44] before reaching nymph stage. Mirid *S. singularis* has a very long life cycle (eggs to adults). It is on average 40 days with a minimum of 36 days [30] and a maximum of 50 days [11]. The percentage of hatching eggs is globally 96.53% as the eggs are protected in the pods cortex. During

the five nymph instars, the individuals move within a cacao tree by walk to feed on the pods and shoots. The nymphs are able to feed just after the eggs hatching. Twenty five days are needed to complete the nymph development considering 5 days in average per instar [11]. Globally, the total nymph survivorship is around 68% [1]. The average daily rate of survival of the nymphs (considering all the five instars) was estimated around 98.5% (estimated using biological data). At the emergence there is on average one female for 0.71 male [11] (this gives a sex ratio $r = 1/1.71 \approx 0.58$; in fact, sex ratio varies between 0.5 and 0.6). Females *S. singularis* mate with one male 6 to 10 days after their emergence. The first eggs are observed in average 10 days after emergence, so 4 to 8 days after mating (estimated using biological data). Indeed, after this mating period females are considered as mature. On average 72.1% of immature females become mature females [30]. After the emergence, adults (males and females) fly from one cocoa tree to another ensuring the spatial dispersion of the individuals and causing the spatial distribution of the damage in the plots. It is likely the females do not lay all their eggs on the same pod. The average fecundity per female is around 50.7 larvae or 52.5 eggs and the fecundity period lasts on average 16 days [16, 18, 45, 2, 73]. The daily survival of mirids adult is around respectively 98.14% for immature females, 92.8% for mature females and 93% for males (estimated thanks to [2, 44, 45, 11, 16]). On average, 50 to 60 days are needed to obtain a new generation of mirids [11]. This long life period for an insect to grow is a key factor for the dynamic of mirid populations.

Mirids population dynamics varied greatly during the year. Density of population is likely to be influenced by pods availability on the trees and by external conditions like weather [15]. The mirid population is low on cocoa during the period from February to March. From June to July, the populations start to grow more or less rapidly. The peak of the population appears between September and November when the pods are almost mature [11, 50, 2, 3]. It is also assumed that unfavourable climatic conditions (high temperature and low pluviometry) can cause declining fertility of females and increased mortality of individuals [15] that lead to lower mirid populations observed in plantations from November-December to June. We now formulate a model based on the life cycle of *S. singularis*, summarized in Fig. 2.1. We use a stage structured model. We consider three main stages in the development of the mirid: the egg stage (E), the nymph stage (L) (nymphs and pupae) and the adult stage, subdivided into immature female (F_1), mature female (F_2) and male (M). According

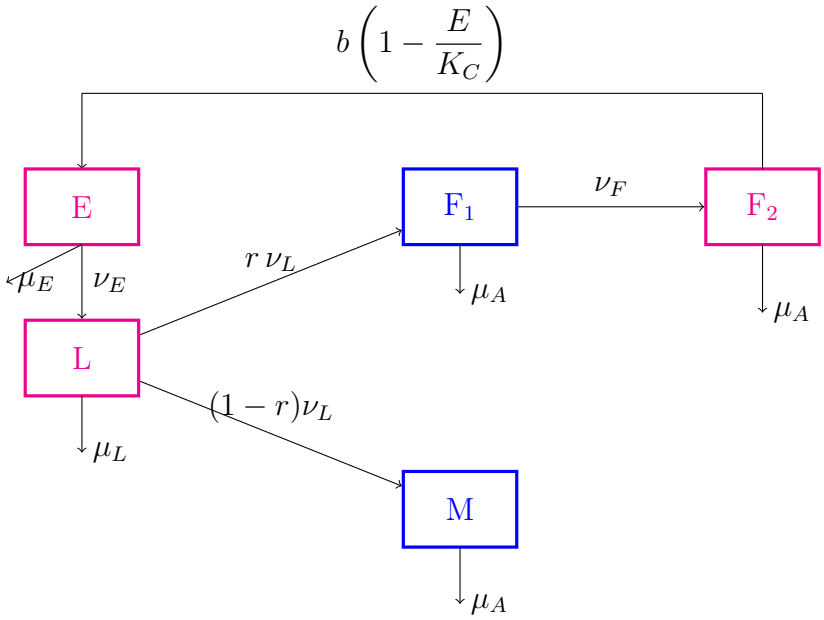

Figure 2.1: Life cycle of *Sahlbergella singularis*

to the flow diagram given in Fig. 2.1, we derive the following ODES model:

$$\begin{cases} \dot{E} = b\,F_2\left(1-\dfrac{E}{K_C}\right) - (\nu_E+\mu_E)\,E, \\ \dot{L} = \nu_E\,E - (\nu_L+\mu_L)\,L, \\ \dot{F_1} = r\,\nu_L\,L - (\nu_F+\mu_A)\,F_1, \\ \dot{F_2} = \nu_F F_1 - \mu_A F_2, \\ \dot{M} = (1-r)\nu_L L - \mu_A M, \end{cases} \tag{2.1}$$

with non-negative initial conditions:

$$\begin{cases} E(0)=E^0, \quad L(0)=L^0, \quad F_1(0)=F_1^0, \\ F_2(0)=F_2^0, \quad M(0)=M^0. \end{cases} \tag{2.2}$$

The biological parameters are described as follows: r is the sex ratio; b is the mean number of eggs laid by an adult female mirid per day that have emerged as nymphs, K_C is the maximal carrying capacity related to the mean daily number of pods per area (ha), μ_E, μ_L and μ_A represents respectively the eggs, nymphs and adults daily mortality rate, ν_E and ν_L are respectively the transition rate from the egg to nymph stage and the nymph to adult stage; $(1/(\nu_E+\mu_E)$ and $(1/(\nu_L+\mu_L)$ are respectively the mean time a mirid stays in the egg and nymph stage (measured in days); ν_F is the transition rate from the immature female stage to mature female stage; $1/(\nu_F+\mu_A)$ is the mean lifespan of an immature female mirid, measured in days.

The non linear term $r\,b\,F_2\left(1-\frac{E}{K_C}\right)$ is related to a specific behaviour of some insects species, like *Aedes* mosquito [74, 75], and also mirids, known as skip-oviposition behaviour. Indeed, according to expert's knowledge, mirids (*S. singularis*) are able to select their breeding sites. Some cocoa trees, particularly suitable for nymph development, show greater damage, which leads to the degradation of the foliage and the formation of orthotropic (or greedy) shoots [1]. Thus, if breeding sites, in a given area, already contain a lot of eggs, then females will not deposit eggs or only very few. That is why, the oviposition rate $r\,b\,F_2$ is limited by the available space in breeding sites, $\left(1-\frac{E}{K_C}\right)$, which implies that the birth rate in the eggs compartment is modelled by the non linear term $r\,b\,F_2\left(1-\frac{E}{K_C}\right)$. Table 2.1, page 43, summarizes the parameters and their biological meaning.

Table 2.1: **Parameters of model (2.1).**

Parameters	Biological significance	Unit
b	Mean number of eggs laid by a mature female	female^{-1}days^{-1}
K_C	Maximal carrying capacity related to the mean daily number of pods per ha	
$1/\nu_L$	Duration of the development of nymphs	days
$1/\nu_F$	Time necessary for an immature female to become mature	days
μ_L	Mortality of nymphs	days^{-1}
μ_A	Mortality of adults	days^{-1}
μ_E	Mortality of eggs	days^{-1}
$1/\nu_E$	Time necessary for an egg to become nymph	days

2.1.2 Study of the ODEs model

Lemma 2.1. *: Assume that the initial conditions of the model system (2.1) satisfy (2.2), then the model system (2.1) has a unique maximal solution* $X=(E,L,F,A,M)$.

Proof:

Model system (2.1) can be written as a Cauchy problem:

$$\dot{X(t)} = F(X(t)) \tag{2.3}$$

where

$$F(X(t)) = \begin{pmatrix} bF_2(t)\left(1 - \dfrac{E(t)}{K_C}\right) - (\nu_E + \mu_E)E(t) \\ \nu_E E(t) - (\nu_L + \mu_L)L(t) \\ r\nu_L L(t) - (\nu_F + \mu_A)F_1(t) \\ \nu_F\, F_1(t) - \mu_A\, F_2(t) \\ (1-r)\nu_L L(t) - \mu_A M(t) \end{pmatrix}$$

$F(X(t))$ is continuously differentiable ($\mathcal{C}^1$). Then, using the Cauchy-Lipschitz theorem, system (2.1) has a unique maximal solution.

□

Lemma 2.2. *: Assume that the initial conditions $L(0) = L^0$, $F_1(0) = F_1^0$, $F_2(0) = F_2^0$ and $M(0) = M^0$ of the model system (2.1) are positive, then all solutions of the model system (2.1) are positive.*

Proof:

Model system (2.1) can be written as follows:

$$\dot{X}(t) = A(X(t))X(t), \tag{2.4}$$

where

$$X(t) = (E(t), L(t), F_1(t), F_2(t), M(t))^T$$

and

$$A(X(t)) = \begin{pmatrix} -\dfrac{bA}{K_C} - (\nu_E + \mu_E) & 0 & 0 & b & 0 \\ \nu_E & -(\nu_L + \mu_L) & 0 & 0 & 0 \\ 0 & r\,\nu_L & -(\nu_F + \mu_A) & 0 & 0 \\ 0 & 0 & \nu_F & -\mu_A & 0 \\ 0 & (1-r)\nu_L & 0 & 0 & -\mu_A \end{pmatrix}$$

Integrating system of differential equation yields

$$\dot{X}(t) = A(X(t))X(t) \Longrightarrow X(t) = X_0 \exp\left(\int_0^t A(X(s))ds\right),$$

where $X_0 = (E^0, L^0, F_1^0, F_2^0, M^0)$ is an initial condition. Thus, if X_0 satisfy (2.2), then for all $t \geq 0$, $X(t) > 0$. We can conclude that all solutions of $L(t)$, $F(t)$ and $M(t)$ with non-negative initial conditions is non-negative, then $X(t) \in \mathbb{R}^4_+$. Consequently, if the initial data are in $\mathbb{R}^5_+$, the solutions stays in $\mathbb{R}^5_+$: $E = 0$, $L = 0$, $F_1 = 0$, $F_2 = 0$ and $M = 0$ are vertical and horizontal null lines respectively. Thus, the trajectories can not cut these axes: so model system (2.1) is biologically well posed.

Theorem 2.1. *The compact*

$$\Omega = \{(E, L, F_1, F_2, M) \in \mathbb{R}^5_+; E(t) \leq K_C,\ L(t) \leq \frac{\nu_E\, K_C}{\nu_L + \mu_L}\ \ F_1(t) \leq \frac{r\,\nu_L\,\nu_E\,K_C}{(\nu_L+\mu_L)(\mu_A+\nu_F)}, \quad (2.5)$$
$$F_2(t) \leq \frac{r\,\nu_L\,\nu_F\,\nu_E\,K_C}{\mu_A(\nu_L+\mu_L)(\nu_F+\mu_A)} \text{ and } M(t) \leq \frac{(1-r)\,\nu_L\,\nu_E\,K_C}{\mu_A(\nu_L+\mu_L)}\}$$

is positively invariant by (2.1).

Proof: Lemma 2.2 shows the positivity of solutions. Let us prove the boundness of the solurions:

- Let us prove that $E(t) \leq K_C$ for al $t \geq t_0$.

  Let us suppose that there exists $\varepsilon > 0$ such that

  $$t_1 \leq t_1 + \varepsilon < T \quad \text{and} \quad E(t_1+\varepsilon) > K_C.$$

  Let us define

  $$t_1^* = \inf\{t \geq t_1,\, L(t) \geq K_C\} \text{ then } E(t_1^*) = K_C.$$

  Thus,

  $$E(t) = E(t_1^*) + \dot{E}(t_1^*)(t-t_1^*) + o(t-t_1^*) \quad \text{and} \quad \dot{E}(t_1^*) = -(\nu_E+\mu_E)E(t_1^*) < 0.$$

  So, there exists $\varepsilon_1 > 0$ such that

  $$t_1^* \leq t < t_1^* + \varepsilon_1 \quad \text{and} \quad E(t_1^*) < K_C.$$

  This is absurd because $t_1^* = \inf\{t \geq t_1,\, E(t) \geq K_C\}$. Consequently, $E(t) \leq K_C$ for all $t \geq t_0$.

- By integrating equations in L, F_1, F_2 and M separately, we find the born of each popuation. Consequently, solutions of our model are bounded and Ω is positively invariant for the model.

□

Now, we will derive some quantitative analysis of system (2.1).

Proposition 2.1. *Model (2.1) always has a trivial equilibrium* $X_0 = (0,0,0,0,0)$ *and the basic offspring number is given by:*

$$\mathcal{N}_0 = \frac{r\,b\,\nu_L\,\nu_F\,\nu_E}{\mu_A(\nu_E+\mu_E)(\nu_F+\mu_A)(\nu_L+\mu_L)}. \quad (2.6)$$

$\mathcal{N}_0$ *represents the mean number of adults female produced by one adult female over its lifespan. It is sometimes called the basic offspring number.*

Proof:

The jacobian is given by:

$$J(X) = \begin{pmatrix} -(\nu_E + \mu_E) - \dfrac{b\,F_2}{K_C} & 0 & 0 & b\left(1 - \dfrac{E}{K_C}\right) & 0 \\ \nu_E & -(\nu_L + \mu_L) & 0 & 0 & 0 \\ 0 & r\,\nu_L & -(\nu_F + \mu_A) & 0 & 0 \\ 0 & 0 & \nu_F & -\mu_A & 0 \\ 0 & (1-r)\,\nu_L & 0 & 0 & -\mu_A \end{pmatrix}. \tag{2.7}$$

Around the trivial equilibrium $X_0 = (0,0,0,0,0)^T$, one has

$$J(X_0) = \begin{pmatrix} -(\nu_E + \mu_E) & 0 & 0 & b & 0 \\ \nu_E & -(\nu_L + \mu_L) & 0 & 0 & 0 \\ 0 & r\,\nu_L & -(\nu_F + \mu_A) & 0 & 0 \\ 0 & 0 & \nu_F & -\mu_A & 0 \\ 0 & (1-r)\,\nu_L & 0 & 0 & -\mu_A \end{pmatrix}.$$

$J(X_0)$ is a Metzler matrix and can be written as a following block matrix:

$$J(X_0) = \begin{pmatrix} A & B \\ C & D \end{pmatrix},$$

where

$$A = \begin{pmatrix} -(\nu_E + \mu_E) & 0 & 0 \\ \nu_E & -(\nu_L + \mu_L) & 0 \\ 0 & r\nu_L & -(\nu_F + \mu_A) \end{pmatrix}, \quad B = \begin{pmatrix} b & 0 \\ 0 & 0 \\ 0 & 0 \end{pmatrix},$$

$$C = \begin{pmatrix} 0 & 0 & \nu_F \\ 0 & (1-r)\nu_L & 0 \end{pmatrix} \quad et \quad D = \begin{pmatrix} -\mu_A & 0 \\ 0 & -\mu_A \end{pmatrix}.$$

Matrix $J(X_0)$ is Metzler stable if and only if matrix A and $D - CA^{-1}B$ are Metzler stable [76].

Matrix A has three negative eigenvalues: $-(\nu_E + \mu_E)$, $-(\nu_L + \mu_L)$ and $-(\nu_F + \mu_A)$. So A is Metzler stable.

Now, we prove that matrix $D - CA^{-1}B$ is Metzler stable. A simple calculation gives

$$A^{-1} = \frac{1}{\det(A)} \begin{pmatrix} (\nu_L + \mu_L)(\nu_F + \mu_A) & 0 & 0 \\ -\nu_E(\nu_F + \mu_A) & (\nu_E + \mu_E)(\nu_F + \mu_A) & \\ r\nu_E\nu_L & -r\nu_L(\nu_E + \mu_E) & (\nu_E + \mu_E)(\nu_F + \mu_A) \end{pmatrix}.$$

where

$$\det(A) = -(\nu_E + \mu_E)(\nu_L + \mu_L)(\nu_F + \mu_A)$$

This leads to

$$CA^{-1}B = \frac{1}{\det(A)} \begin{pmatrix} r\,b\,\nu_E\,\nu_F\,\nu_L & 0 \\ (1-r)\,b\,\nu_E\,(\nu_F+\mu_A) & 0 \end{pmatrix},$$

then

$$D - CA^{-1}B = \begin{pmatrix} -\mu_A + \dfrac{r\,b\,\nu_E\,\nu_L\,\nu_F}{(\nu_E+\mu_E)(\nu_L+\mu_L)(\nu_F+\mu_A)} & 0 \\ \dfrac{(1-r)\,b\,\nu_E\,(\nu_F+\mu_A)}{(\nu_E+\mu_E)(\nu_L+\mu_L)(\nu_F+\mu_A)} & -\mu_A \end{pmatrix}.$$

Matrix $D - CA^{-1}B$ is Metzler stable if and only if

$$\frac{r\,b\,\nu_E\,\nu_L\,\nu_F}{\mu_A\,(\nu_E+\mu_E)\,(\nu_L+\mu_L)\,(\nu_F+\mu_A)} \leq 1.$$

The basic offspring number is

$$\mathcal{N}_0 = \frac{r\,b\,\nu_E\,\nu_L\,\nu_F}{\mu_A\,(\nu_E+\mu_E)\,(\nu_L+\mu_L)\,(\nu_F+\mu_A)}.$$

□

Lemma 2.3. *System (2.1) has two possible equilibria:*

(i) a trivial equilibrium $X^0 = (0,0,0,0,0)$ which always exists and is an asymptotic equilibrium for the system.

(ii) a positive equilibrium $X^* = (E^*, L^*, F_1^*, F_2^*, M^*)$, defined as follows:

$$E^* = \frac{(\mathcal{N}_0 - 1)}{\mathcal{N}_0} K_C,\ L^* = \frac{\nu_E}{\nu_L+\mu_L} E^*,\ F_1^* = \frac{r\,\nu_E\,\nu_L}{(\nu_L+\mu_L)(\nu_F+\mu_A)} E^*, \tag{2.8}$$
$$F_2^* = \frac{r\,\nu_E\,\nu_L\,\nu_F}{\mu_A(\nu_L+\mu_L)(\nu_F+\mu_A)} E^* \text{ and } M^* = \frac{(1-r)\,\nu_E\,\nu_L}{\mu_A(\nu_L+\mu_L)} E^*.$$

which exists when $\mathcal{N}_0 > 1$.

Proof Setting the fifth equations of model (2.1) equal to zero, we find equilibria define in (2.8).

□

System (2.1) is a cooperative system [66]. Then, the dynamic of system (2.1) is summarized in the following theorem:

Theorem 2.2. *Assume that $(E^0, L^0, F_1^0, F_2^0, M^0) \in \Omega$.*

(i) When $\mathcal{N}_0 \leq 1$, the trivial equilibrium X^0 is globally asymptotically stable, which means that the mirid population will dwindle until extinction, whatever the initial population.

(ii) When $\mathcal{N}_0 > 1$, the trivial equilibrium X^0 is unstable, and the positive equilibrium X^* is globally asymptotically stable, which means that the mirid population persists.

Proof: It suffices to verify the assumptions of theorem 1.12.

(i) When $\mathcal{N}_0 \leq 1$, model system (2.1) has only the trivial equilibrium X^0. By taking $a = 0$ and

$$b = \left(K_C, \frac{2\nu_E\, K_C}{\nu_L + \mu_L}, \frac{3\, r\, \nu_L\, \nu_E\, K_C}{(\nu_L + \mu_L)(\nu_F + \mu_A)}, \frac{4\, r\, \nu_E\, \nu_L\, \nu_F\, K_C}{\mu_A(\nu_L + \mu_L)(\nu_F + \mu_A)}, \frac{2\,(1-r)\,\nu_E\,\nu_L\, K_C}{\mu_A(\nu_L + \mu_L)} \right),$$

we have $f(a) = 0$ and $f(b) \leq 0$. Thus, according to Theorem 1.12, the trivial equilibrium X^0 is globally asymptotically stable on $[0, b]$, hence on Ω when $\mathcal{N}_0 \leq 1$.

(ii) When $\mathcal{N}_0 > 1$, there exists $\varepsilon > 0$ such that $\mathcal{N}_0 > 1 + \varepsilon$. Let E_ε sufficiently small such that

$$E_\varepsilon \leq \varepsilon, \quad L_\varepsilon = \frac{\nu_E(1+\varepsilon)}{(\nu_L + \mu_L)\,\mathcal{N}_0}\, E_\varepsilon, \quad F_{1\varepsilon} = \frac{r\,\nu_L\,(1+\varepsilon)}{(\nu_F + \mu_A)\mathcal{N}_0}\, L_\varepsilon,$$
$$F_{2\varepsilon} = \frac{(\nu_E + \mu_E)\,(1+\varepsilon)^2}{b\mathcal{N}_0^2}\, E_\varepsilon, \quad M_\varepsilon = \frac{(1-r)\,\nu_L\,(1+\varepsilon)}{\mu_A\,\mathcal{N}_0}\, L_\varepsilon$$

Let $b_\varepsilon = (E_\varepsilon, L_\varepsilon, F_{1\varepsilon}, F_{2\varepsilon}, M_\varepsilon)$. Then, from the right-hand side of (2.1) and the fact that $\mathcal{N}_0 > 1 + \varepsilon$ and $K_C \gg 1$, we deduce:

$$f(b_\varepsilon) \geq \begin{pmatrix} \varepsilon\,(\nu_E + \mu_E)(1+\varepsilon)^2 \left(1 - \dfrac{1+\varepsilon}{K_C}\right) E_\varepsilon \\ \nu_E \left(1 - \dfrac{1+\varepsilon}{\mathcal{N}_0}\right) E_\varepsilon \\ r\,\nu_L \left(1 - \dfrac{1+\varepsilon}{\mathcal{N}_0}\right) L_\varepsilon \\ \nu_F \left(1 - \dfrac{1+\varepsilon}{\mathcal{N}_0}\right) F_{1\varepsilon} \\ (1-r)\,\nu_L \left(1 - \dfrac{1+\varepsilon}{\mathcal{N}_0}\right) L_\varepsilon \end{pmatrix} > 0.$$

Hence, according to Theorem 1.12, equilibrium X^* is globally asymptotically stable on $[b_\varepsilon, b]$. Since b_ε can be selected to be smaller than any $x > 0$, we have that X^* is asymptotically stable on Ω with basin of attraction $\tilde{\Omega} = \Omega \setminus \{(0,0,0,0,0)\}$. This also implies that X^0 is unstable.

□

2.1.3 Sensitivity analysis

It is important to know the relative importance of some factors that maintain or not a mirid population. We may estimate the sensitivity index of $\mathcal{N}_0$ with respect to a parameter p, as follows:

$$\gamma_p^{\mathcal{N}_0} = \frac{\partial \mathcal{N}_0}{\partial p}.\frac{p}{\mathcal{N}_0} \tag{2.9}$$

Straightforward calculation leads to the following result:

$$\begin{aligned}
&\gamma_r^{\mathcal{N}_0} = \gamma_b^{\mathcal{N}_0} = 1, \quad \gamma_{\nu_E}^{\mathcal{N}_0} = \frac{\mu_E}{\nu_E(\nu_E+\mu_E)},\\
&\gamma_{\nu_L}^{\mathcal{N}_0} = \frac{\mu_L}{\nu_L(\nu_L+\mu_L)}, \quad \gamma_{\nu_F}^{\mathcal{N}_0} = \frac{\mu_F}{\nu_F(\nu_F+\mu_A)},\\
&\gamma_{\mu_E}^{\mathcal{N}_0} = -\frac{1}{\nu_E+\mu_E}, \quad \gamma_{\mu_L}^{\mathcal{N}_0} = -\frac{1}{\nu_L+\mu_L}, \quad \gamma_{\mu_A}^{\mathcal{N}_0} = -\frac{\nu_F}{\mu_A(\nu_F+\mu_A)}
\end{aligned}$$

Clearly, r and b have the strongest impact on $\mathcal{N}_0$. However, this gives us only partial informations. In particular, we will now focus on the variables E, L, F_1, F_2 and M. That is why, we derive some global sensitivity analysis using two well-known methods: the eFast and the LHS-PRCC methods. The eFast method given in Fig.2.2, page 50, highlights first-order effects (main effects) and total effects (main and all interaction effects) of the parameters on the Model Outputs. Complementary to the eFast method, we derived a LHS-PRCC sensitivity analysis given in Fig.2.3, page 51. LHS-PRCC stands for Latin Hypercube Sampling and PRCC for Partial rank correlation coefficient. These two methods give complementary information. Indeed the PRCC method provides mainly information about how the outputs is impacted if we increase (or decrease) the inputs of a specific parameter while the eFast indicates which parameter uncertainty has the greatest impact on the output variability (see for instance [77] for further explanations). In Table 2.2, page 51, we provide ranges of values for the model parameters. These ranges were estimated based on the Data obtained by Babin and collaborators.

As expected, variation of the carrying capacity K_C has strong an impact on all variables, and also μ_A. For the transition rates ν_L, ν_E, ν_F, and the mortality rate μ_L, their impact is weaker, but according to the LHS-PRCC analysis, is not negligible. Thus obviously, among all parameters, the parameters K_C, μ_A, ν_L, ν_E, ν_F, and μ_L are the most important parameters to estimate. Finally, according to the sensitivity analysis method that is considered b does not have the same impact. However, we think that this is an important parameter too.

2.1.4 Mirid system with periodic coefficients

In this section, we consider the previous model, but with periodic time-dependent parameters, since we know that most of the parameters may depend on the environment. In fact, mirids dynamics

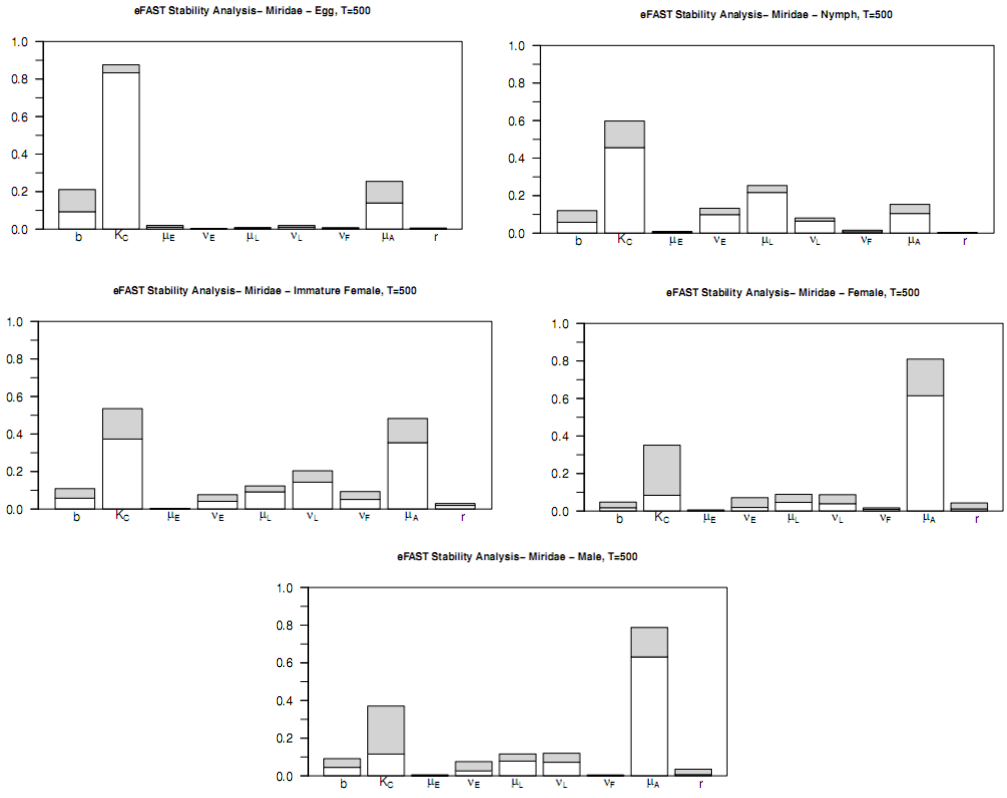

Figure 2.2: e-FAST Sensitivity analysis at $T = 500$. White bar:first-order effects; Sum of white and grey bars: total effect.

Table 2.2: Range of values for the parameters of system (2.1).

Parameters	Range	Source
r	$[0.5, 0.6]$	estimated
b	$[1.5; 4]$	estimated
K_C	$[1, 10000]$	estimated
ν_L	$[1/35, 1/10]$	estimated
ν_F	$[1/10, 1/6]$	estimated
μ_L	$[1/100, 1/10]$	estimated
μ_A	$[1/100, 1/10]$	estimated
μ_E	$[1/100, 1/10]$	estimated
ν_E	$[1/10, 1/20]$	estimated

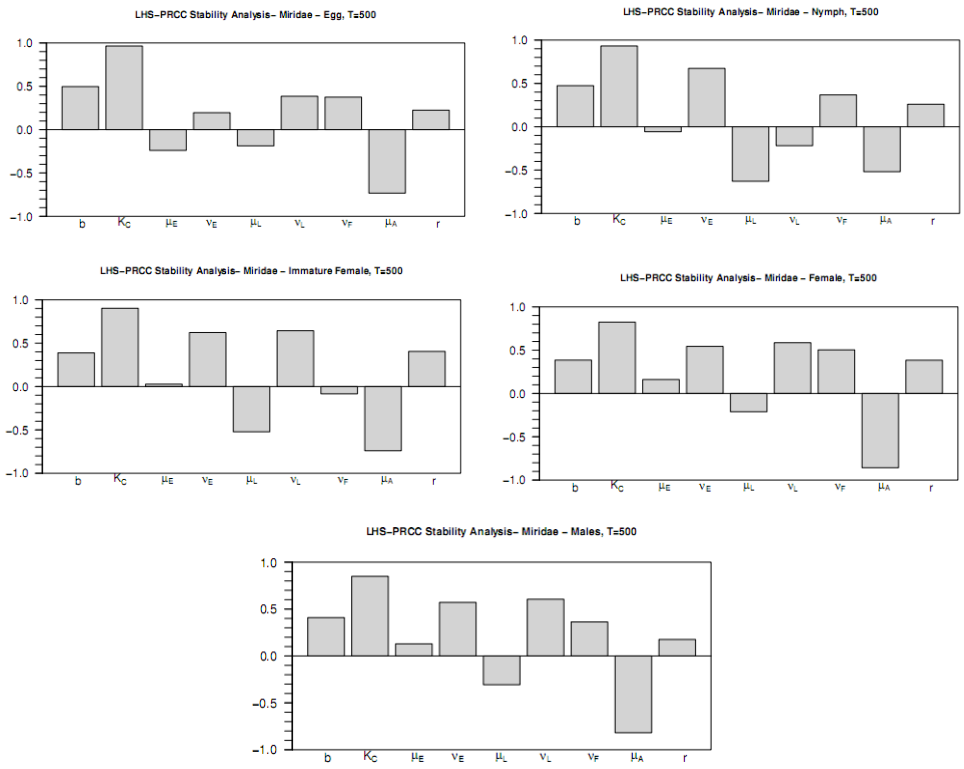

Figure 2.3: LHS-PRCC Sensitivity analysis at $T = 500$.

vary greatly during the year; density of populations is likely to be influenced by pods avail ability on the trees. In [30], it is admitted that lower mirid populations observed in the plots during a certain period of the year is due to the declining fertility of females and increasing mortality of individuals. Thus it seems that development parameters (longevity, fecundity, mortality) of mirids vary depending

on season.

We assume that all those parameters are T-periodic functions and are bounded: below, by a non negative minimal value, and above by a positive maximal value, that is $p_{min} \leq p(t) \leq p_{max}$ for all $t \geq 0$, and $p = r$, b, μ_L, μ_A, μ_E, ν_L, ν_F, ν_E or K_C. We also split the carrying capacity in two parts, $K_C(t) + C$: $K_C(t)$, the mean number of pods available for breeding, and C, the alternative breeding sites including other tree hosts, like *Cola nitida, Ceiba pentandra* [1]. Thus, Model (2.1) becomes

$$\begin{cases} \dot{E} = b(t)\, F_2 \left(1 - \dfrac{E}{C + K_C(t)}\right) - (\nu_E(t) + \mu_E(t))\, E, \\ \dot{L} = \nu_E(t)\, E - (\nu_L(t) + \mu_L(t))\, L, \\ \dot{F}_1 = r(t)\, \nu_L(t)\, L - (\nu_F(t) + \mu_A(t))\, F_1, \\ \dot{F}_2 = \nu_F(t)\, F_1 - \mu_A(t) F_2, \\ E(0) = E^0, \quad L(0) = L^0, \quad F_1(0) = F_1^0, \quad F_2(0) = F_2^0 \end{cases} \tag{2.10}$$

System (2.10) enters the family of periodic concave cooperative system with a concave non-linearity ([64],[65]). In fact:

We will use a theorem 1.14 (see Chapter 1) proved in [65]. We have:

$$F(t,x) = \begin{pmatrix} b(t)\, F_2 \left(1 - \dfrac{E}{C + K_C(t)}\right) - (\nu_E(t) + \mu_E(t))\, E \\ \nu_E(t)\, E - (\nu_L(t) + \mu_L(t))\, L \\ r(t)\, \nu_L(t)\, L - (\nu_F(t) + \mu_A(t))\, F_1 \\ \nu_F(t)\, F_1 - \mu_A(t) F_2 \end{pmatrix},$$

where $x = (E, L, F_1, F_2)^T$. Obviously, F is continuously differentiable and T-periodic. According to Cauchy-Lipschitz theorem, we have existence of a positive and bounded solution. Since all time-dependent parameters are positive, we verify easily property (i) in Definition 1.9.

Let us compute the Jacobian

$$D_x F(t,x) = \begin{pmatrix} a & 0 & 0 & b(t)\left(1 - \dfrac{E}{K_C(t) + C}\right) \\ \nu_E(t) & -(\nu_L(t) + \mu_L(t)) & 0 & 0 \\ 0 & r(t)\nu_L(t) & -(\nu_F(t) + \mu_A(t)) & 0 \\ 0 & 0 & \nu_F(t) & -\mu_A(t) \end{pmatrix}$$

with

$$a = -\left(\nu_E(t) + \mu_E(t) + \frac{b(t) F_2}{K_C(t) + C}\right)$$

It is straightforward to verify (ii) in Definition 1.9. In addition, $D_x F(t,x)$ is irreducible for each $(t,x) \in \mathbb{R} \times \mathbb{R}^n_+$. Thus, Theorem 1.13 applies to system (**??**) and we deduce that every solution x,

with $x(t_0) \geq 0$, can be continued in $[t_0, \infty]$ with $x(t) \geq 0$ for $t \geq t_0$.

Now, let us compute $D_x F(t,0)$, that is

$$D_x F(t,0) = \begin{pmatrix} -(\nu_E(t) + \mu_E(t)) & 0 & 0 & b(t) \\ \nu_E(t) & -(\nu_L(t) + \mu_L(t) & 0 & 0 \\ 0 & r(t)\nu_L(t) & -(\nu_F(t) + \mu_A(t)) & 0 \\ 0 & 0 & \nu_F(t) & -\mu_A(t) \end{pmatrix}$$

According to Theorem 1.13, if the Floquet multipliers of $D_x F(t,0)$ lie inside or on the unit circle, then $\lim_{t\to\infty} x(t) = 0$. In contrary, if any Floquet multiplier lies outside the unit circle, and according to the fact that $F(t,0) \equiv 0$ and x is a bounded solution, we deduce that system (**??**) has a unique non-zero T-periodic solution $x_{per}(t)$.

In general, the determination of Floquet multipliers is extremely difficult. That is why, we will now consider an additional result [64] recalled in Appendix B (see Theorem 1.14). This is an algebraic criterion, related to the study of $A(t) = D_x F(t,0)$.

Let us estimate $\underline{\mathrm{A}}$ and $\overline{A}$, lower and upper bounds of Matrix $A(t)$. Using the fact that all time-dependent parameters have positive lower and upper bounds, we deduce

$$\underline{\mathrm{A}} = \begin{pmatrix} -(\nu_{E,max} + \mu_{E,max}) & 0 & 0 & b_{min} \\ \nu_{E,min} & -(\nu_{L,max} + \mu_{L,max}) & 0 & 0 \\ 0 & r_{min}\nu_{L,min} & -(\nu_{F,max} + \mu_{A,max}) & 0 \\ 0 & 0 & \nu_{F,min} & -\mu_{A,max} \end{pmatrix}$$

and

$$\overline{A} = \begin{pmatrix} -(\nu_{E,min} + \mu_{E,min}) & 0 & 0 & b_{max} \\ \nu_{E,max} & (\nu_{E,min} + \mu_{E,min}) & 0 & 0 \\ 0 & r_{max}\nu_{L,max} & -(\nu_{F,min} + \mu_{A,min}) & 0 \\ 0 & 0 & \nu_{F,max} & -\mu_{A,min} \end{pmatrix}.$$

Then according to Theorem 1.14, we have to study the principal minors of $-\underline{\mathrm{A}}$ and $-\overline{A}$. All diagonal terms of $-\underline{\mathrm{A}}$ and $-\overline{A}$ are positive. In fact it suffices to compute $\det(-\overline{A})$ and $\det(-\underline{\mathrm{A}})$, that is

$$\begin{aligned} \det(-\overline{A}) = &-(\nu_{E,min} + \mu_{E,min})(\nu_{L,min} + \mu_{L,min})(\nu_{F,min} + \mu_{A,min})\mu_{A,min} \\ &+ b_{max} r_{max} \nu_{E,max} \nu_{L,max} \nu_{F,max}, \end{aligned}$$

$$\begin{aligned} \det(-\underline{\mathrm{A}}) = &(\nu_{E,max} + \mu_{E,max})(\nu_{L,max} + \mu_{L,max})(\nu_{F,max} + \mu_{A,max})\mu_{A,max} \\ &- b_{min} r_{min} \nu_{L,min} \nu_{F,min}. \end{aligned}$$

Thus $\det(-\overline{A}) \geq 0$ if

$$b_{max} r_{max} \nu_{L,max} \nu_{F,max} \geq (\nu_{E,min} + \mu_{E,min})\,(\nu_{L,min} + \mu_{L,min})(\nu_{F,min} + \mu_{A,min})\mu_{A,min},$$

and $\det(-\underline{A}) < 0$ if

$$(\nu_{E,max} + \mu_{E,max})\,(\nu_{L,max} + \mu_{L,max})(\nu_{F,max} + \mu_{A,max})\mu_{A,max} < b_{min} r_{min} \nu_{L,min} \nu_{F,min}.$$

In fact, the previous results are related to the time dependent basic offspring number

$$\mathcal{N}_0(t) = \frac{r\, b(t)\nu_E(t)\nu_L(t)\nu_F(t)}{\mu_A(t)(\nu_E(t) + \mu_E(t))\,(\nu_F(t) + \mu_A(t))\,(\nu_L(t) + \mu_L(t))},$$

such that $\mathcal{N}_{0,min} \leq \mathcal{N}_0(t) \leq \mathcal{N}_{0,max}$, where

$$\mathcal{N}_{0,min} = \frac{r_{min}\, b_{min} \nu_{E,min} \nu_{L,min} \nu_{F,min}}{(\nu_{E,max} + \mu_{E,max})\,(\nu_{max} + \mu_{max})\,(\nu_{F,max} + \mu_{A,max})\mu_{A,max}},$$

and

$$\mathcal{N}_{0,max} = \frac{r_{max}\, b_{max}\, \nu_{E,max} \nu_{L,max} \nu_{F,max}}{(\nu_{E,min} + \mu_{E,min})\,(\nu_{min} + \mu_{min})\,(\nu_{F,min} + \mu_{A,min})\mu_{A,min}}.$$

According to Theorem 1.14, we deduce

Theorem 2.3. *:*

(i) If $\mathcal{N}_{0,max} \leq 1$, then the solution of system (2.10) converges to the trivial equilibrium X^0.

(ii) If $\mathcal{N}_{0,min} > 1$, then system (2.10) admits a unique periodic solution that attracts all initial condition in Ω.

According to the sensitivity analysis, an interesting and particular case is when we assume that all parameters are constant, except K_C. Then $\overline{A} = \underline{A}$, and thus $\mathcal{N}_{0,max} = \mathcal{N}_{0,min} = \mathcal{N}_0$. Thus, theorem 2.3 reduces to

Theorem 2.4. *(i) If $\mathcal{N}_0 \leq 1$, then the solution of system (2.10) converges to the trivial equilibrium X^0.*

(ii) If $\mathcal{N}_0 > 1$, then system (2.10) admits a unique periodic solution which attracts all initial condition in Ω.

In fact, we recover the same results than for the constant parameters problem, except that the constant positive equilibrium is now periodic of period T.

It is important to notice that K_C constant is relevant in the case where the cocoa production is almost constant along the year. This is realistic in Central America where there is no real seasonality. By contrast, in Cameroon, they are two rainy season: a long one, and a short one. There the seasonality is clearly marked, which has an impact on cacao production. That is why we consider a periodic function for K_C.

Numerical simulation

Now, we will illustrate our theoretical results. We will use the values of the monthly mean number of pods using data extrapolated, obtained in Cameroon, from [73] to construct our periodic function $K_C(t)$. According to the data from [73] and the knowledge about the mean number of pods over the year, our daily estimated data are recapitulated in Table 2.3.

Table 2.3: **Mean number of pods per days**

Months	June	July	August	September	October	November	
$K_C(t)$	0	$\frac{32000}{31}$	$\frac{160000}{31}$	$\frac{416000}{30}$	$\frac{544000}{31}$	$\frac{304000}{31}$	
Months	December	January	February	March	April	May	June
$K_C(t)$	$\frac{416000}{31}$	$\frac{120000}{31}$	$\frac{8000}{28}$	0	0	0	0

We suppose that the function $K_C(t)$ is periodic, of period $T = 365$ days. We use the cubic spline interpolation to derive the time evolution of $K_C(t)$ along a year. Using cubic Hermite spline, we obtain a polynomial interpolation (Daily estimation of $K_C(t)$) given in Fig. 2.4, page 56. Figure 2.4, page 56 represents the daily estimation of pods number in the plot. $K_C(t)$.

When the parameter K_C is constant, we used a classical scheme already well implemented under Matlab (ode23s) for numerical simulations and we consider that the number of pods K_C is constant, we evaluate the average daily value estimated with the data of Table 2.3, that is

$$\overline{K}_C = \frac{1}{365}\int_1^{365} K_C(t)dt.$$

.

When K_C is periodic, following [62], we consider a nonstandard numerical scheme to preserve most of the qualitative properties of the continuous model, like positivity, equilibria, stability and instability whatever the time step $\Delta t > 0$. We consider the values of parameters given in Table 2.4.

In Cameroon, cacao is not cultivated alone. Cacaoculture is doing in agroforests which are systems of culture in which main culture (cacao) is associated with many other cultures. These culture constitute alternative resource for mirids in the absence of pods. Since in our models, we consider that the resource are the pods, alternative resource may always be the other parts of the tree: it is

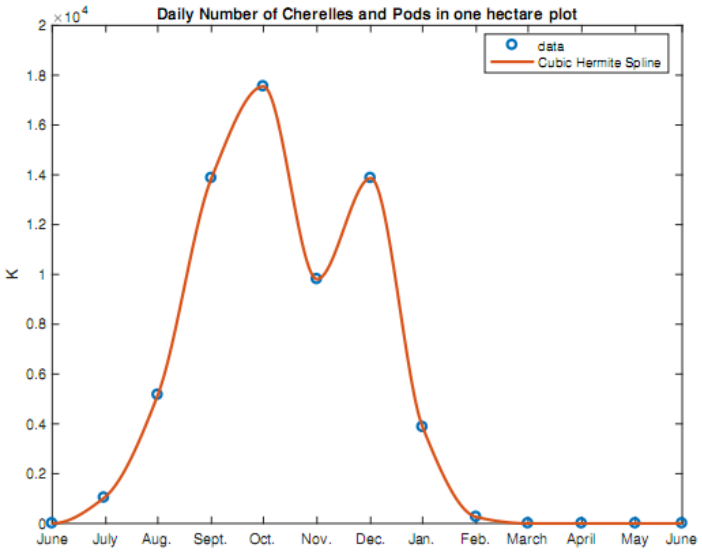

Figure 2.4: Daily estimation of $K_C(t)$ along a year

represented by the parameter C. We illustrate our numerical simulations for two values of C: $C = 5$ (alternative resource is not important) and $C = 100$ (alternative resource is important). All the given values have been estimated thanks to [2, 44, 45, 11, 16].

Table 2.4: Values of constant parameters

Parameters	Case $\mathcal{N}_0 < 1$	Case $\mathcal{N}_0 > 1$	Source
r	0.58	0.58	[11]
b	3.28	3.28	Estimated
ν_E	1/15	1/15	Estimated
ν_L	1/25	1/25	Estimated
ν_F	1/10	1/10	Estimated
μ_E	0.05	0.001	Estimated
μ_L	0.15	0.03	Estimated
μ_A	0.15	0.07	Estimated
$\mathcal{N}_0$	**0.6103**	**9.0002**	**Equation (2.6)**

Using Matlab, we have done numerical simulations in order to validate theoretical results obtained. In Fig. 2.5, page 57, we illustrate the theoretical results when the carrying capacity K_C is constant, that is $\overline{K}_C = 5482$, with initial conditions $(E, L, F_1, F_2, M) = (0, 0, 0, 10, 10)$. As expected, when

$\mathcal{N}_0 < 1$, the population decays till extinction, while, when $\mathcal{N}_0 > 1$, the population reaches rapidly the positive equilibrium. However, in Cameroon, having a constant number of pods along the year is not realistic. That's why in the next simulations, we consider a more realistic case, with the same parameters values.

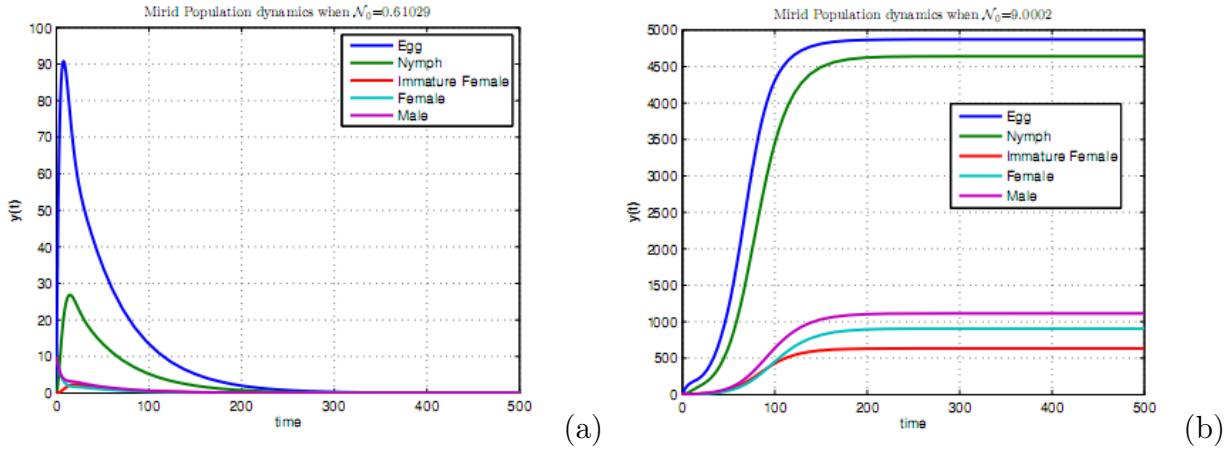

(a) (b)

Figure 2.5: Time Evolution of mirid population when $K_C = 5482$; (a)$\mathcal{N}_0 < 1$; (b)$\mathcal{N}_0 > 1$.

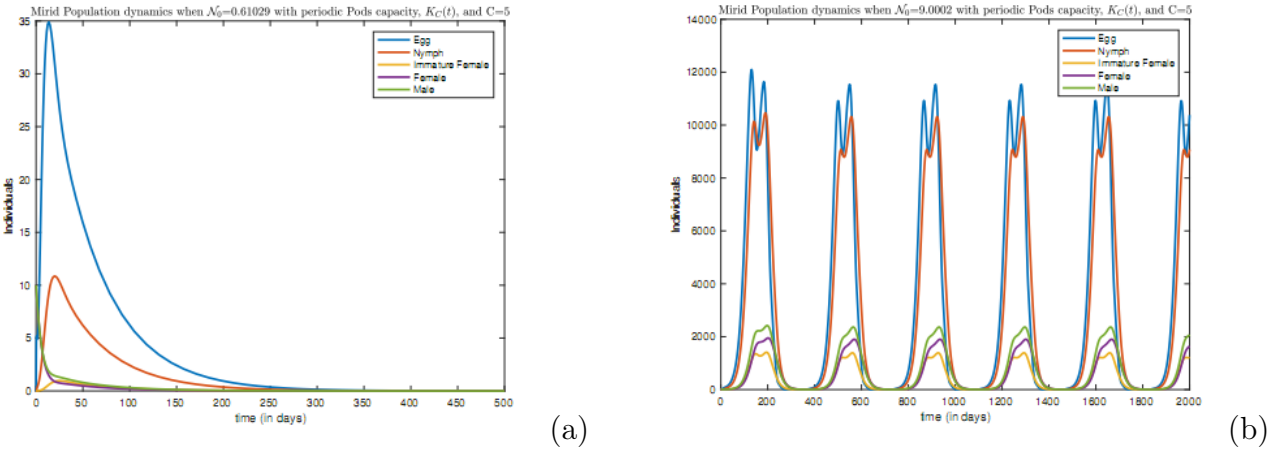

(a) (b)

Figure 2.6: Time Evolution of mirid population when K_C is periodic and $C = 5$; (a) $\mathcal{N}_0 < 1$; (b) $\mathcal{N}_0 > 1$.

In Figs. 2.6 and 2.7, page 57, we illustrate the previous results when the carrying capacity K_C is periodic and alternative resource is $C = 100$. In the case where $\mathcal{N}_0 > 1$, the dynamic of mirids follows the dynamic of pods, as expected. However, the size of the population seems to be large. More alternative resource is important, more the size of the populations seems to be large. A way to control mirid's population may be to reduce alternative resource in the plots. However, it is not realistic since agroforestery favour the culture of many things in the same plot at the same time.

In the continuation of our work, we will build a new mathematical model in order to have a better dynamic of mirid's population.

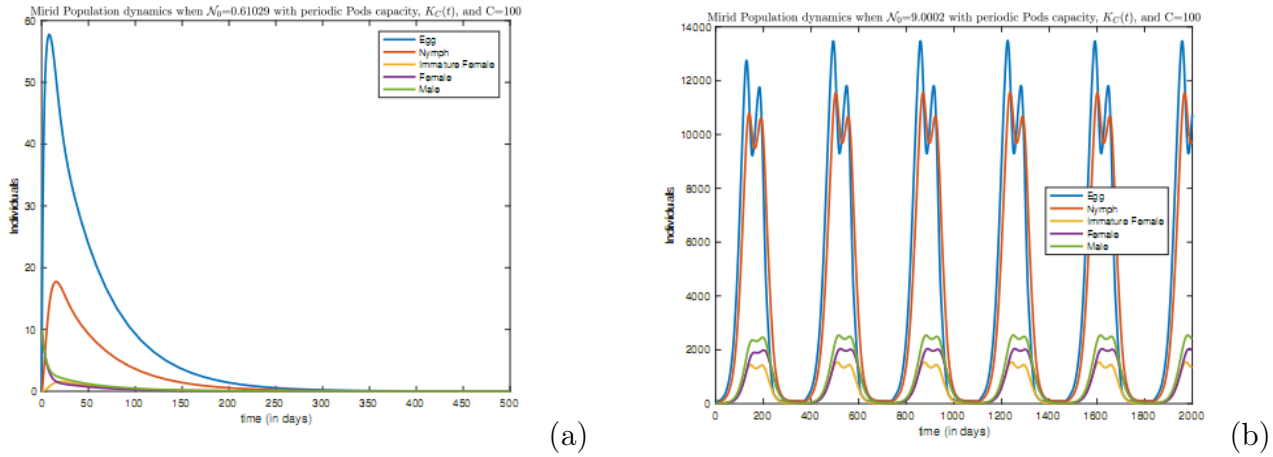

Figure 2.7: Time Evolution of mirid population when K_C is periodic and $C = 100$; (a) $\mathcal{N}_0 < 1$; (b) $\mathcal{N}_0 > 1$.

2.2 A model with delays

In the previous section, we studied the time evolution of mirid population as if the transition to one stage of development to another is immediate. Biologically, this is not correct: let us return on the biological life cycle of *S. singularis* given in Fig. 2.8, page 58. In fact, each individual needs to stay a certain amount of time in each compartment to complete its stage, in particular in the egg, nymph and non-mature female stages: there exists τ_1 days between egg-laying and appearing of new nymphs; τ_2 days between nymphs and emergence to adults. In addition, female needs τ_3 days to become mature before being able to lay eggs. In this section, we will take into account some of these previous times leading to time-delayed model with delays.

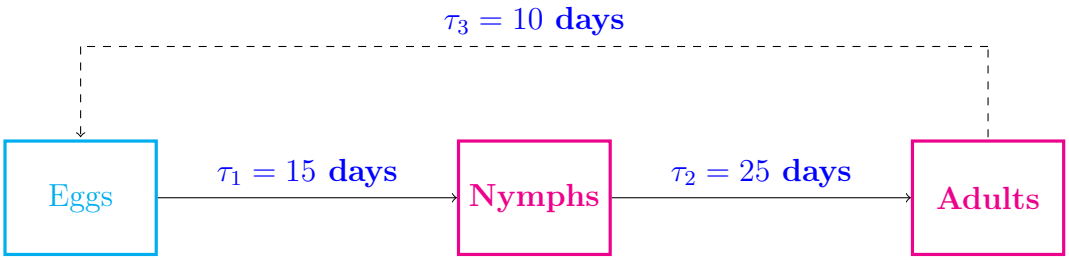

Figure 2.8: Life cycle of *S. singularis*

Now, it is possible to take into account different biological facts. In particular, based on the literature, we know that after deposition, eggs need (in mean) $\tau_1 = 15$ days to hatch and enter the nymphs compartment. b always represents the mean daily number of eggs laid by an adult female. $\tau_2 = 25$ days represent the required time for nymphs to achieve their development and become adults. So only a proportion $e^{-\tau_2 \mu_L}$ of Nymphs will survive and become adults, . Thus $\nu_E\, e^{-\tau_2 \mu_L} E(t-\tau_2)$ represents the transition rate from eggs to adults, after τ_2 days in the Nymphs compartment. The term $r\, e^{-\tau_3 \mu_A}$ represents the proportion of immature adults that will deposit eggs, after τ_3 of maturation.

Altogether, we obtain the following "two-delays" model:

$$\begin{cases} \dfrac{dE}{dt} = r\, b\, e^{-\tau_3 \mu_A}\, A(t-\tau_3) \left(1 - \dfrac{E}{K_C}\right) - (\nu_E + \mu_E)\, E, \\ \dfrac{dA}{dt} = \nu_E\, e^{-\tau_2 \mu_L}\, E(t-\tau_2) - \mu_A\, A \end{cases} \tag{2.11}$$

where initial conditions $\varphi \in \mathcal{C}([-\tau;0],\mathbb{R}^2)$ with $\tau = \max(\tau_2,\tau_3)$. $\mathcal{C}([-\tau;0],\mathbb{R}^2)$ denote $\mathcal{C}([-\tau;0],\mathbb{R}^2)$ the Banach space of continuous functions mapping the interval $[-\tau;0]$ into $\mathbb{R}^2$ with the topology of uniform convergence; i.e. for $\varphi \in \mathcal{C}([-\tau;0],\mathbb{R}^2)$, the norm of φ is defined as $\|\varphi\| = \sup_{-\tau\le\theta\le 0} |\varphi(\theta)|$ where $|.|$ is a norm of $\mathbb{R}^2$. $A = F_1 + F_2 + M$ and this is why the sex ratio r enters the E equation in Eq. (2.11).

System (2.11) can be rewritten as follows:

$$\begin{cases} \dfrac{dx_1}{dt} = \alpha x_2(t-\tau_3) \left(1 - \dfrac{x_1}{K_C}\right) - \beta x_1, \\ \dfrac{dx_2}{dt} = \gamma\, x_1(t-\tau_2) - \delta x_2, \end{cases} \tag{2.12}$$

where

$$\alpha = r\, b\, e^{-\tau_3 \mu_A}, \qquad \beta = \nu_E + \mu_E, \qquad \gamma = \nu_E\, e^{-\tau_2 \mu_L}, \qquad \delta = \mu_A.$$

Theorem 2.5. *The right-hand side of system (2.12) is continuous and Lipschitzian in x. Thus, according to the standard theory of Delay Differential Equations [78], system (2.12) admits a unique solution for each continuous initial condition $\varphi \in \mathcal{C}([-\tau;0],\mathbb{R}^2)$ where $\tau = \max(\tau_2,\tau_3)$.*

Theorem 2.6. *The domain*

$$\mathcal{D} = \left\{ x \in \mathbb{R}^2_+ / x_1 \le K_C, \quad x_2 \le \frac{\gamma K_C}{\delta} \right\}$$

is positively invariant for the model (2.12).

System (2.12) can be rewritten as follows

$$x'(t) = f(x(t), x(t-\tau_3), x(t-\tau_2)) = f(x, Y), \tag{2.13}$$

where $Y = (x(t-\tau_3), x(t-\tau_2))$. Following [66], it is important to notice that system (2.10) without delays reduces to a cooperative irreducible system. In fact the delayed system is cooperative too. Indeed, according to [66, 67], we can show that f verifies the quasimonotone condition, defined as follows in [66, 67]

$$\phi, \psi \in \mathcal{D}, \phi \leq \psi \text{ and } \phi_i(0) = \psi_i(0) \quad \text{implies} \quad f_i(\phi) \leq f_i(\psi). \tag{2.14}$$

In fact, it suffices to use Theorem 4.5 [67], page 308, i.e. to show that f is cooperative to deduce that (2.14) holds for f, that is

$$\frac{\partial f_i}{\partial x_j}(x, Y) \geq 0, \quad \text{for } i \neq j, \tag{2.15}$$

$$\frac{\partial f_i}{\partial y_j^k}(x, Y) \geq 0, \quad \text{for all } i, j, k. \tag{2.16}$$

Obviously, since the non-delayed model is cooperative, condition (2.15) is verified. Let us now check condition (2.16):

$$\frac{\partial f_1}{\partial y_1^1}(x, Y) = 0, \quad \frac{\partial f_1}{\partial y_2^1}(x, Y) = \alpha(1 - \frac{x_1}{K_C}) \geq 0, \tag{2.17}$$

$$\frac{\partial f_2}{\partial y_1^2}(x, Y) = \gamma > 0, \quad \frac{\partial f_2}{\partial y_2^2}(x, Y) = 0. \tag{2.18}$$

Since the previous conditions are verified we deduce that f is quasi-monotone, which implies that if the initial condition is positive (with at most one zero component), then the solution x is still non-negative, i.e. $x(t) \geq 0$.

Similarly, using the fact that the initial condition $\phi \in \mathcal{D}$, we have $x_1 \leq K_C$, and $x_2 \leq \frac{\gamma K_C}{\delta}$, for $t \in [-\tau, 0]$. Using these inequalities in (2.12), we infer that this is still true when $t \in [0, \tau]$. Iterating this reasoning, we finally deduce that $x(t) \in \mathcal{D}$ for all $t \geq 0$.

Proposition 2.2. *A direct computation shows that system (2.12) admits two equilibria: the trivial ones,* $\mathbf{0} = (0, 0)$*, and*

$$\mathbf{x}^* = \left(\left(1 - \frac{\beta\delta}{\alpha\gamma}\right) K_C, \frac{\gamma}{\delta}\left(1 - \frac{\beta\delta}{\alpha\gamma}\right) K_C\right) = \left(\left(1 - \frac{1}{\mathcal{R}}\right) K_C, \frac{\gamma}{\delta}\left(1 - \frac{1}{\mathcal{R}}\right) K_C\right),$$

when $\mathcal{R} > 1$ *where*

$$\mathcal{R} = \frac{\alpha\gamma}{\beta\delta} = \frac{r\, b\, \nu_E\, e^{-\tau_2\mu_L - \tau_3\mu_A}}{\mu_A\,(\nu_E + \mu_E)}. \tag{2.19}$$

$\mathcal{R}$ *represents the basic offspring number for the delayed model (2.12).*

Note that

$$\mathcal{R} = \frac{\alpha\gamma}{\beta\delta} = \frac{r\, b\, \nu_E\, e^{-\tau_2\mu_E - \tau_3\mu_A}}{\mu_A\,(\nu_E + \mu_E)} < \mathcal{N} = \frac{r\, b\, \nu_E\, \nu_L\, \nu_F}{\mu_A\,(\nu_E + \mu_E)\,(\nu_L + \mu_L)\,(\nu_F + \mu_A)}.$$

Thus, for some parameters values, we may have $\mathcal{N} > 1$ and $\mathcal{R} < 1$; the delayed model is more realistic than the non-delayed model.

There is no need to study the stability/instability of the equilibria. Indeed, according to [66] (Chapter 5), there is a nice property pointed out about cooperative irreducible time-delay systems: the asymptotic stability of each equilibrium is preserved for the delay differential system (2.10), whatever the values taken by the delays. In particular, when $\mathcal{R} \leq 1$ ($\mathcal{R} > 1$), all orbits are attracted by $\mathbf{0}$ ($\mathbf{x}^*$). In other words, to study the long term behaviour of cooperative time-delay systems it suffices to study the cooperative systems without delay(s).

This result implies that the use of delays does not change the long-time behaviour of the time-dependent system (2.10). However, when the system is non-autonomous and periodic, its behaviour may be different in the transient period from the non-delayed non-autonomous periodic system as it is showed in the forthcoming simulations (see Fig. 2.11, page 64), and Fig.2.12, page 65).

Remark 2.1. *The previous time-delayed system is considered with fixed delays. A possible extension, for future work would be to consider time varying delays, $\tau_i(t)$, since it seems obvious to consider that the developmental time in each stage may change according to environmental parameters, like temperature, rainfall.... Finally, distributed delays could be considered. Unfortunately for both cases, we do not have data.*

2.2.1 Sensitivity analysis

Finally, like for the non-delayed model, it is interesting to provide a global sensitivity analysis at different time $T = 100$ and $T = 500$: see Fig. 2.9, page 62.

Clearly, the parameters μ_L, and μ_A are the most sensitive parameters, and the delays play mainly a role in the transient phase ($T = 100$) and no more at equilibrium, contrary to the carrying capacity K_C, even if this parameter is far less sensitive than in the previous non-delayed model. This clearly shows the importance of estimating efficiently these parameters in different environmental or semi-field conditions. It also very interesting to compare the sensitivity analysis between two models that are supposed to model the same system.

2.2.2 Numerical simulation

Now, we illustrate all the different stability cases, i.e. when $\mathcal{R} < 1$ and $\mathcal{R} > 1$. The time-delayed Model is solved using Matlab and the dde23 function. In Table 2.4, page 56 we summarize the parameters values used in the next simulations but we attribute the new values of parameter μ_L.

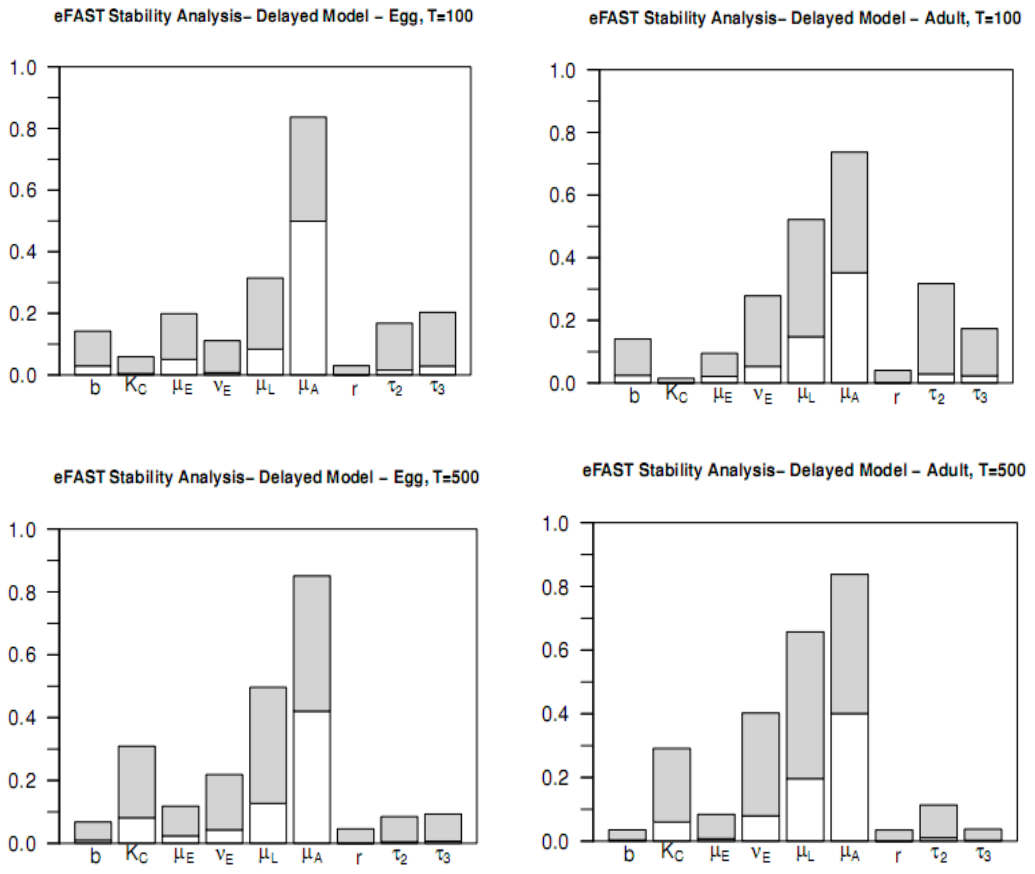

Figure 2.9: E-Fast Sensitivity analysis of the Time-Delay Model

Then, the values of parameters for those simulations are consigned in Table 2.5, page 63.

We now derive numerical simulations with $K_C = 5482$ constant and K_C periodic, like in the previous section. We choose as initial conditions $(E(0), A(0)) = (0, 50)$.

In Fig. 2.10, page 64, we illustrate the previous results when the carrying capacity K_C is constant. When $\mathcal{R} < 1$, mirids population decays till extinction and when $\mathcal{R} > 1$, mirids population converge to a positive equilibrium.

As expected, when t goes to infinity, the time-delayed model with constant parameters responds exactly like the non-delayed model, except that the threshold parameters is not exactly the same. When $\mathcal{R} < 1$ (> 1), the system converges to the trivial (positive) equilibrium. In fact, with the same parameters, the deterministic model may converge to the positive equilibrium, while the time-delay model converges to the trivial equilibrium.

Figs. 2.11, page 64 and 2.12, page 65 represent the time evolution of mirids with K_C periodic and for different values for C, namely $C = 5$ and $C = 100$. When $\mathcal{R} \leq 1$, mirid population decays rapidly till extinction, whatever the values taken by C. In contrary, when $\mathcal{R} > 1$, mirid population converges

Table 2.5: Values of constant parameters for the time-delay model

Parameters	Case $\mathcal{R} < 1$	Case $\mathcal{R} > 1$	Source
b	3.28	3.28	Estimated
τ_2	25	25	Estimated
τ_3	10	10	Estimated
μ_A	0.1	0.07	Estimated
r	0.58	0.58	[11]
μ_L	0.1	0.03	Estimated
ν_E	1/15	1/15	Estimated
μ_E	0.001	0.001	Estimated
$\mathcal{R}$	**0.566**	**6.28**	**Equation (2.19)**

to a periodic solution, as expected, but with different amplitudes related ted to C, indicating the importance of alternative resources in the maintenance and the size of the population. The simulations seem to be in good agreement with field observations. It seems also to be obvious that the removal of alternative resources should be part of control strategies to lower the impact of the mirids. Compared to the time-delayed model, the non-delayed model overestimates the population. Thus, even if from the mathematical point of view the long term behaviour is the same, the time-delayed model provides better estimate of the population size along the year than the non-delayed model. We would like to emphasize that our study was very difficult because of the lack of population data. Many parameters values were estimated using raw data obtained in the field by Babin, in 2008, in Cameroon. We use these data to estimate several parameters like mortality of eggs, nymphs and adults (μ_E, μ_L and μ_A), fecundity of adults female (b), the mean duration of immature females stage ($1/\nu_F$) and the mean necessary time for development of eggs. For some parameters (the sex-ratio r, the mean duration of egg stage ($1/\nu_E$) and the mean duration of nymph stage ($1/\nu_L$)), we used data from [30] because it was the last experiment on *S. singularis* life cycle, realized in Cameroon. The most difficult data to obtain was the daily evolution of pods number in the plot. Using data from [73] and also based on our knowledge about the mean pods density per hectare, we construct our periodic function $K_C(t)$ which represent the daily appearance of pods and cherelle in the plot. However, mirids also feed and lay eggs on young shoots that lead to important damage able to cause the destruction of the tree over the years. It will be important to take into account this aspect and model the daily appearance of young shoots in the plot by a function ($S(t)$ for example). Then, it will be relevant to know the mirid frequency of feeding on host plants to have a good idea about the parameter C

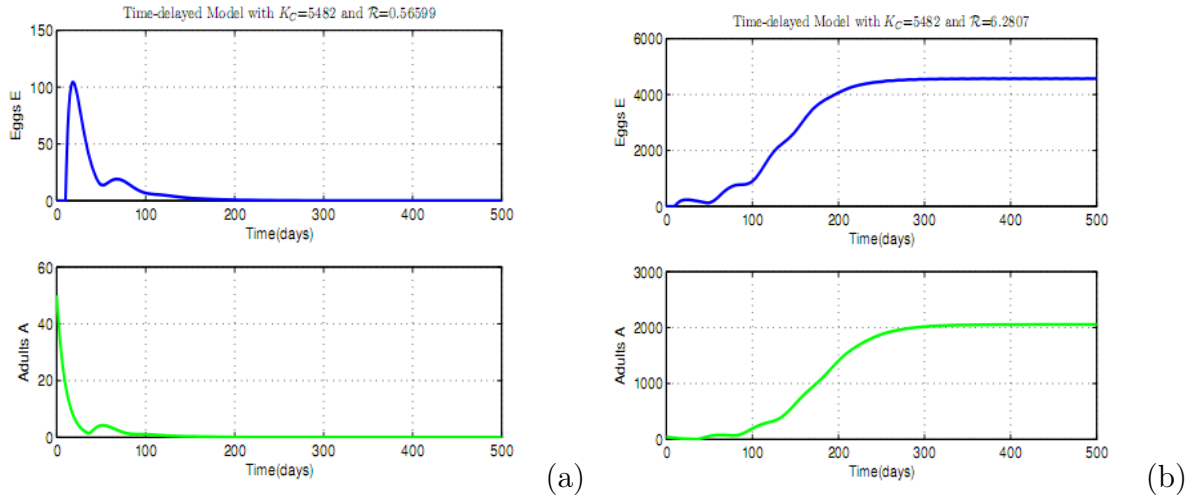

(a) (b)

Figure 2.10: Time evolution of the Eggs and Adult Compartments for the time-delay model with constant parameters, $K_C = 5482$, with: (a) $\mathcal{R} < 1$, (b) $\mathcal{R} > 1$

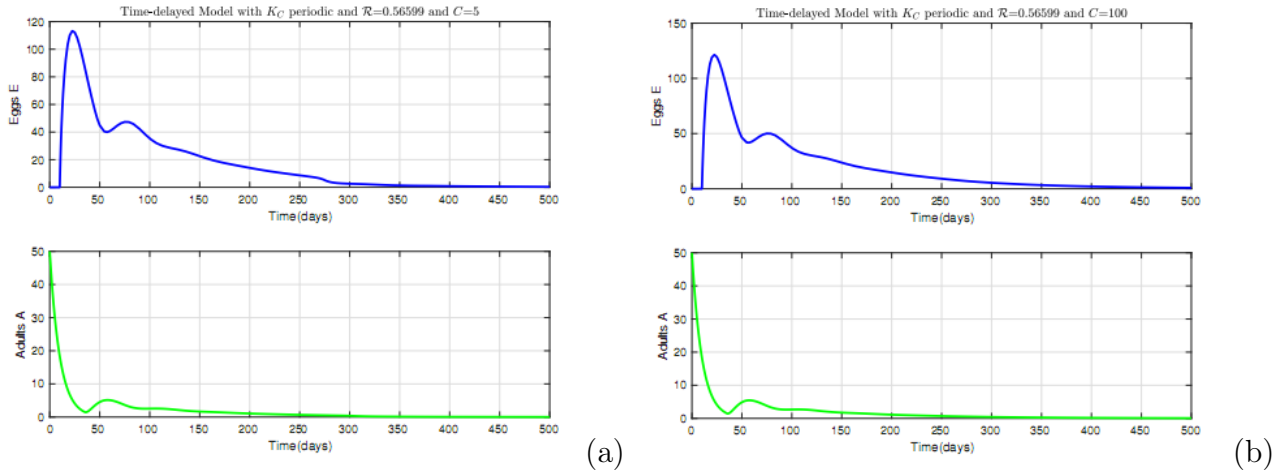

(a) (b)

Figure 2.11: Time evolution of the Eggs and Adult Compartments for the time-delay model with constant parameters, K_C periodic, such that $\mathcal{R} < 1$, with: (a) $C = 5$ (b) $C = 100$.

because the time-evolution of mirids also depends on it considering that if C is large, the level of mirid population increase. In our numerical simulations, we attributed to this parameter two values $C = 5$ and $C = 100$. According to these results, we suggest that it will be important to have several experiences in the field: to better estimate the daily appearance on pods and shoots in the plot, to have a good idea about the parameters of development of mirids and also to better estimate the parameter C.

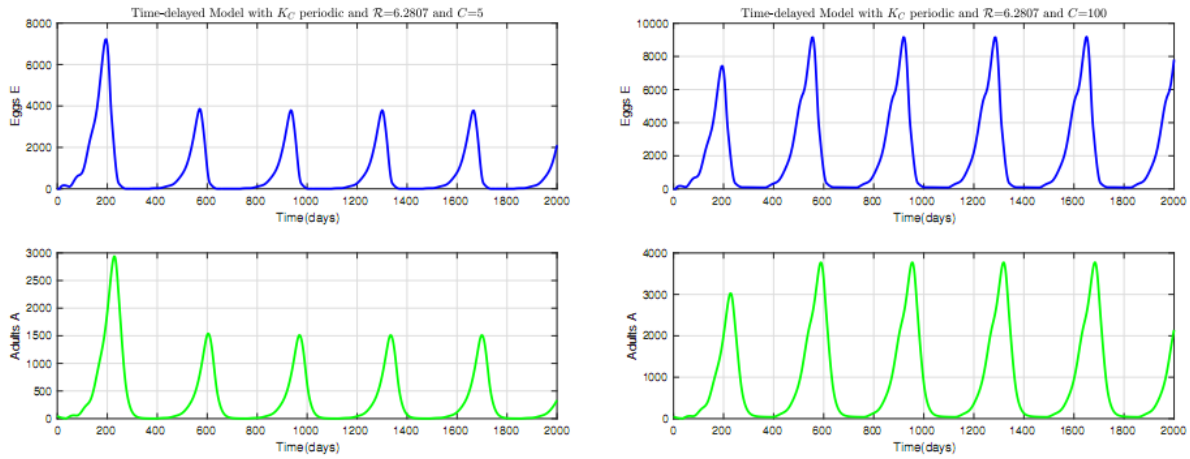

Figure 2.12: Time evolution of the Eggs and Adult Compartments for the time-delay model with constant parameters, K_C periodic, such that $\mathcal{R} > 1$, with: (a) $C = 5$ (b) $C = 100$.

2.3 Application to control strategies

Understanding the population dynamic of *S. singularis* is crucial for monitoring, forecasting and, then, controlling this pest population. Recent work in Ghana indicates (using the visual hand-height assessment method) that mirid populations (predominately nymphs) began to increase rapidly in April with an initial peak in May, followed by a rapid build-up in June [20]. In Cameroon, mirid /population is low on cacao from February to March. From June to July, the populations start to grow more or less rapidly depending on external conditions like weather and fruits production on the trees. The peak of the population appears between September and November when the pods are almost mature [30].

Even if the chemical control remains inevitable in many agrosystems, cultural methods, varietal characters of tolerance to insects, action of auxiliaries entomophages and entomopathogenic agents, as well as the prospects offered by mediators chemicals are to be taken into account to reduce the dependency of the pesticide culture.

Several methods are developed in order to control mirid population among which cultural management, varietal management, chemical management and semio-chemical management:

- Cultural management, based on managing the system structure and composition to create unfavourable conditions for the development of mirids populations. All agronomic practices entering into the conduct of culture are concerned: sowing, associated crops, the density of populations, weeding, control of plant growth and fertilization.

- Varietal management, which consists in replacing the cacao varieties traditionally cultivated with more resistant and/or tolerant varieties to mirid attacks.
- Chemical management, based on chemical insecticide used. This is the most widespread and efficient strategy to control mirid population in Cameroon. The chemical insecticides are applied twice to three times a year [9] (see also the CIRAD report published for cocoa producers.)
- Semio-chemical management which consists of using synthetic sexual pheromone traps [26] which increases adult mortality (trapping), and prevents male insects finding females and mating (mating-disruption), and thus reduces the fecundity of female.
- last but not least, as showed in the previous simulations, a reduction of mirids alternative host (resources), i.e. decrease C, is also essential to have an efficient control.

In Cameroon context, chemical management is the main way to control mirids population. In the following section, using the precedent delayed model, we will show the impact of chemical applications on the level of mirid population. We will successively the case of one, two and three applications per year (as recommended by CIRAD).

2.3.1 Chemical control

In Cameroon, mirids populations are mainly controlled by chemical insecticides. Three treatments are recommended per year: in June/July and August/September (propagation of mirids population); in November/December [79]. We will consider the impact of one treatment, two treatments and, finally three treatments. We will make a comparative study of treatments applied in systems with cacao only, $C = 5$, and in agroforestry systems composed of cacao and associated trees that could be secondary resource for mirids, $C = 100$.

According to the expert's knowledge and field observations, the insecticide has a decaying death rate over 8 weeks, that is summarized in Table 2.6: .

Table 2.6: Time dependent death-rate of chemical treatment

Time (in days) after the release	1	3	8	16	24	32	40	48	56	60
Insecticide death rate	1	1	0.9	0.2	0.1	0.05	0.025	0.01	0	0

Using cubic Hermite spline, we obtain a polynomial interpolation (Daily estimation of efficiency of treatment) given in Fig. 2.13, page 67. Figure 2.13, page 67 represents the daily estimation of pods number in the plot.

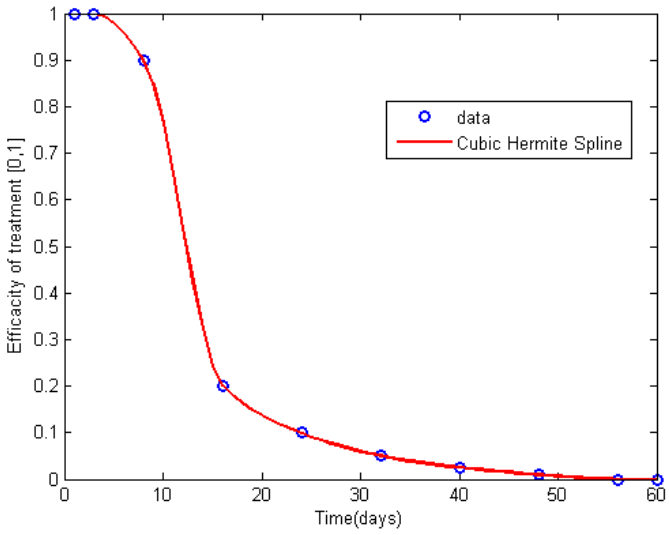

Figure 2.13: Efficiency of chemical treatment in the plot.

Remark 2.2. *Synthetic insecticides like λ-cyhalothrine and Imidacloprid have a long residual effect, but it depends on several environmental factors, like rainfall. That is why Table 2.6 provides only a feedback from field experts according to the locations in Cameroon where these treatments have been studied and are already used.*

We start our numerical simulations at the end of June, a period where the number of pods is increasing in the plot. We treat the plot respectively one, two, or three time(s) per year, as recommended to Cacao producers. We compare the efficacy between each treatment. The periods of treatment are given as follows:

- **Treatment One**: with only one application per year
  (beginning of) July ($t = 395, 760, 1125, 1490, 1855$).
- **Treatment Two**: with two applications per year
  July ($t = 395, 760, 1125, 1490, 1855$) and September ($t = 457, 822, 1187, 1552, 1917$) (see [**?**], page 20).
- **Treatments Three**: with three applications per year
  July ($t = 395, 760, 1125, 1490, 1855$), September ($t = 457, 822, 1187, 1552, 1917$), and November ($t = 518, 883, 1248, 1613, 1978$) (see [**?**], page 20).

It is worth to mention that the periodicity of the two last treatments coïncides with the duration of the chemical treatment after spreading. In Figs. 2.14, page 68, Fig. 2.15, page 68, and Fig. 2.16,page

69, we present the results obtained with the different treatments in two cases: $C = 5$ and $C = 100$. The case $C = 5$ represents a full cacao crops, while $C = 100$ may represent a cacao crop in an agro-forestry system, where additional resources (host trees) are available for mirids.

We show that 2 treatments are sufficient (more than 90% reduction of the population) when C is small. An additional (third) treatment is particularly recommended when C is large, i.e. $C = 100$. These results are relevant with real observations in different type of plots, at least in Cameroon.

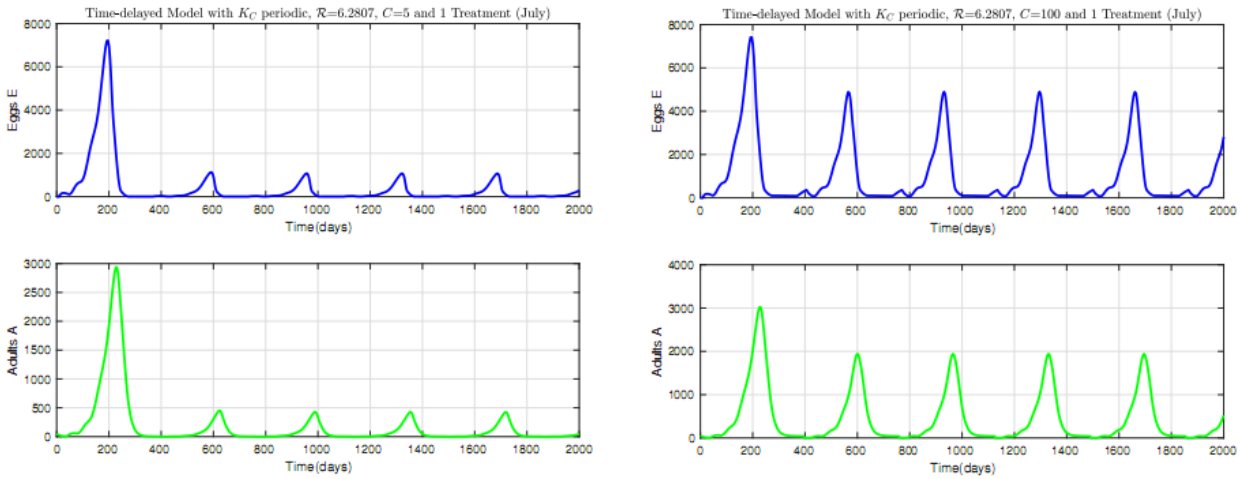

Figure 2.14: Time evolution of Mirids using only one treatment in the plot per year: (a) $C = 5$, (b) $C = 100$.

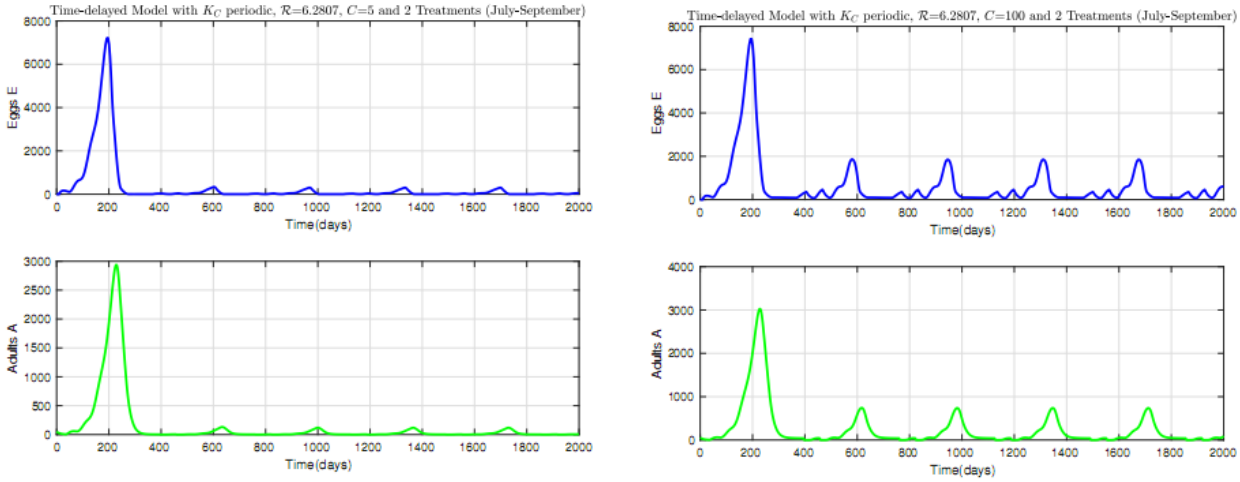

Figure 2.15: Time evolution of Mirids using two treatments per year in the plot: (a) $C = 5$, (b) $C = 100$.

Numerical simulations proves that more alternative resource is great, more the mirid population

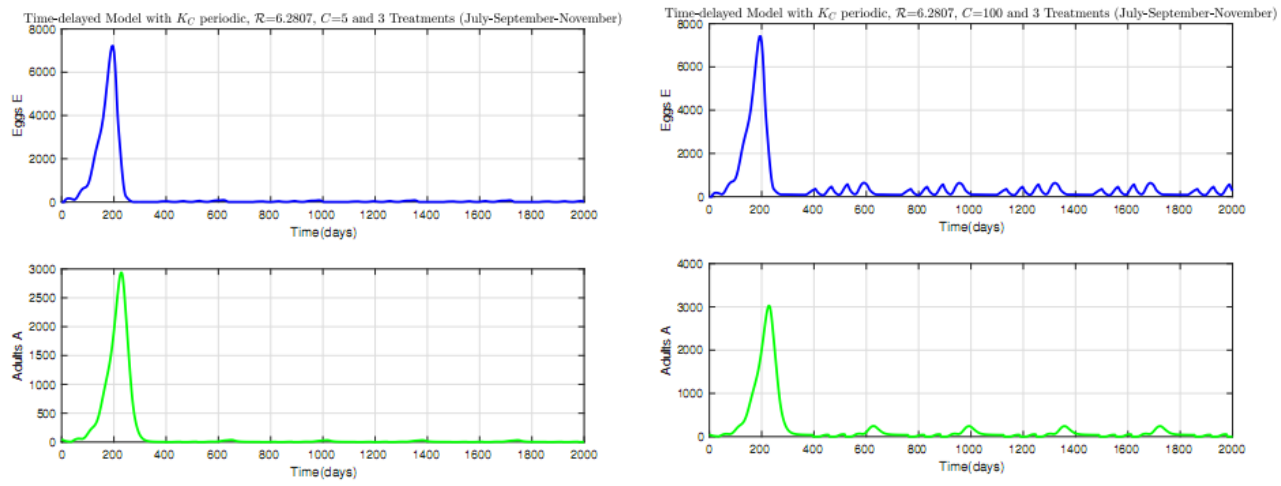

Figure 2.16: Time evolution of Mirids using three treatments per year in the plot: (a) $C = 5$, (b) $C = 100$.

increase even if there is not pods (main resource) in the plot. In Cameroonian's context where cacaoculture is done in agroforesteries systems, it will be good or beneficial to improve the control in these such systems.

Although chemical insecticides are very efficient to control mirids, their recurrent use is widely questioned due to the immediate adverse effects that they cause in ecosystems via environmental pollution (impact non targeted species), induce resistance in the mirid population, and to the toxic effects on human health. In addition, these chemical products are very expensive. That is why, it could be more advantageous to consider sustainable control strategies, like for instance, mating disruption and trapping [26, 80].

2.3.2 Semio-chemical control

Mating disruption consists of introducing an artificial stimuli, like pheromones or para-pheromones, to confuse individuals, and, thus, disrupt mate localization, leading to long-term reduction of the population. In our case, we roughly assume that this implies a decrease of the female fecundity. Thus, for instance, if we reduce the daily female fecundity from 3.28 to 2, the mirid population decreases: see Fig.2.17, page 70. Another way to control mirids is the use of traps. Traps increase the adult mortality rate, μ_A. For instance, if we increase the mortality μ_A from 0.07 to 0.1, we observe a great reduction of the level of mirid population (see the time evolution of mirids in Fig. 2.18, page 70). According to the sensitivity analysis, the adult mortality μ_A is a sensitive parameter for the delayed model such that any increase may have a strong negative impact on the population.

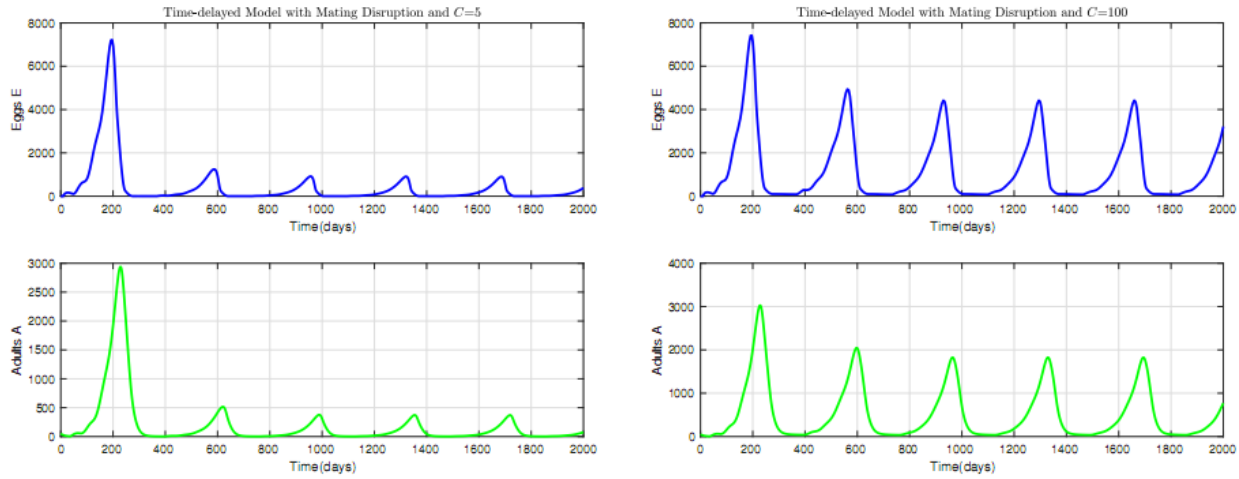

Figure 2.17: Time evolution of Mirids with control using mating disruption: (a) $C = 5$, (b) $C = 100$.

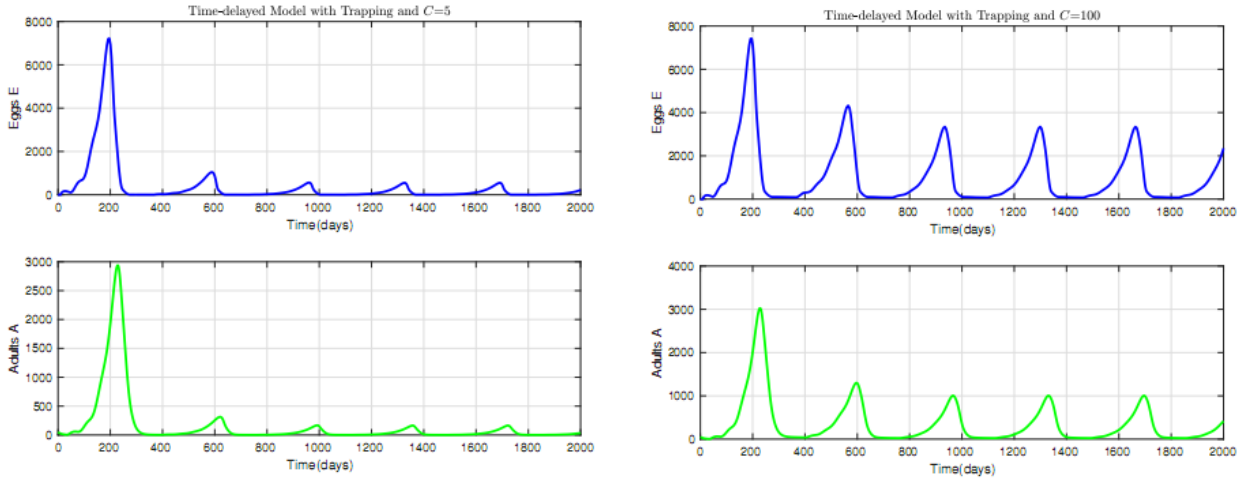

Figure 2.18: Time evolution of Mirids with control using trapping: (a) $C = 5$, (b) $C = 100$.

In general, combining the two previous methods of control (mating disruption and trapping), improve the previous results (see Fig. 2.19, page 71). This combination allows to reach a low level of population, right after the first year.

2.3.3 Comparative study between chemical control and semio-chemical control

We summarize in Table 2.7, page 71 the impact of each treatment in the reduction of the wild

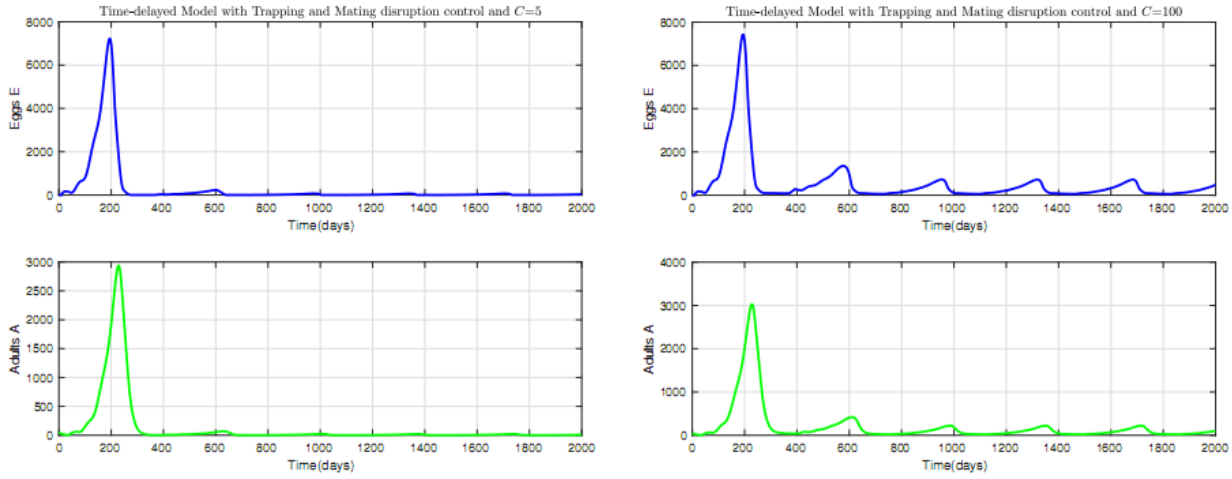

Figure 2.19: Time evolution of Mirids with control combining trapping and mating disruption; (a) $C = 5$, (b) $C = 100$.

population.

Table 2.7: Efficacy of each treatment - Percentage of reduction of the wild population

	Treatment 1	Treatment 2	Treatment 3
$C = 5$	74.8%	92.9%	97.8%
$C = 100$	58.7%	84.8%	94.1%

.

We summarize in table Table 2.8, page 71, the efficiency of each control methods. According to the given results, it seems possible to have a very efficient control of mirids without using chemical control. Clearly the combination of Mating and Trapping gives the best results whatever the values taken by C. This is in good agreement with recent field experiments [80]. .

Table 2.8: Efficacy of Trapping, Matting, and Trapping-Mating - Percentage of reduction of the wild population

	Mating	Trapping	Trapping& Mating
$C = 5$	70.5%	85.5%	96.5%
$C = 100$	49.4%	71.0%	90.1%

In this chapter, we studied the dynamics of a cocoa pest, mirids. From the best of our knowledge it is the first time that mathematical models are developed to study mirid pest. We first build a generic

stage-structured ODE model to simulate the dynamic of the pest population considering the resource (available cocoa pods and additional tree hosts) as constant or as a periodic function. Our model enters the family of cooperative system, which facilitates its study. Thus, we show that there exists a threshold parameters, $\mathcal{N}_0$, also called the basic offspring number, that summarizes the dynamics of the system: when it is less than one, then the mirid population decreases till extinction; when it is greater than one, then mirids population persists. Then, based on the mirid's development stages and times, we also develop a cooperative delay model with two delays. We derive a theoretical study and estimate the related basic offspring number, $\mathcal{R}$. We illustrate the theoretical results through numerical simulations. We show that the outputs of the delayed system are more realistic than the non-delayed ODE model. We also highlighted that the presence of additional hosts can help the capsid population to maintain when pods are not available. Last but not least, for both models, we derive a sensitivity analysis that shows that the carrying capacity and the mortality rates are the most sensitive parameters.

In the previous simulations, we showed that a biological control strategy (using Mating and Trapping) can be a very good alternative to the use of insecticides. Last but not least, if it is possible, the reduction of alternative hosts in the plots is also an additional way to improve the efficacy of both controls.

Thus in the following chapter, we will develop a generic mirid model which take into account the semio-chemical control using mating-disruption and trapping.

3

Miridae control using sex-pheromones, trapping. Modeling, analysis and simulations.

The focus of this chapter is to study a mathematical model to get a better understanding on the dynamics of the mirid population under mating disruption and trapping. Based on [4] and [81], we built a generic mathematical delayed model of mirid population, modelling mating and trapping in order to study the effort required in terms of traps or sex-pheromone, to reduce the population size below harmful level. We obtain a piecewise smooth (PWS) systems of delayed differential equations. We analyse this model and provide numerical simulations to highlight the theoretical results. This chapter has been submitted for publication at the revue "*Nonlinear analysis: Application to real world*".

In fact mirids are responsible of several damages on cocoa in Africa especially in Cameroon. Their presence leads to the enormous losses of production difficult to estimate, but can reach $30-40\%$ of potential production. Mirids are very harmful and lead to the destruction of the plot over the time. They also have a capacity to develop resistance on treatments and to adapt to wide range of hosts and/or climate conditions. However, pest management is essential to prevent devastating impact on economy, food security, social life, health and biodiversity. Nowadays, in Cameroon, it is proved that chemical control is the best ways to control mirid population. However, although chemical insecticides are very efficient to control mirids, their recurrent use is widely questioned due to the immediate adverse effects on the environment such as reduction the mirid natural enemies and production that they cause in ecosystems via environmental pollution (impact non targeted species), induce resistance on the mirid population, and to the toxic effects on human health. In addition, these chemical products are very expensive.

In the previous chapter, we built and study several models (with and without delays) of mirids

population and also several control strategies, including chemical treatment, mating disruption and trapping. We showed that the use of three applications of chemical treatment is equivalent to the combination of mating disruption and trapping. These two methods are less expensive and less toxic than chemical management and respect specific ecological and toxicological environmentally friendly requirements. In this paper, we will model more specifically the use of sex pheromones to trap males and thus disturb matings, in order to eliminate or decay the population. In Cameroon, we used different blends of the two components hexyl (R)-3-((E)-2- butenoyloxy)-butyrate and hexyl (R)-3-hydroxybutyrate) of the *S. singularis* female sex pheromone for tests. Traps used are delta or rectangular white-coloured traps, made out of recycled polyethylene and cardboard. In the two years experiment, conducted by [26], a total of 361 adults of *S. singularis* (359 males and two females) were caught. The highest numbers of mirids were found in traps with pheromone blends that combined a monoester and a diester, compared with traps with the diester or the mono-ester individually and control traps with no pheromone. Rectangular traps also caught significantly more mirids compared with delta traps. Finally, in a recent work [80], the authors studied the impact of pheromone trap density (per ha) for mass trapping cacao mirids. It is clearly stated that this is a Male Annihilation technique, with the objective of reducing the male population in order to lower the mirid population under an economical threshold.

3.1 A sex-structured model of mirid population

In this section, we consider a generic delayed model to describe the dynamics of *S. singularis*. The flow diagram is represented in Fig. 3.2, page 76. Based on biological and behavioural assumptions, we consider two main developments stages: eggs (E) and adults (females F and A and male M). Indeed, after being laid, the eggs need, on average, $\tau_1 = 15$ days to become nymphs. These nymphs need $\tau_2 = 25$ days to complete the nymph's development and become adult males or females. After emergence, sexual immature female mate with males (attracted by sex pheromones released by the females) and then they need approximately $\tau_3 = 10$ days before being able to deposit eggs (in fact this is the time needed for the appearance of mature eggs in the ovarioles [82]). This is summarized in Fig. 3.1, page 75.

We denote by $e^{-\tau_2 \mu_L}$ the proportion of nymphs respectively which survive the nymph stage. After mating, F becomes mated females A that need an additional period of maturation, τ_3, in order to lay eggs [82]. However, only a proportion, $e^{-\tau_3 \mu_A}$ of A females will deposit eggs. Thus, we have four compartments for our delayed model: E which represent egg's compartment, F which represent

females which need mating to lay eggs; A which represent females after mating and M which represent the males.

Females release pheromone in order to attract males for mating. The mating between males and females is modelled as in [80]: as long as the male density is such that $\gamma\, M \geq F$, then all Females F will be inseminated and move to the compartment A, at rate ν_F . In contrary, if, for any reason, the male density is scarce, i.e. $\gamma\, M \leq F$ then the number of females F that will move to the compartment A is related to the number of Males, M. The other parts of the compartmental model follow the model developed in [4].

The biological parameters are described as follows: r is the sex ratio; b is the mean number of eggs laid by an adult female mirid per day that have emerged as nymphs, K_C is the maximal carrying capacity related to the mean daily number of pods per area (ha), μ_E, μ_M, μ_F and μ_A represents respectively the eggs, male, females daily mortality rate, ν_E is the transition rate from the egg to the next stage; $1/(\nu_E + \mu_E)$ is the mean time a mirid stays in the egg stage (measured in days); ν_F is the transition rate from the sex-immature female stage to mature female stage.

As already explained in [4], the non linear term $r\, b\, F_2\, (1 - E/K_C)$ is related to a skip-oviposition behaviour. Indeed, according to expert's knowledge, mirids (*S. singularis*) are able to select their breeding sites according to their level of occupation.

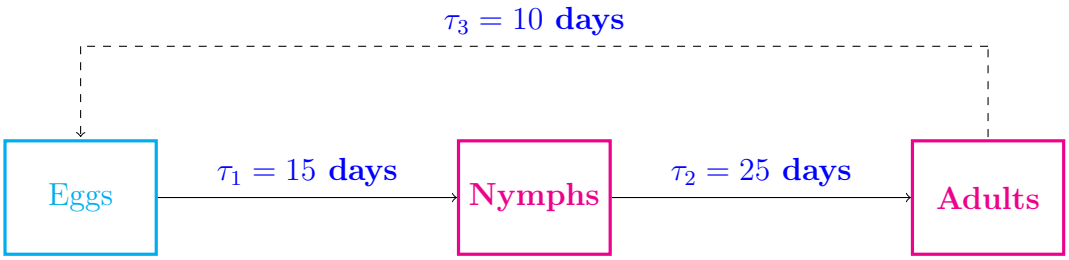

Figure 3.1: Life cycle of *S. singularis*

According to the diagram given in Fig. 3.2, we derive the delay differential system (3.1):

$$\begin{cases} \dot{E}(t) = b\, e^{-\tau_3\, \mu_A}\, A(t-\tau_3) \left(1 - \dfrac{E(t)}{K}\right) - (\nu_E + \mu_E)\, E(t), \\ \dot{F}(t) = r\, \nu_E\, e^{-\tau_2\, \mu_L}\, E(t-\tau_2) - \nu_F\, \min\left(\dfrac{\gamma\, M(t)}{F(t)}, 1\right) F(t) - \mu_F\, F(t), \\ \dot{A}(t) = \nu_F\, \min\left(\dfrac{\gamma\, M(t)}{F(t)}, 1\right) F(t) - \mu_A\, A(t), \\ \dot{M}(t) = (1-r)\, \nu_E\, e^{-\tau_2\, \mu_L}\, E(t-\tau_2) - \mu_M\, M(t). \end{cases} \tag{3.1}$$

Parameters of model (3.1) are recapitulated in Table 3.1.

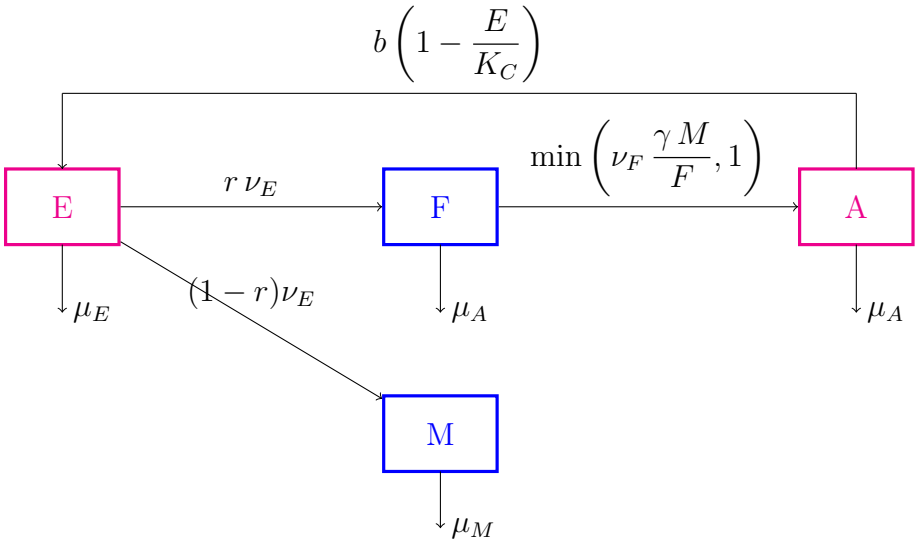

Figure 3.2: *Sahlbergella singularis* control model using mating disruption and trapping.

3.2 Control using mating disruption and trapping

In order to maintain a low level a mirid population, we consider a control using sex pheromone traps. The objective is to perturb the mating but also to reduce the number of males in order to reduce the overall population. More precisely, we take into account two aspects for the control. The first consists of disturbing the mating between males and females to reduce the fertilisation opportunities, which in turn, reduces the number of offspring. This is done using traps that are releasing a female pheromone lure to which males are attracted. This leads to a reduction in the number of males available for mating near the females, and decreases the opportunity for fertilisation. The efficiency of mating disruption depends on the strength of the lure or on the number of traps in an area. The second aspect of the control is the trapping potential of the trap. We assume that the lure traps also contain an insecticide which can kill the captured insects.

In order to take in account the effect of the lures, we consider the approach proposed by Barclay and Van den Driessche ([83, 84]). That is, the strength of the lure is represented as the quantity of pheromones released by an equivalent number of wild females. Thus, in the model the effect of the lure corresponds to the attraction of YP additional females. In such a setting, the total number of "females" attracting males is $F + F_p$ [83]. Then, males have a probability $\frac{F}{F+F_p}$ to be attracted to wild females and a probability $\frac{F_p}{F+F_p}$ to be attracted to the pheromone traps. Let γ be the number of females that can be inseminated by a single male, then the transfer rate from F to A does not exceed $\nu_F \frac{\gamma M}{F+F_p}$. When $\nu_F \frac{\gamma M}{F+F_p} > 1$, the population is in male abundance state and the transfer

Table 3.1: **Parameters of model (2.1).**

Parameters	Biological significance	Unit
b	Mean number of eggs laid by a mature female	female^{-1}days^{-1}
r	sex ratio	
K	Maximal carrying capacity related to the mean daily number of pods per ha	
$1/\nu_L$	Duration of the development of nymphs	days
$1/\nu_F$	Time necessary for an immature female to become mature	days
μ_L	Mortality of nymphs	days^{-1}
μ_A	Mortality of adults females	days^{-1}
μ_M	Mortality of adults males	days^{-1}
μ_F	Mortality of immature females	days^{-1}
μ_E	Mortality of eggs	days^{-1}
$1/\nu_E$	Time necessary for an egg to become nymph	days
γ	The number of females that can be inseminated by a single male	

rate is ν_F and when $\nu_F \dfrac{\gamma\, M}{F+F_p} < 1$, the population is in a male scarcity state and the transfer rate is $\nu_F \dfrac{\gamma\, M}{F+F_p}$. Altogether, the transfer rate is $\min\left(\nu_F \dfrac{\gamma\, M}{F+F_p}, 1\right)$.

Parameter α represents the maximum capture rate by trapping, the ratio $\dfrac{F_p}{F+F_p}$ represents the attractiveness of the traps. The new flow diagram is represented in Fig. 3.3, page 78. According to the flow diagram, and taking into account the life cycle of *S. singularis*, we obtain a new mating disruption and trapping control model is given by model (3.2).

$$\begin{cases} \dot{E}(t) = b\, e^{-\tau_3 \mu_A}\, A(t-\tau_3) \left(1 - \dfrac{E(t)}{K}\right) - (\nu_E + \mu_E)\, E(t), \\ \dot{F}(t) = r\, \nu_E\, e^{-\tau_2 \mu_L}\, E(t-\tau_2) - \nu_F \min\left(\dfrac{\gamma\, M(t)}{F(t)+F_p}, 1\right) F(t) - \mu_F\, F(t), \\ \dot{A}(t) = \nu_F \min\left(\dfrac{\gamma\, M(t)}{F(t)+F_p}, 1\right) F(t) - \mu_A\, A(t), \\ \dot{M}(t) = (1-r)\, \nu_E\, e^{-\tau_2 \mu_L}\, E(t-\tau_2) - \left(\mu_M + \alpha \dfrac{F_p}{F(t)+F_p}\right) M(t). \end{cases} \tag{3.2}$$

Model (3.2), like model (3.1), enters the family of piece-wise dynamical systems with delay differential

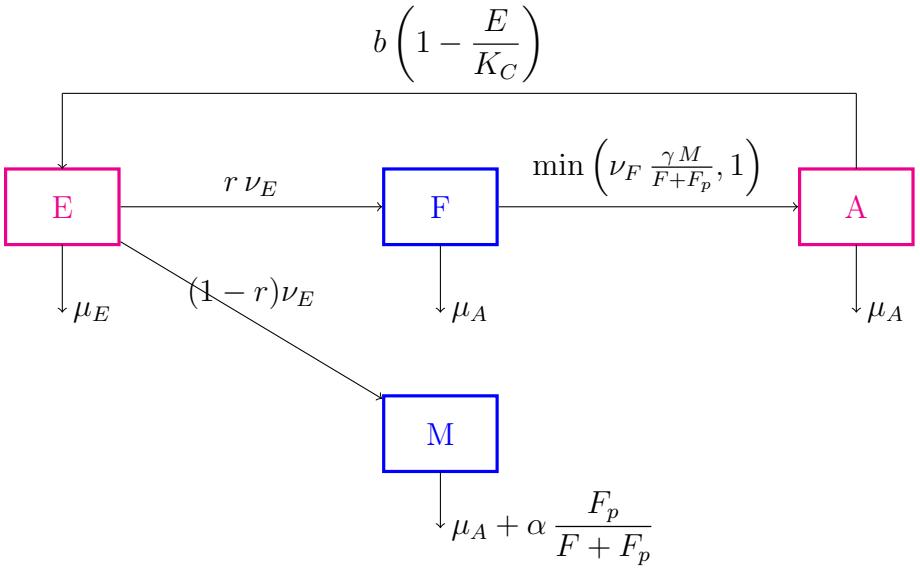

Figure 3.3: *Sahlbergella singularis* control model using mating disruption and trapping.

equations (shortly, PWS-DDE) (See Chapter 1, Section 1.3). The switching manifold is defined as follows

$$\sum := \{x \in \mathbb{R}^4_+, \quad F + F_p = \gamma\, M\}$$

Model (3.1) can be rewritten in the form:

$$\frac{dx}{dt} = f(x) := \begin{cases} f_1(x, x_{\tau_2}, x_{\tau_3}) & if \quad F + F_p \leq \gamma\, M \\ f_2(x, x_{\tau_2}, x_{\tau_3}) & if \quad F + F_p \geq \gamma\, M \end{cases} \tag{3.3}$$

where

$$x = (E, F, A, M)^t$$

,

$$f_1(x, x_{\tau_2}, x_{\tau_3}) = \begin{pmatrix} b\, e^{-\tau_3\,\mu_A}\, A(t-\tau_3)\left(1-\frac{E(t)}{K}\right) - (\nu_E + \mu_E)\, E(t) \\ r\,\nu_E\, e^{-\tau_2\,\mu_L}\, E(t-\tau_2) - (\nu_F + \mu_F)\, F(t) \\ \nu_F\, F(t) - \mu_A\, A(t) \\ (1-r)\,\nu_E\, e^{-\tau_2\,\mu_L}\, E(t-\tau_2) - \left(\mu_A + \alpha\frac{F_p}{F(t)+F_p}\right) M(t) \end{pmatrix} \tag{3.4}$$

and

$$f_2(x, x_{\tau_2}, x_{\tau_3}) = \begin{pmatrix} b\, e^{-\tau_3\,\mu_A}\, A(t-\tau_3)\left(1-\frac{E(t)}{K}\right) - (\nu_E + \mu_E)\, E(t) \\ r\,\nu_E\, e^{-\tau_2\,\mu_L}\, E(t-\tau_2) - \nu_F\,\frac{\gamma\, M(t)}{F(t)+F_p}\, F(t) - \mu_F\, F(t) \\ \nu_F\,\frac{\gamma\, M(t)}{F(t)+F_p}\, F(t) - \mu_A\, A(t) \\ 1-r)\,\nu_E\, e^{-\tau_2\,\mu_L}\, E(t-\tau_2) - \left(\mu_A + \alpha\frac{F_p}{F(t)+F_p}\right) M(t) \end{pmatrix} \tag{3.5}$$

When $\tau_2 = \tau_3 = 0$, system (3.3) is exactly the same system studied in [81]. We will use the related results in our study.

The aim of this chapter is to investigate the existence of equilibria of model (3.2) and their asymptotic properties. Like in [81], the theoretical analysis of the model is carried out for two cases: male abundance and male scarcity. These two cases are separated by the hyperplane $\sum$. The analysis of the two systems can be carried out independently on the orthant $\mathbb{R}^4_+$. The obtained results will be merged into a general theorem for the system (3.2).

3.2.1 Case with Male abundance: $\gamma M > F + F_p$

In this case, the system can be written in the vector form

$$\frac{dx}{dt} = f_1(x, x_\tau), \tag{3.6}$$

with $x = (E, F, A, M)^T$ and f_1 is given by the equation (3.4).

Theorem 3.1. *The right hand side of system (3.6), f_1, is continuous and Lipschitzian in x. Thus, according to the standard theory of delay differential equations [78], for each continuous initial condition $\psi \in \mathcal{C}([-\tau, 0], \mathbb{R}^4)$, where $\tau = \max(\tau_2, \tau_3)$, uniqueness and local existence of the solution are guaranteed.*

Note also, that, without delay, we recover the cooperative system studied in [81]. As explained in [4], some cooperative systems with delay can enjoy some nice properties such that their long term behaviour is similar to the cooperative system without delay. Let $Y = (x(t - \tau_3), x(t - \tau_2))$, $x = (E, F, A, M)^T$. System (3.6) verifies the, so-called, quasimonotone (QM) condition if

(a) $\dfrac{\partial f_{1,i}}{\partial x_j} \geq 0$ for $i \neq j$

(b) $\dfrac{\partial f_{1,i}}{\partial Y_j^k} \geq 0$ for all i, k.

Condition (a) is verified since the non delayed model is a cooperative system. Let us verify condition (b):

One has:

$$\frac{\partial f_{1,1}}{\partial Y_3^1} = b\, e^{-\tau_3\,\mu_F}\left(1-\frac{E(t)}{K_C}\right) \geq 0, \quad \frac{\partial f_{1,1}}{\partial Y_j^1} = 0 \quad \forall\ j=1,2,4, \quad \frac{\partial f_{1,1}}{\partial Y_j^2} = 0 \quad \forall\ j=1,2,3,4$$

$$\frac{\partial f_{1,2}}{\partial Y_1^2} = r\,\nu_E\, e^{-\tau_2\,\mu_L}, \quad \frac{\partial f_{1,2}}{\partial Y_j^2} = \frac{\partial f_{1,2}}{\partial Y_k^1} = 0 \quad \forall\ j=2,3,4 \quad \forall\ k=1,2,3,4,$$

$$\frac{\partial f_{1,3}}{\partial Y_j^1} = \frac{\partial f_{1,3}}{\partial Y_j^1} = 0, \quad \forall\ j=1,2,3,4$$

$$\frac{\partial f_{1,4}}{\partial Y_1^2} = (1-r)\,\nu_E\, e^{-\tau_2\,\mu_L} \geq 0, \quad \frac{\partial f_{1,4}}{\partial Y_j^2} = \frac{\partial f_{1,4}}{\partial Y_k^1} = 0 \quad \forall\ j\in\{2,3,4\} \quad \forall\ k\in\{1,2,3,4\}.$$

Then the (QM) condition is verified. This implies that if the initial condition is non negative (with at most one zero component) then the solution of system (6) is still non negative i.e $x(t)\geq 0$. Moreover, the (QM) condition guarantees the stability of each equilibrium of the non delayed system is preserved for the delayed system. In other words, it suffices to study the following non delayed system

$$\frac{dx}{dt} = f_1(x) \tag{3.7}$$

to deduce the behaviour of the time delayed system (3.6). As already emphasized, system (3.7) has already been studied in [81], using [85, 86].

Theorem 3.2. *The basic offspring number for the model (3.6) is*

$$\mathcal{R} = \frac{r\,b\,\nu_E\,\nu_F\,e^{-\tau_2\,\mu_L}\,e^{-\tau_3\,\mu_A}}{\mu_A\,(\nu_E+\mu_E)\,(\nu_F+\mu_F)} \tag{3.8}$$

and applying Theorem 9 [81] we deduce:

(i) The system (3.6) defines a positive dynamical system on $\mathbb{R}^4_+$.

(ii) Model (3.6) always has a trivial equilibrium $\mathbf{0}=(0,0,0,0)$ which is globally asymptotically stable when $\mathcal{R}\leq 1$.

(iii) If $\mathcal{R}>1$, model (3.6) has two equilibria: a trivial equilibrium $\mathbf{0}$ and a unique positive equilibrium $X*=(E^*,F^*,A^*,M^*)$ where

$$E^* = \left(1-\frac{1}{\mathcal{R}}\right)K, \quad F^* = \frac{r\,\nu_E\,e^{-\tau_2\,\mu_L}}{(\mu_F+\mu_F)}\,E^*, \quad A^* = \frac{\nu_F}{\mu_A}\,F^*,$$

$$M^* = \frac{M^0}{\mu_M+\alpha\,\dfrac{F_p}{F^*+F_p}}\,E^* \quad \textit{with} \quad M^0 = (1-r)\,\nu_E\,e^{-\tau_2\,\mu_L}\,E^*.$$

Positive equilibrium is globally asymptotically stable if $\mathcal{R}>1$ on

$$\mathbb{R}^4_+\setminus\{\mathbf{0}\} = \{x\in\mathbb{R}^4_+,\ E=F=A=M=0\}.$$

Remark 3.1. *When $\alpha = 0$, we recover the positive equilibrium when no control occurs. It is important to notice that the effect on the control only impact the value of the Male equilibrium.*

The positive equilibrium X^* is called a regular (virtual) equilibrium of model (3.6) if and only if $F^* + F_p < (>)\gamma M^*$ which is equivalent to $F_p < F_p^*$ where

$$F_p^* = \frac{1}{\alpha + \mu_M}\left(\gamma M^0 - \mu_M F^*\right) = \frac{\nu_E e^{-\tau_2 \mu_L}}{\mu_M + \alpha}\left[\gamma(1-r) - \frac{r\,\mu_M}{(\nu_F + \mu_F)}\right] E^* \tag{3.9}$$

Therefore, we deduce that

- If $F_p < F_p^*$, positive equilibrium X^* is a regular equilibrium of (3.6).
- If $F_p > F_p^*$, positive equilibrium X^* is a virtual equilibrium of (3.6).

The threshold F_p^* determines the maximum level of control below which the control has essentially no effect on an established mirid population. More precisely, as stated in the previous remark, the effect of pheromone releases is only limited to the males compartment, all other compartments remain at their natural equilibrium. Thus females will continue to deposit as many eggs (inside fruits) as before the control.

Thus, thanks to the (QM) condition, and, using Theorem 3.2, we deduce the following results in the DDE "male abundance" case:

Theorem 3.3. *(i) The system (3.6) defines a positive dynamical system on $\mathbb{R}^4_+$.*

(ii) System (3.6) always has one equilibrium, $\mathbf{0} = (0,0,0,0)$, which is globally asymptotically stable when $\mathcal{R} \leq 1$.

(iii) When $\mathcal{R} > 1$, model (3.6) has an additional (unique) positive equilibrium X^*, which is globally asymptotically stable on $\mathbb{R}^4_+ \setminus \{\mathbf{0}\}$

The positive equilibrium is a regular equilibrium if $F_p < F_p^*$ and it is a virtual equilibrium if $F_p > F_p^*$.

Remark 3.2. *As already highlighted for the non-delayed system, the threshold F_p^* determines the maximum level of control below which the control has essentially no effect on an established pest population for the delayed model.*

3.2.2 Case with male scarcity: $\gamma M < F + F_p$

In this case, the system can be written in the vector form

$$\frac{dx}{dt} = f_2(x, x_\tau), \tag{3.10}$$

with $x = (E, F, A, M)^T$ and f_2 is given by the equation (3.5).

Theorem 3.4. *: Existence and uniqueness of solutions*

The right hand side of system (3.10) is continuous and Lipschitzian in x. Thus, according to the standard theory od Delay Differential Equations [78], system admits a unique solution for each continuous initial condition $\varphi \in \mathcal{C}([-\tau, 0], \mathbb{R}^2_+)$ where $\tau = \max(\tau_2, \tau_3)$. The domain

$$\Omega := \quad \{x \in \mathbb{R}^4 : E \leq K,\ F < \frac{r\,\nu_E\,e^{-\tau_2\mu_L}\,K}{\mu_F},\ A \leq \frac{(1-r)\,\gamma\,\nu_F\,\nu_E\,e^{-\tau_2\mu_L}\,K}{\mu_A\,\mu_M},$$
$$M \leq \frac{(1-r)\,\nu_E\,e^{-\tau_2\mu_L}\,K}{\mu_M}\} \tag{3.11}$$

is positively invariant for system (3.10).

Proof:

Let $(t_0, X_0) = (E^0, F^0, A^0, M^0) \in \mathbb{R}_+ \times \mathbb{R}^4_+)$ and $([t_0, T[, X = (L, F_1, F_2, M))$ be the maximal solution of the delayed equation (3.10) with initial condition (t_0, X_0); $T \in]t_0, +\infty]$.

Let us prove that $E(t) \leq K$ for al $t \geq 0$.

Let us suppose that there exists $\varepsilon > 0$ such that

$$t_1 \leq t_1 + \varepsilon < T \quad \textit{and} \quad L(t_1 + \varepsilon) > K.$$

Let us define

$$t_1^* = \inf\{t \geq t_1,\ E(t) \geq K\}\ \textit{then}\ \ E(t_1^*) = K.$$

Thus,

$$E(t) = E(t_1^*) + \dot{E}(t_1^*)(t - t_1^*) + o(t - t_1^*) \quad \textit{and} \quad \dot{E}(t_1^*) = -(\nu_L + \mu_L)E(t_1^*) < 0.$$

So, there exists $\varepsilon_1 > 0$ such that

$$t_1^* \leq t < t_1^* + \varepsilon_1 \quad \textit{and} \quad E(t_1^*) < K.$$

This is absurd because $t_1^* = \inf\{t \geq t_1,\ E(t) \geq K\}$. Consequently, $E(t) \leq K$ for all $t \geq 0$. Moreover, we have:

$$\begin{aligned}
\dot{F}(t) &= r\,\nu_E\,e^{-\tau_2\mu_L}\,E(t-\tau_2) - \frac{\nu_F\,\gamma\,M(t)\,F(t)}{F(t)+F_p} - \mu_F\,F(t)\\
&\leq r\,\nu_E\,e^{-\tau_2\mu_L}\,E(t-\tau_2) - \mu_F\,F(t)\\
\dot{A}(t) &= \frac{\nu_F\,\gamma\,M(t)\,F(t)}{F(t)+F_p} - \mu_A\,A(t) \leq \nu_F\,\gamma\,M(t) - \mu_A\,A(t)\\
\dot{M}(t) &= (1-r)\nu_E e^{-\tau_2\mu_L}E(t-\tau_2) - \left(\mu_A + \alpha\frac{F_p}{F(t)+F_p}\right)M(t)\\
&\leq 1-r)\,\nu_E\,e^{-\tau_2\,\mu_L}\,E(t-\tau_2) - \mu_M\,M(t).
\end{aligned} \tag{3.12}$$

Solving Eq. (3.12), we have

$$F(t) \leq \frac{r\,\nu_E\,e^{-\tau_2\mu_L}\,K}{\mu_F};\quad M(t) \leq \frac{(1-r)\,\nu_E\,e^{-\tau_2\mu_L}\,K}{\mu_M};\quad A(t) \leq \frac{(1-r)\,\nu_E\,\nu_F\,\gamma\,e^{-\tau_2\mu_L}\,K}{\mu_A\,\mu_M} \tag{3.13}$$

The local existence and uniqueness of solutions follows from the standard DDE theory (since f is Lipschitz, which is the minimum required). Further, system (3.10) is dissipative. This provides the global existence of solutions on the interval $[0, +\infty)$.

□

Proposition 3.1. *There exists a threshold $F_p^{**} > 0$ of F_p such that*

- *If $F_p > F_p^{**}$ the only equilibrium os system (3.10) on $\mathbb{R}^4_+$ is $\mathbf{0}$.*
- *If $0 < F_p < F_p^{**}$, system (3.10) has three equilibria on $\mathbb{R}^4_+$, $\mathbf{0}$ and two positive equilibria.*

In addition, $\mathbf{0}$ is absolutely stable equilibrium.

Proof:

The proof follows the proof in [81], page 447. Setting the right-hand side of system (3.10) equal to zero, and after some straightforward calculations, we get the following equation in E to solve:

$$\psi(E) := E\,\xi(E)\,\phi(E) = \eta(F_p, E) \tag{3.14}$$

where

$$\xi(E) = \gamma\,(1-r)\,e^{-\tau_2\,\mu_L}\,\nu_E\,\nu_F\,e^{-\tau_3\,\mu_A}\,b\left(1-\frac{E}{K}\right) - \mu_A(\alpha+\mu_M)(\nu_E+\mu_E), \tag{3.15}$$

$$\eta(F_p, E) = \mu_A\,\mu_F\,\mu_M(\nu_E+\mu_E)\,b\,e^{-\tau_3\,\mu_A}\left(1-\frac{E}{K}\right)F_p \tag{3.16}$$

and

$$\phi(E) = b\,e^{-\tau_3\,\mu_A}\,r\,\nu_E\,e^{-\tau_2\,\mu_L}\left(1-\frac{E}{K}\right) - \mu_A\,(\nu_E+\mu_E). \tag{3.17}$$

Therefore, assuming that E_{eq} is a positive root of (3.14), the other components of the non trivial equilibria of (3.10) are:

$$F_{eq} = \frac{\phi(E_{eq})}{\mu_F\,b\,e^{-\tau_3\,\mu_A}\left(1-\frac{E}{K}\right)}\,E_{eq} \tag{3.18}$$

$$A_{eq} = \frac{(\nu_E+\mu_E)}{b\,e^{-\tau_3\,\mu_A}\left(1-\frac{E}{K}\right)}\,E_{eq} \tag{3.19}$$

$$M_{eq} = \frac{(1-r)\,\nu_E\,e^{-\tau_2\,\mu_L}}{\mu_M + \alpha\dfrac{F_p}{F_{eq}+F_p}}\,E_{eq}. \tag{3.20}$$

Further, to ensure $F_{eq} > 0$, we need to have $\phi(E_{eq}) > 0$, that is E_{eq} must satisfy the condition:

$$E_{eq} < K\left(1 - \frac{\mu_A\,(\nu_E + \mu_E)}{r\,b\,\nu_E\,e^{-\tau_2\,\mu_L}\,e^{-\tau_3\,\mu_F}}\right) \tag{3.21}$$

In fact, according to the definition of $\psi(E)$, it is straightforward to check that *psi* admits two real positive roots on $[0,\, K]$,

$$E_1 = \left(1 - \frac{\mu_A\,(\nu_E + \mu_E)}{r\,b\,e^{-\tau_2\,\mu_L}\,e^{-\tau_3\,\mu_A}}\right)K \quad \textit{and} \quad E_2 = \left(1 - \frac{\mu_A\,(\nu_E + \mu_E)(\alpha + \mu_M)}{\gamma\,(1-r)\,b\,\nu_E\,\nu_F\,e^{-\tau_2\,\mu_L}\,e^{-\tau_3\,\mu_A}}\right)K$$

provided that

$$\frac{\mu_A\,(\nu_E + \mu_E)}{r\,b\,e^{-\tau_2\,\mu_L}\,e^{-\tau_3\,\mu_A}} < 1 \quad \textit{and} \quad \frac{\mu_A\,(\nu_E + \mu_E)(\alpha + \mu_M)}{\gamma\,(1-r)\,b\,\nu_E\,\nu_F\,e^{-\tau_2\,\mu_L}\,e^{-\tau_3\,\mu_A}} < 1.$$

Thus, only the points of intersection between the straight line $\eta(F_p, E)$ and the cubic $\psi(E)$ that belong to $[0,\, \min\{E_1,\, E_2\}]$ are intersect for us: see Fig 3.4, 84. We denote by F_p^{**} the value of F_p

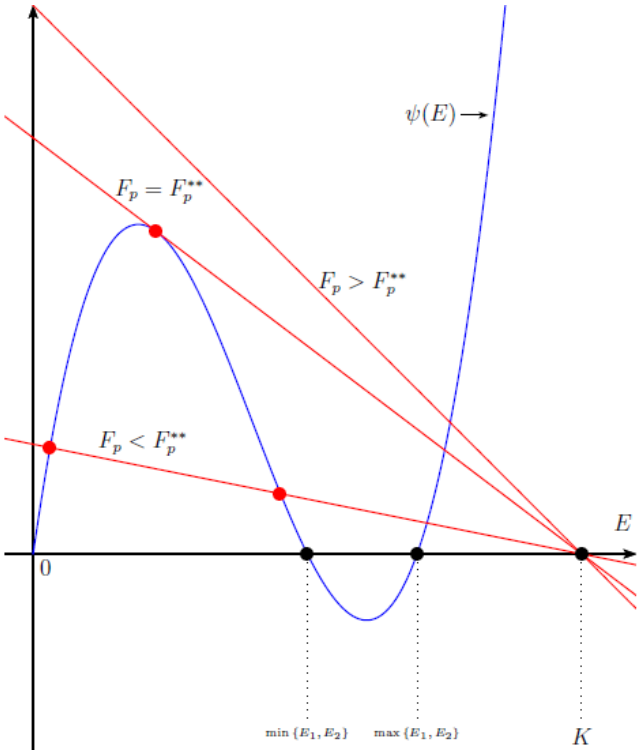

Figure 3.4: Intersection between $\psi(E)$ (in blue) and $\eta(F_p, E)$ (in red) for three values of F_p

such that the line $\eta(F_p, E)$ is tangent to the indicated section of the graph ϕ. Then, it is clear that for $F_p > F_p^{**}$ there is no intersection between $\eta(F_p, E)$ and ψ (no positive equilibrium) while if $0 < F_p < F_p^{**}$, there are two such points of intersection (2 positive equilibria).

Finally, straightforward calculations shows that trivial equilibrium **0** is an absolutely stable equilibrium of system (3.10)

□

3.2.3 Study of the bifurcation for the threshold F_p^* and F_p^{**}

Assume $0 < F_p < F_p^{**}$. Let $E_{eq}^{(1)}$ and $E_{eq}^{(2)}$, $E_{eq}^{(1)} < E_{eq}^{(2)}$ be the roots of (3.14) when $0 < F_p < F_p^{**}$ and denote the respective equilibria by $X^{(1)}$ and $X^{(2)}$. To show that any equilibrium of (3.10) is a regular equilibrium of 3.1, we need to show that it belongs to the male scarcity region. Using the previous relationships, it suffices to study the sign of $F_{eq} + F_p - \gamma\, M_{eq}$.

In fact,

$$F_{eq} + F_p - \gamma\, M_{eq} = \frac{1}{\mu_M + \alpha \dfrac{F_p}{F_{eq} + F_p}} (\mu_M\, (F_{eq} + F_p) + \alpha\, F_p - \gamma\, (1 - r)\, \nu_E\, e^{-\tau_2\, \mu_L}\, E_{eq})$$

Thus, studying the sign of $F_{eq} + F_p - \gamma\, M_{eq}$ is equivalent to study the sign of

$$\Gamma = \mu_M\, F_{eq} - \gamma\, (1 - r)\, \nu_E\, e^{-\tau_2\, \mu_L}\, E_{eq}) + (\alpha + \mu_M)\, F_p.$$

In fact we have

$$\begin{aligned}
\Gamma &= \left(\mu_M \frac{\phi(E_{eq})}{\mu_F\, b\, e^{-\tau_3\, \mu_A} \left(1 - \dfrac{E_{eq}}{K}\right)} - \gamma\, (1 - r)\, \nu_E\, e^{-\tau_2\, \mu_L} \right) E_{eq} + (\alpha + \mu_M)\, F_p \\
&= r\, \nu_E\, e^{-\tau_2\, \mu_L} \left(\frac{r\, \mu_M}{\mu_F} - \frac{\mu_M\, \mu_A\, (\nu_E + \mu_E)}{\mu_F\, b\, e^{-\tau_3\, \mu_A} \left(1 - \dfrac{E_{eq}}{K}\right)} - \gamma\, (1 - r) \right) E_{eq} + (\alpha + \mu_M)\, F_p
\end{aligned}$$

Using the inequality $E_{eq}^{(1)} < E_{eq}^{(2)} < E^*$, we have:

$$\begin{aligned}
\Gamma &\geq r\, \nu_E\, e^{-\tau_2\, \mu_L} \left(\frac{r\, \mu_M}{\mu_F} - \frac{\mu_M\, \mu_A\, (\nu_E + \mu_E)}{\mu_F\, b\, e^{-\tau_3\, \mu_A} \left(1 - \dfrac{E^*}{K}\right)} - \gamma\, (1 - r) \right) E_{eq} + (\alpha + \mu_M)\, F_p \\
&= r\, \nu_E\, e^{-\tau_2\, \mu_L} \left(\frac{r\, \mu_M}{\mu_F} - \frac{\mu_M\, \mu_A\, (\nu_E + \mu_E)\, \mathcal{R}}{\mu_F\, b\, e^{-\tau_3\, \mu_A}} - \gamma\, (1 - r) \right) E_{eq} + (\alpha + \mu_M)\, F_p \\
&= r\, \nu_E\, e^{-\tau_2\, \mu_L} \left(\frac{r\, \mu_M}{\nu_F + \mu_F} - \gamma\, (1 - r) \right) + (\alpha + \mu_M)\, F_p
\end{aligned}$$

Using (3.9), page 81, we deduce

$$(\mu_M\, F_{eq} - \gamma\, (1 - r)\, \nu_E\, e^{-\tau_2\, \mu_L}\, E_{eq}) + (\alpha + \mu_M)\, F_p = \frac{(\alpha + \mu_M)}{E^*} (F_p\, E^* - E_{eq}\, F_p^*).$$

Since $E_{eq}^{(1)} < E_{eq}^{(2)} < E^*$, then $F_p\, E^* - E_{eq}\, F_p^* > (F_p - F_p^*)\, E_{eq}$. Using the fact that $F_p^* < F_p$, then $F_p\, E^* - E_{eq}\, F_p^* > 0$, such that $F_{eq} + F_p - \gamma\, M_{eq} > 0$. Therefore, in this case, $X^{(1)}$ and $X^{(2)}$ are both in the male scarcity region. Hence, they are also equilibria of (3.2).

If $F_p < F_p^*$ and $E_{eq} > E^*$, considering the fact that for $0 < F_p < F_p^*$, we have $E_{eq}^{(1)} < E^* < E_{eq}^{(2)}$ and using the same method as previously, we obtain $F_p + F_{eq} - \gamma\, M_{eq} < 0$. Therefore, $X^{(2)}$ is not in

the male scarcity region. Hence, it is not an equilibrium of (3.2). Taking into consideration the above results regarding $X^{(1)}$ and $X^{(2)}$, we obtain the following theorem for the model (3.2).

Theorem 3.5. *Let $F_p > 0$. The following holds for model (3.2):*

(a) Trivial equilibrium $\mathbf{0}$ *is an asymptotically stable equilibrium.*

(b) If $0 < F_p < F_p^*$, there are two positive equilibria $X^{(1)}$ and x^*, where x^* is asymptotically stable.

- *If $F_p^* < F_p < F_p^{**}$, there are two positive equilibria $X^{(1)}$ and $X^{(2)}$.*
- *If $F_p > F_p^{**}$, there is no positive equilibrium*

3.2.4 Long term behaviour of system (3.2) when $F_p > 0$

The previous theorem shows us that the dynamics of the system may vary according to the level of control. In particular, as long as $0 < F_p < F_p^*$, the control has essentially no effect on an established population. Even if $F_p^* < F_p < F_p^{**}$, the effect are negligible (on an established population). here, we intend to derive results that may help us to define appropriate control strategies.

Due to the term $-\nu_F \dfrac{\gamma\, M(t)}{F(t)+F_p}\, F(t)$ in the equation for the F compartment, the right hand side of (3.10) is not quasi-monotone. By removing this non-linear term, we obtain an upper DDE system, that admits a unique positive equilibrium $\overline{x}$ that is an upper solution of (3.10). Since $f_2(x,y)$ is non decreasing in y, according to Theorem 3.6 in [87], we deduce $x \leq \overline{x}$.

Thus, following [81], we consider the following upper system, as an auxiliary system of system (3.10):

$$\frac{dx}{dt} = g_2(x, x_\tau), \tag{3.22}$$

with $x = (E, F, A, M)^T$ and

$$g_2(x) = \begin{pmatrix} b\, e^{-\tau_3 \mu_A}\, A(t-\tau_3) \left(1 - \dfrac{E(t)}{K}\right) - (\nu_E + \mu_E)\, E(t) \\ r\, \nu_E\, e^{-\tau_2 \mu_L}\, E(t-\tau_2) - \mu_F\, F(t) \\ \nu_F\, \dfrac{\gamma\, M(t)}{F(t)+F_p}\, F(t) - \mu_A\, A(t) \\ (1-r)\, \nu_E\, e^{-\tau_2 \mu_L}\, E(t-\tau_2) - \left(\mu_A + \alpha \dfrac{F_p}{F(t)+F_p}\right) M(t) \end{pmatrix} \tag{3.23}$$

System (3.22) is cooperative time delayed system: The QM condition is verified. Hence, the stability of each equilibrium for the non delayed model is preserved for the delayed system. It suffices to study the non delayed system

$$\frac{dx}{dt} = g(x) \tag{3.24}$$

to deduce the long term behaviour of the time delayed system.

Let us first set

$$\mathcal{R}_M = \frac{(1-r)\,b\,\nu_E\,\gamma\; nu_F\, e^{-\tau_2\,\mu_L}\, e^{-\tau_3\,\mu_A}}{\mu_A\,\mu_M\,(\nu_E+\mu_E)} \tag{3.25}$$

While $\mathcal{R}$, the basic offspring number, represents the number of offsprings produced by one single female during its mean lifespan, $\mathcal{R}_M$ represents the number of offsprings produced by one male during its mean lifespan.

We have the following result:

Theorem 3.6. *1. The non delayed system (3.24) defines a positive dynamical system on $\mathbb{R}^4_+$.*

2. There exists a threshold value $\overline{F}_p^{**}$ such that

(i) if $F_p > \overline{F}_p^{**}$, trivial equilibrium $\mathbf{0}$ is GAS on $\mathbb{R}^4_+$

(ii) If $F_p = \overline{F}_p^{**}$ and $\mathcal{R}_M > 1$, then system (3.24) has two equilibria: $\mathbf{0}$ and one positive equilibrium $\bar{X}_1$. The basin of attraction of trivial equilibrium contains the set $\{x \in \mathbb{R}^4_+ : 0 \le x \le \bar{X}_1\}$. The basin of attraction of $\bar{X}_1$ contains the set $\{x \in \mathbb{R}^4_+ : x \ge \bar{X}_1,\, E \le K\}$.

- *if $0 < F_p < \overline{F}_p^{**}$ and $\mathcal{R}_M > 1$, then system (3.24)*

The first assertion is obvious. Setting the first, second, and fourth terms in (3.23) equal to zero, we derive

$$\bar{F} = \frac{r\,\nu_E\, e^{-\tau_2\mu_L}}{\mu_F}\bar{E}, \quad \bar{A} = \frac{(\nu_E+\mu_E)}{b\, e^{-\tau_3\,\mu_A}\left(1-\dfrac{\bar{E}}{K}\right)}\bar{E}, \quad \bar{M} = \frac{((1-r)\,\nu_E\, e^{-\tau_2\,\mu_L})\,(\bar{F}+F_p)}{\mu_M\,\bar{F}+(\mu_M+\alpha)\,F_p}\bar{E}$$

Solving the third equation equal to zero and substituting the expressions for $\bar{F}$, $\bar{A}$ and $\bar{M}$ above, we obtain an equation for $\bar{E}$ in the form

$$E\phi(E) = \eta(F_p, E), \tag{3.26}$$

with

$$\begin{aligned} \eta(F_p, E) &= \mu_M r \nu_E e^{-\tau_2\mu_L} E + \mu_F\,(\alpha+\mu_M)\,F_P \\ \phi(E) &= (\mu_F+\nu_F)(1-r)\nu_E e^{-\tau_2\mu_L}\gamma\mathcal{R}\left(1-\frac{E}{K}\right) \end{aligned} \tag{3.27}$$

In other words, if (3.26) admits roots, they are intersection between a parabola and a straight line: see Fig. 3.5, page 88.

In fact, solving (3.26) is equivalent to solve the following quadratic equation

$$\begin{aligned} \frac{\mathcal{R}(1-r)\nu_E e^{-\tau_2\mu_L}\,(\nu_F+\mu_F)\,\gamma}{K}E^2 + \nu_E e^{-\tau_2\mu_L}\,(\mu_M r - \mathcal{R}(1-r)\,(\nu_F+\mu_F)\,\gamma)\,E + \\ +\mu_F\,(\alpha+\mu_M)\,F_p = 0. \end{aligned}$$

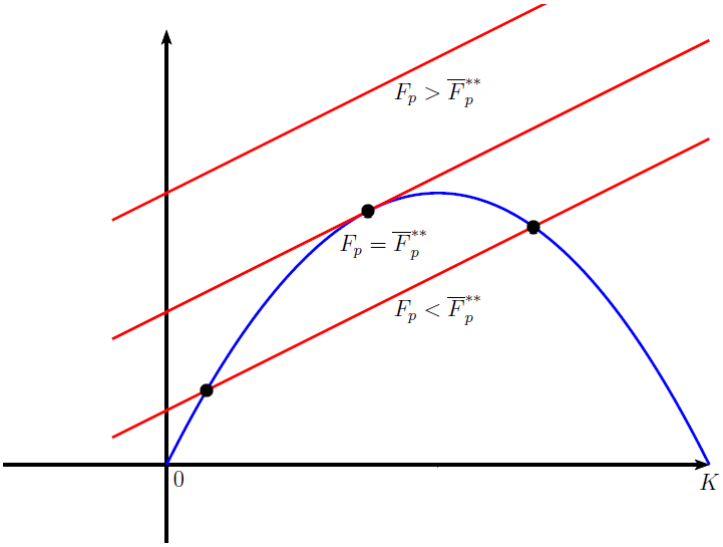

Figure 3.5: Intersections between the graphs of $E\phi(E)$ (in blue) and $\eta(F_p, E)$ (in red) for different values of F_p. The black dots represent the intersection points on the interval $[0, K]$.

Then, we estimate the discriminant

$$\Delta = \left(\nu_E e^{-\tau_2 \mu_L} \left(\mu_M r - \mathcal{R}(1-r)\left(\nu_F + \mu_F\right)\gamma\right)\right)^2 - 4\frac{\mathcal{R}(1-r)\nu_E e^{-\tau_2\mu_L}\left(\nu_F+\mu_F\right)\gamma}{K}\mu_F\left(\alpha+\mu_M\right)F_p$$

or equivalently

$$\Delta = \left(\nu_E e^{-\tau_2 \mu_L} \mu_M r \left(1 - \mathcal{R}_M\right)\right)^2 - 4\frac{\mathcal{R}(1-r)\nu_E e^{-\tau_2\mu_L}\left(\nu_F+\mu_F\right)\gamma}{K}\mu_F\left(\alpha+\mu_M\right)F_p$$

Clearly, if $F_p > \overline{F}_p^{**}$, with

$$\overline{F}_p^{**} = \frac{\left(\nu_E e^{-\tau_2 \mu_L} \mu_M r \left(1 - \mathcal{R}_M\right)\right)^2}{4\mathcal{R}(1-r)\left(\nu_F+\mu_F\right)\gamma\mu_F\left(\alpha+\mu_M\right)}K,$$

then $\Delta < 0$, and no positive real roots exist. Otherwise, when $F < \overline{F}_p^{**}$, two real roots exist. If in addition, we assume that

$$\mathcal{R}_M > 1,$$

then, we obtain the following positive real roots $\bar{E}_1 < \bar{E}_2$:

$$\bar{E}_1 = \frac{1}{2}\left(\frac{\nu_E e^{-\tau_2\mu_L}\mathcal{R}(1-r)\left(\nu_F+\mu_F\right)\gamma - \mu_M r - \sqrt{\Delta}}{\mathcal{R}(1-r)\nu_E e^{-\tau_2\mu_L}\left(\nu_F+\mu_F\right)\gamma}\right)K$$

$$\bar{E}_2 = \frac{1}{2}\left(\frac{\nu_E e^{-\tau_2\mu_L}\mathcal{R}(1-r)\left(\nu_F+\mu_F\right)\gamma - \mu_M r + \sqrt{\Delta}}{\mathcal{R}(1-r)\nu_E e^{-\tau_2\mu_L}\left(\nu_F+\mu_F\right)\gamma}\right)K.$$

Using (3.26) and (3.27), it is straightforward to show that $\bar{E}_1 < \bar{E}_2 < K$. Assume $F_p > \overline{F}_p^{**}$, then

setting

$$\bar{y}_q = \begin{pmatrix} K \\ \dfrac{r\,\nu_E\,e^{-\tau_2\mu_L}}{\mu_F}q \\ \dfrac{\gamma\nu_F(1-r)\,\nu_E\,e^{-\tau_2\,\mu_L}}{\mu_M} \\ \dfrac{(1-r)\,\nu_E\,e^{-\tau_2\,\mu_L}}{\mu_M} \end{pmatrix},$$

where q is any real number, such that $q \geq K$. We check that $g_2(\bar{y}_q, \bar{y}_q) \leq 0$. Thus, by Theorem 7 [81], $\mathbf{0}$ is GAS on $\Omega_K = \bigcup_{q\geq K}[\mathbf{0}, \bar{y}_q]$, which implies that $\mathbf{0}$ is GAS on $\mathbb{R}^4_+$ since Ω_K is an absorbing set.

□

Using the previous results, and assuming $\mathcal{R} > 1$ and $\mathcal{R}_M > 1$, we can deduce the following results for the delayed system (3.22)

Theorem 3.7. *There exists a threshold value $\overline{F}_p^{**}$ such that*

(i) if $F_p > \overline{F}_p^{**}$, $\mathbf{0}$ is the only equilibrium for the system (3.22)

(ii) if $0 < F_p < \overline{F}_p^{**}$, $\mathcal{R} > 1$, and $\mathcal{R} > \dfrac{\mu_M r}{(1-r)\,(\nu_F+\mu_F)\,\gamma}$, we have $\bar{E}_1$, $\bar{E}_2 \in [0, K]$.the system has three equilibria: trivial equilibrium $\mathbf{0}$ and two positive equilibria $\bar{X}_1$ and $\bar{X}_2$ such that $\bar{X}_1 < \bar{X}_2$.

Since model (3.22) is a delayed cooperative model, we can deduce from [81] the following result about the stability of equilibria:

Theorem 3.8. *Let $F_p > 0$. Then, the following holds for the model (3.22):*

- *If $0 < F_p \leq \overline{F}_p^{**}$, then the basin of attraction of the trivial equilibrium contains $\{x \in \mathbb{R}^4_+ : x \leq \bar{X}_{1,F_p}\}$.*
- *If $F_p \geq \overline{F}_p^{**}$, then trivial equilibrium is GAS on $\mathbb{R}^4_+$.*

Finally we can deduce the following GAS result for the PWS-DDE system (3.1).

Theorem 3.9. *Let $F_p > 0$ then the following hold for the model (2.1):*

- *If $0 < F_p \leq \overline{F}_p^{**}$, then the basin of attraction of $\mathbf{0}$ contains $\{x \in \mathbb{R}^4_+ : x \leq \bar{X}_{1,F_p}\}$.*
- *If $F_p \geq \overline{F}_p^{**}$, then $\mathbf{0}$ is GAS on $\mathbb{R}^4_+$.*

In fact, the last theorem is very useful to derive a long term control strategy. Indeed, if the control stops, the system will automatically recover. In the other hand, using only long time massive releases of pheromones is not a sustainable option. However, we know that once the non-massive control starts, i.e. $0 < F_p < F_p^{**}$, the system become bistable, such that locally, at least in $\{x \in \mathbb{R}^4_+ : x \leq \bar{X}_{1,F_p}\}$, $\mathbf{0}$ is stable and attractive, for a given (small) amount of pheromones, F_p.

3.2.5 Control strategy related to the level of infestation of Mirids

The previous theoretical results highlighted two strategies

- When the mirid population is small or at an invading stage (not established in the field, but starting to settle), thanks to the size of the plot, a limited number of traps (small of pheromones) can be sufficient to control it. In other words, knowing the the population size, it could be possible to estimate F_p such that the mirid population belongs to the basin of attraction of $\mathbf{0}$ for a certain amount of Pheromone, $0 < F_p < \overline{F}_P^{**}$.
- When the population is large, at equilibrium for instance, then, to reduce the population, we need to increase the number of traps in order to release enough pheromones/Fake females to use the GAS property of $\mathbf{0}$ when $F_P > \overline{F}_P^{**}$. This is what we called the "maximal treatment". Thus, according to the GAS of $\mathbf{0}$, there exists $t^* > 0$, such that for $t > t^*$, the mirid population become small enough such that a small amount of pheromones is sufficient to maintain the population under a given threshold, $X^{(1)}$, the lowest equilibrium for a given (low preferably) amount of pheromones $F_p^{(1)} << \overline{F}_p^{**}$. This is what we called the "minimal treatment". Altogether, when the population is large, the best way to control it is to consider a maximal treatment, followed by a minimal treatment.

To summarize the "maximal-minimal treatment" strategy: for a given amount of pheromones, $F_p > \overline{F}_P^{**}$, it suffices to estimates the time, t^*, necessary to enter $[\mathbf{0}, X^{(1}[$ for a given amount $F_p^{(1)} << \overline{F}_P^{**}$. Since $X^{(1)}$ cannot be estimated analytically, we can only estimate the minimum time, t^*, numerically. This is what is illustrated in the next subsection.

3.2.6 Applications - Numerical simulations

In this section, we will prove numerically the theoretical results obtained. The values used for the next simulations are given in Table 3.2, page 90 (taken from [4]), leading to the case $\mathcal{R} = 4.5547 > 1$ and $\mathcal{R}_M = 7.4211$.

b	r	K	$1/\nu_L$	$1/\nu_F$	μ_L	μ_A	μ_M	μ_F	μ_E	$1/\nu_E$	α	γ
3.28	0.58	5000	25	10	0.01	0.08	0.08	0.08	0.001	15	0.1	1

Table 3.2: Values used for simulations of model (2.1) with $\mathcal{R} > 1$ [4] and $\mathcal{R}_M > 1$

According to the theoretical part and the parameters values, for a maximal control, we need to release more than $\overline{F}_p^{**} \approx 1162$ fake females (per ha), in other words for any value of F_p larger

than $\overline{F}_p^{**}$, the system will converge to $\mathbf{0}$ for t sufficiently large. However, as explained above, we are not interested in a permanent maximal treatment, but we only want to reach (rapidly) a level of population where the damages can be acceptable and where the population can be controlled with a small amount of pheromones. That is why we choose $F_p^{(1)}$ to estimate $X^{(1)}$ and thus target the box $[\mathbf{0}, X^{(1)} - \epsilon]$, for a given $0 < \epsilon << 1$. In the sequel, we initiate the simulations at the wild equilibrium. We choose $F_p = 100$ such that we estimate numerically $X^{(1)} = (95.1836, 35.8291, 4.4550, 13.5112)$ (the red dot in Fig. 3.7, page 92). Hence, in the next simulations, for a given $F_p > \overline{F}_p^{**}$, we estimate the minimum time necessary to enter $[\mathbf{0}, X^{(1)} - \epsilon]$. In Figs. 3.6 and 3.7, page 91, we present an example

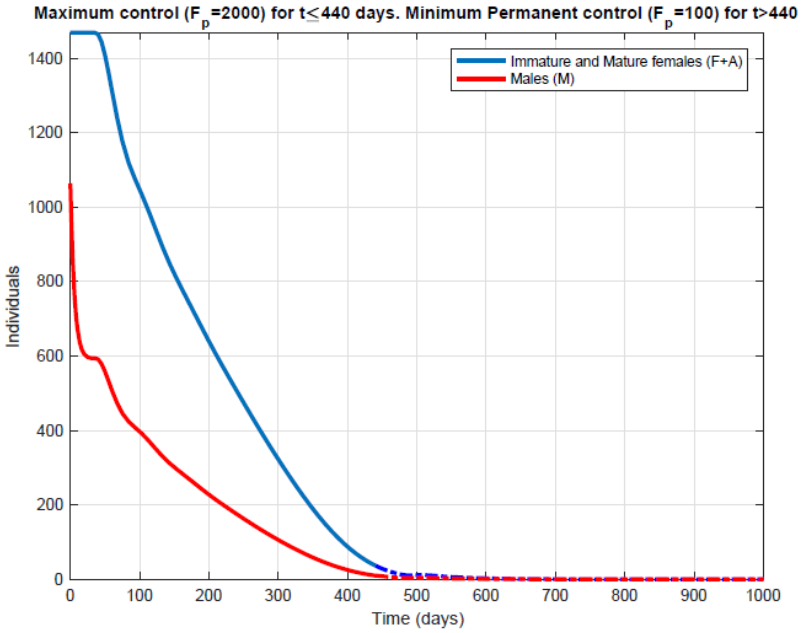

Figure 3.6: Mating disruption and Trapping Control with, first $F_p = 2000$, then $F_p = 100$ once the system has reach the basin of attraction of $\mathbf{0}$ for $F_p = 100$.

of the control strategy described above: first, we consider a large amount of pheromones traps, such that $F_p = 2000$, to use the GAS property of $\mathbf{0}$, in order to reach the box $[\mathbf{0}, X^{(1)}[$, where $X^{(1)}$ is estimated based on the targeted level of control, i.e. $F_p^{(1)} = 100$. Numerically, we estimate that 440 days of maximum treatment are necessary to enter the basin $[\mathbf{0}, X^{(1)}[$. Then, for all $t > 440$ days, we remove some pheromones traps in order to reach the value $F_p^{(1)} = 100$: the system continues to converge to $\mathbf{0}$, thanks to the LAS property of $\mathbf{0}$ in $[\mathbf{0}, X^{(1)}[$, when $F_p^{(1)} = 100$.

Note, that the previous results correspond to the case when male trapping occurs, $\alpha = 0.1$. If we assume that there is no trapping, i.e. $\alpha = 0$, then the $M_{T_1} \approx 3576$, and also the minimal time necessary to enter the basin $[\mathbf{0}, X^{(1)}[$ increases to 536 days but we have to use the double amount of pheromones (fake females) $M_T = 4000$. That is why the combination of mating disruption and

trapping is of utmost importance, not only to minimize the duration of the treatment but also to minimize the release of pheromones.

Fig. 3.7(a) shows different phase of the control: a first phase, where only the male population is reducing, then the eggs population, before the whole system $(E + F + A + M)$ starts to decay. This shows that in constant environmental conditions (constant parameters) the duration of the control is crucial. In Fig. 3.7(b), the green box represents the basin $[\mathbf{0}, X^{(1)}]$: the red trajectory represents the trajectory when the control is defined by $F_p = 100$. Of course, in that case, since $\mathbf{0}$ is LAS in $[\mathbf{0}, X^{(1)}]$, the system continues to decay (slowly) to $\mathbf{0}$.

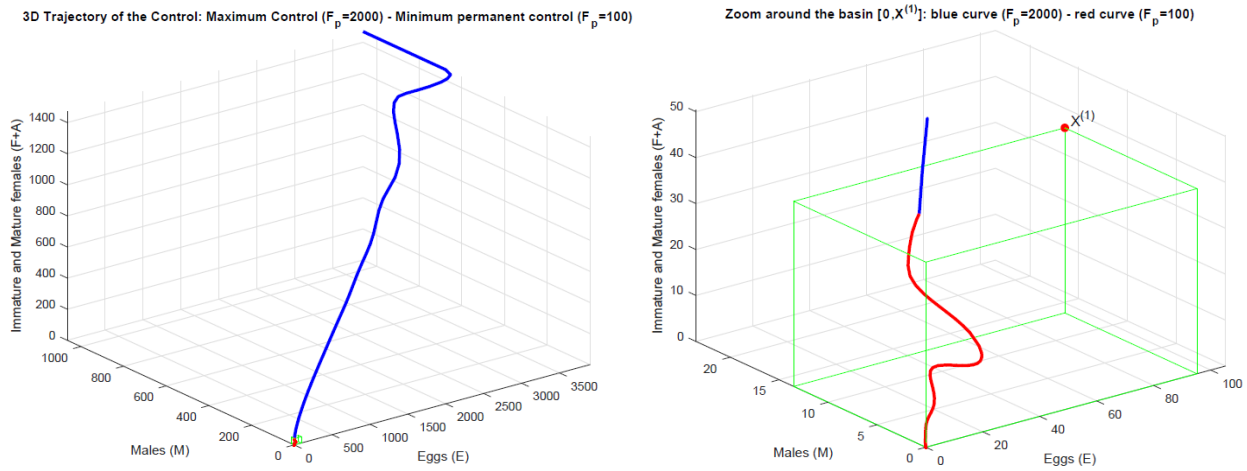

Figure 3.7: Control with first $F_p = 2000$, then $F_p = 100$ once the system has reach the basin of attraction of $\mathbf{0}$ for $F_p = 100$.

Of course, the time necessary to enter the basin $[\mathbf{0}, X^{(1)}]$ depends on the initial maximum control, the larger, the shorter the time needed. However, as showed in Fig. 3.8, page 93, it seems that choosing F_p between 2000 and 4000 provides the more interesting results. However, the cost of pheromones need to be taken into account in order to derive the best strategies. The previous strategy is based on two given values for F_p. Other strategies based on the use of several values for F_p could be chosen in order to reduce progressively the amount of pheromones and to use the LAS of $\mathbf{0}$ in the box $[\mathbf{0}, X^{(1)}_{F_p}]$, for a given F_p. However, from a practical point of view, reducing F_p, while convenient on the paper, seems to be more difficult from a practical point of view.

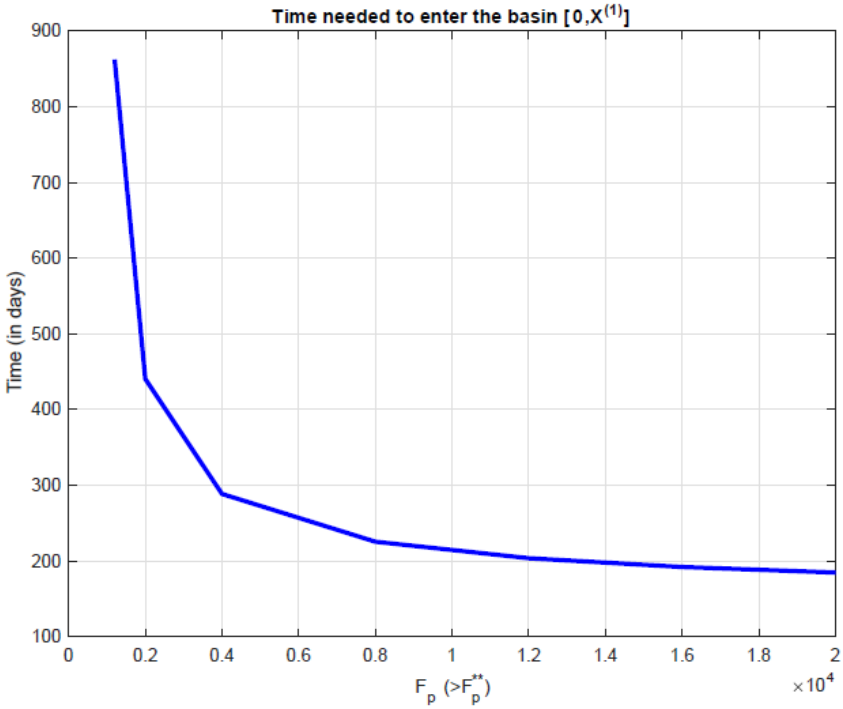

Figure 3.8: Time needed to enter the basin $[\mathbf{0}, X^{(1)}]$ for a given $F_p > F_p^{**}$.

3.3 About mating disruption strategy when the pods carrying capacity is periodic

Like in [4], we have to consider that the mirid population dynamics is mainly related to the presence/absence of pods, but not only. Indeed, the cacao production in Cameroon is seasonal, which is not the case, for instance, in Central America. Thus, in Cameroon, the pods carrying capacity, K, is not constant but has to be approximated by a yearly periodic function. Last but not least, we know that, in the absence of pods, mirids can maintain in the area using secondary host plants, like *Cola nitida*, or *Ceiba pentandra* [1]. Thus finally, we consider the following pods carrying capacity $K(t) + C$, where $C > 0$ is a given constant, equal to 100 [4], and $K(t)$ is defined as in [4] (see Table 1.2, page 10).

In that case, the control strategy is rather different than in the constant coefficients case. Here, knowing the inter-period (from March to June), when no cocoa pods are available, is rather crucial: it seems obvious to start the control at the beginning of this period , i.e. in March, in order to use the LAS property of model (3.3), when $K(t) \equiv 0$, to avoid the establishment of the mirid population within the cocoa plantation when $K(t)$ rises again (in July).

3.3 About mating disruption strategy when the pods carrying capacity is periodic

We thus consider the following non-autonomous periodic DDE-PWS system

$$\frac{dx}{dt} = f(x, x_\tau, t) := \begin{cases} f_1(x, x_{\tau_2}, x_{\tau_3}, t) & \text{if} \quad F + F_p \leq \gamma\, M \\ f_2(x, x_{\tau_2}, x_{\tau_3}, t) & \text{if} \quad F + F_p \geq \gamma\, M \end{cases} \tag{3.28}$$

where $x = (E, F, A, M)^t$,

$$f_{1,per}(x, x_\tau, t) = \begin{pmatrix} b\, e^{-\tau_3\, \mu_A}\, A(t-\tau_3) \left(1 - \dfrac{E(t)}{C + K(t)}\right) - (\nu_E + \mu_E)\, E(t) \\ r\, \nu_E\, e^{-\tau_2\, \mu_L}, E(t-\tau_2) - (\nu_F + \mu_F)\, F(t) \\ \nu_F\, F(t) - \mu_A\, A(t) \\ (1-r)\, \nu_E\, e^{-\tau_2\, \mu_L}\, E(t-\tau_2) - \left(\mu_M + \alpha \dfrac{F_p}{F(t) + F_p}\right) M(t) \end{pmatrix} \tag{3.29}$$

and

$$f_{2,per}(x, x_\tau, t) = \begin{pmatrix} b\, e^{-\tau_3\, \mu_A}\, A(t-\tau_3) \left(1 - \dfrac{E(t)}{C + K(t)}\right) - (\nu_E + \mu_E)\, E(t) \\ r\, \nu_E\, e^{-\tau_2\, \mu_L}\, E(t-\tau_2) - \nu_F \gamma \dfrac{M(t)}{F(t) + F_p}\, F(t) - \mu_F\, F(t) \\ \nu_F\, \gamma \dfrac{F(t)}{F(t) + F_p}\, M(t) - \mu_A\, A(t) \\ 1-r)\, \nu_E\, e^{-\tau_2\, \mu_L}\, E(t-\tau_2) - \left(\mu_M + \alpha \dfrac{F_p}{F(t) + F_p}\right) M(t) \end{pmatrix} \tag{3.30}$$

The methodology to study the periodic PWS-DDE (3.28) follows the methodology of the previous sections, thanks to the fact that $0 < C \leq K(t) \leq K_{\max} + C$. Indeed, for $i = 1, 2$, it is straightforward to check that

$$f_{i,C}(x, x_\tau) \leq f_{i,per}(x, x_\tau, t) \leq f_{i,C+K_{\max}}(x, x_\tau), \quad \text{for all } t > 0. \tag{3.31}$$

1. In the male abundance case, $f_{1,C}$ and $f_{1,C+K_{\max}}$ are delayed system that verify the (QM) condition. Thus, using (3.31), and applying Theorem 5.1.1 [66], we deduce that

$$x_{1,C}(t) \leq x_{1,per}(t) \leq x_{1,C+K_{\max}}(t), \quad \text{for all } t > 0.$$

where $x_{1,per}$ is the solution of the periodic male abundance equation, $x_{1,C}$ and $x_{1,C+K_{\max}}$ are respectively solutions of the autonomous male abundance system (3.6), with $K \equiv C$ and $K \equiv C + K_{\max}$ respectively. Thus, using Theorem 3.3, page 81, we can deduce

Theorem 3.10.

- *Assume $\mathcal{R}_0 < 1$, then $x_{1,per}$ converges to* $\mathbf{0}$.
- *Assume $\mathcal{R}_0 > 1$, then the male abundance system is permanent, i.e. $x_{1,per} > 0$ for all $t > 0$.*

where $\mathcal{R}_0$ is defined in (3.8).

Remark 3.3. *Following [4], when $\mathcal{R}_0 > 1$, it is possible to show that the male abundance system converges to a unique periodic solution, $x^*_{per}(t)$, defined as follows:*

$$E^*_{per}(t) = \left(1 - \frac{1}{\mathcal{R}}\right)(C + K(t)), \quad F^*_{per}(t) = \frac{r\,\nu_E\,e^{-\tau_2\,\mu_L}}{\mu_F + \nu_F}\,E^*_{per}(t),$$

$$A^*_{per}(t) = \frac{\nu_F}{\mu_A}\,F^*_{per}(t), \quad M^*_{per}(t) = \frac{(1-r)\,\nu_E\,e^{-\tau_2\,\mu_L}}{\mu_M + \alpha\,\dfrac{F_p}{F^*_{per}(t) + F_p}}\,E^*_{per}(t).$$

2. The male scarcity case is rather more difficult to study. However, we can use the second inequality (3.31): $f_{2,per}(t,x,y)$ is nondecreasing in y; thus, according to Theorem 3.6 in [87], page 29, we deduce that $x_{2,per} \leq x_{2,C+K_{\max}}$, such that the methodology developed in section 3.2.2, page 81, can be applied to the system

$$\frac{dx}{dt} = f_{2,C+K_{\max}}(x, x_\tau).$$

Hence, we deduce that there exists $\overline{F}^{**}_{p,C+K_{\max}} > 0$ such that $\mathbf{0}$ is GAS when $F_p > \overline{F}^{**}_{p,C+K_{\max}} > 0$, i.e. $x_{2,C+K_{\max}}$ converges to $\mathbf{0}$ and so is $x_{2,per}$ as t goes to $+\infty$.

However, for a practical application, this result is not interesting since the amount of pheromones to release can be very large.

Another possibility is to focus on the case where $K \equiv 0$ from March to June, such that we know that periodic system reduces to the autonomous system with carrying capacity C, in other word: $f_{i,per}(x, x_\tau) = f_{i,C}(x, x_\tau)$. In that case, we are able to estimate $\overline{F}^{**}_{p,C}$. When $C = 100$, then $\overline{F}^{**}_{p,C} \approx 23.23$

3.3.1 Periodic case - Simulations

As explained above we focus on the period from March to June, i.e, we adapt the starting time of our control: either a the end of Period or at the beginning. Then, we consider two starting times: $t = 390$ (beginning of July), see Fig. 3.10; and $t = 300$ (beginning of March), see Fig. 3.11. When choosing $F_p = 20$ as the targeted amount of pheromones, we are looking at the time t^* necessary to enter $[\mathbf{0}, X^{(1)}[$, with $X^{(1)} = (27.11, 10.20, 1.70, 4.04)$.

As illustrated in Fig. 3.10, starting lately within the no-production period, at $t = 390$, will have an effect during the production period, with a population fourth times less than without control, and it is only after 470 days of $F_p = 100$ treatment that the trajectory enter the box $[\mathbf{0}, X^{(1)}[$ and then continues to decay to zero with $F_p = 20$.

In contrary, starting the treatment early, at $t = 300$, within the no-production period, the population decreases rapidly, and in 217 days, the trajectory enter the box $[\mathbf{0}, X^{(1)}[$ and then continues

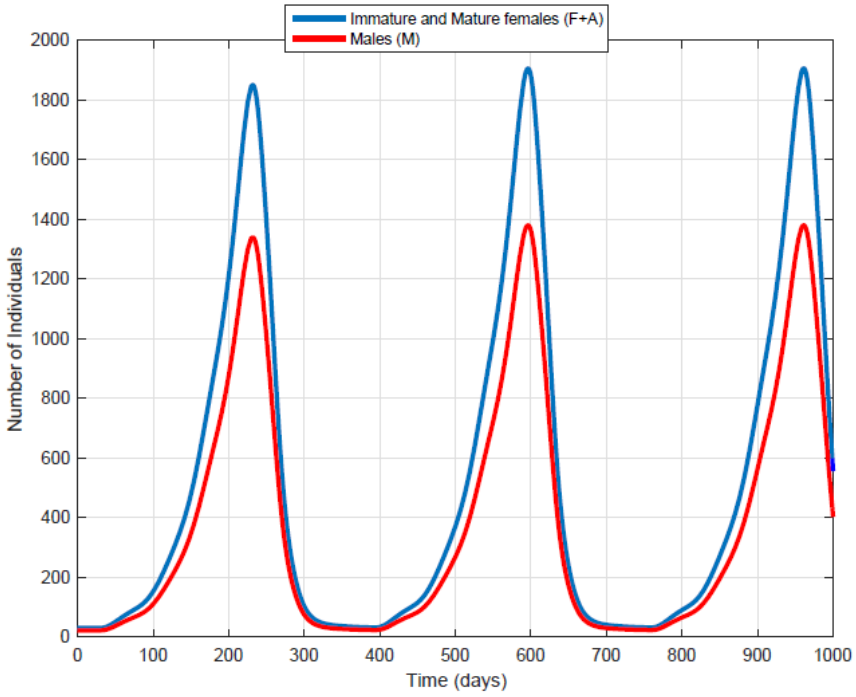

Figure 3.9: Time evolution of the periodic system, without control

to decay to zero with $F_p = 20$. In addition, the population has become so small, that even when the pods are back, the mirid population stay within $[\mathbf{0}, X^{(1)}[$, event with a small amount of pheromones, $F_p = 20$.

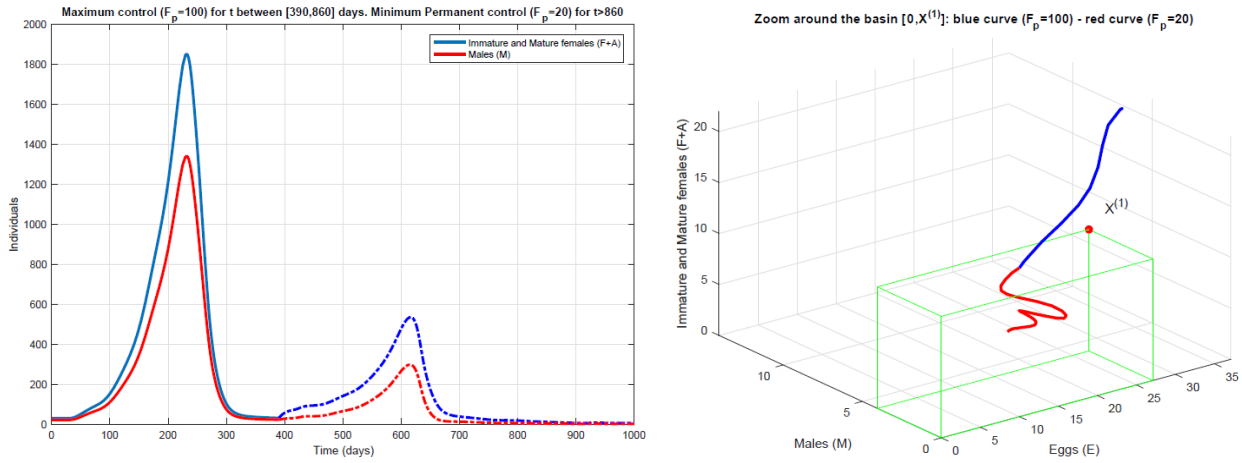

Figure 3.10: Control with first $F_p = 100$, then $F_p = 20$ once the system has reach the basin of attraction of $\mathbf{0}$ (dotted lines) for a control starting at $t_{start} = 390$: (a) trajectories of the system (b) Zoom of the trajectory near $[\mathbf{0}, X^{(1)}[$.

In fact, the periodic case, for mating disruption and trapping control, is the most favorable case,

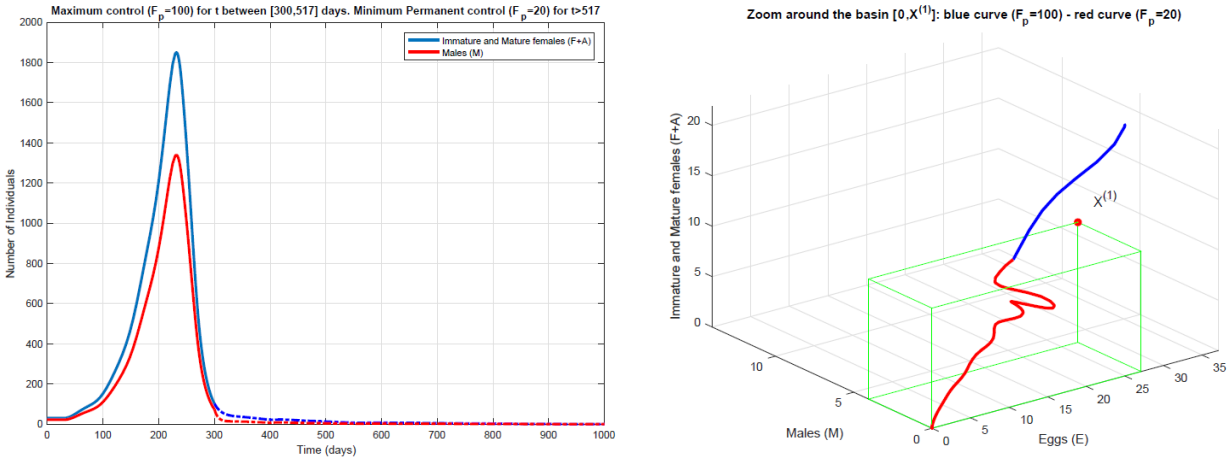

Figure 3.11: Control with first $F_p = 100$, then $F_p = 20$ once the system has reach the basin of attraction of $\mathbf{0}$ (dotted lines) for a control starting at $t_{start} = 300$: (a) trajectories of the system (b) Zoom of the trajectory near $[\mathbf{0}, X^{(1)}[$.

as we can use the no-production period, and thus when the mirid population is at its lowest, to be very efficient, especially if the treatment starts early (beginning of March, for instance).

3.4 Conclusion

We have considered a mating disruption and trapping model to study the opportunity of using sex-pheromones to control a mirid population. We obtain a PWS-DDE model, a kind of model that is not so common in Mathematical Biology. Thanks to the previous works by some of the authors and a suitable use of the Monotone System theory, we were able to provide theoretical results that helped us to provide interesting strategies that could be used in the field.

Of course, this work provides only partial inside on this complex system. Using a temporal approach, we implicitly assume that mirids and pheromones are homogeneously distributed, which is not the case in the field. A next step would be to take into account the spatial component, like in [88]. Last, but not least, it is well known that mirids aggregate on some particular trees, such that aggregation and dispersion processes should be taken into account, and also the impact of these behaviors in terms of the distribution and the density of the pheromone traps. This may require another modeling approach, thanks to the fact that very few knowledge are available thanks to pheromone spreading, mirid sensitivity to pheromone, etc.

GENERAL CONCLUSION

This thesis focused on the mathematical modelling and simulation of the time evolution of miridae in the plots in Cameroon with application to control. The main objective was to better estimate the level of miridae in the plot. We propose the models based on the life-cycle of the mirids taking into account the delays in the maturation processes at different stages of the life-cycle of the mirid. The main contribution of the work are found in chapter 2 and 3. These chapters are related to the publication and the submission of the paper [4] and [89] respectively.

The chapter 1 is devoted to the literature review on cacao, miridae and interaction between cacao and miridae. We present the main bug of cacao *S. singularis*, we described its life cycle, its biology and ecology. After this, we present the main mathematical tools especially the theory of monotone systems, the theory of delay differential equations and the theory of piecewise smooths systems which help us for the analysis of our models.

The first contribution presented in Chapter 2 is a deterministic model to describe the time evolution of miridae and its application to control. We first build a generic stage-structured cooperative ODE model to simulate the dynamic of the pest population considering the resource (available cocoa pods and additional tree hosts) as constant or as a periodic function. We also develop a cooperative delay model with two delays. We also highlighted that the presence of additional hosts can help the capsid population to maintain when resource (pods) are not available. We apply the control (biological, chemical and semio-chemical) to reduce the level of miridae in the plot. The main control strategy is the use of insecticide, but since chemical products are very expensive and harmful for the health of farmers, we propose a biological control. Through simulations, we showed that a biological control strategy (using Mating disruption and Trapping) can be a very good alternative to the use of insecticides. Last but not least, if it is possible, the reduction of alternative hosts in the plots is also an additional way to improve the efficacy of both controls.

The second contribution of this work has been displayed in Chapter 3. We focus more specially on one of te control methods studied in chapter 2. We develop a generic mirid model which take into account the semio-chemical control using mating-disruption and trapping. We consider an additional number of females named "fake females" to disturb the mating and accrue the male's mortality.

Models enter the theory of piecewise dynamical system. We studied the delayed model and we obtained a good dynamic. We exhibit two levels of control F_p^* and F_p^{**} which corresponds to "minimal and maximal treatment" respectively: this is the main result of this chapter. These two threshold are indicators to better control Miridae. For an efficient control, it is likely to set up new experiments in order to have many knowledge about pheromone spreading and mirid sensitivity to pheromone.

A possible extension of this work consists in explicitly taking into account the spatial dispersion of Miridae in mathematical model. Two possible approaches can be done: a meta-population model which takes into account the migration to one plot to another or the dispersion of Miridae modelled using Partial Differential Equations (PDE). Another extension of this work consists in evaluation of damages caused by mirids in terms of losses of production in mathematical model. An approach consists in formulation of a mathematical model taking into account the time evolution of mirids and the pods on different stages of development (cherelle, young pod and ripe pods). This study will intend to improve te estimation of losses of production, to prevent and avoid the destruction of the plants. The main objective is to develop mathematical models that answer the following questions: What is the real impact of the interaction between Miridae and cacao in the plot in Cameroon? After how long, a plot left under the influence of mirids can be completely destroyed?.

All these preliminary results obtained in this thesis encourage us to go further, that is to set up new experiments in the field in order to obtain additional data, the appearance of shoots on cacao which can be consider as an additional resource of mirids (in this thesis, we only consider pods as main resource of mirids). In the third chapter in this thesis, we consider an additional number of females namely "fake females". This number is evaluated by the quantity of sex pheromone. We suggest to set up new experiments in the field in order to estimate the quantity of sex pheromone which is equivalent to one female. So that, with the two thresholds obtained in the third chapter (F_p^* and F_p^{**}), an effective control can be applied in the plot.

A

Appendix

We introduces some of the key mathematical theories and methodologies relevant to the thesis (the material presented in this chapter are mostly standard definitions and results obtained from the literature).

A.1 Equilibria of Linear and Non-linear Systems

Consider the system of ordinary differential equation (ODEs) below (where a dot represents differentiation with respect to time $\left(\frac{d}{dt}\right)$):

$$\dot{x} = f(x, t, \mu), \quad x \in U \subset \mathbb{R}^n, \quad t \in \mathbb{R} \quad \text{and} \quad \mu \in V \subset \mathbb{R}^p, \tag{A.1}$$

where, U and V are open sets in $\mathbb{R}^n$ and $\mathbb{R}^p$, respectively, and μ is a parameter. The right-hand side function, $f(x, t, \mu)$, of equation (32) is called a vector field. ODEs which explicitly depend on time are called *non-autonomous*, while those that are independent of time are called *autonomous*.

Consider the following general autonomous system:

$$\dot{x} = f(x), \quad x \in \Omega \subset \mathbb{R}^n. \tag{A.2}$$

Definition A.1. *[90]: An equilibrium solution of the system (33) is given by $x = \bar{x} \in \mathbb{R}^n$; where $f(\bar{x}) = 0$. The vector or point $\bar{x}$ is called an equilibrium point.*

Theorem A.1. *(Fundamental Existence-Uniqueness Theorem [91]): Let Ω be an open subset of $\mathbb{R}^n$ containing x_0 and assume that $f \in \mathcal{C}^1(\Omega)$. Then, there exists an $a > 0$ such that the initial value problem (IVP):*

$$\dot{x} = f(x), \quad x(0) = x_0. \tag{A.3}$$

has a unique solution $x(t)$ on the interval $[-a, a]$

Theorem A.2. *[92]: Let $z(t)$ satisfy*

$$z^{'} \leq az + b, \quad z(0) = z_0,$$

for constants a, b. Then for $t \geq 0$

$$z(t) \leq e^{at} z_0 + \frac{b}{a}\left(e^{at} - 1\right), \quad a \neq 0,$$

and

$$z(t) \leq z_0 + bt, \quad a = 0.$$

Definition A.2. *[92]: System (33) is said to define a dynamical system on a set $\Omega \subset \mathbb{R}^n$ if, for every $x_0 \in \Omega$ there exists a unique solution of (33) which is defined for all $t \in [0, \infty)$ and remaining in Ω for all $t \in [0, \infty)$*

Definition A.3. *[92]: The Jacobian matrix of f at the equilibrium point $\bar{x}$ denoted by $Df(\bar{x})$, is the matrix of partial derivatives of f evaluated at $\bar{x}$. It is given by:*

$$J(\bar{x}) = \begin{bmatrix} \frac{\partial f_1}{\partial x_1}(\bar{x}) & \cdots & \frac{\partial f_1}{\partial x_n}(\bar{x}) \\ \vdots & \vdots & \vdots \\ \frac{\partial f_n}{\partial x_1}(\bar{x}) & \cdots & \frac{\partial f_n}{\partial x_n}(\bar{x}) \end{bmatrix}$$

Definition A.4. *[92]: Let $x = \bar{x}$ be an equilibrium solution of (33). Then $\bar{x}$ is called hyperbolic if none of the eigenvalues of $Df(\bar{x})$ has zero real part. An equilibrium point that is not hyperbolic is called non-hyperbolic.*

A.2 Stability of solutions and bifurcations

Definition A.5. *(Evolution Semi-group) : For an autonomous dynamical systems on Ω, we define its evolution semi-group operator (solution map or flow map) to be the map $\Phi_t : \Omega \longrightarrow \Omega$ such that the solution of system (33) $u(t) = \Phi_t u_0$ or $\Phi_t(u_0) = x(t; u_0)$. That is, Φ_t maps the initial data u_0 to the solution at time t.*

The terminology semi-group for the evolution operator Φ is motivated by the following properties

(a) For any $s, t > 0$, $\Phi(t + s) = \Phi_t \Phi_s = \Phi_s \Phi_t$,

(b) For $t = 0$, $\Phi(0) = I$, the identity operator.

Definition A.6. *[90]: An equilibrium point $\bar{x}$ of the autonomous dynamical systems (33) is said to be*

(1.) *Stable if for any $\epsilon > 0$ there exists $\delta = \delta(\epsilon) > 0$ such that if $x(0) \in \Omega(\bar{x}, \delta)$ then $x(t) \in \omega(\bar{x}, \epsilon)$ for all $t \geq 0$. Equivalently, for all $x(0) \in \mathbb{R}^n$ if $||x(0) - \bar{x}|| \leq \delta$ then $||x(t) - \bar{x}|| \leq \epsilon$ for all $t \geq 0$.*

(2.) *Locally attractive if* $||x(t) - \bar{x}|| \longrightarrow 0$ *as* $t \longrightarrow \infty$ *for all* $||x(0) - \bar{x}||$ *sufficiently small.*

(3.) *Locally asymptotically stable if* $\bar{x}$ *is stable and locally attractive. For an asymptotically stable equilibrium point* $\bar{x}$ *of system (33), the set of all initial data* $x(0) = x_0$ *such that*

$$\lim_{t \longrightarrow \infty} \Phi_t(x_0) = \bar{x}$$

is said to be the basin of attraction of $\bar{x}$*.*

(4.) *Globally attractive if (2) holds for any* $x(0) \in \Omega$ *i.e. the basin of attraction of* $\bar{x}$ *is* Ω*.*

(5.) *Globally asymptotically stable if (1) and (4) hold.*

(6.) *Unstable if it is not stable, i.e., (1) fails to hold.*

Interpretation of stability is given below

Remark A.1. *: An equilibrium point* $\bar{x}$ *is stable if the autonomous dynamical systems can be forced to remain in any neighbourhood of* $\bar{x}$ *by appropriate choice of initial condition. It is asymptotically stable if, in addition, any solution starting near the steady state approaches it as* $t \longrightarrow \infty$*. Thus, the basin of attraction of an asymptotically stable equilibrium point includes a neighbourhood of the equilibrium.*

Theorem A.3. *[90]: Consider the differential equation*

$$\dot{x} = Ax, \tag{A.4}$$

where A *is a* $n \times n$ *matrix and dot, represents differentiation with respect to time. Let* A *have eigenvalues* $\{\lambda_i\}_{i=1}^{l}$*,* $l \leq n$*. Then*

(i) *The origin is asymptotically stable if and only if* $Re(\lambda_i) < 0$ *for all* i*.*

(ii) *If* $Re(\lambda_i) \leq 0$ *for all* i*, and those eigenvalues with* $Re(\lambda_i) = 0$ *are non-defective (*λ *has multiplicity* $k \leq 1, k = 0, 1, ...$*), then the origin is stable.*

Definitions .6 cannot easily be used in practice. Fortunately, the method of linearisation permits to reduce the analysis to the user-friendly Theorem .13. The simplest natural way to proceed would have been to replace system (33) by its linearised system . The starting point is the following:

The linearised form of (33), near $\bar{x}$, is given by

$$u^{'} = Ju, \tag{A.5}$$

where f is assumed to be of class C^1.

Theorem A.4. *(Hartman-Grobman Theorem [92]): Assume that f in (33) is of class C^1 and consider a hyperbolic equilibrium point $\bar{x}$ of the dynamical system defined by (33). Then, there exist $\delta > 0$, a neighbourhood $N \subset \mathbb{R}^n$ of the origin and a homeomorphism h from the ball $B = \{x \in \mathbb{R}^n : ||x - \bar{x}|| < \delta\}$ onto N such that*

$$u(t) := h(x(t)) \quad \textit{solves (36) if and only if } x(t) \textit{ solves system (33).}$$

A direct implication of the Hartman-Grobman Theorem is that an orbit structure near a hyperbolic equilibrium solution is (topologically) qualitatively-equivalent to the orbit structure given by the associated linearised (around the equilibrium) dynamical system.

A.2.1 Basic offspring number

In ecology, there exists a threshold from an underlying concept in determining the spread or a decline of a population of bugs. The basic offspring number $\mathcal{N}_0$ is the average number of adults females generate by one adult female during all its lifespan. Its equivalent in epidemiology is the basic reproduction number, denoted by $\mathcal{R}_0$, which is the average number of secondary cases generated by a single infected individual during its entire period of infectiousness when introduced into a completely susceptible population [93, 94].

The threshold quantity $\mathcal{N}_0$ typically determine whether pest population persist in the plot ($\mathcal{N}_0 > 1$) or decay still to extinction ($\mathcal{N}_0 \leq 1$): this is the stability of trivial equilibrium. If $\mathcal{N}_0 > 1$, the usual situation is that there is a positive equilibrium which is asymptotically stable. This exchange of stability between the trivial and positive equilibrium occurs at $\mathcal{N}_0 = 1$, and is referred as forward bifurcation (or transcritical bifurcation).

For simple models, the basic reproduction number or the basic offspring number is the product of the infection rate and the duration of infectiousness. But usually the next generation operator method is used to compute $\mathcal{N}_0$ and permits to establish the local asymptotic stability of the associated disease-free equilibrium. The method is described below using the formulation and notations in [95].

Let $x = (x_1, ..., x_n)$, be the number of individuals in each compartment with each $x_i \geq 0$ and the first m compartments correspond to infected individuals. Define X_s to be the set of all disease-free states, that is,

$$X_s = \{x \geq 0 \mid x_i = 0,\ i = 1, ..., m\}.$$

The disease transmission model consists of nonnegative initial conditions together with the following system of equations:

$$\dot{x}_i = f_i(x) = \mathcal{F}_i(x) - \mathcal{V}_i(x), \quad i = 1, ..., n, \tag{A.6}$$

where $\mathcal{V}_i(x) = \mathcal{V}_i^-(x) - \mathcal{V}_i^+(x)$, $\mathcal{F}_i(x)$ be the rate of appearance of new infections in compartment i, $\mathcal{V}_i^+(x)$ be the rate of transfer of individuals into compartment i by all other means and $\mathcal{V}_i^-(x)$ be the rate of transfer of individuals out of compartment i. The functions are differentiable at least twice and satisfy assumptions (A1)-(A5) described below

(A1) if $x \geq 0$, then $\mathcal{F}_i$, $\mathcal{V}_i^+(x)$, $\mathcal{V}_i^-(x) \geq 0$ for $i = 1, ..., n$.

(A2) if $x_i = 0$ then $\mathcal{V}_i^+ = 0$. In particular, if $x \in X_s$ then $\mathcal{V}_i^+ = 0$ for $i = 1, ..., m$.

(A3) $\mathcal{F}_i = 0$ if $i > m$.

(A4) if $x \in X_s$ then $\mathcal{F}_i(x) = 0$ and $\mathcal{V}_i^+(x) = 0$ for $i = 1, ..., m$.

(A5) If $\mathcal{F}(x) = 0$ is set to zero, then all eigenvalues of $Df(x_0)$ have negative real parts, where $Df(x_0)$ is the derivative evaluated at the Disease Free Equilibrium, x_0 (i.e., the Jacobian matrix).

Let A be a square matrix with non-positive off-diagonal and non-negative diagonal entries as shown below

$$A = \begin{bmatrix} a_{11} & -a_{12} & -a_{13} & \cdots \\ -a_{21} & a_{22} & -a_{23} & \cdots \\ -a_{31} & -a_{32} & a_{33} & \cdots \\ \vdots & \vdots & \vdots & \ddots \end{bmatrix}$$

where the a_{ij} are nonnegative. Furthermore, let A be expressed as

$$A = sI - B, s > 0, B \geq 0. \tag{A.7}$$

Definition A.7. *(M-Matrix [96]): Any matrix A of the form (38) for which $s \geq \rho(B)$, (where $\rho(B)$ is the spectral radius of B), is called an M-matrix.*

Lemma A.1. *(Van den Driessche and Watmough [95]) If x_0 is a DFE of (37) and $f_i(x)$ satisfies (A1)-(A5), then the derivatives $D\mathcal{F}(x_0)$ and $D\mathcal{V}(x_0)$ are partitioned as*

$$D\mathcal{F}(x_0) = \begin{bmatrix} F & 0 \\ 0 & 0 \end{bmatrix} \text{ and } D\mathcal{V}(x_0) = \begin{bmatrix} V & 0 \\ J_3 & J_4 \end{bmatrix},$$

where $\mathcal{F}$ and $\mathcal{V}$ are the $m \times m$ matrices defined by $F = \left[\frac{\partial \mathcal{F}_i}{\partial x_j}(x_0)\right]$ and $V = \left[\frac{\partial \mathcal{V}_i}{\partial x_j}(x_0)\right]$ with $1 \leq i, j \leq m$. Further, F is non-negative, V is a non-singular M-matrix and J_3, J_4 are matrices associated with the transition terms of the model, and all eigenvalues of J_4 have positive real part.

The following theorem states that $\mathcal{R}_0$ is a threshold quantity that govern the persistence or effective control (elimination of the disease)

Theorem A.5. *(Van den Driessche and Watmough [95]): Consider the disease transmission model given by (37) with $f(x)$ satisfying conditions (A1)-(A5). If x_0 is a DFE of the model, then x_0 is locally asymptotically stable if $\mathcal{R}_0 < 1$, but unstable if $\mathcal{R}_0 > 1$, where $\mathcal{R}_0$ is defined by $\mathcal{R}_0 = \rho(FV^{-1})$*

The formulation above has been extended by Wang and Zhao [97] to compute the reproduction ratio for disease transmission models in a periodic environment.

Local stability stated by Theorem .15 mean that a sufficiently small flow of infectious individuals will not generate outbreak of the disease unless $\mathcal{R}_0 > 1$.

A.2.2 Bifurcation

A dynamical system typically involves a number of parameter values, in addition to the state variables. Bifurcation is a point in parameter space where equilibrium appear, disappear, or change stability [98]. Typically, in epidemic modeling, bifurcation occurs when the associated reproduction number equals unity. There are different types of bifurcations, such as saddle-node, transcritical, pitchfork, Hopf bifurcations and backward. The centre manifold theorem (in particular, Theorem 4.1 in [98] reproduced below for convenience) is used to establish the presence of backward or fordward bifurcation phenomenon.

Theorem A.6. *(Castillo-Chavez and Song [98]): Consider the following general system of ordinary differential equations with a parameter Φ:*

$$\frac{dz}{dt} = f(x, \Phi) \ , \qquad f : \mathbb{R}^n \times \mathbb{R} \qquad \text{and} \qquad f \in C^2(\mathbb{R}^n, \mathbb{R}), \tag{A.8}$$

where 0 is an equilibrium point of the system (that is, $f(0, \Phi) \equiv 0$ for all Φ) and assume

1. *$A = D_z f(0,0) = \left(\frac{\partial f_i}{\partial z_j}(0,0)\right)$ is the linearization matrix of system (39) around the equilibrium 0 with Φ evaluated at 0. Zero is a simple eigenvalue of A and other eigenvalues of A have negative real parts;*

2. *Matrix A has a right eigenvector u and a left eigenvector v (each corresponding to the zero eigenvalue). Let f_k be the k^{th} component of f and*

$$a = \sum_{k,i,j=1}^{n} v_k u_i u_j \frac{\partial^2 f_k}{\partial x_i \partial x_j}(0,0) \qquad \text{and} \qquad b = \sum_{k,i=1}^{n} v_k u_i \frac{\partial^2 f_k}{\partial x_i \partial \Phi}(0,0),$$

then, the local dynamics of the system around the equilibrium point 0 is totally determined by the signs of a and b.

(1) *$a > 0$, $b > 0$. When $\Phi < 0$ with $|\Phi| \ll 1$, 0 is locally asymptotically stable and there exists a positive unstable equilibrium; when $0 < \Phi \ll 1$, 0 is unstable and there exists a negative, locally asymptotically stable equilibrium;*

(2) *$a < 0$, $b < 0$. When $\Phi < 0$ with $|\Phi| \ll 1$, 0 is unstable; when $0 < \Phi \ll 1$, 0, is locally asymptotically stable equilibrium, and there exists a positive unstable equilibrium;*

(3) *$a > 0$, $b < 0$. When $\Phi < 0$ with $|\Phi| \ll 1$, 0 is unstable and there exists a locally asymptotically stable negative equilibrium; when $0 < \Phi \ll 1$, 0 is stable, and a positive unstable equilibrium appears;*

(4) *$a < 0$, $b > 0$. When Φ changes from negative to positive, 0 changes its stability from stable to unstable. Correspondingly a negative unstable equilibrium becomes positive and locally asymptotically stable.*

In particular, a backward bifurcation occurs at $\Phi = 0$ when condition (1) holds.

A.3 Irreducible Cooperative Systems

Consider the autonomous system (33), where f is continuously differentiable on an open subset $\mathcal{D} \subset \mathbb{R}^n$. Let $\Phi_t(x)$ denote the solution of system (33) with initial value x.

Definition A.8. *([99]): f is said to be of Type K in D if for each i; $f_i(a) \leq f_i(b)$ for any two points $a, b \in D$ satisfying $a \leq b$.*

The Type K Condition can easily be identified from the sign structure of the Jacobian matrix of the system (33). The following definition describes this structure.

Definition A.9. *([99]): D is p-convex if $tx + (1-t)y \in D$ for all $t \in [0,1]$ whenever $x, y \in D$ and $x \leq y$*

It is clear that if D is a convex set, then it is also p-convex. Furthermore, if D is a p-convex subset of $\mathbb{R}^n$ and

$$\frac{\partial f_i}{\partial x_j} \geq 0, \quad i \neq j, \quad x \in \mathcal{D}, \tag{A.9}$$

then f is of type K in D.

Definition A.10. *([99]): System (33) is said to be a cooperative system if (40) holds on the p-convex domain $\mathcal{D}$: It is called a competitive system on $\mathcal{D}$ if $\mathcal{D}$ is p-convex and the inequalities (40) are reversed:*

$$\frac{\partial f_i}{\partial x_j} \leq 0, \quad i \neq j, \quad x \in \mathcal{D}. \tag{A.10}$$

Definition A.11. *([99]): An $n \times n$ matrix $A = (a_{i,j})$ is irreducible if for every nonempty, proper subset $\mathcal{I}$ of the set $N = \{1, 2, \cdots, n\}$; there is an $i \in I$ and $j \in \mathcal{D} \setminus \mathcal{I}$ such that $a_{i,j} \neq 0$.*

Definition A.12. *([99]): System (33) is called irreducible in $\mathcal{D}$ if the Jacobian matrix of the system (33) is an irreducible matrix for every $x \in \mathcal{D}$.*

Theorem A.7. *: Suppose system (33) is irreducible and cooperative in $\mathcal{D}$. Then*

$$\frac{\partial \Phi_t}{\partial x} \gg 0, \quad t > 0.$$

Furthermore, if $x_0, y_0 \in \mathcal{D}$ satisfy $x_0 < y_0$; $t > 0$ and if $\Phi_t(x_0)$, $\Phi_t(y_0)$ are defined, then

$$\Phi_t(x_0) \ll \Phi_t(y_0), \quad t > 0.$$

A.4 Uniform persistence theory

Suppose X is a metric space with a metric d: Let $P : X \longrightarrow X$ be a continuous map and $X_0 \subset X$ is an open set. Define $\partial X_0 = X \setminus X_0$, and $M_\partial = \{x \in \partial X_0 : P^m(x) \in \partial X_0, \forall \geq 0\}$, which may be empty.

Definition A.13. *(Periodic Solution): A solution $x(t)$ is said to be periodic if $x(t + T) = x(t)$ for all t, for some $T > 0$.*

Proposition A.1. *(Properties of Poincaré Map)*

1. *$P^0 := I$, where I is the identity operator;*
2. *$P^{n+1} := P \circ P^n$*
3. *$P^{-n-1} := P^{-1} \circ P^{-n}$.*

Definition A.14. *([100]): A bounded set A is said to attract a bounded set B in X if*

$$\limsup_{m \longrightarrow \infty, x \in B} d(P^m(x), A) = 0.$$

- *A subset $A \subset X$ is said to be an attractor for f if A is nonempty, compact and invariant $(P(A) = A)$, and A attracts some open neighborhood of itself.*
- *A global attractor for $P : X \longrightarrow X$ is an attractor that attracts every point in X.*
- *For a nonempty invariant set M, the set $W^s(M) := \left\{x \in X : \lim_{m \to \infty} d(P^m(x), A) = 0\right\}$ is called the stable set of M.*

It should be recalled that a continuous mapping $P : X \longrightarrow X$ is said to be point-dissipative if there is a bounded set B_0 in X such that B_0 attracts each point in X.

Definition A.15. *([100]): P is said to be uniformly-persistent with respect to $(X_0, \partial X_0)$ if there exists an $\upsilon > 0$ such that $\liminf_{m \longrightarrow \infty} d(P^m(x), \partial X_0) \geq \upsilon$ for all $x \in X_0$.*

Definition A.16. *([100]): P is said to be weakly uniformly-persistent with respect to $(X_0, \partial X_0)$ if there exists an $\upsilon > 0$ such that $\limsup_{m \longrightarrow \infty} d(P^m(x), \partial X_0) \geq \upsilon$ for all $x \in X_0$.*

Theorem A.8. *([100]): Assume that*

1. *$P(X_0) \subset X_0$ and P has a global attractor A.*
2. *There exists a finite sequence $\mathcal{M} = \{M_1, M_2, ..., M_k\}$ of disjoint, compact, and isolated invariant sets in ∂X_0 such that*
   - *$\Omega(M_\partial) = \cup_{x \in M_\partial} \omega(x) \subset \cup_{i=1}^{k} M_i$;*
   - *no subset of $\mathcal{M}$ forms a cycle in ∂X_0;*
   - *M_i is isolated in X;*
   - *$W^s(M_i) \cap X_0 = \varnothing$ for each $1 \leq i \leq k$*

Then, there exists $\eta > 0$ such that $\liminf_{n \to \infty} d\left(P^n(x), \partial X_0\right) \geq \eta$ for all $x \in X_0$.

Theorem A.9. *([100]): Let $P : X \longrightarrow X$ be a continuous map with $P(X_0) \subset X_0$. Assume P has a global attractor A. Then weak uniform-persistence implies uniform-persistence*

Theorem A.10. *([100]): Let $T(t)$ be an ω-periodic semiflow on X with $T(t)(X_0) \subset X_0$; for all $t \geq 0$: Assume that $S = T(\omega)$ satisfies the following:*

1. *$S : X \longrightarrow X$ is dissipative;*
2. *S is compact.*

Then, uniform-persistence of S with respect to $(X_0; \partial X_0)$ implies that of $T(t)$.

Theorem A.11. *([100]): Let $S : X \longrightarrow X$ be a continuous map with $S(X_0) \subset X_0$. Assume*

1. *$S : X \longrightarrow X$ is dissipative;*
2. *S is compact;*
3. *S is uniformly-persistent with respect to $(X_0, \partial X_0)$.*

Then, there exists a global attractor A_0 for S in X_0, and S has a coexistence state $x_0 \in A_0$.

Bibliography

[1] R. Babin. *Contribution à l'amélioration de la lutte contre le miride du cacaoyer* Sahlbergella singularis *Hagl. (Hemiptora: Miridae). Influence des facteurs agro-écologiques sur la dynamique des populations du ravageur.* Thèse de Doctorat, Université Paul Valéry-Montpellier III, biologie des populations et écologie, 2009.

[2] J. C. Anikwé, A. A. Omoloye, F. A. J. C. Okelana, and R Babin. Novel rearing technique, development biology, fecundity and morphometrics of the brown cocoa mirid *Sahlbergella singularis* haglung in nigeria. *16th International Cocoa Research Conference*, 2010.

[3] F. K. N'guessan, H. A. N'guessan, P. W. N'guessan, N. N'Dri Kouame, and Y. Tano. Variations saisonniÃ¨res des populations de mirides du cacaoyer dans la région de l'indénié-djuablin en côte d'ivoire. *Journal of Applied Biosciences*, 83:7595–7605, 2014.

[4] Djoukwe Tapi M, Bagny Beihle, S Bowong, and Y Dumont. Models for miridae, a cocoa insect pest. application in control strategies. *Mathematical Methods in the Applied Sciences.*

[5] Jean Braudeau. Le cacaoyer. Technical report, GP Maisonneuve & Larose, 1969.

[6] P. Jagoret. *Analyse et évaluation de systèmes agroforestiers complexes sur le long terme : Application aux systèmes de culture à base de cacaoyer au Centre Cameroun..* Thèse soutenue pour l'obtention du titre de Docteur de Montpellier Supagro., 2011.

[7] Guy Mossu. Le cacaoyer: Le techinicien d'agriculture tropical. *Maisonneuve et Larose*, 1990.

[8] Dieudonne Alemagi, Peter A Minang, Lalisa A Duguma, Anderson Kehbila, Faith Ngum, M Noordwijk, OE Freeman, C Mbow, J de Leeuw, and D Catacutan. Pathways for sustainable intensification and diversification of cocoa agroforestry landscapes in cameroon. *Climate-Smart Landscapes: Multifunctionality in Practice. ASB Partnership for The Tropical Forest margins*, pages 347–359, 2014.

[9] G. K. Ayenor, N Roling, A. van Huis, B. Padi, and D Obeng-Ofori. Assessing the effectiveness of a local agricultural research committee in diffusing sustainable cocoa production practices: the case of capsid control in ghana. *International Journal of Agricultural Sustainability*, 5, 2007.

[10] R. Babin, C. Fenouillet, L. Legavre, T.and Blondin, C. Calatayud, A-M. Risterucci, and M-P Chapuis. Isolation and characterization of twelve polymorphic microsatellite loci for the cocoa mirid bug sahlbergella singularis. *International journal of molecular sciences*, 13(4):4412–4417, 2012.

[11] R. Babin, B. H. D. Bisselua, L. Dibog, and J. P. Lumaret. Rearing method and life table data for the cocoa mirid bug *Sahlbergella singularis* haglund (hemiptera: Miridae). *Journal of Applied Entomology*, 132:366–374, 2008.

[12] Emile M Lavabre, J Decelle, and P Debord. Recherches sur les variations de populations de mirides (capsides) en côte d'ivoire. *Café, Cacao, Thé*, 6(4):287–295, 1962.

[13] F Varlet and D Berry. Réhabilitation de la protection phytosanitaire des cacaoyers et caféiers du cameroun. tome i: rapport principal, 1997.

[14] E. M. Lavabre. Systématique des mirides du cacaoyer. in : Les mirides du cacaoyer. *E.M. Lavabre Ed., G.-P. Maisonneuve et Larose, Paris*, pages 47–70, 1977a.

[15] R. Babin, M. Gerben ten Hoopen, C. Cilas, F. Enjalric, Yede, P. Gendre, and J. P. Lumaret. Impact of shade on the spatial distribution of *Sahlbergella singularis* in traditional cocoa agroforests. *Agricultural and Forest Entomology*, 12:69–79, 2010.

[16] G. Williams. Field observations on the cacao mirids, *Sahlbergella singularis* hagl. and *Distantiella theobroma* (dist.), in the gold coast. part i. mirid damage. *Bulletin of Entomological Research*, 44:101–119, 1953a.

[17] J. Carayon. Caractères généraux des hémiptères bryocorinae. in: Les mirides du cacaoyer. *E. M. Lavabre Ed., G-P. Maisonneuve et Larose, Paris*, pages 13–34, 1977.

[18] Philip Frank Entwistle et al. *Pests of cocoa.* 1972.

[19] Richard Adu-Acheampong, Janice Jiggins, Arnold van Huis, Anthony Richmond Cudjoe, Victress Johnson, Owuraku Sakyi-Dawson, Kwasi Ofori-Frimpong, Paul Osei-Fosu, Ebenezer Tei-Quartey, William Jonfia-Essien, et al. The cocoa mirid (hemiptera: Miridae) problem: evidence

to support new recommendations on the timing of insecticide application on cocoa in ghana. *International Journal of Tropical Insect Science*, 34(1):58–71, 2014.

[20] Godfred Kweku Awudzi, Mercy Asamoah, Frank Owusu-Ansah, Paul Hadley, Paul Edwin Hatcher, and Andrew James Daymond. Knowledge and perception of ghanaian cocoa farmers on mirid control and their willingness to use forecasting systems. *International Journal of Tropical Insect Science*, 36(1):22–31, 2016.

[21] Sarah A Laird, Gabriel Leke Awung, and Rita J Lysinge. Cocoa farms in the mount cameroon region: biological and cultural diversity in local livelihoods. *Biodiversity and Conservation*, 16(8):2401–2427, 2007.

[22] Denis J Sonwa, Bernard A Nkongmeneck, Stephan F Weise, Maturin Tchatat, Akin A Adesina, and Marc JJ Janssens. Diversity of plants in cocoa agroforests in the humid forest zone of southern cameroon. *Biodiversity and Conservation*, 16(8):2385–2400, 2007.

[23] G. Matthews, T. Wiles, and P Baleguel. A survey of pesticide application in cameroon. *Crop Protection*, 22(5):707–714, 2003.

[24] B Padi, GK Owusu, and NK Kumah. A record of desplatsia dewevrei (de wild & th. dur.)(tiliales: Tiliaceae) as an alternative and potential breeding host plant for the cocoa mirid sahlbergella singularis hagl. In *Proceedings of the 12th International Cocoa Research Conference, Salvador, Bahia, Brazil*, pages 31–37, 1996.

[25] L. Dibog, R. Babin, A. Amang, J. Mbang, B. Decazy, S. Nyassé, C. Cilas, and A. B. Eskes. Effect of genotype of cocoa (theobroma cacao) on attractiveness to the mirid sahlbergella singularis (hemiptera: Miridae) in the laboratory. *Pest Management Science*, 64:977–980, 2008.

[26] Raymond J Mahob, Regis Babin, Gerben M ten Hoopen, Luc Dibog, David R Hall, and Charles F Bilong Bilong. Field evaluation of synthetic sex pheromone traps for the cocoa mirid sahlbergella singularis (hemiptera: Miridae). *Pest management science*, 67(6):672–676, 2011.

[27] Emmanuel F Torquebiau. A renewed perspective on agroforestry concepts and classification. *Comptes Rendus de l'Academie des Sciences-Series III-Sciences de la Vie*, 323(11):1009–1017, 2000.

[28] Emmanuel Torquebiau. *L'agroforesterie: des arbres et des champs*. L'Harmattan, 2007.

[29] Geneviève Michon and H De Foresta. Agroforests: pre-domestication of forest trees or true domestication of forest ecosystems? *NJAS wageningen journal of life sciences*, 45(4):451–462, 1997.

[30] R. Babin, J. C. Anikwé, L. Dibog, and J. P. Lumaret. Effets of cocoa trees phenology and canopy microclimate on the performance of the mirid bug *Sahlbergella singularis*. *Entomologia Experimentalis et Applicata*, 141:25–34, 2011.

[31] Cynthia Gidoin. *Relations entre structure du peuplement végétal et bioagresseurs dans les agroforêts à cacaoyers. Application à trois bioagresseurs du cacaoyer: la moniliose au Costa Rica, la pourriture brune et les mirides au Cameroun.* PhD thesis, Montpellier Supagro; Ecole nationale superieure agronomique de montpellier-AGRO M, 2013.

[32] J Nya Ngatchou. Etat d'avancement des travaux de genetique et d'amelioration du cacaoyer au cameroun proceedings. In *7. International Cocoa Research Conference4-12 Nov 1979Douala (Cameroon)*, number 633.74063 I61p 1979. Cocoa Producers' Alliance, Lagos (Nigeria), 1981.

[33] G. A. R. Wood and RA Lass. *Cocoa*. John Wiley & Sons, 2008.

[34] Michel Ndoumbe-Nkeng and Ivan Sache. Lutte contre la pourriture brune des cabosses du cacaoyer au cameroun: Améliorer les connaissances épidémiologiques afin d'intervenir au bon moment. *Phytoma-La Défense des Végétaux*, (562):10–12, 2003.

[35] M Boulay. Thesis, m. sc, université laval, québec g1k 7p4 (canada). etude de la phenologie de differents hybrides de cacaoyer associes a six especes d'arbre d'ombrage.

[36] PJM Salef. Growth, flowering and fruiting of cacao under controlled soil moisture conditions. *Journal of Horticultural Science*, 45(2):99–118, 1970.

[37] Edward O Wilson. *The future of life*. Vintage, 2002.

[38] Philippe Lachenaud and Bertrand Sallée. Les cacaoyers spontanés de guyane. localisation, écologie et morphologie. *Café, cacao, thé*, 37(2):101–113, 1993.

[39] Philippe Petithuguenin. Les conditions naturelles de production du cacao en côte d'ivoire, au ghana et en indonésie. *Plantations, recherche, développement*, 5(6):393–411, 1998.

[40] Gerben Martijn Ten Hoopen and Ulrike Krauss. Biological control of cacao diseases. In *Cacao diseases*, pages 511–566. Springer, 2016.

[41] G. Delvare and H. P. Aberlenc. Les insectes d'afrique et d'amérique tropicale : clés pour la reconnaissance des familles. *Montpellier, CIRAD/PRIFAS,*, page 302, 1989.

[42] Emile M Lavabre. Recherches sur une méthode économique de contrôle des mirides du cacaoyer. *Café, Cacao, Thé*, 4(1):16–25, 1960.

[43] PF Entwistle, GAR Wood, and RA Lass. Insects and cocoa. *Cocoa, Forth Edition*, pages 366–443, 1985.

[44] R. Kumar and A.K Ansari. Biology, immature stages and rearing of cocoa-capsids (miridae: Heteroptera). *Zoological Journal of the Linnean Society*, 54:1–29, 1974.

[45] A. Youdeowei. The life cycles of the cocoa mirids *Sahlbergella singularis* hagl. and *Distantiella theobroma* dist. in nigeria. *Journal of Natural History*, 7:217–223, 1973.

[46] R. Babin, L. Dibog, and D. B. H Bisselua. Description et évaluation d'une nouvelle méthode d'élévage et d'éléments de biologie de *Sahlbergella singularis* hagl. (hemiptera: Miridae), principal ravageur du cacaoyer au cameroun. *Actes de la 15e Conférence Internationale sur la recherche Cacaoyère au Cameroun, San Jose, Costa Rica*, pages 1297–1303, 2006.

[47] KF N'Guessan, AB Eskes, and P Lachenaud. Résistance des principaux groupes génétiques de cacaoyer (theobroma cacao) aux mirides (sahlbergella singularis) en côte d'ivoire. *Sci. Nat*, 3(1):19–27, 2006.

[48] KF N'Guessan, JAK N'Goran, and AB Eskes. Resistance of cacao (theobroma cacao l.) to sahlbergella singularis (hemiptera: Miridae): investigation of antixenosis, antibiosis and tolerance. *International Journal of Tropical Insect Science*, 28(4):201–210, 2008.

[49] D. G. Gibbs, A. D. Pickett, and D. Leston. Seasonal population changes in cocoa capsids (hemiptera, miridae) in ghana. *Bulletin of Entomological Research*, 58:279–293, 1968.

[50] F. K. N'Guessan and N Coulibaly. Dynamique des populations de mirides et de quelques autres déprédateurs du cacaoyer dans la région ouest de la côte d'ivoire. *Proceedings of the 13th International Cocoa Research Conference*, pages 425–435, 2000. Cocoa Producer's Alliance, Malaysia.

[51] Dennis Leston. The flight behaviour of cocoa-capsids (hemiptera: Miridae). *Entomologia Experimentalis et Applicata*, 16(1):91–100, 1973.

[52] A Youdeowei. Aspects of flight in the cocoa mirids *S. singularis* hagl. and *D. theobroma* dist. (heteroptera: Miridae). *Actes de la* 4^{eme} *Conférence sur la Recherche Cacaoyère, St Augustine, Trinitad et Tobago*, pages 532–538, 1972.

[53] S. H. Crowdy. Observations on the pathogenicity of *Calonectria rigidiuscula* (berk. and br.) sacc. on *Theobroma cacao* l. *The Annals of Applied Biology*, 34:45–59, 1947.

[54] L. Mahot, R. Babin, L. Dibog, P.R. Tondje, and C. Bilong. Biocontrol of cocoa mirid *S. singularis* hagl. (hemiptera: Miridae) with *Beauveria bassiana* vuillemin. first results of activities carried out irad, cameroon. *INCOPED* 5^{th} *International seminar on cocoa pests and diseases, SanJose, Costa Rica*, page 14 [Abstract], 2006.

[55] Ovide Arino, Moulay Lhassan Hbid, and E Ait Dads. *Delay Differential Equations and Applications: Proceedings of the NATO Advanced Study Institute held in Marrakech, Morocco, 9-21 September 2002*, volume 205. Springer Science & Business Media, 2007.

[56] JK Hale. Smv lunel introduction to functional differential equations. *Springer-Verlag, New York*, 19:437–443, 1993.

[57] Morris W Hirsch. Systems of differential equations that are competitive or cooperative. iv: Structural stability in three-dimensional systems. *SIAM journal on mathematical analysis*, 21(5):1225–1234, 1990.

[58] Morris W Hirsch. Stability and convergence in strongly monotone dynamical systems. *J. reine angew. Math*, 383(1):53, 1988.

[59] Jiang Ji-Fa. On the global stability of cooperative systems. *Bulletin of the London Mathematical Society*, 26(5):455–458, 1994.

[60] John Smillie. Competitive and cooperative tridiagonal systems of differential equations. *SIAM journal on mathematical analysis*, 15(3):530–534, 1984.

[61] Abraham Berman and Robert J Plemmons. *Nonnegative matrices in the mathematical sciences*, volume 9. Siam, 1994.

[62] R. Anguelov, Y. Dumont, and J. M.-S Lubuma. On nonstandard finite difference schemes in biosciences. In Michael Todorov, editor, *Proceedings of the 4th International Conference on Application of Mathematics in Technical and Natural Sciences (AMiTaNS'11)*, volume 1487, pages 212–223. American Institute of Physics - AIP Conference Proceedings, 2012.

[63] Morris W Hirsch. Systems of differential equations that are competitive or cooperative ii: Convergence almost everywhere. *SIAM Journal on Mathematical Analysis*, 16(3):423–439, 1985.

[64] J Jifa. The algebraic criteria for the asymptotic behaviour of cooperative systems with concave nonlinearities. *J. Syst. Sci. Complex.*, 6(3):193, 1993.

[65] H. L Smith. Cooperative system of differential equations with concave nonlinearities,. *Nonlinear Anal,: Theory, Meth. Appl.*, 10(10):1037–1052, 1986.

[66] H. L Smith. Monotone dynamical systems: An introduction to the theory of competitive and cooperative systems. *American Mathematical Society*, 41, 2008.

[67] H. Smith and M Hirsch. Monotone dynamical systems. In A.Canada, P.Drabek, and A.Fonda, editors, *Handbook of Differential Equations , Ordinary Differential Equations (volume 2)*, pages 239–357. Elsevier North-Holland, 2005.

[68] L. Lu. Numerical stability of the theta-methods for systems of differential equations with several delay terms. *Journal of Computational and Applied Mathematics*, 34(3):291–304, 1991.

[69] M. Bernado, A. R. Champneys, P. Kowalczk, A. B. Nordmark, G. O. Tost, and P. T. Piroinen.

[70] J. P. LaSalle. The stability of dynamical systems. *Society for Industrial and Applied Mathematics, Philadelphia. With an appendix:"Limiting equations and stability of non-autonomous ordinary differential equations" by Z. Artstein, Regional Conference Series in Applied Mathematics.*, 1976.

[71] David Barton. Stability calculations for piecewise-smooth delay equations. *I. J. Bifurcation and Chaos*, 19:639–650, 02 2009.

[72] Mario Bernardo, Chris Budd, Alan Richard Champneys, and Piotr Kowalczyk. *Piecewise-smooth dynamical systems: theory and applications*, volume 163. Springer Science & Business Media, 2008.

[73] D. H. B. Bisselua, Yede, and S. Vidal. Dispersion models and sampling of cacao mirid bug *Sahlbergella singularis* (hemiptera: Miridae) on theobroma cacao in southern cameroon. *Environmental Entomology*, 40(1):111–119, 2011.

[74] T.J. Davis, P. Kaufman, and D Hogsette, J. Kline. The effects of larval habitat quality on aedes albopictus skip oviposition. *J. Am. Mosq. Control Assoc.*, 31, 2015.

[75] F.V.S. De Abreu, M.M. Morais, S.P. Ribeiro, and A.E Eiras. Influence of breeding site availability on the oviposition behaviour of aedes aegypti. *Memórias Do Insti- tuto Oswaldo Cruz*, 110, 2015.

[76] J. C. Kamgang and G. Sallet. Computation of threshold conditions for epidemiological models and global stability of the disease-free equilibriun (dfe). *Mathematical Biosciences*, 213:1–12.

[77] S. Marino, I.B. Hogue, C.J. Ray, and D.E Kirschner. A methodology for performing global uncertainty and sensitivity analysis in systems biology. *Journal of theoretical biology*, 254(1):178–196, 2008.

[78] J.K Hale. *Theory of Functional differential equations*, volume 3 of *Applied Mathematical Sciences*. Springer, New York, 1977.

[79] K. Edoh, Adabe and E.L. Ngo-Samnick. Cocoa: production and processing. *Edited by Engineers Without Borders (ISF Cameroon, Douala) and The Technical Centre for Agricultural and Rural Cooperation (CTA, Wageningen, The Netherlands).*

[80] JE Sarfo, CAM Campbell, and DR Hall. Design and placement of synthetic sex pheromone traps for cacao mirids in ghana. *International Journal of Tropical Insect Science*, 38(2):122–131, 2018.

[81] Roumen Anguelov, Claire Dufourd, and Yves Dumont. Mathematical model for pest–insect control using mating disruption and trapping. *Applied Mathematical Modelling*, 52:437–457, 2017.

[82] Joseph Easmon Sarfo. *Behavioural responses of cocoa mirids, Sahlbergella singularis Hagl and Distantiella theobroma Dist.(Heteroptera: Miridae), to sex pheromones.* PhD thesis, University of Greenwich, 2013.

[83] H Barclay and P Van den Driessche. Pheromone trapping models for insect pest control. *Researches on population ecology*, 25(1):105–115, 1983.

[84] Hugh J Barclay and Jorge Hendrichs. Models for assessing the male annihilation of bactrocera spp. with methyl eugenol baits. *Annals of the Entomological Society of America*, 107(1):81–96, 2014.

[85] Y. Dumont and J. M Tchuenche. Mathematical studies on the sterile insect technique for the chikungunya disease and aedes albopictus,. *Journal of Mathematical Biology*, 65(5):809–854, 2012.

[86] Martin Strugarek, Hervé Bossin, and Yves Dumont. On the use of the sterile insect release technique to reduce or eliminate mosquito populations. *Applied Mathematical Modelling*, 68:443–470, 2019.

[87] Hal L Smith. *An introduction to delay differential equations with applications to the life sciences*, volume 57. Springer New York, 2011.

[88] Roumen Anguelov, Claire Dufourd, and Yves Dumont. Simulations and parameter estimation of a trap-insect model using a finite element approach. *Mathematics and Computers in Simulation*, 133:47–75, 2017.

[89] Djoukwe Tapi M, Bagny Beihle, and Y Dumont. Miridae control using sex-pheromones trapping. modeling, analysis and simulations. *Nonlinear Analysis: Real World Applications.*

[90] Stephen Wiggins. *Introduction to Applied Nonlinear Dynamical Systems and Chaosl.* 2000.

[91] Perko L. *Difierential Equations and Dynamical Systems.*, volume 7. 2000.

[92] Mohammad A. Safi. *Mathematical Analysis of The Role of Quarantine and Isolation in Epidemiology.* PhD thesis, 2010.

[93] Anderson R.M. and May R.M. *Infectious Disease of Humans.* 1991.

[94] Diekmann O. and Heesterbeek J. A. P. On the definition and computation of the basic reproduction ratio r_0 in the model of infectious disease in heterogeneous populations. *J Math Biol*, 2:265–382, 1990.

[95] van den Driessche P. and Watmough J. Reproduction numbers and sub-threshold endemic equilibria for compartmental models of disease transmission. *Math Bios*, 180:29–28, 2002.

[96] Plemmons R. J. and Berman A. *Nonnegative matrices in the mathematical sciences.* 1994.

[97] Wang W. and Zhao X-Q. Threshold dynamics for compartmental epidemic models in periodic environments. *Journal of Dynamics and Differential Equations*, 20:699–717, 2008.

[98] Castillo-Chavez C. and Song B. Dynamical models of tuberculosis and their applications. *Math Bio sci Eng*, 1:361–404, 2004.

[99] Smith H. L. Monotone dynamical systems: An introduction to the theory of competitive and cooperative systems. *American Mathematical Society.*, page 41, 2008.

[100] Zhao X.-Q. Dynamical systems in population biology. *Springer-Verlag, New York*, 2003.

Received: 3 July 2017 | Revised: 20 March 2018 | Accepted: 11 April 2018

DOI: 10.1002/mma.5063

SPECIAL ISSUE PAPER

WILEY

Models for Miridae, a cocoa insect pest. Application in control strategies

Djoukwe Tapi[1,2,7] | Bagny Beihle[3,8,9] | S. Bowong[1,2,7] | Y. Dumont[4,5,6,7]

[1]Department of Mathematics and Computer Science, The University of Douala, Douala, Cameroon

[2]UMI 209 IRD/UPMC UMMISCO, University of Yaounde I, Cameroon

[3]CIRAD, UPR Bioagresseurs, 30501 Turrialba, Costa Rica

[4]CIRAD, Umr AMAP, Pretoria, South Africa

[5]AMAP, Univ Montpellier, CIRAD, CNRS, INRA, IRD, Montpellier, France

[6]University of Pretoria, Department of Mathematics and Applied Mathematics, Pretoria, South Africa

[7]EPITAG, LIRIMA, France

[8]Bioagresseurs, Univ Montpellier, CIRAD, Montpellier, France

[9]IRAD, BP 2123 Yaoundé, Cameroon

Correspondence
Y. Dumont, CIRAD, Umr AMAP, Pretoria, South Africa.
Email: yves.dumont@cirad.fr

Communicated by: R. Anguelov

Funding information
DP-PCP Agroforesterie Cameroon; CIRAD; IRD; INRIA-LIRIMA

MSC Classification: 34A12; 34C12; 34K28; 92D25

Cocoa mirid, *Sahlbergella singularis*, is one of the major pests of cocoa in West Africa. It is responsible of several damages in plots. In this paper, we study the dynamics of this pest. Based on biological and ecological partial knowledge, we develop 2 cooperative mathematical models that aim to describe the time dynamics of the cocoa mirids. We first develop a cooperative stage-structured model, derived some qualitative results, and a sensitivity analysis study in order to determine the most important parameters. Assuming that all parameters are or not periodic, we obtain conditions that allow the persistence or not of the population. We highlight the influence of cocoa pods variation along the year on the time evolution of the population. Then, we derive a 2-stage cooperative time-delay model, with 2 delays, that takes into account the eggs' development time and the females' maturation time. We illustrate our theoretical results with some simulations and show that the delayed system provides the best results compared with real observations. Finally, we focus on chemical control that is commonly used in Cameroon and compare it to a new biological control, mixing mating disrupting and trapping. We discuss the results and provide future perspectives based on this work.

KEYWORDS
cocoa pest, delays, mathematical models, pest control, *Sahlbergella singularis*, simulation

1 | INTRODUCTION

Cacao is a cash crop mainly cultivated in African countries (Ivory Coast, Ghana, Nigeria, and Cameroon) that ensures around 72% of the world production [ICCO 2016]. Cocoa (*Theobroma cacao*) is essential for the livelihood of millions of small producers in Africa especially in Cameroon.[1] African production of cocoa is seriously impacted by 2 important diseases the Cocoa Swollen Shoot Virus (CSSV) and the black pod rot (up to 80%-90% losses[2]) and by the damage caused by 2 pests: *Sahlbergella singularis* and *Distantiella theobroma* known as mirid bugs or cacao capsids.[3,4] These species, which originate from the forests of central Africa, have very similar life histories and regularly live together in cacao-based agroforestry systems.[5] In Cameroon, *S. singularis* is nowadays the most common and the most harmful species for the production. Mirid bugs feed preferentially on *Theobroma cacao,* but other species like *Cola nitida* and *Ceiba*

pentandra are known to be alternative hosts when cacao resource is unavailable. The immature (5 instars) and adult stages of these sucking insects used to feed on the sap of young semi-lignified branches, on plant tissues by injecting a digestive saliva, on buds and on fruits.[6-9] Mirid damage on the pod is relatively superficial since the pods cortex is very thick. In general, mirids attacks on the pods are characterized by black dots (feeding lesion) around the peduncle of mature pods. Indeed, there is no obvious link between the intensity of feeding lesions on mature pods and an impact on beans quality.[10] Very few losses are noted at this stage. However, lesion caused to young fruit (less than 10 cm and less than 2 months old), called cherelle, increase fruit abortion and impact directly the ongoing production.[10] This fruit stage is vulnerable to mirids attacks. Indeed, the most harmful damage that is also the less obvious to quantify is the damage caused to cocoa vegetative growth parts. Those lesions prevent sap circulation favoring leaves fall and branches death that is characteristic of mirids attacks. Extensive feeding by mirids on branches results in the degradation of the canopy of discrete groups of trees, which can be up to 100 and are referred as mirid pockets. Mirid pockets are generally located in the sunniest areas of plantations.[8] The impact of mirids on cacao tree is a long-term impact as cacao is a perennial plant, which can produce for more than 20 years. Damage of mirid bugs on the cocoa tree are cumulated over time and can lead to premature aging of plantations and to the rapid death of the most severely damaged trees.[6,11,12] Losses due to mirids are difficult to estimate but can reach 30% to 40% of potential production[13,14] depending on the system management strategy. In fact, mirids attacks are known to be the most harmful in full sun plantations. In multi-strata and highly diversified[15-17] cacao-based agroforestry system as the one that is widespread in Cameroon, shade management is a relevant option to control mirid population.[8] But shade management is a long-term process that is sometimes difficult to set up for the farmers given antagonistic effects on black pod disease. Whatever the type of system considered, synthetic insecticides of the neonicotinoid family, such as λ-cyhalothrine and imidacloprid,[3,18] are still the main input used to control these pests.[19] Since 1970, the economic threshold for phytosanitary intervention has been fixed at 0.7 mirids/tree in Cameroon[8] and 0.6 mirids/tree in Ghana.[20] These indicators based on mirid populations are however difficult to evaluate regarding the ecology of the species. In fact, it is challenging to count mirids individuals (immatures and adults) on the field since they used to hide during the day to avoid direct light. It is likely a relatively low level of mirid population can cause important damage in the plantation. Mirids do not pullulate in the plantations even during the peak period. Due to controversial effects of chemical insecticide use, alternative cocoa pest control methods have been developed including cultural management, varietal management,[21] as well as semio-chemical management, using synthetic sexual pheromone traps,[22] or the use of plant extracts as pesticides.[3] Considering the difficulty to estimate mirid population and to obtain long-term data on the field, the mathematical approach appears as the most relevant option to forecast the efficiency of control strategy. In that sense, the aim of this work is to develop some (generic) mathematical models of mirid population to better predict its time evolution in a plot under different management strategies. A first compartmental model, with constant or periodic parameters, is developed based on the mirid life cycle. We make some theoretical analysis, a sensitivity analysis and provide some numerical simulations. Then, we develop a second model, time-delayed model, based on the previous ones, in order to better take into account the developmental time at different stage. After a brief theoretical analysis, we provide some numerical simulations without and with control efforts, and we discuss the results.

The paper is organized as follows. In Section 2, we formulate a first ODE model: for this model, we make a theoretical study, a sensitivity analysis, and some numerical simulations. In Section 3, we formulate a delay model. After a brief study, we do some numerical simulations, and we compare with the previous model without delay. In Section 4, we compare chemical and biological controls and discuss their efficiency. Finally, in Section 5, we conclude and propose several experimental and theoretical studies in order to improve our knowledge and extend our work.

2 | MIRIDS ODES MODELS

To build the models, we recall here what we know about the biology and ecology of Mirids. The life cycle of *S. singularis* is composed of 3 stages: egg stage, nymph stage, and adult stage that develop mainly on pods either on shoots. The eggs are individually inserted into the host plant tissues[23] principally in the cortex of pods and sometimes under the bark of young shoots.[24] The incubation period of eggs is on average 15 days with a minimum of 9 days[25] and a maximum of 21 days[26] before reaching nymph stage. Mirid *S. singularis* has a very long life cycle (eggs to adults). It is on average 40 days with a minimum of 36 days[27] and a maximum of 50 days.[5] The percentage of hatching eggs is globally 96.53% as the eggs are protected in the pods cortex. During the 5 nymph instars, the individuals move within a cacao tree by walk to feed on the pods and shoots. The nymphs are able to feed just after the eggs hatching.

Twenty-five days are needed to complete the nymph development considering 5 days in average per instar.[5] Globally, the total nymph survivorship is around 68%.[28] The average daily rate of survival of the nymphs (considering all the 5 instars) was estimated around 98.5% (estimated using biological data). At the emergence, there is on average one female for 0.71 male[5] (this gives a sex ratio $r = 1/1.71 \approx 0.58$; in fact, sex ratio varies between 0.5 and 0.6). Females *S. singularis* mate with one male 6 to 10 days after their emergence. The first eggs are observed in average 10 days after emergence, so 4 to 8 days after mating (estimated using biological data). Indeed, after this mating period females are considered as mature. On average 72.1% of immature females become mature females.[27] After the emergence, adults (males and females) fly from one cocoa tree to another ensuring the spatial dispersion of the individuals and causing the spatial distribution of the damage in the plots. It is likely the females do not lay all their eggs on the same pod. The average fecundity per female is around 50.7 larvae or 52.5 eggs, and the fecundity period lasts on average 16 days.[6,12,25,29,30] The daily survival of mirids adult is around respectively 98.14% for immature females, 92.8% for mature females, and 93% for males (estimated thanks to other works[5,6,25,26,29]). On average, 50 to 60 days are needed to obtain a new generation of mirids.[5] This long life period for an insect to grow is a key factor for the dynamic of mirid populations.

Mirids population dynamics varied greatly during the year. Density of population is likely to be influenced by pods availability on the trees and by external conditions like weather.[8] The mirid population is low on cocoa during the period from February to March. From June to July, the populations start to grow more or less rapidly. The peak of the population appears between September and November when the pods are almost mature.[5,29,31,32] It is also assumed that unfavorable climatic conditions (high temperature and low pluviometry) can cause declining fertility of females and increased mortality of individuals[8] that lead to lower mirid populations observed in plantations from November to December to June.

We now formulate a model based on the life cycle of *S. singularis* that is summarized in Figure 1. We use a stage-structured model. We consider 3 main stages in the development of the mirid: the egg stage (E), the nymph stage (L) (nymphs and pupae), and the adult stage. The adult stage is subdivided into immature female (F_1), mature female (F_2), and male (M). According to Figure 1, we derive the following ODES model:

$$\begin{cases} \dot{E} = bF_2\left(1-\dfrac{E}{K_C}\right)-(\nu_E+\mu_E)E, \\ \dot{L} = \nu_E E-(\nu_L+\mu_L)L, \\ \dot{F_1} = r\nu_L L-(\nu_F+\mu_A)F_1, \\ \dot{F_2} = \nu_F F_1-\mu_A F_2, \\ \dot{M} = (1-r)\nu_L L-\mu_A M, \end{cases} \tag{1}$$

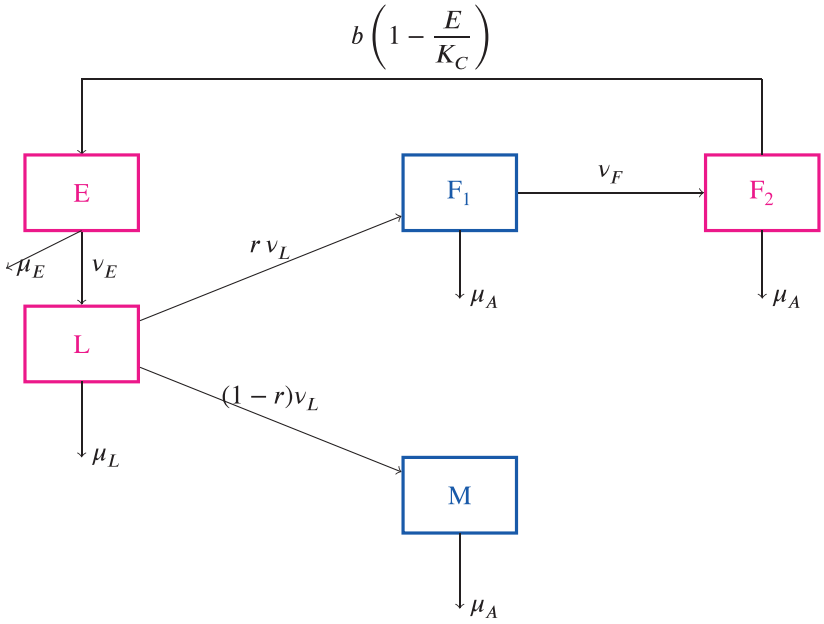

FIGURE 1 Life cycle of *Sahlbergella singularis* [Colour figure can be viewed at wileyonlinelibrary.com]

with nonnegative initial conditions:

$$\begin{cases} E(0) = E^0, & L(0) = L^0, & F_1(0) = F_1^0, \\ F_2(0) = F_2^0, & M(0) = M^0. \end{cases} \tag{2}$$

The biological parameters are described as follows: r is the sex ratio; b is the mean number of eggs laid by an adult female mirid per day that have emerged as larvae; K_C is the maximal carrying capacity related to the mean daily number of pods per area (ha); μ_E, μ_L, and μ_A represent respectively the eggs, nymphs, and adults daily mortality rate; ν_E and ν_L are respectively the transition rate from the egg to nymph stage and the nymph to adult stage; $(1/(\nu_E+\mu_E)$ and $(1/(\nu_L+\mu_L)$ are respectively the mean time a mirid stays in the egg and nymph stage (measured in days); ν_F is the transition rate from the immature female stage to mature female stage; and $1/(\nu_F+\mu_A)$ is the mean life span of an immature female mirid, measured in days.

The nonlinear term $rbF_2\left(1-\frac{E}{K_C}\right)$ is related to a specific behavior of some insects species, like *Aedes* mosquito[33,34] and also mirids, known as skip-oviposition behavior. Indeed, according to expert's knowledge, mirids (*S. singularis*) are able to select their breeding sites. Some cocoa trees, particularly suitable for development larvae, show greater damage, which leads to the degradation of the foliage and the formation of orthotropic (or greedy) shoots.[28] Thus, if breeding sites, in a given area, already contain a lot of eggs, then females will not deposit eggs or only very few. That is why, the oviposition rate rbF_2 is limited by the available space in breeding sites, $\left(1-\frac{E}{K_C}\right)$, which implies that the birth rate in the eggs compartment is modeled by the nonlinear term $rbF_2\left(1-\frac{E}{K_C}\right)$. Table 1, page 4, summarizes the parameters and their biological meaning.

The right-hand side of system (1) is continuously differentiable ($\mathcal{C}^1$). Then, using the Cauchy-Lipschitz theorem, system (1) has a unique maximal solution. If the initial data are in $\mathbb{R}^5_+$, the solutions stay in $\mathbb{R}^5_+$: $E = 0$, $L = 0$, $F_1 = 0$, $F_2 = 0$ and $M = 0$ are vertical and horizontal null lines, respectively. Thus, the trajectories can not cut these axes: so model system (1) is biologically well posed. It is straightforward to show that the compact

$$\begin{aligned} \Omega = \Bigg\{ & (E, L, F_1, F_2, M) \in \mathbb{R}^5_+; E(t) \le K_C,\ L(t) \le \frac{\nu_E K_C}{\nu_L + \mu_L} F_1(t) \le \frac{r\nu_L \nu_E K_C}{(\nu_L + \mu_L)(\mu_A + \nu_F)}, \\ & F_2(t) \le \frac{r\nu_L \nu_F \nu_E K_C}{\mu_A(\nu_L + \mu_L)(\nu_F + \mu_A)} \text{ and } M(t) \le \frac{(1-r)\nu_L \nu_E K_C}{\mu_A(\nu_L + \mu_L)} \Bigg\} \end{aligned} \tag{3}$$

is positively invariant by (1). Now, we will derive some quantitative analysis of system (1). Let us consider the following threshold:

$$\mathcal{N}_0 = \frac{rb\nu_L \nu_F \nu_E}{\mu_A(\nu_E + \mu_E)(\nu_F + \mu_A)(\nu_L + \mu_L)}. \tag{4}$$

TABLE 1 Parameters of model (1)

Parameters	Biological significance	Unit
b	Mean number of eggs laid by a mature female	days^{-1}
K_C	Maximal carrying capacity related to the mean	
	daily number of pods per ha	
$1/\nu_L$	Duration of the development of nymphs	days
$1/\nu_F$	Time necessary for an immature female to become mature	days
μ_L	Mortality of nymphs	days^{-1}
μ_A	Mortality of adults	days^{-1}
μ_E	Mortality of eggs	days^{-1}
$1/\nu_E$	Time necessary for an egg to become nymph	days

$\mathcal{N}_0$ represents the mean number of adults female produced by one adult female over its life span. It is sometimes called the basic offspring number.

Lemma 2.1. *System (1) has 2 possible equilibria:*

(1) a trivial equilibrium $X^0 = (0,0,0,0,0)$, which always exists
(2) a positive equilibrium $X^* = (E^*, L^*, F_1^*, F_2^*, M^*)$ defined as follows:

$$E^* = \frac{(\mathcal{N}_0 - 1)}{\mathcal{N}_0} K_C,\ L^* = \frac{\nu_E}{\nu_L + \mu_L} E^*,\ F_1^* = \frac{r\nu_E\nu_L}{(\nu_L + \mu_L)(\nu_F + \mu_A)} E^*,$$
$$F_2^* = \frac{r\nu_E\nu_L\nu_F}{\mu_A(\nu_L + \mu_L)(\nu_F + \mu_A)} E^* \text{ and } M^* = \frac{(1-r)\nu_E\nu_L}{\mu_A(\nu_L + \mu_L)} E^*, \tag{5}$$

which exists when $\mathcal{N}_0 > 1$.

It is straightforward to verify that system (1) is a cooperative system.[35] We briefly recall its definition. Let us consider an n-dimensional autonomous differential system:

$$\dot{x} = f(x), \qquad x(0) = x_0, \tag{6}$$

where f is a given vector function, ie, $f = (f)_i$, with $f_i: \mathbb{R}^n \to \mathbb{R}$. System (6) is called cooperative if for every $i, j \in \{1,2,\dots,n\}$ such that $i \neq j$, the function $f_i(x_1, \dots, x_n)$ is monotone increasing with respect to x_j. For cooperative system, the global asymptotic stability of an equilibrium can be studied by the following theorem:

Theorem 2.1. *System (6) is a cooperative system. Let $a, b \in \Omega$ such that $a < b$, $[a,b] \subset \Omega$ and $f(b) \leq 0 \leq f(a)$; where $[a,b] = \{x \in \mathbb{R}^5, a \leq x \leq b\}$.* [36] *Then (6) defines a (positive) dynamical system on [a,b]. Moreover, if [a,b] contains a unique equilibrium p then p is globally asymptotically stable on [a,b].*

The dynamic of system (1) is summarized in the following theorem:

Theorem 2.2. *Assume that $(E^0, L^0, F_1^0, F_2^0, M^0) \in \Omega$.*

(1) When $\mathcal{N}_0 \leq 1$, the trivial equilibrium X^0 is globally asymptotically stable, which means that the mirid population will dwindle until extinction, whatever the initial population.
(2) When $\mathcal{N}_0 > 1$, the trivial equilibrium is unstable and the positive equilibrium X^* is globally asymptotically stable, which means that the mirid population persists.

Proof. It suffices to verify the assumptions of theorem.[36]

(1) When $\mathcal{N}_0 \leq 1$, model system (1) has only the trivial equilibrium X^0. By taking $a = 0$ and $b = \left(K_C, \frac{2\nu_E K_C}{\nu_L + \mu_L}, \frac{3r\nu_L\nu_E K_C}{(\nu_L + \mu_L)(\nu_F + \mu_A)}, \frac{4r\nu_E\nu_L\nu_F K_C}{\mu_A(\nu_L + \mu_L)(\nu_F + \mu_A)}, \frac{2(1-r)\nu_E\nu_L K_C}{\mu_A(\nu_L + \mu_L)}\right)$, we have $f(a) = 0$ and $f(b) \leq 0$. Using theorem 6,[36] the trivial equilibrium X^0 is globally asymptotically stable on $[0, b]$; hence, on Ω when $\mathcal{N}_0 \leq 1$.
(2) When $\mathcal{N}_0 > 1$, there exists $\varepsilon > 0$ such that $\mathcal{N}_0 > 1 + \varepsilon$. Let E_ε sufficiently small such that

$$E_\varepsilon \leq \varepsilon, \quad L_\varepsilon = \frac{\nu_E(1+\varepsilon)}{(\nu_L + \mu_L)\mathcal{N}_0} E_\varepsilon, \quad F_{1\varepsilon} = \frac{r\nu_L(1+\varepsilon)}{(\nu_F + \mu_A)\mathcal{N}_0} L_\varepsilon,$$
$$F_{2\varepsilon} = \frac{(\nu_E + \mu_E)(1+\varepsilon)^2}{b\mathcal{N}_0^2} E_\varepsilon, \quad M_\varepsilon = \frac{(1-r)\nu_L(1+\varepsilon)}{\mu_A \mathcal{N}_0} L_\varepsilon.$$

Let $b_\varepsilon = (E_\varepsilon, L_\varepsilon, F_{1\varepsilon}, F_{2\varepsilon}, M_\varepsilon)$. Then, from the right-hand side of (1) and the fact that $\mathcal{N}_0 > 1 + \varepsilon$ and $K_C \gg 1$, we deduce

$$f(b_\varepsilon) \geq \begin{pmatrix} \varepsilon(\nu_E+\mu_E)(1+\varepsilon)^2\left(1-\frac{1+\varepsilon}{K_C}\right)E_\varepsilon \\ \nu_E\left(1-\frac{1+\varepsilon}{\mathcal{N}_0}\right)E_\varepsilon \\ r\nu_L\left(1-\frac{1+\varepsilon}{\mathcal{N}_0}\right)L_\varepsilon \\ \nu_F\left(1-\frac{1+\varepsilon}{\mathcal{N}_0}\right)F_{1\varepsilon} \\ (1-r)\nu_L\left(1-\frac{1+\varepsilon}{\mathcal{N}_0}\right)L_\varepsilon \end{pmatrix} > 0.$$

Hence, it follows[36] from theorem 6 that equilibrium X^* is globally asymptotically stable on $[b_\varepsilon, b]$. Since b_ε can be selected to be smaller than any $x>0$, we have that X^* is asymptotically stable on Ω with basin of attraction $\tilde{\Omega} = \Omega \setminus \{(0,0,0,0,0)\}$. This also implies that X^0 is unstable.

2.1 | Sensitivity analysis

It is important to know the relative importance of some factors that maintain or not a mirid population. We may estimate the sensitivity index of $\mathcal{N}_0$ with respect to a parameter p, as follows:

$$\gamma_p^{\mathcal{N}_0} = \frac{\partial \mathcal{N}_0}{\partial p}.\frac{p}{\mathcal{N}_0}. \tag{7}$$

Straightforward calculation leads to the following result:

$$\gamma_r^{\mathcal{N}_0} = \gamma_b^{\mathcal{N}_0} = 1, \quad \gamma_{\nu_E}^{\mathcal{N}_0} = \frac{\mu_E}{\nu_E(\nu_E+\mu_E)},$$
$$\gamma_{\nu_L}^{\mathcal{N}_0} = \frac{\mu_L}{\nu_L(\nu_L+\mu_L)}, \quad \gamma_{\nu_F}^{\mathcal{N}_0} = \frac{\mu_F}{\nu_F(\nu_F+\mu_A)},$$
$$\gamma_{\mu_E}^{\mathcal{N}_0} = -\frac{1}{\nu_E+\mu_E}, \quad \gamma_{\mu_L}^{\mathcal{N}_0} = -\frac{1}{\nu_L+\mu_L}, \quad \gamma_{\mu_A}^{\mathcal{N}_0} = -\frac{\nu_F}{\mu_A(\nu_F+\mu_A)}.$$

Clearly, r and b have the strongest impact on $\mathcal{N}_0$. However, this gives us only partial informations. In particular, we will now focus on the variables E, L, F_1, F_2, and M. That is why, we derive some global sensitivity analysis using 2 well-known methods: the eFast and the LHS-PRCC methods. The eFast method given in Figure 2, page 8, highlights first-order effects (main effects) and total effects (main and all interaction effects) of the parameters on the model outputs. Complementary to the eFast method, we derived an LHS-PRCC sensitivity analysis given in Figure 3, page 9. LHS stands for Latin hypercube sampling and PRCC for partial rank correlation coefficient. These 2 methods give complementary information. Indeed, the PRCC method provides mainly information about how the outputs is impacted if we increase (or decrease) the inputs a specific parameter while the eFast indicates which parameter uncertainty has the greatest impact on the output variability (see, for instance, Marino et al[37] for further explanations).

In Table 2, page 7, we provide ranges of values for the model parameters. These ranges were estimated based on the data obtained by Babin and collaborators.

As expected, variation of the carrying capacity K_C has a strong impact on all variables, and also μ_A. For the transition rates ν_L, ν_E, ν_F, and the mortality rate μ_L, their impact is weaker, but according to the LHS-PRCC analysis is not negligible. Thus obviously, among all parameters, the parameters K_C, μ_A, ν_L, ν_E, ν_F, and μ_L are the most important parameters to estimate. Finally, according to the sensitivity analysis method that is considered b does not have the same impact. However, we think that this is an important parameter too.

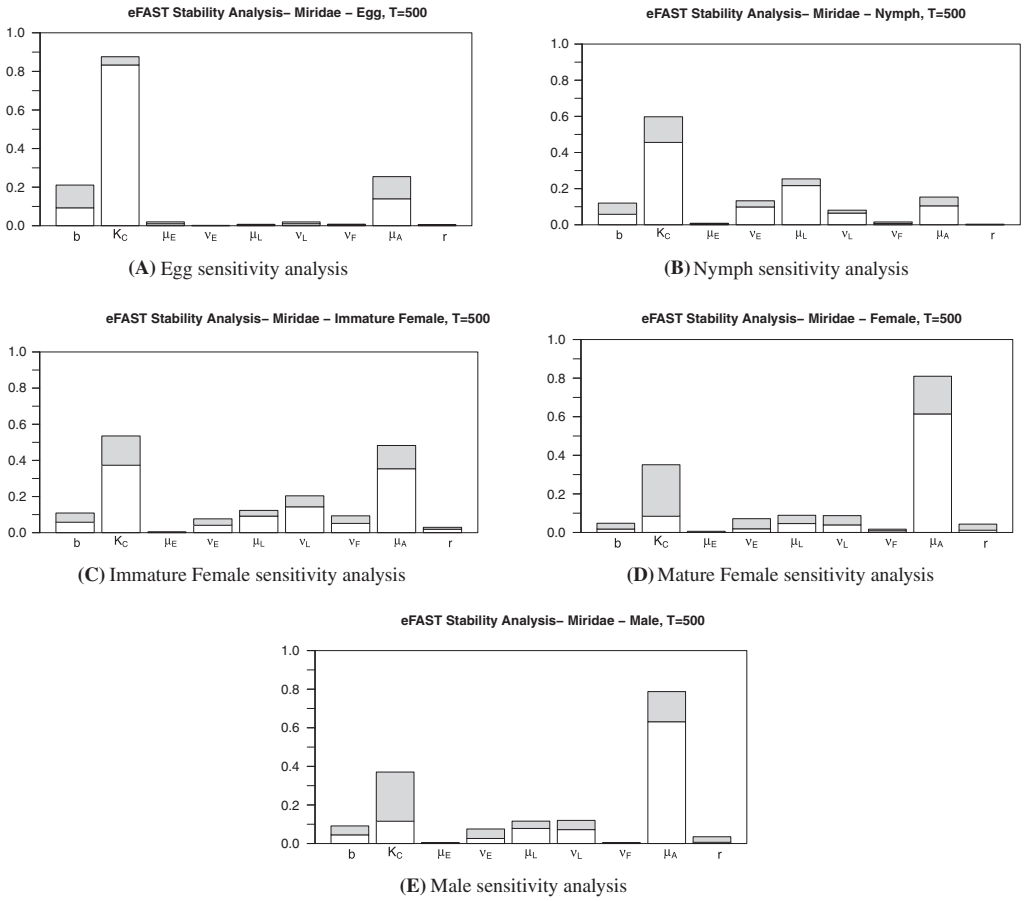

(A) Egg sensitivity analysis

(B) Nymph sensitivity analysis

(C) Immature Female sensitivity analysis

(D) Mature Female sensitivity analysis

(E) Male sensitivity analysis

FIGURE 2 eFAST sensitivity analysis at T=500. White bar: first-order effects; sum of white and gray bars: total effect

2.2 | Mirid system with periodic coefficients

In this section, we consider the previous model, but with periodic time-dependent parameters, since we know that most of the parameters may depend on the environment. In fact, mirids dynamics vary greatly during the year; density of populations is likely to be influenced by pods avail ability on the trees. In Babin et al,[27] it is admitted that lower mirid populations observed in the plots during a certain period of the year is due to the declining fertility of females and increasing mortality of individuals. Thus, it seems that development parameters (longevity, fecundity, and mortality) of mirids vary depending on season. We assume that all those parameters are T-periodic functions and are bounded: below, by a nonnegative minimal value, and above by a positive maximal value, that is, $p_{min} \leq p(t) \leq p_{max}$ for all $t \geq 0$, and $p = r, b, \mu_L, \mu_A, \mu_E, \nu_L, \nu_F, \nu_E$, or K_C. We also split the carrying capacity in 2 parts, $K_C(t)+C$: $K_C(t)$, the mean number of pods available for breeding, and C, the alternative breeding sites including new shoots and other tree hosts, like *Cola nitida, Ceiba pentandra*. [28] Thus, Model (1) becomes

$$\begin{cases} \dot{E} = b(t)F_2\left(1-\dfrac{E}{C+K_C(t)}\right)-(\nu_E(t)+\mu_E(t))E, \\ \dot{L} = \nu_E(t)E-(\nu_L(t)+\mu_L(t))L, \\ \dot{F_1} = r(t)\nu_L(t)L-(\nu_F(t)+\mu_A(t))F_1, \\ \dot{F_2} = \nu_F(t)F_1-\mu_A(t)F_2, \\ E(0)=E^0, \quad L(0)=L^0, \quad F_1(0)=F_1^0, \quad F_2(0)=F_2^0. \end{cases} \tag{8}$$

In fact, system (8) enters the family of periodic concave cooperative system with a concave nonlinearity. [38,39]

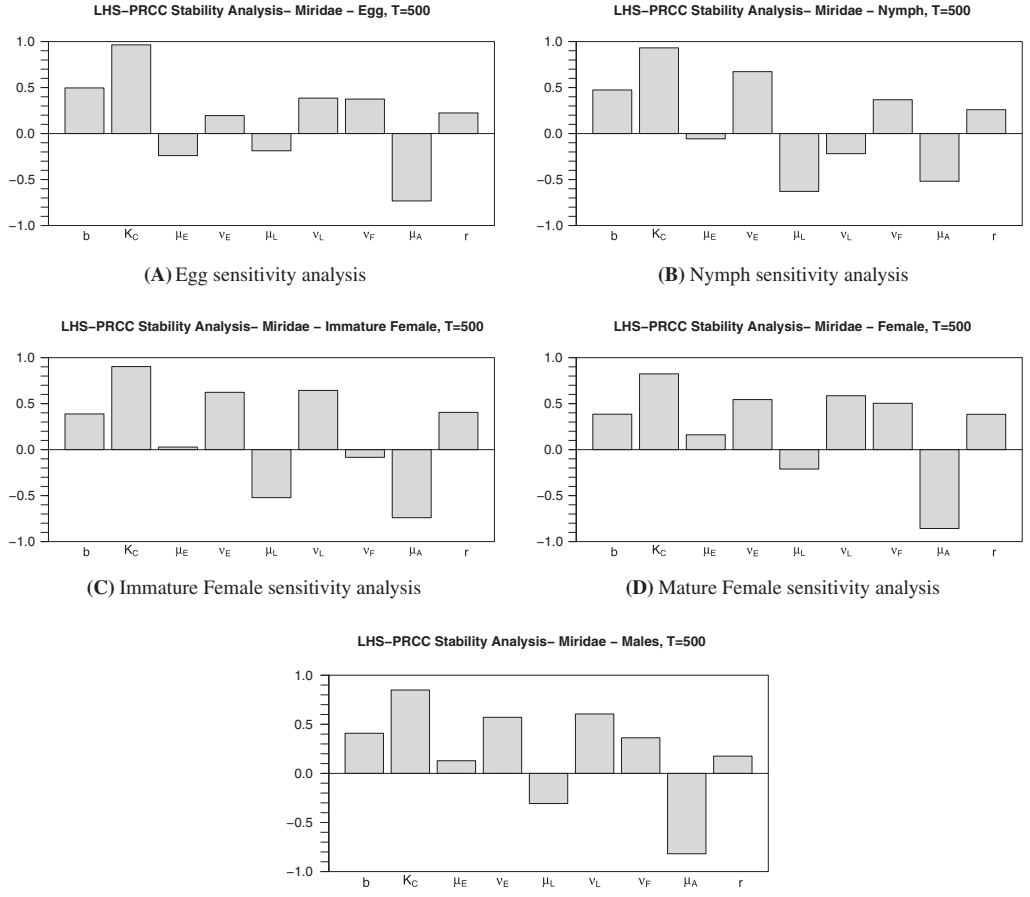

(A) Egg sensitivity analysis

(B) Nymph sensitivity analysis

(C) Immature Female sensitivity analysis

(D) Mature Female sensitivity analysis

(E) Male sensitivity analysis

FIGURE 3 Latin hypercube sampling (LHS)–partial rank correlation coefficient (PRCC) sensitivity analysis at T=500

Definition 2.1. Let us consider a n-dimensional autonomous differential system:

$$\dot{x} = F(t,x), \qquad x \in \mathbb{R}^n. \tag{9}$$

The system of differential Equations 9 is called cooperative with concave nonlinearities if

(i) $\dfrac{\partial F_i}{\partial x_j} \geq 0,\ i \neq j$ for each $(t,x) \in \mathbb{R}_+ \times \mathbb{R}_+^n$.

(ii) $x > y > 0$ implies $D_x F(t,y) > D_x F(t,x)$.

TABLE 2 Range of values for the parameters of system (1)

Parameters	Range	Source
r	[0.5,0.6]	estimated
b	[1.5;4]	estimated
K_C	[1,10000]	estimated
ν_L	[1/35,1/10]	estimated
ν_F	[1/10,1/6]	estimated
μ_L	[1/100,1/10]	estimated
μ_A	[1/100,1/10]	estimated
μ_E	[1/100,1/10]	estimated
ν_E	[1/10,1/20]	estimated

We will use a theorem (Theorem 2.5, in appendix A) proved in Smith.[39] We have

$$F(t,x)=\begin{pmatrix} b(t)F_2\left(1-\dfrac{E}{C+K_C(t)}\right)-(\nu_E(t)+\mu_E(t))E \\ \nu_E(t)E-(\nu_L(t)+\mu_L(t))L \\ r(t)\nu_L(t)L-(\nu_F(t)+\mu_A(t))F_1 \\ \nu_F(t)F_1-\mu_A(t)F_2 \end{pmatrix},$$

where $x=(E,L,F_1,F_2)^T$. Obviously, F is continuously differentiable and T-periodic. According to Cauchy-Lipschitz theorem, we have existence of a positive and bounded solution. Since all time-dependent parameters are positive, we verify easily property (1) in Definition 2.1.
Let us compute the Jacobian

$$D_xF(t,x)=\begin{pmatrix} -\left(\nu_E(t)+\mu_E(t)+\dfrac{b(t)F_2}{K_C(t)+C}\right) & 0 & 0 & b(t)\left(1-\dfrac{E}{K_C(t)+C}\right) \\ \nu_E(t) & -(\nu_L(t)+\mu_L(t)) & 0 & 0 \\ 0 & r(t)\nu_L(t) & -(\nu_F(t)+\mu_A(t)) & 0 \\ 0 & 0 & \nu_F(t) & -\mu_A(t) \end{pmatrix}.$$

It is straightforward to verify (2) in Definition 2.1. In addition, $D_xF(t,x)$ is irreducible for each $(t,x)\in\mathbb{R}\times\mathbb{R}^n_+$. Thus, Theorem 2.5 applies to system (9), and we deduce that every solution x, with $x(t_0)\geq 0$, can be continued in $[t_0,\infty]$ with $x(t)\geq 0$ for $t\geq t_0$. Now, let us compute $D_xF(t,0)$, that is,

$$D_xF(t,0)=\begin{pmatrix} -(\nu_E(t)+\mu_E(t)) & 0 & 0 & b(t) \\ \nu_E(t) & -(\nu_L(t)+\mu_L(t) & 0 & 0 \\ 0 & r(t)\nu_L(t) & -(\nu_F(t)+\mu_A(t)) & 0 \\ 0 & 0 & \nu_F(t) & -\mu_A(t) \end{pmatrix}.$$

According to Theorem 2.5, if the Floquet multipliers of $D_xF(t,0)$ lie inside or on the unit circle, then $\lim_{t\to\infty}x(t)=0$. In contrary, if any Floquet multiplier lies outside the unit circle, and according to the fact that $F(t,0)\equiv 0$ and x is a bounded solution, we deduce that system (9) has a unique nonzero T-periodic solution $x_{per}(t)$.

In general, the determination of Floquet multipliers is extremely difficult. That is why, we will now consider an additional result[38] recalled in appendix A (see Theorem 2.6). This is an algebraic criterion, related to the study of $A(t)=D_xF(t,0)$. Let us estimate $\underline{A}$ and $\bar{A}$, lower and upper bounds of matrix $A(t)$. Using the fact that all time-dependent parameters have positive lower and upper bounds, we deduce

$$A=\begin{pmatrix} -(\nu_{E,max}+\mu_{E,max}) & 0 & 0 & b_{min} \\ \nu_{E,min} & -(\nu_{L,max}+\mu_{L,max}) & 0 & 0 \\ 0 & r_{min}\nu_{L,min} & -(\nu_{F,max}+\mu_{A,max}) & 0 \\ 0 & 0 & \nu_{F,min} & -\mu_{A,max} \end{pmatrix},$$

and

$$\bar{A}=\begin{pmatrix} -(\nu_{E,min}+\mu_{E,min}) & 0 & 0 & b_{max} \\ \nu_{E,max} & (\nu_{E,min}+\mu_{E,min}) & 0 & 0 \\ 0 & r_{max}\nu_{L,max} & -(\nu_{F,min}+\mu_{A,min}) & 0 \\ 0 & 0 & \nu_{F,max} & -\mu_{A,min} \end{pmatrix}.$$

Then according to Theorem 2.6, we have to study the principal minors of $-\underline{A}$ and $-\overline{A}$. All diagonal terms of $-\underline{A}$ and $-\overline{A}$ are positive. In fact, it suffices to compute $\det(-\overline{A})$ and $\det(-\underline{A})$, that is,

$$\det(-\overline{A}) = -(\nu_{E,min}+\mu_{E,min})(\nu_{L,min}+\mu_{L,min})(\nu_{F,min}+\mu_{A,min})\mu_{A,min} + b_{max}r_{max}\nu_{E,max}\nu_{L,max}\nu_{F,max},$$
$$\det(-\underline{A}) = (\nu_{E,max}+\mu_{E,max})(\nu_{L,max}+\mu_{L,max})(\nu_{F,max}+\mu_{A,max})\mu_{A,max} - b_{min}r_{min}\nu_{L,min}\nu_{F,min}.$$

Thus, $\det(-\bar{A}) \geq 0$ if

$$b_{max}r_{max}\nu_{L,max}\nu_{F,max} \geq (\nu_{E,min}+\mu_{E,min})(\nu_{L,min}+\mu_{L,min})(\nu_{F,min}+\mu_{A,min})\mu_{A,min},$$

and $\det(-\underline{A}) < 0$ if

$$(\nu_{E,max}+\mu_{E,max})(\nu_{L,max}+\mu_{L,max})(\nu_{F,max}+\mu_{A,max})\mu_{A,max} < b_{min}r_{min}\nu_{L,min}\nu_{F,min}.$$

In fact, the previous results are related to the time dependent basic offspring number

$$\mathcal{N}_0(t) = \frac{r\,b(t)\nu_E(t)\nu_L(t)\nu_F(t)}{\mu_A(t)(\nu_E(t)+\mu_E(t))(\nu_F(t)+\mu_A(t))(\nu_L(t)+\mu_L(t))},$$

such that $\mathcal{N}_{0,min} \leq \mathcal{N}_0(t) \leq \mathcal{N}_{0,max}$, where

$$\mathcal{N}_{0,min} = \frac{r_{min}\,b_{min}\nu_{E,min}\nu_{L,min}\nu_{F,min}}{(\nu_{E,max}+\mu_{E,max})(\nu_{max}+\mu_{max})(\nu_{F,max}+\mu_{A,max})\mu_{A,max}},$$

and

$$\mathcal{N}_{0,max} = \frac{r_{max}\,b_{max}\,\nu_{E,max}\nu_{L,max}\nu_{F,max}}{(\nu_{E,min}+\mu_{E,min})(\nu_{min}+\mu_{min})(\nu_{F,min}+\mu_{A,min})\mu_{A,min}}.$$

According to Theorem 2.6, we deduce

Theorem 2.3.

(i) If $\mathcal{N}_{0,max} \leq 1$, then the solution of system (8) converges to the trivial equilibrium X^0.

(ii) If $\mathcal{N}_{0,min} > 1$, then system (8) admits a unique periodic solution, which attracts all initial condition in Ω.

According to the sensitivity analysis, an interesting and particular case is when we assume that all parameters are constant, except K. Then $\overline{A} = \underline{A}$, and thus, $\mathcal{N}_{0,max} = \mathcal{N}_{0,min} = \mathcal{N}_0$. Thus, Theorem 2.3 reduces to

Theorem 2.4.

(i) If $\mathcal{N}_0 \leq 1$, then the solution of system (8) converges to the trivial equilibrium X^0.

(ii) If $\mathcal{N}_0 > 1$, then system (8) admits a unique periodic solution, which attracts all initial condition in Ω.

In fact, we recover the same results than for the constant parameters problem, except that the constant positive equilibrium is now periodic of period T.

It is important to notice that K_C constant is relevant in the case where the cocoa production is almost constant along the year. This is realistic in Central America where there is no real seasonality. By contrast, in Cameroon, they are 2 rainy season: a long one and a short one. There, the seasonality is clearly marked, which has an impact on cacao production. That is why we consider a periodic function for K_C.

2.3 | Numerical simulations

Now, we will illustrate our theoretical results. We will use the values of the monthly mean number of pods using data extrapolated, obtained in Cameroon, from Bisselua et al[30] to construct our periodic function $K_C(t)$. According to the data from Bisselua et al[30] and the knowledge about the mean number of pods over the year, our daily estimated data are recapitulated in Table 3.

We suppose that the function $K_C(t)$ is periodic, of period $T = 365$ days. We use the cubic spline interpolation to derive the time evolution of $K_C(t)$ along a year. Using cubic Hermite spline, we obtain a polynomial interpolation (daily estimation of $K_C(t)$) given in Figure 4, page 11. Figure 4, page 11, represents the daily estimation of pods number in the plot. $K_C(t)$.

TABLE 3 Mean number of pods per days

Mo	Jun	Jul	Aug	Sept	Oct	Nov	Dec	Jan	Feb	Mar	Apr	May	Jun
$K_C(t)$	0	$\frac{32\ 000}{31}$	$\frac{160\ 000}{31}$	$\frac{416\ 000}{30}$	$\frac{544\ 000}{31}$	$\frac{304\ 000}{31}$	$\frac{416\ 000}{31}$	$\frac{120\ 000}{31}$	$\frac{8000}{28}$	0	0	0	0

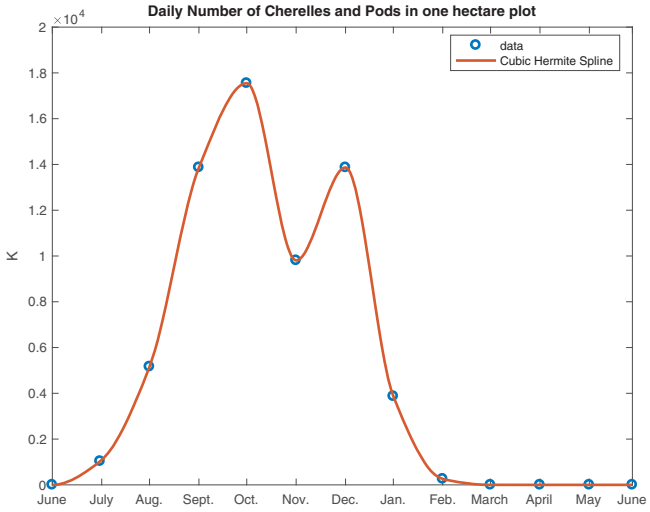

FIGURE 4 Daily estimation of $K_C(t)$ along a year [Colour figure can be viewed at wileyonlinelibrary.com]

When the parameter K_C is constant, we used a classical scheme already well implemented under matlab (ode23s) for numerical simulations, and we consider that the number of pods K_C is constant; we evaluate the average daily value estimated with the data of Table 3, that is,

$$\overline{K}_C = \frac{1}{365}\int_1^{365} K_C(t)dt.$$

When K_C is periodic, following Anguelov et al,[40] we consider a nonstandard numerical scheme to preserve most of the qualitative properties of the continuous model, like positivity, equilibria, stability, and instability whatever the time step $\Delta t > 0$. We consider the values of parameters given in Table 4. We illustrate our numerical simulations for 2 values of C: $C = 5$, and $C = 100$. All the given values have been estimated thanks to other works.[5,6,25,26,29]

In Figure 5, page 12, we illustrate the theoretical results when the carrying capacity K_C is constant, that is, $\overline{K}_C = 5482$, with initial conditions (E, L, F_1, F_2, M)=(0,0,0,10,10). As expected, when $\mathcal{N}_0$<1, the population decays till extinction,

TABLE 4 Values of constant parameters

Parameters	Case $\mathcal{N}_0$<1	Case $\mathcal{N}_0$>1	Source
r	0.58	0.58	[5]
b	3.28	3.28	Estimated
ν_E	1/15	1/15	Estimated
ν_L	1/25	1/25	Estimated
ν_F	1/10	1/10	Estimated
μ_E	0.05	0.001	Estimated
μ_L	0.15	0.03	Estimated
μ_A	0.15	0.07	Estimated
$\mathcal{N}_0$	0.6103	9.0002	Equation 4

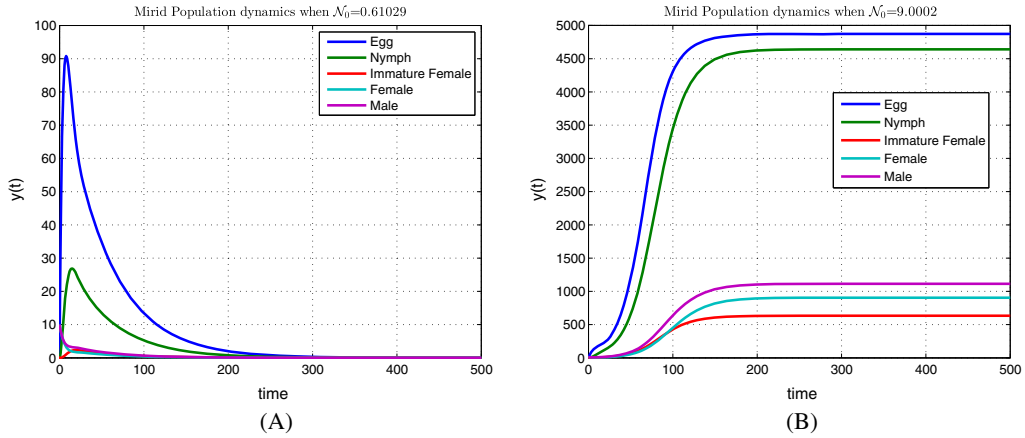

FIGURE 5 Time evolution of mirid population when $K_C = 5482$. A, $\mathcal{N}_0$<1. B, $\mathcal{N}_0$>1 [Colour figure can be viewed at wileyonlinelibrary.com]

while, when $\mathcal{N}_0$>1, the population reaches rapidly the positive equilibrium. However, in Cameroon, having a constant number of pods along the year is not realistic. That is why in the next simulations, we consider a more realistic case, with the same parameters values. In Figures 6 and 7, page 13, we illustrate the previous results when the carrying capacity K_C

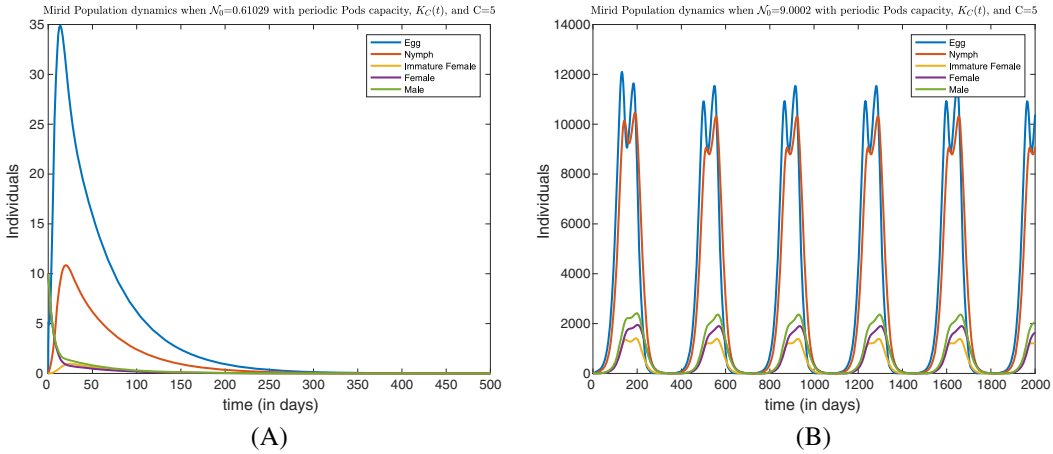

FIGURE 6 Time evolution of mirid population when K_C is periodic and C=5. A, $\mathcal{N}_0$<1. B, $\mathcal{N}_0$>1 [Colour figure can be viewed at wileyonlinelibrary.com]

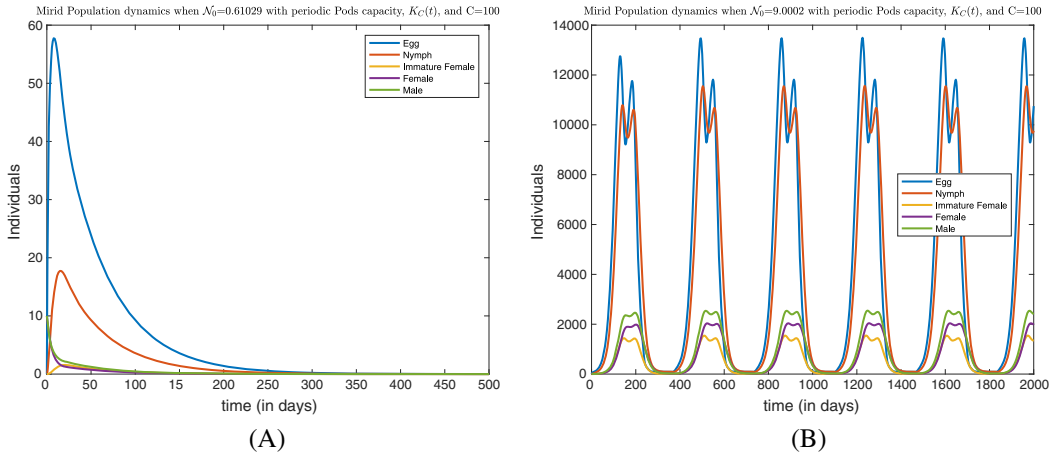

FIGURE 7 Time evolution of mirid population when K_C is periodic and C=100. A, $\mathcal{N}_0$<1. B, $\mathcal{N}_0$>1 [Colour figure can be viewed at wileyonlinelibrary.com]

is periodic. However, in the case where $\mathcal{N}_0 > 1$, the dynamic of mirids follows the dynamic of pods, as expected. However, the size of the population seems to be large compared with real observations (see, for instance, Bisselua et al [30]).

3 | A MODEL WITH DELAYS

In the previous section, we studied the time evolution of mirid population as if the transition to one stage of development to another is immediate. Biologically, this is not correct: let us return on the biological life cycle of *S. singularis* given in Figure 8, page 14. In fact, each individual needs to stay a certain amount of time in each compartment to complete its stage, in particular in the egg, nymph, and nonmature female stages: there exists τ_1 days between egg-laying and appearing of new nymphs; τ_2 days between nymphs and emergence to adults. In addition, female needs τ_3 days to become mature before being able to lay eggs. In this section, we will take into account some of these previous times leading to time-delayed model with delays.

Now, it is possible to take into account different biological facts. In particular, based on the literature, we know that after deposition, eggs need (in mean) τ_1=15 days to hatch and enter the nymphs compartment. b always represents the mean daily number of eggs laid by an adult female. τ_2=25 days represent the required time for nymphs to achieve their development and become adults. So only a proportion $e^{-\tau_2\mu_L}$ of nymphs will survive and become adults. Thus, $\nu_E e^{-\tau_2\mu_L}E(t-\tau_2)$ represents the transition rate from eggs to adults, after τ_2 days in the nymphs compartment. The term $re^{-\tau_3\mu_A}$ represents the proportion of immature adults that will deposit eggs, after τ_3 of maturation.

Altogether, we obtain the following "two-delays" model:

$$\begin{cases} \dfrac{dE}{dt} = rbe^{-\tau_3\mu_A}A(t-\tau_3)\left(1-\dfrac{E}{K_C}\right)-(\nu_E+\mu_E)E, \\ \dfrac{dA}{dt} = \nu_E e^{-\tau_2\mu_L}E(t-\tau_2)-\mu_A A. \end{cases} \tag{10}$$

It can be rewritten as follows:

$$\begin{cases} \dfrac{dx_1}{dt} = \alpha x_2(t-\tau_3)\left(1-\dfrac{x_1}{K_C}\right)-\beta x_1, \\ \dfrac{dx_2}{dt} = \gamma x_1(t-\tau_2)-\delta x_2, \end{cases} \tag{11}$$

where

$$\alpha = rbe^{-\tau_3\mu_A}, \qquad \beta = \nu_E+\mu_E, \qquad \gamma = \nu_E e^{-\tau_2\mu_L}, \qquad \delta = \mu_A.$$

The right-hand side of system (11) is continuous and Lipschitzian in x. Thus, according to the standard theory of delay differential equations,[41] system (11) admits a unique solution for each continuous initial condition $\varphi \in \mathcal{C}([-\tau;0],\mathbb{R}^2)$ where $\tau = \max(\tau_3,\tau_2)$. We denote $\mathcal{C}([-\tau;0],\mathbb{R}^2)$ the Banach space of continuous functions mapping the interval $[-\tau;0]$ into $\mathbb{R}^2$ with the topology of uniform convergence; ie, for $\varphi \in \mathcal{C}([-\tau;0],\mathbb{R}^2)$, the norm of φ is defined as $\|\varphi\| = \sup_{-\tau\le\theta\le 0}|\varphi(\theta)|$ where $|.|$ is a norm of $\mathbb{R}^2$.

Let

$$\mathcal{D} = \left\{x\in\mathbb{R}^2_+ / x_1 \le K_C, \quad x_2 \le \frac{\gamma K_C}{\delta}\right\}.$$

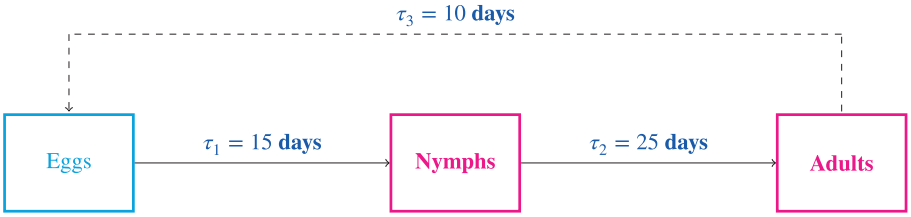

FIGURE 8 Life cycle of *Sahlbergella singularis* with maturation times [Colour figure can be viewed at wileyonlinelibrary.com]

System (11) can be rewritten as follows:

$$x'(t) = f(x(t), x(t-\tau_3), x(t-\tau_2)) = f(x, Y), \tag{12}$$

where $Y=(x(t-\tau_3), x(t-\tau_2))$. Following Smith,[35] it is important to notice that system (8) without delays reduces to a cooperative irreducible system. In fact, the delayed system is cooperative too. Indeed, according to Smith[35] and Smith and Hirsch,[42] we can show that f verifies the quasimonotone condition, defined as follows in Smith[35] and Smith and Hirsch[42]:

$$\phi, \psi \in \mathcal{D}, \phi \leq \psi \text{ and } \phi_i(0) = \psi_i(0) \quad \text{implies} \quad f_i(\phi) \leq f_i(\psi). \tag{13}$$

In fact, it suffices to use theorem 4.5,[42] page 308, ie, to show that f is cooperative to deduce that (13) holds for f, that is,

$$\frac{\partial f_i}{\partial x_j}(x, Y) \geq 0, \quad \text{for } i \neq j, \tag{14}$$

$$\frac{\partial f_i}{\partial y_j^k}(x, Y) \geq 0, \quad \text{for all } i, j, k. \tag{15}$$

Obviously, since the nondelayed model is cooperative, condition (14) is verified. Let us now check condition (15):

$$\frac{\partial f_1}{\partial y_1^1}(x, Y) = 0, \quad \frac{\partial f_1}{\partial y_2^1}(x, Y) = \alpha\left(1-\frac{x_1}{K_C}\right) \geq 0, \tag{16}$$

$$\frac{\partial f_2}{\partial y_1^2}(x, Y) = \gamma > 0, \quad \frac{\partial f_2}{\partial y_2^2}(x, Y) = 0. \tag{17}$$

Since the previous conditions are verified, we deduce that f is quasimonotone, which implies that if the initial condition is positive (with at most one zero component), then the solution x is still nonnegative, ie, $x(t) \geq 0$. Similarly, using the fact that the initial condition $\phi \in \mathcal{D}$, we have $x_1 \leq K_C$, and $x_2 \leq \frac{\gamma K_C}{\delta}$, for $t \in [-\tau, 0]$. Using these inequalities in (11), we infer that this is still true when $t \in [0, \tau]$. Iterating this reasoning, we finally deduce that $x(t) \in \mathcal{D}$ for all $t \geq 0$. A direct computation shows that system (11) admits 2 equilibria: the trivial ones, $\mathbf{0} = (0,0)$, and

$$\mathbf{x}^* = \left(\left(1-\frac{\beta\delta}{\alpha\gamma}\right)K_C, \frac{\gamma}{\delta}\left(1-\frac{\beta\delta}{\alpha\gamma}\right)K_C\right) = \left(\left(1-\frac{1}{\mathcal{R}}\right)K_C, \frac{\gamma}{\delta}\left(1-\frac{1}{\mathcal{R}}\right)K_C\right),$$

when $\mathcal{R}>1$ where

$$\mathcal{R} = \frac{\alpha\gamma}{\beta\delta} = \frac{rb\nu_E e^{-\tau_2\mu_L - \tau_3\mu_A}}{\mu_A(\nu_E + \mu_E)}. \tag{18}$$

Note that

$$\mathcal{R} = \frac{\alpha\gamma}{\beta\delta} = \frac{rb\nu_E e^{-\tau_2\mu_E - \tau_3\mu_A}}{\mu_A(\nu_E + \mu_E)} < \mathcal{N} = \frac{rb\nu_E\nu_L\nu_F}{\mu_A(\nu_E + \mu_E)(\nu_L + \mu_L)(\nu_F + \mu_A)}.$$

Thus, for some parameters values, we may have $\mathcal{N}>1$ and $\mathcal{R}<1$.

There is no need to study the stability/instability of the equilibria. Indeed, according to Smith[35] (chapter 5), there is a nice property pointed out about cooperative irreducible time-delay systems: the asymptotic stability of each equilibrium is preserved for the delay differential system (8), whatever the values taken by the delays. In particular, when $\mathcal{R} \leq 1$ ($\mathcal{R}>1$), all orbits are attracted by $\mathbf{0}$ ($\mathbf{x}^*$). In other words, to study the long-term behavior of cooperative time-delay systems, it suffices to study the cooperative systems without delay(s).

This result implies that the use of delays does not change the long-time behavior of the time-dependent system (8). However, when the system is nonautonomous and periodic, its behavior may be different in the transient period from the nondelayed nonautonomous periodic system as it is showed in the forthcoming simulations (see Figure 11, page 18, and Figure 12, page 18).

Remark 3.1. The previous time-delayed system is considered with fixed delays. A possible extension, for future work would be to consider time varying delays, $\tau_i(t)$, since it seems obvious to consider that the developmental time in each stage may change according to environmental parameters, like temperature and rainfall. Finally, distributed delays could be considered. Unfortunately for both cases, we do not have data.

Finally, like for the nondelayed model, it is interesting to provide a global sensitivity analysis at different time $T = 100$ and $T = 500$ (see Figure 9, page 16). Clearly, the parameters μ_L and μ_A are the most sensitive parameters, and the delays play mainly a role in the transient phase ($T = 100$) and no more at equilibrium, contrary to the carrying capacity, K_C, even if this parameter is far less sensitive than in the previous nondelayed model. This clearly shows the importance of estimating efficiently these parameters in different environmental or semifield conditions. It also very interesting to compare the sensitivity analysis between 2 models that are supposed to model the same system.

3.1 | Numerical simulation

Now, we illustrate all the different stability cases, ie, when $\mathcal{R}<1$ and $\mathcal{R}>1$. The time-delayed Model is solved using matlab and the dde23 function. In Table 4, page 12, we summarize the parameters values used in the next simulations, but we attribute the new values of parameter μ_L. Then, the values of parameters for those simulations are consigned in Table 5, page 17.

We now derive numerical simulations with $K_C = 5482$ constant and K_C periodic, like in the previous section. We choose as initial conditions $(E(0), A(0))=(0,50)$.

In Figure 10, page 17, we illustrate the previous results when the carrying capacity K_C is constant. When $\mathcal{R}<1$, mirids population decays till extinction and when $\mathcal{R}>1$, mirids population converge to a positive equilibrium.

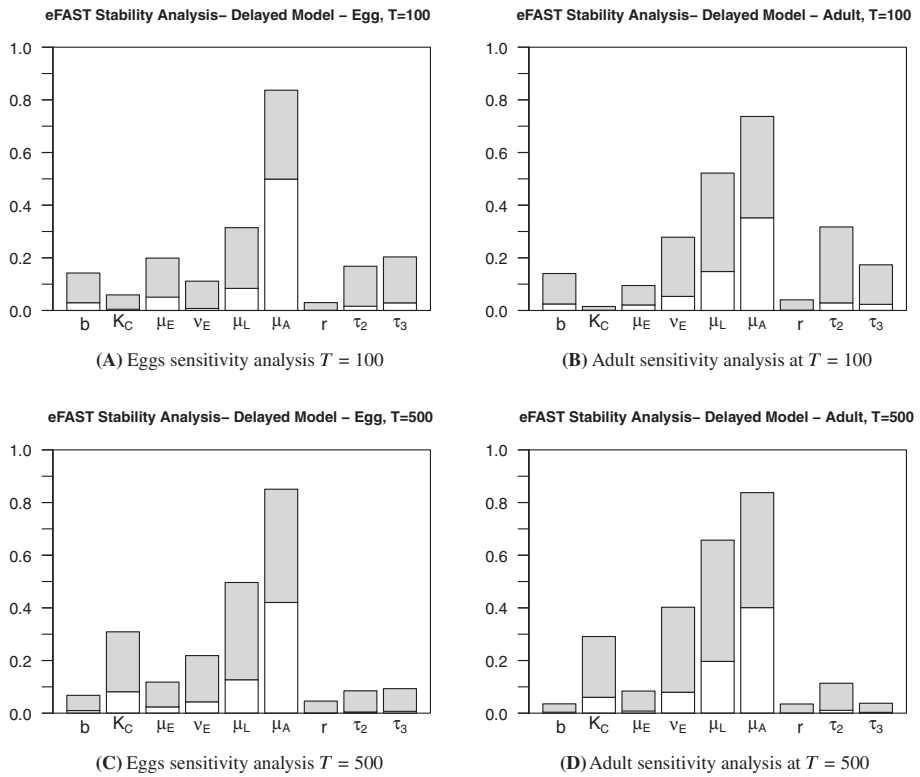

(A) Eggs sensitivity analysis $T = 100$

(B) Adult sensitivity analysis at $T = 100$

(C) Eggs sensitivity analysis $T = 500$

(D) Adult sensitivity analysis at $T = 500$

FIGURE 9 eFast sensitivity analysis of the time-delay model

TABLE 5 Values of constant parameters for the time-delay model

Parameters	Case $\mathcal{R}<1$	Case $\mathcal{R}>1$	Source
b	3.28	3.28	Estimated
τ_2	25	25	Estimated
τ_3	10	10	Estimated
μ_A	0.1	0.07	Estimated
r	0.58	0.58	Babin et al[5]
μ_L	0.1	0.03	Estimated
ν_E	1/15	1/15	Estimated
μ_E	0.001	0.001	Estimated
$\mathcal{R}$	0.566	6.28	Equation 18

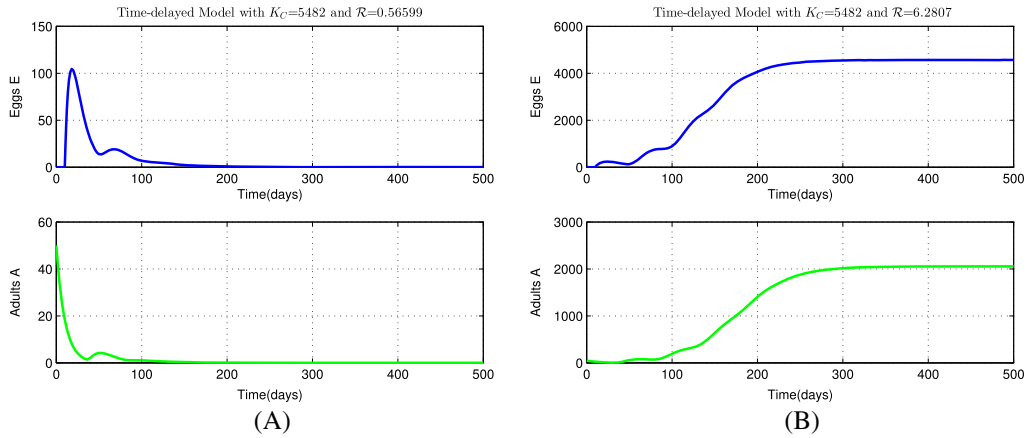

FIGURE 10 Time evolution of the eggs and adult compartments for the time-delay model with constant parameters, $K_C = 5482$, with A, $\mathcal{R}<1$; B, $\mathcal{R}>1$ [Colour figure can be viewed at wileyonlinelibrary.com]

As expected, when t goes to infinity, the time-delayed model with constant parameters responds exactly like the nondelayed model, except that the threshold parameters is not exactly the same. When $\mathcal{R}<1$ (>1), the system converges to the trivial (positive) equilibrium. In fact, with the same parameters, the deterministic model may converge to the positive equilibrium, while the time-delay model converges to the trivial equilibrium.

Figures 11, page 18, and 12, page 18, represent the time evolution of mirids with K_C periodic and for different values for C, namely, C=5 and C=100. When $\mathcal{R}\leq 1$, mirid population decays rapidly till extinction, whatever the values taken by C. In contrary, when $\mathcal{R}>1$, mirid population converges to a periodic solution, as expected, but with different amplitudes related to C, indicating the importance of alternative resources in the maintenance and the size of the population. The simulations seem to be in good agreement with field observations. It seems also to be obvious that the removal of alternative resources should be part of control strategies to lower the impact of the mirids. Compared with the time-delayed model, the nondelayed model overestimates the population. Thus, even if from the mathematical point of view the long-term behavior is the same, the time-delayed model provides better estimate of the population size along the year than the nondelayed model.

We would like to emphasize that our study was very difficult because of the lack of population data. Many parameters values were estimated using raw data obtained in the field by Babin, in 2008, in Cameroon. We use these data to estimate several parameters like mortality of eggs, nymphs, and adults (μ_E, μ_L, and μ_A), fecundity of adults female (b), the mean duration of immature females stage ($1/\nu_F$) and the mean necessary time for development of eggs. For some parameters (the sex ratio r, the mean duration of egg stage ($1/\nu_E$) and the mean duration of nymph stage ($1/\nu_L$)), we used data from Babin et al[27] because it was the last experiment on *S. singularis* life cycle realized in Cameroon. The most difficult data to obtain were the daily evolution of pods number in the plot. Using data from Bisselua et al[30] and also based on our knowledge about the mean pods density per hectare, we construct our periodic function $K_C(t)$,

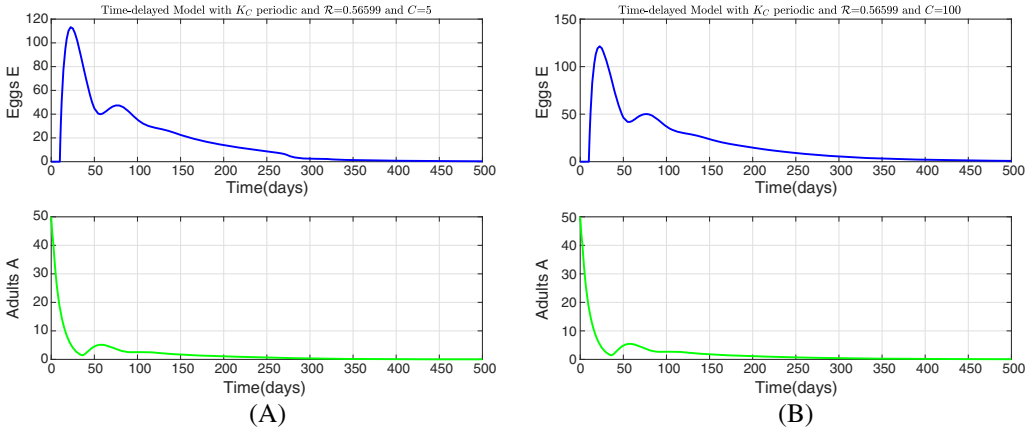

FIGURE 11 Time evolution of the eggs and adult compartments for the time-delay model with constant parameters, K_C periodic, such that $\mathcal{R}<1$, with A, $C=5$; B, $C=100$ [Colour figure can be viewed at wileyonlinelibrary.com]

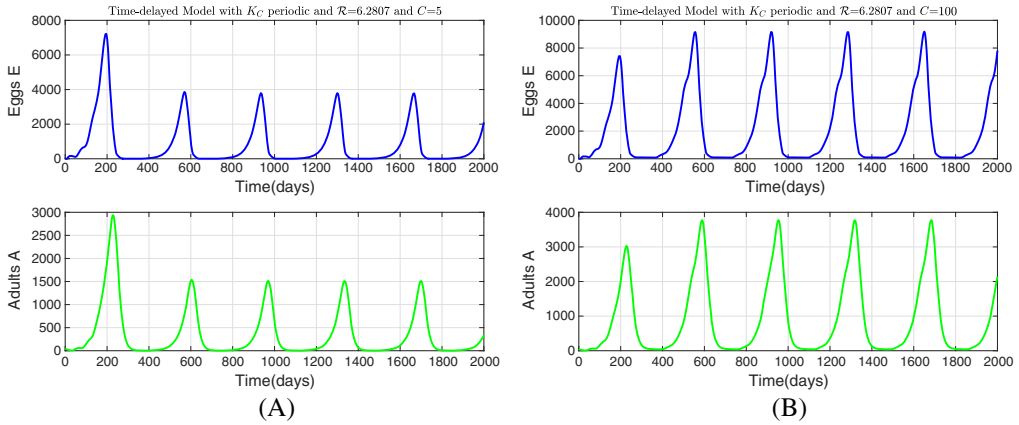

FIGURE 12 Time evolution of the Eggs and Adult Compartments for the time-delay model with constant parameters, K_C periodic, such that $\mathcal{R}>1$, with A, $C=5$; B, $C=100$ [Colour figure can be viewed at wileyonlinelibrary.com]

which represent the daily appearance of pods and cherelle in the plot. However, mirids also feed and lay eggs on young shoots that lead to important damage able to cause the destruction of the tree over the years. It will be important to take into account this aspect and model the daily appearance of young shoots in the plot by a function ($S(t)$ for example). Then, it will be relevant to know the mirid frequency of feeding on host plants to have a good idea about the parameter C because the time evolution of mirids also depends on it considering that if C is large, the level of mirid population increase. In our numerical simulations, we attributed to this parameter 2 values $C=1$ and $C=100$. According to these results, we suggest that it will be important to have several experiences in the field: to better estimate the daily appearance on pods and shoots in the plot, to have a good idea about the parameters of development of mirids and also to better estimate the parameter C.

4 | ABOUT MIRID CONTROLS

Several methods are used to control mirid population among which:

- cultural management, based on managing the system structure and composition to create unfavorable conditions for the development of mirids populations.
- varietal management, which consists in replacing the cacao varieties traditionally cultivated with more resistant and/or tolerant varieties to mirid attacks.

- chemical management, based on chemical insecticide used. This is the most widespread and efficient strategy to control mirid population in Cameroon. The chemical insecticides are applied 2 to 3 times a year[3] (see also page 20 in [18])
- semio-chemical management, which consists of using synthetic sexual pheromone traps[22] which increases adult mortality (trapping) and prevents male insects finding females and mating (mating disruption) and thus reduces the fecundity of female.
- last but not least, as shown in the previous simulations, a reduction of mirids alternative host (resources), ie, decrease C, is also essential to have an efficient control.

Understanding the population dynamic of *S. singularis* is crucial for monitoring, forecasting and, then, controlling this pest population. Recent work in Ghana indicates (using the visual hand-height assessment method) that mirid populations (predominately nymphs) began to increase rapidly in April with an initial peak in May, followed by a rapid buildup in June.[43] In Cameroon, mirid/population is low on cacao from February to March. From June to July, the populations start to grow more or less rapidly depending on external conditions like weather and fruits production on the trees. The peak of the population appears between September and November when the pods are almost mature.[27]

In Cameroon, mirids populations are mainly controlled by chemical insecticides. Three treatments are recommended per year: in June/July and August/September (propagation of mirids population); in November/December.[18] We will consider the impact of one treatment, 2 treatments, and, finally, 3 treatments. We will make a comparative study of treatments applied in systems with cacao only, $C=5$, and in agroforestry systems composed of cacao and associated trees that could be secondary resource for mirids, $C=100$. According to the expert's knowledge and field observations, the insecticide has a decaying death rate over 8 weeks that is summarized in Table 6.

> *Remark* 1. Synthetic insecticides like λ-cyhalothrine and imidacloprid have a long residual effect, but it depends on several environmental factors, like rainfall. That is why Table 6 provides only a feedback from field experts according to the locations in Cameroon where these treatments have been studied and are already used.

We start our numerical simulations at the end of June, a period where the number of pods is increasing in the plot. We treat the plot respectively 1, 2, or 3 time(s) per year, as recommended to cacao producers. We compare the efficacy between each treatment. The periods of treatment are given as follows:

- Treatment 1, with only one application per year: (beginning of) July (t=395,760,1125,1490,1855).
- Treatment 2, with 2 applications per year: July (t=395,760,1125,1490,1855) and September (t = 457,822,1187,1552,1917) (see Edoh Adabe and Ngo-Samnick,[18] page 20).
- Treatments 3, with 3 applications per year: July (t = 395,760,1125,1490,1855), September (t = 457,822,1187,1552,1917), and November (t = 518,883,1248,1613,1978)(see Edoh Adabe and Ngo-Samnick,[18] page 20).

It is worth to mention that the periodicity of the 2 last treatments coincides with the duration of the chemical treatment after spreading. In Figures 13, page 20, 14, page 20, and 15,page 21, we present the results obtained with the different treatments in 2 cases: $C=5$ and $C=100$. The case $C=5$ represents a full cacao crops, while $C=100$ may represent a cacao crop in an agroforestry system, where additional resources (host trees) are available for mirids.

We summarize in Table 7, page 19, the impact of each treatment in the reduction of the wild population.

As expected, 2 treatments are sufficient (more than 90% reduction of the population) when C is small. An additional (third) treatment is particularly recommended when C is large, ie, $C=100$. These results are relevant with real observations in different type of plots, at least in Cameroon.

Although chemical insecticides are very efficient to control mirids, their recurrent use is widely questioned because of the immediate adverse effects that they cause in ecosystems via environmental pollution (impact nontargeted species), the induced resistance in the mirid population, and to the toxic effects on human health. In addition, these chemical products are very expensive. That is why, it could be more advantageous to consider sustainable control strategies,

TABLE 6 Time-dependent death rate of chemical treatment

Time (d) After the Release	1	3	8	16	24	32	40	48	56	60
Insecticide death rate	1	1	0.9	0.2	0.1	0.05	0.025	0.01	0	0

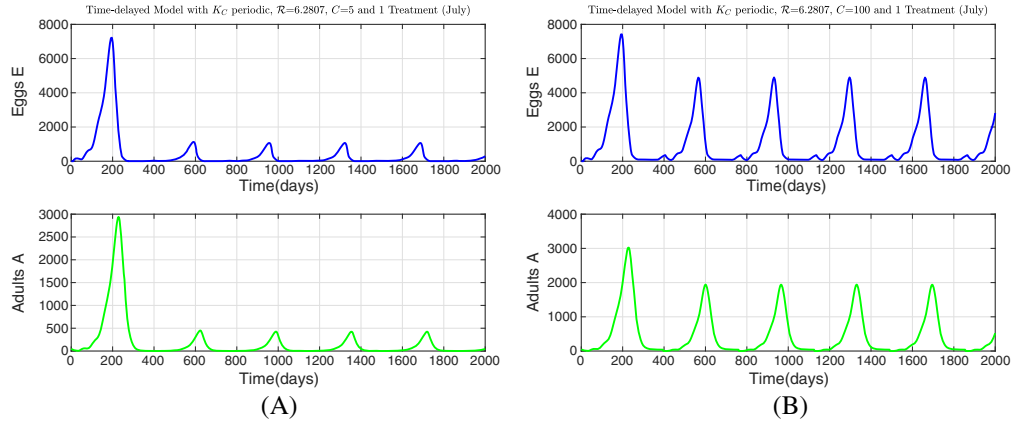

FIGURE 13 Time evolution of mirids using only one treatment in the plot per year: A, C=5; B, C=100 [Colour figure can be viewed at wileyonlinelibrary.com]

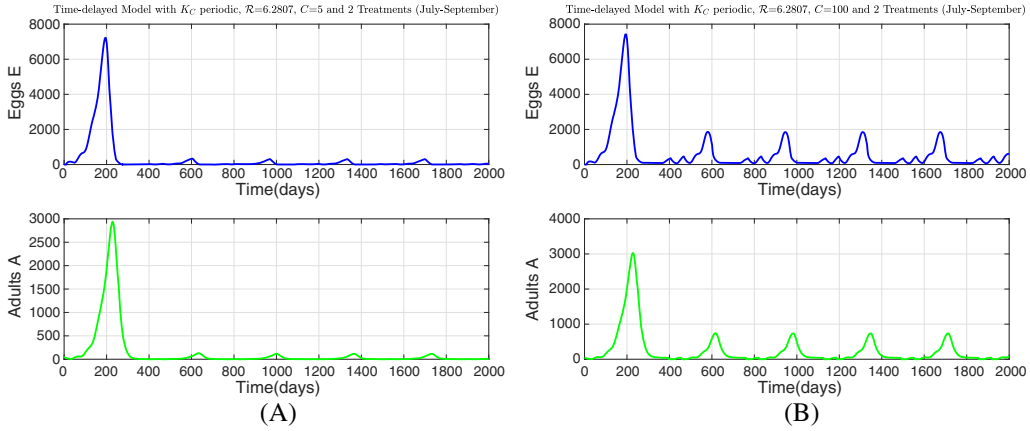

FIGURE 14 Time evolution of mirids using 2 treatments per year in the plot: A, C=5; B, C=100 [Colour figure can be viewed at wileyonlinelibrary.com]

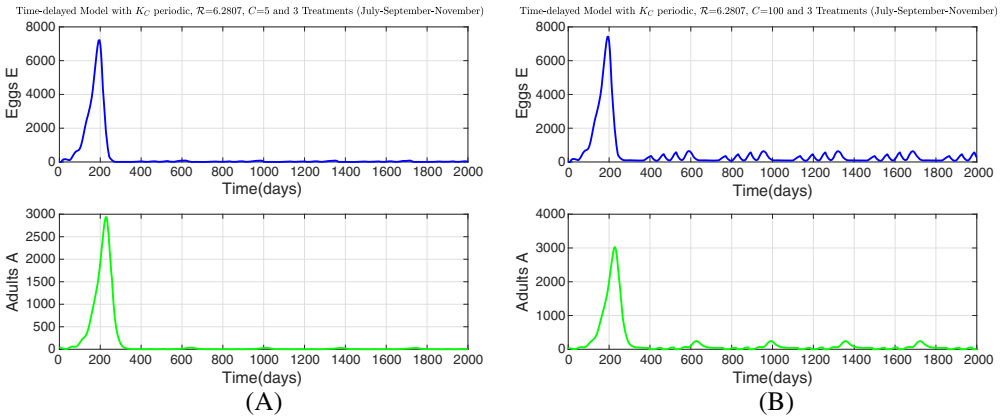

FIGURE 15 Time evolution of mirids using 3 treatments per year in the plot: A, C=5; B, C=100 [Colour figure can be viewed at wileyonlinelibrary.com]

TABLE 7 Efficacy of each treatment—percentage reduction of the wild population

	Treatment 1	Treatment 2	Treatment 3
C=5	74.8%	92.9%	97.8%
C=100	58.7%	84.8%	94.1%

like for instance, mating disruption and trapping. [22,44] Mating disruption consists in introducing an artificial stimulus, like pheromones or para-pheromones, to confuse individuals and, thus, to disrupt mate localization, leading to long-term reduction of the population. In our case, we roughly assume that this implies a decrease of the female fecundity. Thus, for instance, if we reduce the daily female fecundity from 3.28 to 2, the mirid population decreases (see Figure 16, page 21).

Another way to control mirids is the use of traps. Traps increase the adult mortality rate, μ_A. For instance, if we increase the mortality μ_A from 0.07 to 0.1, we observe a great reduction of the level of mirid population (see the time evolution of mirids in Figure 17, page 22). According to the sensitivity analysis, the adult mortality μ_A is a sensitive parameter for the delayed model such that any increase may have a strong negative impact on the population.

In general, combining the 2 previous methods of control (mating disruption and trapping), improve the previous results (see Figure 18, page 22). This combination allows to reach a low level of population, right after the first year.

We summarize in Table 8, page 21, the efficiency of each control methods. According to the given results, it seems possible to have a very efficient control of mirids without using chemical control. Clearly the combination of mating and trapping gives the best results whatever the values taken by C. This is in good agreement with recent field experiments.[44]

In the previous simulations, we showed that a biological control strategy (using mating and trapping) can be a very good alternative to the use of insecticides. Last but not least, if it is possible, the reduction of alternative hosts in the plots is also an additional way to improve the efficacy of both controls.

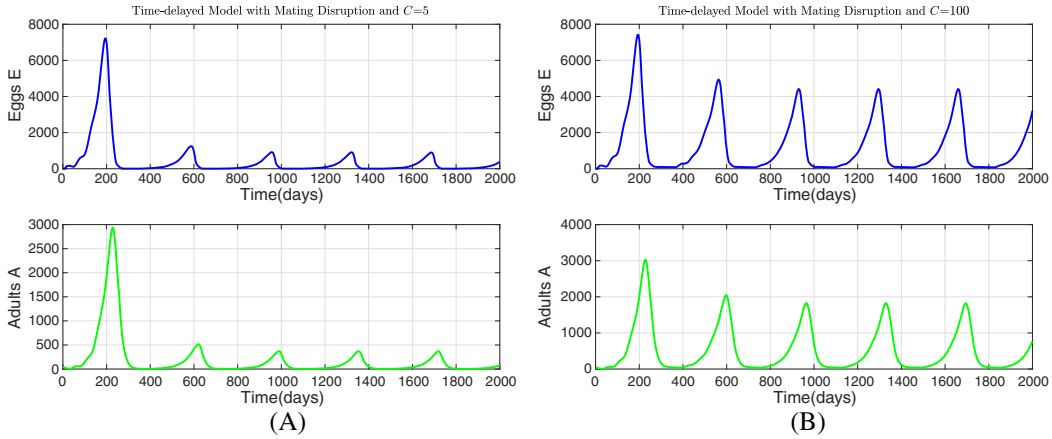

FIGURE 16 Time evolution of mirids with control using mating disruption: A, C=5; B, C=100 [Colour figure can be viewed at wileyonlinelibrary.com]

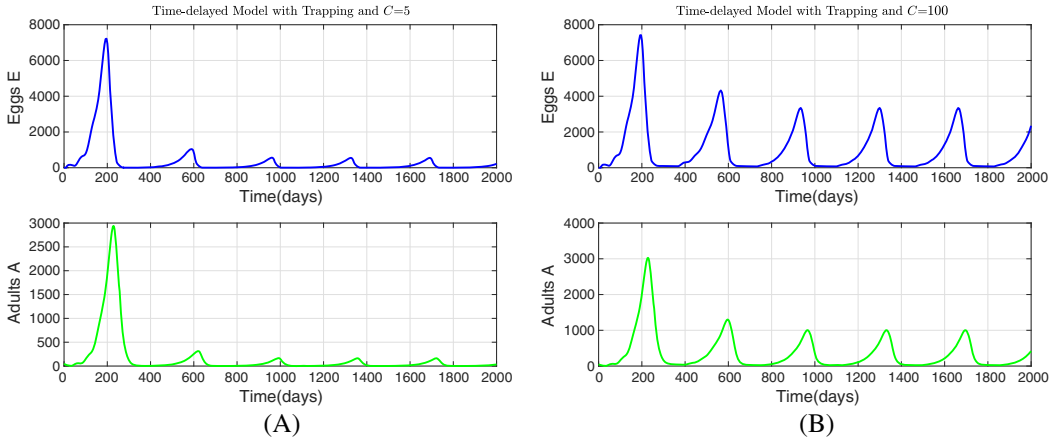

FIGURE 17 Time evolution of mirids with control using trapping: A, C=5; B, C=100 [Colour figure can be viewed at wileyonlinelibrary.com]

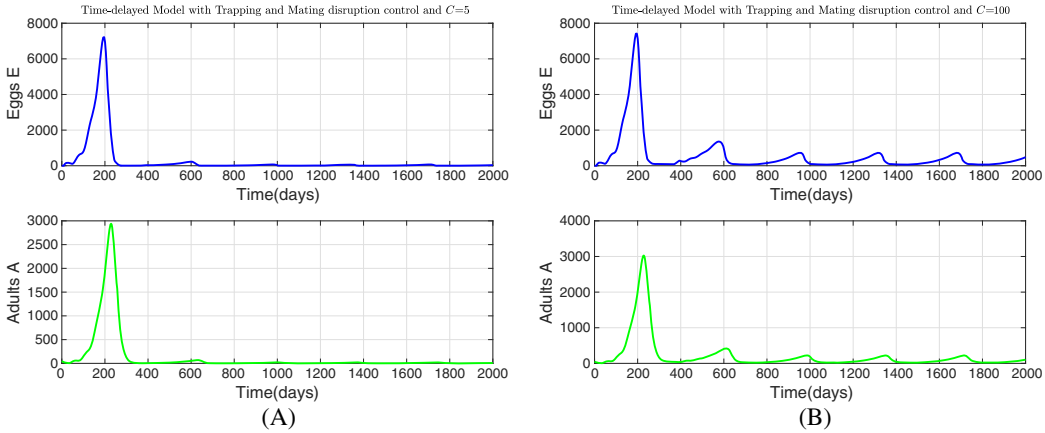

FIGURE 18 Time evolution of mirids with control combining trapping and mating disruption: A, C=5; B, C=100 [Colour figure can be viewed at wileyonlinelibrary.com]

TABLE 8 Efficacy of trapping, mating, and trapping-mating-percentage reduction of the wild population

	Mating	Trapping	Trapping&Mating
C=5	70.5%	85.5%	96.5%
C=100	49.4%	71.0%	90.1%

5 | CONCLUSION

In this paper, we studied the dynamics of a cocoa pest, mirids. From the best of our knowledge, it is the first time that mathematical models are developed to study mirid pest. We first build a generic stage-structured ODE model to simulate the dynamic of the pest population considering the resource (available cocoa pods and additional tree hosts) as constant or as a periodic function. Our model enters the family of cooperative system, which facilitates its study. Thus, we show that there exists a threshold parameters, $\mathcal{N}_0$, also called the basic offspring number, that summarizes the dynamics of the system: if it is less than one, then the mirid population decreases till whatever the availability of resources; when it is great than one, then mirids population persists. We also derive a sensitivity analysis that highlights that most of the parameters values are important to estimate. Then, based on the mirid's development stages and times, we also developed a delayed model. We derive a basic offspring number $\mathcal{R}$ and, since our system is a cooperative system, the study of the nondelayed model is sufficient to derive the long-term dynamics of the delayed system. We illustrate the theoretical results through numerical simulations. We show that the outputs of the delayed system seem to be more realistic than the nondelayed ODE model. We also highlighted that the presence of additional hosts can help the capsid population to maintain when pods are not available.

As an application, another objective of our work was to study ongoing mirid control strategies in Cameroon. We evaluated the impacts of chemical control and biological control (using mating disruption and trapping). Chemical control is used since a long time in Cameroon. It is very efficient when, at least, 2 treatments per year are applied. Our numerical simulations are in good agreement with the phytosanitary recommendations. However, we show that mating disrupting and trapping can be as efficient as chemical control, while being less detrimental to the environment. Of course, the reduction of additional hosts will improve the efficacy of the control.

These preliminary results encourage us to go further, that is, (1) to develop a model where mating disrupting and trapping are modeled, like in Anguelov et al,[45,46] (2) to couple our models to a pod growth model in order to take into account the impact of mirids on cocoa pods, (3) to take into account the spatial distribution of mirids using a metapopulation approach or a partial differential equation approach like in Dufourd and Dumont,[47] and (4) to set up new experiences in the field in order to obtain additional and new data in order to improve our knowledge, to estimate some biological and ecological parameters in different environmental conditions, in order to better model the time dynamic of the mirids, and thus to improve their control.

ACKNOWLEDGEMENTS

The first author is grateful to the DP-PCP Agroforesterie Cameroon, CIRAD, IRD, and INRIA-LIRIMA for logistical and financial support during the preparation and the finalization of this manuscript.

ORCID

Bagny Beihle http://orcid.org/0000-0002-4789-7076
S. Bowong http://orcid.org/0000-0001-8909-1225
Y. Dumont http://orcid.org/0000-0003-4817-685X

REFERENCES

1. Alemagi D, Minang PA, Duguma LA, Kehbila A, Ngum F. Pathways for sustainable intensification and diversification of cocoa agroforestry landscapes in Cameroon. In: Minang PA, van Noordwijk M, Freeman OE, Mbow C, de Leeuw J, Catacutan D, eds. *Climate-Smart Landscapes: Multifunctionality in Practice*. Nairobi, Kenya: World Agroforestry Centre (ICRAF); 2015:347-359.
2. Guest D. Black pod: diverse pathogens with a global impact on cocoa yield. *Phytopathology*. 2007;97(12):1650-1653.
3. Ayenor GK, Roling N, van Huis A, Padi B, Obeng-Ofori D. Assessing the effectiveness of a local agricultural research committee in diffusing sustainable cocoa production practices: the case of capsid control in Ghana. *Int J Agric Sustain*. 2007;5.
4. Babin R, Fenouillet C, Legavre L, Calatayud C, Risterucci A-M, Chapuis M-P. Isolation and characterization of twelve polymorphic microsatellite loci for the cocoa mirid bug Sahlbergella singularis. *Int J Mol Sci*. 2012;13(4):4412-4417.
5. Babin R, Bisselua BHD, Dibog L, Lumaret JP. Rearing method and life table data for the cocoa mirid bug *Sahlbergella singularis* Haglund (Hemiptera: Miridae). *J Appl Entomol*. 2008;132:366-374.
6. Williams G. Field observations on the cacao mirids, Sahlbergella singularis Hagl. and Distantiella theobroma (Dist.), in the Gold Coast. Part I. Mirid damage. *Bull Entomol Res*. 1953;44:101-119.
7. Collingwood CA. Biological control and relations with other insects. In: Lavabre EM, ed. *Les mirides du cacaoyer*. Paris: Maisonneuve et Larose; 1977:237–255IG-P.
8. Babin R, Hoopen M, Cilas C, et al. Impact of shade on the spatial distribution of *Sahlbergella singularis* in traditional cocoa agroforests. *Agric For Entomol*. 2010;12:69-79.
9. Lavabre EM, Decelle J, Debord P. Recherches sur les variations des populations de mirides en côte d'ivoire. *Café Cacao Thé*. 1962;6:287-295.
10. Yede Y, Babin R, Djieto-Lordon C, et al. True bug (Heteroptera) impact on cocoa fruit mortality and productivity. *J Econ Entomol*. 2012;4:1285-1292.
11. Carayon J. Caractères généraux des hémiptères bryocorinae. In: Lavabre EM, ed. *Les mirides du cacaoyer*. Paris: Maisonneuve et Larose; 1977:13–34IG-P.
12. Entwistle PF. *Pests of Cocoa*. London: Longman Group Ltd; 1972.
13. Adu-Acheampong R, Jiggins J, van Huis A, et al. The cocoa mirid (Hemiptera: Miridae) problem: evidence to support new recommendations on the timing of insecticide application on cocoa in Ghana. *Int J Trop Insect Sci*. 2014;34(1):58-71.
14. Awudzi GK, Asamoah M, Owusu-Ansah F, Hadley P, Hatcher PE, Daymond AJ. Knowledge and perception of ghanaian cocoa farmers on mirid control and their willingness to use forecasting systems. *Int J Trop Insect Sci*. 2016;36(1):22-31.
15. Dounias E, Hladick CM. Les agroforêts mvae et yassa du cameroun littoral : Fonctions socioculturelles, structure et composition floristique. In: Hladik CM, Hladik A, Pagezy H, Linares OF, Koppert GJA, FromentA, eds. *L'alimentation en forêt tropicale : Interactions bioculturelles et perspectives de développement*. Paris: UNESCO; 1996:1103-1126.
16. Laird SA, Awung GL, Lysinge RJ. Cocoa farms in the mount cameroon region: biological and cultural diversity in local livelihoods. *Biodivers Conserv*. 2007;16:2401-2427.
17. Sonwa DJ, Nkongmeneck AB, Weise SF, Tchatat M, Adesina AA, Janssens MJ. Diversity of plants in cocoa agroforests in the humid forest zone of Southern Cameroon. *Biodivers Conserv*. 2007:2385-2400.
18. Edoh Adabe K, Ngo-Samnick EL. Cocoa: production and processing. Edited by Engineers Without Borders (ISF Cameroun, Douala) and The Technical Centre for Agricultural and Rural Cooperation (CTA, Wageningen, The Netherlands).
19. Matthews G, Wiles T, Baleguel P. A survey of pesticide application in Cameroon. *Crop Prot*. 2003;22(5):707-714.
20. Padi B, Owusu GK, Kumah NK. A record of desplatsia dewevrei (de wild & th. dur.) (Tiliales: Tiliaceae) as an alternative and potential breeding host plant for the cocoa mirid Sahlbergella singularis hagl. In: Actes de la 12^{Ome} Conférence Internationale sur la Recherche Cacaoyère, San Salvador; 1996; Brésil:31-37.

21. Dibog L, Babin R, Amang A, et al. Effect of genotype of cocoa (theobroma cacao) on attractiveness to the mirid sahlbergella singularis (Hemiptera: Miridae) in the laboratory. *Pest Manag Sci*. 2008;64:977-980.
22. Mahob RJ, Babin R, ten Hoopen GM, et al. Field evaluation of synthetic sex pheromone traps for the cocoa mirid, Sahlbergella singularis(Hemiptera: Miridae). *Pest Manag Sci*. 2011;67:672-676.
23. Lavabre EM. Recherches sur une méthode économique de contrôle des mirides du cacaoyer. *Café Cacao Thé*. 1960;4:16-25.
24. Entwiste PF. Insects and cocoa. In: Wood GAR, Lass RA, eds. *Cocoa*. London: Longman; 1985:366-443.
25. Youdeowei A. The life cycles of the cocoa mirids Sahlbergella singularis Hagl. and Distantiella theobroma dist. *Niger J Nat Hist*. 1973;7:217-223.
26. Kumar R, Ansari AK. Biology, immature stages and rearing of cocoa-capsids (Miridae: Heteroptera). *Zool J Linn Soc*. 1974;54:1-29.
27. Babin R, Anikwé JC, Dibog L, Lumaret JP. Effets of cocoa trees phenology and canopy microclimate on the performance of the mirid bug *Sahlbergella singularis*. *Entomol Exp Appl*. 2011;141:25-34.
28. Babin R. *Contribution à l'amélioration de la lutte contre le miride du cacaoyer* Sahlbergella singularis *hagl. (Hemiptora: Miridae). influence des facteurs agro-écologiques sur la dynamique des populations du ravageur*. Université Paul Valéry-Montpellier III, biologie des populations et écologie: Thèse de Doctorat; 2009.
29. Anikwé JC, Omoloye AA, Okelana FAJC, Babin R. Novel rearing technique, development biology, fecundity and morphometrics of the brown cocoa mirid *Sahlbergella singularis* Haglung in Nigeria; 2010.
30. Bisselua DHB, Yede, Vidal S. Dispersion models and sampling of cacao mirid bug *Sahlbergella singularis* (Hemiptera: Miridae) on *Theobroma* cacao in Southern Cameroon. *Environ Entomol*. 2011;40(1):111-119.
31. N'Guessan FK, Coulibaly N. Dynamique des populations de mirides et de quelques autres déprédateurs du cacaoyer dans la région ouest de la Côte d'Ivoire. In: Proceedings of the 13th International Cocoa Research Conference; 2000; Cocoa Producer's Alliance, Malaysia:425-435.
32. N'Guessan FK, N'Guessan HA, N'Guessan PW, N'Dri Kouame N, Tano Y. Variations saisonnières des populations de mirides du cacaoyer dans la région de l'indénié-djuablin en côte d'ivoire. *J App Biosci*. 2014;83:7595-7605.
33. Davis TJ, Kaufman P, Hogsette D. The effects of larval habitat quality on aedes albopictus skip oviposition. *J Am Mosq Control Assoc*. 2015;31.
34. De Abreu FVS, Morais MM, Ribeiro SP, Eiras AE. Influence of breeding site availability on the oviposition behaviour of aedes aegypti. *Mem Inst Oswaldo Cruz*. 2015;110.
35. Smith HL. Monotone dynamical systems: an introduction to the theory of competitive and cooperative systems. *Amer Math Soc*. 2008;41.
36. Anguelov R, Dumont Y, Lubuma J. Mathematical modeling of sterile insect technology for control of anopheles mosquito. *Comput Math Appl*. 2012;64(3):374-389.
37. Marino S, Hogue IB, Ray CJ, Kirschner DE. A methodology for performing global uncertainty and sensitivity analysis in systems biology. *J Theor Biol*. 2008;254(1):178-196.
38. Jifa J. The algebraic criteria for the asymptotic behaviour of cooperative systems with concave nonlinearities. *J Syst Sci Complex*. 1993;6(3):193.
39. Smith HL. Cooperative system of differential equations with concave nonlinearities. *Nonlinear Anal,: Theory, Meth Appl*. 1986;10(10):1037-1052.
40. Anguelov R, Dumont Y, Lubuma JM-S. On nonstandard finite difference schemes in biosciences. In: Todorov Michael, ed. *Proceedings of the 4th International Conference on Application of Mathematics in Technical and Natural Sciences (Amitans'11)*, Vol. 1487. Varna, Bulgaria: American Institute of Physics—AIP Conference Proceedings; 2012:212-223.
41. Hale JK. *Theory of Functional Differential Equations*, *Applied Mathematical Sciences*, vol. 3. New York: Springer; 1977.
42. Smith H, Hirsch M. Monotone dynamical systems. In: Canada A, Drabek P, Fonda A, eds. *Handbook of Differential Equations, Ordinary Differential Equations (volume 2)*. North-Holland: Elsevier; 2005:239-357.
43. Awudzi GK, Cudjoe AR, Hadley P, Hatcher PE, Daymond AJ. Optimizing mirid control on cocoa farms through complementary monitoring systems. *J Appl Entomol*. 2017;141(4):247-255.
44. Sarfo JE, Campbell CAM, Hall DR. Design and placement of synthetic sex pheromone traps for cacao mirids in Ghana. *Int J Trop Insect Sci*. 2018:1-10.
45. Anguelov R, Dufourd C, Dumont Y. Mathematical model for pest-insect control using mating disruption and trapping. *Appl Math Model*. 2017;52:437-457.
46. Anguelov R, Dufourd C, Dumont Y. Simulations and parameter estimation of a trap-insect model using a finite element approach. *Math Comput Simul*. 2017;133:47-75.
47. Dufourd C, Dumont Y. Impact of environmental factors on mosquito dispersal in the prospect of sterile insect technique control. *Comput Math Appl*. 2013;66(9):1695-1715.

How to cite this article: Tapi D, Beihle B, Bowong S, Dumont Y. Models for Miridae, a Cocoa insect pest. Application in control strategies. *Math Meth Appl Sci*. 2018;1-24. https://doi.org/10.1002/mma.5063

APPENDIX A: MAIN RESULTS OF COOPERATIVE SYSTEMS

Here, we recall useful theorems (theorem 3.1 in Smith[39] and theorem 5.5 in Jifa[38]).

Theorem 2.5. (Smith,[39] theorem 3.1, page 1045) *Let F(t, x) be continuous in* $\mathbb{R}\times\mathbb{R}^n_+$, T-*periodic in t for fixed x and assume* $D_xF(t, x)$ *exists and is continuous in* $\mathbb{R}\times\mathbb{R}^n_+$. *Assume that if* $x \geq 0$, *with* $x_i = 0$, *then* $F_i(t,x)\geq 0$, $1\leq i\leq n$, $t\in\mathbb{R}$. *Assume*

$$(M)\quad \frac{\partial F_i}{\partial x_j}\geq 0,\ i\neq j,\ (t,x)\in\mathbb{R}\times\mathbb{R}^n_+,$$

and

$$D_xF(t,x) \text{is irreducible for each} (t,x)\,\mathbb{R}\times\mathbb{R}^n_+,$$

$$(C)\quad \text{if} 0<x<y, \text{then}\, D_xF(t,x)\geq D_xF(t,y).$$

Then every solution of (9) with $x(t_0)\geq 0$ *can be continued to* $[t_0,\infty]$ *with* $x(t)\geq 0$ *for* $t\geq t_0$.
If $F(t,0)\equiv 0$ *and*

$$z' = D_xF(t,0)z \tag{A1}$$

is the variational equation about $x\equiv 0$, *then* $\lim_{t\to\infty}x(t) = 0$ *for every solution of (9) with* $x(t_0)\geq 0$ *provided all Floquet multipliers of (A1) lie inside or on the unit circle in the complex plane. If any multiplier of (A1) lies outside the unit circle, then one of the following holds: (a) every solution* x(t) *of (9) with* $x(t_0)\geq 0$ *satisfies* $\lim_{t\to\infty}x(t) = \infty$, *or (b) (9) possess a unique nonzero* T-*periodic solution* q(t). *In the latter case,* $q(t) > 0$ *for all* t *and* $\lim_{t\to\infty}x(t) = q(t)$ *for every solution of (9) with* $x(t_0)>0$.
If $F(t,0)\equiv 0$, *then exactly one of the alternatives (a) or (b) occurs, except that* $x(t_0) > 0$ *is replaced by* $x(t_0)\geq 0$ *above.*

Let $A(t)$ be a $n\times n$ continuous matrix in $\mathbb{R}$ τ-periodic in t, denote

$$\overline{a_{ij}} = \max_{0\leq t\leq\tau} a_{ij}(t), \qquad \underline{a}_{ij} = \min_{0\leq t\leq\tau} a_{ij}(t),$$
$$\overline{A} = (\overline{a_{ij}}), \qquad \underline{A} = (\underline{a}_{ij}).$$

Thus,

$$\underline{A}\leq A(t)\leq\overline{A}, \quad for \quad 0\leq t\leq\tau.$$

Let p be a positive real number. To study system (8), we will use the following theorem:

Theorem 2.6. (Jifa,[38] Theorem 5.5, page 203) *Let* F(t, x) *be continuous in* $\mathbb{R}\times\mathbb{R}^n_+$, T-*periodic in* t *for a fixed* x, *and assume* $D_xF(t, x)$ *exists and is continuous in* $\mathbb{R}\times\mathbb{R}^n_+$. *Assume that all solutions are bounded in* $\mathbb{R}^n_+$ *and* F(t,0)=0. *Assume*

- $\frac{\partial F_i}{\partial x_j}\geq 0, \qquad (t,x)\in\mathbb{R}\times\mathbb{R}^n_+,$
- $A(t)=D_xFt,0)$ *are irreducible for any* $t\in\mathbb{R}$.
- *If* $0 < x < y$, *then* $D_xF(t,x)>D_xF(t,y)$.
  Then

(1) *if all principal minors of* $-\bar{A}$ *are nonnegative, then* $\lim_{t\to+\infty}x(t) = 0$ *for every solution of (9) in* $\mathbb{R}^n_+$;
(2) *if* $-\underline{A}$ *has at least one negative principal minor, then (9) possesses a unique positive* T-*periodic solution, which attracts all initial conditions in* $\mathbb{R}^n_+$.

Nonlinear Analysis: Real World Applications 54 (2020) 103082

Contents lists available at ScienceDirect

Nonlinear Analysis: Real World Applications

www.elsevier.com/locate/nonrwa

Miridae control using sex-pheromone traps. Modeling, analysis and simulations

M. Djoukwe Tapi [a,b,h], L. Bagny-Beilhe [c,d], Y. Dumont [e,f,g,h,*]

[a] *Department of Mathematics and Computer Science, University of Douala, Cameroon*
[b] *UMI 209 IRD/UPMC UMMISCO, University of Yaounde I, Cameroon*
[c] *CIRAD, UPR Bioagresseurs, 30501 Turrialba, Costa Rica*
[d] *Bioagresseurs, Univ Montpellier, CIRAD, Montpellier, France*
[e] *CIRAD, UMR AMAP, F-34398 Montpellier, France*
[f] *AMAP, Univ Montpellier, CIRAD, CNRS, INRAE, IRD, Montpellier, France*
[g] *University of Pretoria, Department of Mathematics and Applied Mathematics, Pretoria, South Africa*
[h] *EPITAG, LIRIMA, France*

ARTICLE INFO

Article history:
Received 17 June 2019
Received in revised form 18 December 2019
Accepted 20 December 2019
Available online xxxx

Keywords:
Pest control
Cocoa Pest
Sex-pheromone traps
Delay differential equations
Piecewise-smooth system
Monotone dynamical system

ABSTRACT

Cocoa mirid, *Sahlbergella singularis*, is known to be one of the major pests of cocoa in West Africa. In this paper, we consider a biological control method, based on mating disrupting, using artificial sex pheromones, and trapping, to limit the impact of mirids in plots. We develop and study a piece-wise smooth delayed dynamical system. Based on previous results, a theoretical analysis is provided in order to derive all possible dynamics of the system. We show that two main threshold parameters exist that will be useful to derive long term successful control strategies for different level of infestation. We illustrate and discuss our results when cacao pods production is either constant along the year or seasonal. To conclude, we provide future perspectives based on this work.

1. Introduction

Mirid pests, like *Sahlbergella singularis*, are responsible of several damages on cocoa in Africa, especially in Cameroon. Their presence leads to enormous losses of production and, thus, have an impact on trading and export. Losses due to mirids are difficult to estimate, but can reach 30–40% of the potential production. Mirids are very harmful and can lead to the destruction of cocoa trees over the time. Development of pest management strategies is essential to prevent devastating impact on economy, food security, and biodiversity. Nowadays, in Cameroon, it is known that chemical control is the best way to control mirid population. However, although chemical insecticides are very efficient to control mirids, their recurrent use is widely

* Corresponding author at: CIRAD, UMR AMAP, F-34398 Montpellier, France.
E-mail address: yves.dumont@cirad.fr (Y. Dumont).

https://doi.org/10.1016/j.nonrwa.2019.103082
1468-1218/

questioned due to their immediate adverse effects on the environment such as reduction of mirid natural enemies (impact on non targeted species), environmental pollution in ecosystems, resistance induction in the mirid population, and toxic effects on human health. In addition, these chemical products are very expensive. That is why the reduction of pesticides in cocoa production is becoming an important issue. In [1], we build and studied several models (with and without delays) of mirids population and also several control strategies, including chemical treatment, mating disruption and trapping. We showed that the use of three applications of chemical treatment is equivalent to the combination of mating disruption and trapping. These two methods are less expensive and less toxic than chemical management and respect specific ecological and toxicological environmentally friendly requirements. In this paper, we will model more specifically the use of sex-pheromones to trap males and thus disturb matings, in order to eliminate or decay the population.

In Cameroon, different blends of the two components hexyl (R)-3-((E)-2-butenoyloxy)-butyrate and hexyl (R)-3-hydroxybutyrate) of the *Sahlbergella singularis* female sex pheromone are used for tests. Traps used are delta or rectangular white-colored traps, made out of recycled polyethylene and cardboard. In a two years experiments [2], a total of 361 adults of *S. singularis* (359 males and two females) were caught. The highest numbers of mirids were found in traps with pheromone blends that combined a monoester and a diester. Rectangular traps also capture significantly more mirids than delta traps. Finally, in a recent work [3], the authors studied the impact of pheromone trap density (per ha) for cacao mirids mass trapping. It is clearly stated that this approach is a Male Annihilation Technique (MAT), with the objective of reducing the male population in order to lower the mirid population under an economical threshold.

In [1], the authors developed and studied several mirids population models, including a model with two delays. In [4], YD and co-authors developed and studied a piecewise smooth (PWS) system to model mating disrupting and trapping. Here, we propose to combine both approaches to develop and study a mathematical model to get a better understanding on the dynamics of the mirid population, under mating disruption and trapping. Then, the main objective of this work is to study the effort required in terms of sex-pheromone and trapping, to reduce the population size below harmful level. We obtain a piecewise smooth system of delayed differential equations. Using [1] and [4], we derive a system's analysis in order to provide a reliable and tractable strategy for a long time control. Since cocoa pods production in Cameroon is seasonal we also consider a periodic version of the delay PWS system. Finally, we provide numerical simulations to highlight the theoretical results and our reliable strategy.

The paper is organized as follows: in Section 2, a sex-structured mirid model is built, based on [1] and [4]. In Section 3, like in [4], mating disruption and trapping are included in the sex-structured model; an analysis is provided that allows to build a useful control strategy, that is also illustrated by numerical simulations. Finally, in Section 4, we consider the periodic case. The paper ends with a conclusion where we discuss possible extensions of this work.

2. A sex-structured model of mirid population

We consider a generic delayed model to describe the dynamics of *S. singularis*. The flow diagram is represented in Fig. 2. Based on biological and behavioral assumptions, we consider two main developments stages: eggs (E) and adults (females F and A, and male M). Indeed, after being laid, the eggs need, on average, $\tau_1 = 15$ days to become nymphs. These nymphs need $\tau_2 = 25$ days to complete the nymph's development and become adult males or females. After emergence, sexually mature female mate with males (attracted by sex pheromones released by the females) and then they need approximately $\tau_3 = 10$ days before being able to deposit eggs (in fact this is the time needed for the appearance of mature eggs in the ovarioles [5]). This is summarized in Fig. 1.

We denote by $e^{-\tau_2 \mu_L}$ the proportion of nymphs respectively which survive the nymph stage. After mating, F becomes mated females, A, that need an additional period of maturation, τ_3, in order to lay eggs [5].

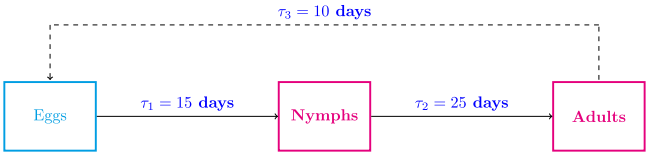

Fig. 1. Life cycle of *S. singularis*.

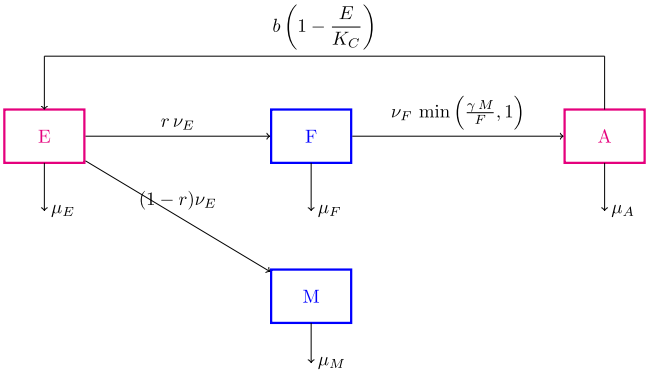

Fig. 2. *Sahlbergella singularis* flow diagram with mating.

However, only a proportion, $e^{-\tau_3\,\mu_A}$, of females A will deposit eggs. Thus, we have four compartments for our delayed model: E, the eggs' compartment, F, the sex-immature females compartment, A, the mated females compartment, and M, the males compartment.

Females release pheromone in order to attract males for mating. The mating between males and females is modeled as in [4]: as long as the male density is such that $\gamma M \geq F$, then all females F will be inseminated and move to the compartment A, at rate ν_F. In contrary, if, for any reason, the male density is scarce, i.e. $\gamma M < F$ then the number of females F that will move to the compartment A is related to the number of Males, M. The other parts of the compartmental model follow the model developed in [1].

The biological parameters are described as follows: r is the sex ratio; b is the mean number of eggs laid by an adult female mirid per day, K_C is the maximal carrying capacity related to the mean daily number of pods per area (ha), μ_E, μ_M, μ_F and μ_A represent respectively the eggs, male, females daily mortality rate, ν_E is the transition rate from the egg to the next stage; $1/(\nu_E + \mu_E)$ is the mean time a mirid stays in the egg stage (measured in days); ν_F is the transition rate from the sex-immature female stage to mature female stage.

As already explained in [1], the non linear term $r\,b\,A\left(1-\frac{E}{K_C}\right)$ is related to a skip-oviposition behavior. Indeed, according to expert's knowledge, mirids (*S. singularis*) are able to select their breeding sites according to their level of occupation.

According to the diagram given in Fig. 2, we derive the following Delay Differential system

$$\begin{cases} \dot{E}(t) = b\,e^{-\tau_3\,\mu_A}\,A(t-\tau_3)\left(1-\dfrac{E(t)}{K_C}\right) - (\nu_E+\mu_E)\,E(t), \\ \dot{F}(t) = r\,\nu_E\,e^{-\tau_2\,\mu_L}\,E(t-\tau_2) - \nu_F\,\min\left(\dfrac{\gamma\,M(t)}{F(t)},1\right)\,F(t) - \mu_F\,F(t), \\ \dot{A}(t) = \nu_F\,\min\left(\dfrac{\gamma\,M(t)}{F(t)},1\right)\,F(t) - \mu_A\,A(t), \\ \dot{M}(t) = (1-r)\,\nu_E\,e^{-\tau_2\,\mu_L}\,E(t-\tau_2) - \mu_M\,M(t). \end{cases} \tag{1}$$

The parameters of model (1) are summarized in Table 1.

Table 1
Parameters of model (1).

Parameters	Biological significance	Unit
b	Mean daily number of eggs laid by a mature female	days^{-1}
r	Sex ratio	–
K_C	Maximal carrying capacity related to the mean	
	Daily number of pods per ha	eggs^{-1}
ν_F	Daily rate from F to A	days^{-1}
μ_A	Death rate of adults females	days^{-1}
μ_M	Death of adults males	days^{-1}
μ_F	Death of sexual immature females	days^{-1}
μ_E	Death rate of eggs	days^{-1}
$1/\nu_E$	Time necessary for an egg to change its stage	days
α	The maximal death rate by sex-pheromone trap	days^{-1}
γ	Daily number of females that can be inseminated by a single male	–
$\tau_1 = \dfrac{1}{\nu_E}$	Average time needed for eggs to become nymphs	days
τ_2	Average time needed for nymphs to become adults	days
τ_3	Average maturation time needed by mated females to deposit eggs	days

3. Control using mating disruption and trapping

In order to maintain a low level a mirid population, we consider a control using sex pheromone traps. The objective is to disrupt the mating by the use of female pheromones, but also to reduce the number of males, by trapping, in order to reduce the overall population. However, to model the pheromones, like in [4], we assume that the release of pheromones is equivalent to the releases of "Fake Females", F_p, such that our approach can be somehow linked to the Sterile Insect Technique (SIT) approach, where sterile males are released to disrupt the mating between wild males and females in order to reduce the number of offsprings and so on (see for instance [6–8] for an overview and results on SIT).

Because of the release of Fake female, F_p, the mating term in the previous system becomes $\min\left(\dfrac{\gamma\, M(t)}{F(t)+F_p}, 1\right)$, such that if the number of Fake females is large enough then $\dfrac{\gamma\, M(t)}{F(t)+F_p} < 1$. Clearly when the mirid population is large, a large number of Fake females is necessary to impact the mating. When Fake females are not released in sufficient numbers, then, the control will have no effect on an established (and large) mirid population. The parameter α represents the maximum capture rate by trapping, the ratio $\dfrac{F_p}{F+F_p}$ represents the attractiveness of the traps. The new flow diagram is represented in Fig. 3. According to the flow diagram given in Fig. 3, and taking into account the life cycle of *S. singularis*, we obtain a new mating disruption and trapping control model

$$\begin{cases} \dot{E}(t) = b\, e^{-\tau_3\, \mu_A}\, A(t-\tau_3)\left(1-\dfrac{E(t)}{K_C}\right) - (\nu_E+\mu_E)\, E(t), \\ \dot{F}(t) = r\, \nu_E\, e^{-\tau_2\, \mu_L}\, E(t-\tau_2) - \nu_F\, \min\left(\dfrac{\gamma\, M(t)}{F(t)+F_p}, 1\right) F(t) - \mu_F\, F(t), \\ \dot{A}(t) = \nu_F\, \min\left(\dfrac{\gamma\, M(t)}{F(t)+F_p}, 1\right) F(t) - \mu_A\, A(t), \\ \dot{M}(t) = (1-r)\, \nu_E\, e^{-\tau_2\, \mu_L}\, E(t-\tau_2) - \left(\mu_M + \alpha \dfrac{F_p}{F(t)+F_p}\right) M(t). \end{cases} \tag{2}$$

Model (2), like model (1), enters the family of piece-wise dynamical systems with delay differential equations (shortly, PWS-DDE) (see Appendix A).

The switching manifold is defined as follows

$$\sum := \left\{(E,F,A,M) \in \mathbb{R}^4_+, \quad F+F_p = \gamma\, M\right\}$$

Model (2) can be rewritten in the form:

$$\frac{dx}{dt} = f(x,x_\tau) := \begin{cases} f_1(x,x_{\tau_2},x_{\tau_3}) & if \quad F+F_p \le \gamma\, M \\ f_2(x,x_{\tau_2},x_{\tau_3}) & if \quad F+F_p \ge \gamma\, M \end{cases} \tag{3}$$

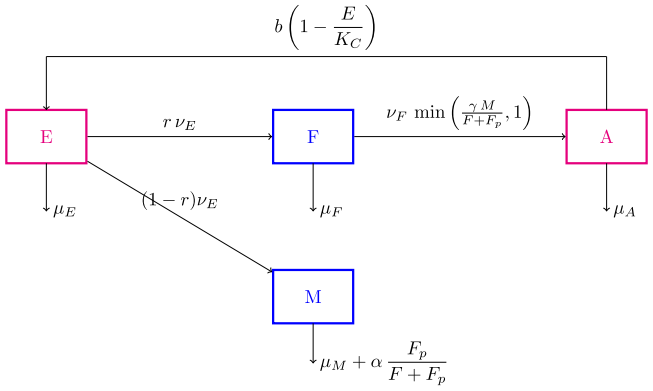

Fig. 3. *Sahlbergella singularis* control model using sex pheromone traps.

where $x=(E,F,A,M)^t$, $x_{\tau_2}=x(t-\tau_2)$, $x_{\tau_3}=x(t-\tau_3)$,

$$f_1(x,x_\tau)=\begin{pmatrix} b\,e^{-\tau_3\,\mu_A}\,A(t-\tau_3)\left(1-\dfrac{E(t)}{K_C}\right)-(\nu_E+\mu_E)\,E(t)\\ r\,\nu_E\,e^{-\tau_2\,\mu_L},E(t-\tau_2)-(\nu_F+\mu_F)\,F(t)\\ \nu_F\,F(t)-\mu_A\,A(t)\\ (1-r)\,\nu_E\,e^{-\tau_2\,\mu_L}\,E(t-\tau_2)-\left(\mu_M+\alpha\dfrac{F_p}{F(t)+F_p}\right)M(t)\end{pmatrix} \tag{4}$$

and

$$f_2(x,x_\tau)=\begin{pmatrix} b\,e^{-\tau_3\,\mu_A}\,A(t-\tau_3)\left(1-\dfrac{E(t)}{K_C}\right)-(\nu_E+\mu_E)\,E(t)\\ r\,\nu_E\,e^{-\tau_2\,\mu_L}\,E(t-\tau_2)-\nu_F\gamma\dfrac{M(t)}{F(t)+F_p}\,F(t)-\mu_F\,F(t)\\ \nu_F\,\gamma\dfrac{F(t)}{F(t)+F_p}\,M(t)-\mu_A\,A(t)\\ (1-r)\,\nu_E\,e^{-\tau_2\,\mu_L}\,E(t-\tau_2)-\left(\mu_M+\alpha\dfrac{F_p}{F(t)+F_p}\right)M(t)\end{pmatrix} \tag{5}$$

When $\tau_2=\tau_3=0$, system (3) is exactly the same system studied in [4]. We will now consider the methodologies developed in [4] and [1] to study system (3).

Like in [4], the theoretical analysis of the model is carried out for two cases: male abundance and male scarcity. These two cases are separated by the hyperplane Σ. The analysis of the two systems can be carried out independently on the orthant $\mathbb{R}^4_+$. The obtained results will be merged into a general theorem for system (3) (or (2)).

3.1. Case with male abundance: $\gamma M > F+F_p$

In this case, system (3) becomes

$$\frac{dx}{dt}=f_1(x,x_\tau). \tag{6}$$

Note that the right hand side of system (6), f_1, is continuous and Lipschitzian in x. Thus, according to the standard theory of delay differential equations [9], for each continuous initial condition $\psi\in\mathcal{C}\left([-\tau,0],\mathbb{R}^4\right)$,

where $\tau = \max\{\tau_2, \tau_3\}$, uniqueness and local existence of the solution are guaranteed. Note also, that, without delay, we recover the cooperative system studied in [4].

As explained in [1], some cooperative systems with delay can enjoy some nice properties such that their long term behavior is similar to the cooperative system without delay. Let $Y = (x(t-\tau_3), x(t-\tau_2))$, $x = (E, F, A, M)^T$. System (6) verifies the, so-called, quasimonotone (QM) condition [10], if

(a) $\dfrac{\partial f_{1,i}}{\partial x_j} \geq 0$ for $i \neq j$

(b) $\dfrac{\partial f_{1,i}}{\partial Y_j^k} \geq 0$ for all i, j, k.

Condition (a) is verified since the non delayed model is a cooperative system. Let us verify condition (b):

$$\begin{aligned}
&\frac{\partial f_{1,1}}{\partial Y_3^1} = b\, e^{-\tau_3 \mu_A} \left(1 - \frac{E(t)}{K_C}\right) \geq 0, \quad \frac{\partial f_{1,j}}{\partial Y_j^1} = 0 \quad \forall\, j = 1, 2, 4.\\
&\frac{\partial f_{1,2}}{\partial Y_2^1} = r\, \nu_E\, e^{-\tau_2 \nu_L}\, e^{-\tau_3 \mu_F} \geq 0, \quad \frac{\partial f_{2,j}}{\partial Y_j^1} = 0 \quad \forall\, j = 2, 3, 4,\\
&\frac{\partial f_{3,j}}{\partial Y_j^1} = 0 \quad \forall\, j = 1, 2, 3, 4,\\
&\frac{\partial f_{1,4}}{\partial Y_1^1} = (1-r)\, \nu_E\, e^{-\tau_2 \nu_L} \geq 0, \quad \frac{\partial f_{4,j}}{\partial Y_j^1} = 0 \quad \forall\, j = 2, 3, 4.
\end{aligned}$$

Then the (QM) condition is verified. This implies that if the initial condition is non negative (with at most one zero component) then the solution of system (6) is still non negative i.e $x(t) \geq 0$. Moreover, the (QM) condition guarantees the stability of each equilibrium of the non delayed system is preserved for the delayed system. In other words, it suffices to study the following non delayed system

$$\frac{dx}{dt} = f_1(x), \tag{7}$$

to deduce the behavior of the time delayed system (6). As already emphasized, system (7) has already been studied in [4], using [10,11].

Setting

$$\mathcal{R} = \frac{r\, b\, \nu_E\, \nu_F\, e^{-\tau_2 \mu_L}\, e^{-\tau_3 \mu_A}}{\mu_A\, (\nu_E + \mu_E)\, (\nu_F + \mu_F)} \tag{8}$$

the so-called basic offspring number, and applying Theorem 9 [4] we deduce

Theorem 3.1.

(i) System (7) defines a positive dynamical system on $\mathbb{R}^4_+$.

(ii) System (7) always has a trivial equilibrium, $\mathbf{0} = (0, 0, 0, 0)$, which is globally asymptotically stable when $\mathcal{R} \leq 1$.

(iii) When $\mathcal{R} > 1$, system has an additional positive equilibrium $X^* = (E^*, F^*, A^*, M^*)$ where

$$\begin{aligned}
E^* &= \left(1 - \frac{1}{\mathcal{R}}\right) K_C, \quad F^* = \frac{r\, \nu_E\, e^{-\tau_2 \mu_L}}{(\nu_F + \mu_F)} \left(1 - \frac{1}{\mathcal{R}}\right) K_C,\\
A^* &= \frac{r\, \nu_E e^{-\tau_2 \mu_L}\, \nu_F}{\mu_A\, (\nu_F + \mu_F)} \left(1 - \frac{1}{\mathcal{R}}\right) K_C, \quad M^* = \frac{M^0}{\mu_M + \dfrac{\alpha\, F_p}{F^* + F_p}}
\end{aligned}$$

with

$$M^0 = (1-r)\, \nu_E e^{-\tau_2 \mu_L} \left(1 - \frac{1}{\mathcal{R}}\right) K_C.$$

Moreover, X^*, is also globally asymptotically stable when $\mathcal{R} > 1$ on

$$\mathbb{R}^4_+ \setminus \{\mathbf{0}\} = \mathbb{R}^4_+ \setminus \{x \in \mathbb{R}^4_+ : E = F = A = M = 0\}.$$

Remark 3.1. When $\alpha = 0$, we recover the positive equilibrium when no control occurs. It is important to notice that the effect on the control only impact the value of the Male equilibrium.

The positive equilibrium X^* is called a regular (virtual) equilibrium of model (7) if and only if $F^* + F_p <$ $(>)\gamma M^*$ which is equivalent to $F_p < F_p^*$, where

$$F_p^* = \frac{1}{\mu_M + \alpha}\left(\gamma M^0 - \mu_M F^*\right) = \frac{\nu_E e^{-\mu_L \tau_2}}{(\alpha + \mu_M)}\left[\gamma(1-r) - \frac{r\,\mu_M}{(\nu_F + \mu_F)}\right] E^*. \tag{9}$$

Therefore, we deduce that

- If $F_p < F_p^*$, the positive equilibrium X^* is a regular equilibrium of (7).
- If $F_p > F_p^*$, the positive equilibrium X^* is a virtual equilibrium of (7).

The threshold F_p^* determines the minimum level of control, i.e. the number of Fake females and thus, indirectly, the number of pheromones traps, below which the control has essentially no effect on an established mirid population. More precisely, as stated in the previous remark, the effect of pheromone traps is only limited to the males compartment (male trapping), all other compartments remain at their natural equilibrium. Thus females will continue to deposit as many eggs (inside pods) as before the control.

Thus, thanks to the (QM) condition, and, using Theorem 3.1, we deduce the following results in the DDE "male abundance" case:

Theorem 3.2.

(i) System (6) defines a positive dynamical system on $\mathbb{R}^4_+$.
(ii) System (6) always has one equilibrium, $\mathbf{0}$, that is globally asymptotically stable when $\mathcal{R} \leq 1$.
(iii) When $\mathcal{R} > 1$, system (6) has an additional (unique) positive equilibrium, $\mathbf{X}^*$, that is globally asymptotically stable on $\mathbb{R}^4_+ \setminus \{\mathbf{0}\}$.

The positive equilibrium is a regular equilibrium if $F_p < F_p^*$ and it is a virtual equilibrium if $F_p > F_p^*$.

Remark 3.2. As already highlighted for the non-delayed system, the threshold F_p^* determines the minimum level of control below which the control has essentially no effect on an established pest population for the delayed model.

3.2. Case with male scarcity: $\gamma M < F + F_p$

In this case, system (3) becomes

$$\frac{dx}{dt} = f_2(x, x_\tau), \tag{10}$$

The right hand side of system (10) is Lipschitz continuous. Thus, according to the standard theory of Delay Differential Equations [9], system (10) admits a unique local solution for each continuous initial condition $\psi \in \mathcal{C}([-\tau_2, 0], \mathbb{R}^2_+)$. In addition, the following domain

$$\Omega := \{\, x \in \mathbb{R}^4_+ : E \leq K_C,\ F < \frac{r\,\nu_E\, e^{-\tau_2 \mu_L}\, e^{-\tau_3 \mu_F}\, K_C}{\mu_F},\ A \leq \frac{(1-r)\,\gamma\,\nu_F\,\nu_E\, e^{-\tau_2 \mu_L}\, K_C}{\mu_A\,\mu_M},$$
$$M \leq \frac{(1-r)\,\nu_E\, e^{-\tau_2 \mu_L}\, K_C}{\mu_M}\} \tag{11}$$

is positively invariant for system (10). Global existence on $[0, +\infty)$ of the solution follows by dissipativity of (10). Then, we derive

Proposition 3.1. *There exists a threshold $F_p^{**} > 0$ of F_p such that*

- *If $F_p > F_p^{**}$ the only equilibrium of system (10) on $\mathbb{R}^4_+$ is $\mathbf{0}$.*
- *If $0 < F_p < F_p^{**}$, system (10) has three equilibria on $\mathbb{R}^4_+$, $\mathbf{0}$ and two positive equilibria.*

In addition, $\mathbf{0}$ is an absolutely stable equilibrium.

Proof. The proof follows the proof of Theorem 4 [4], page 446. However, for reader's convenience we provide it in Appendix B, with additional explanations. □

Similarly, we show

Theorem 3.3 (*Bifurcation Study of F_p^* and F_p^{**}*)**.** *Let $F_p > 0$. The following holds for system (2):*

- *$\mathbf{0}$ is an absolutely stable equilibrium.*
- *If $0 < F_p < F_p^*$, there are two positive equilibria $X^{(1)}$ and X^*, where X^* is asymptotically stable.*
- *If $F_p^* < F_p < F_p^{**}$, there are two positive equilibria $X^{(1)}$ and $X^{(2)}$.*
- *If $F_p > F_p^{**}$, there is no positive equilibrium*

Proof. The proof follows the proof of Theorem 15 [4], page 449. However, for reader's convenience we provide it in Appendix C. □

The stability properties of $X^{(1)}$ and $X^{(2)}$ are not easy to obtain theoretically. However, numerical simulations show that $X^{(1)}$ is unstable while $X^{(2)}$ is stable. Also, when $F_p > F_p^{**}$, $\mathbf{0}$ is Globally Asymptotically Stable. As F_p increases and passes through F_p^* the regular equilibrium X^* collides with the virtual equilibrium $X^{(2)}$, such that X^* becomes virtual and $X^{(2)}$ becomes regular. The bifurcation diagram in Fig. 4, summarizes the previous properties, where the equilibrium values of $F + A$ are given as function of the bifurcation parameter F_p. The blue (red) solid line represents locally (globally) asymptotically stable equilibria, while the blue dotted line represents unstable equilibria.

About the long term behavior of system (2) when $F_p > 0$

The previous Theorem shows us that the dynamics of the system may vary according to the level of control. In particular, as long as $0 < F_p < F_p^*$, the control has essentially no effect on an established population. Even if $F_p^* < F_p < F_p^{**}$, the effect are negligible (on an established population). Here, we intend to derive results that may help us to define appropriate control strategies.

Due to the term $-\nu_F \dfrac{\gamma M(t)}{F(t) + F_p} F(t)$ in (5), the right hand side of (10) is not quasi-monotone. By removing this nonlinear term, we obtain an upper DDE system, that admits a unique positive solution $\overline{x}$ that is an upper solution of system (10). Since $f_2(x, y)$ is nondecreasing in y, according to Theorem 3.6 in [12], page 29, we deduce that $x \leq \bar{x}$.

Thus, following [4], we consider the following upper system, as an auxiliary system of system (10):

$$\frac{dx}{dt} = g_2(x, x_\tau), \tag{12}$$

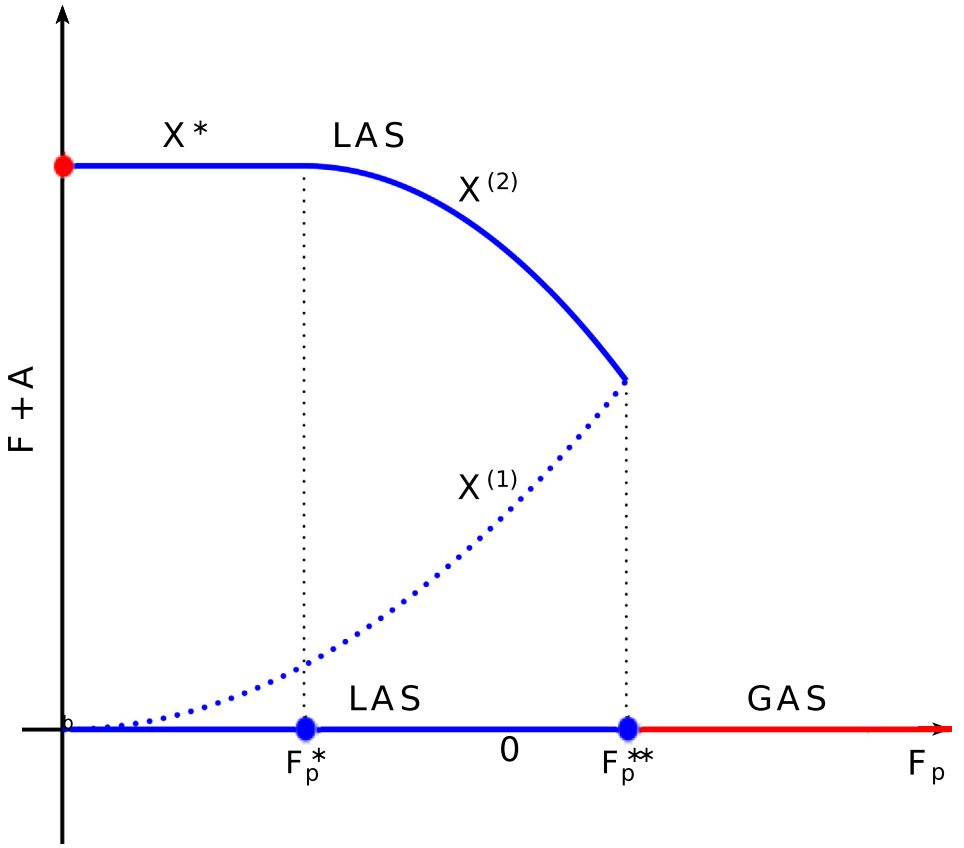

Fig. 4. Bifurcation diagram of the values of $F + A$ at equilibrium with respect to the values of F_p for system (2).

with $x = (E, F, A, M)^T$ and

$$g_2(x, x_\tau) = \begin{pmatrix} b\, e^{-\tau_3\, \mu_A} A(t-\tau_3) \left(1 - \dfrac{E(t)}{K_C}\right) - (\nu_E + \mu_E)\, E(t) \\ r\, \nu_E\, e^{-\tau_2\, \mu_L}\, E(t-\tau_2) - \mu_F\, F(t) \\ \nu_F\, \dfrac{\gamma\, M(t)}{F(t) + F_p}\, F(t) - \mu_A\, A(t) \\ (1-r)\, \nu_E\, e^{-\tau_2\, \mu_L}\, E(t-\tau_2) - \left(\mu_A + \alpha \dfrac{F_p}{F(t) + F_p}\right) M(t) \end{pmatrix} \tag{13}$$

System (12) is a cooperative time delayed system: the (QM) condition is verified. Hence, the stability of each equilibrium for the non delayed system is preserved for the delayed system. It suffices to study the non delayed system to deduce the long term behavior of the time delayed system:

$$\frac{dx}{dt} = g_2(x, x_0). \tag{14}$$

Let us first set

$$\mathcal{R}_M = \frac{(1-r)\, b\, \nu_E\, \gamma \nu_F\, e^{-\tau_2\, \mu_L}\, e^{-\tau_3\, \mu_A}}{\mu_A\, (\nu_E + \mu_E)\, \mu_M} \tag{15}$$

While $\mathcal{R}$, the basic offspring number, represents the number of offsprings produced by one single female during its mean lifespan, $\mathcal{R}_M$ represents the number of offsprings produced by one male during its mean lifespan.

We show the following

Theorem 3.4.

(1) The non delayed system (14) defines a positive dynamical system on $\mathbb{R}^4_+$.
(2) There exists a threshold value $\bar{F}_p^{**}$ *such that*

(i) if $F_p > \bar{F}_p^{**}$, $\mathbf{0}$ *is GAS on* $\mathbb{R}^4_+$.
(ii) if $F_p = \bar{F}_p^{**}$, *and* $\mathcal{R}_M > 1$, *then system (14) has two equilibria:* $\mathbf{0}$ *and one positive equilibria* $\bar{X}_1$. *The basin of attraction of trivial equilibrium contains the set* $\{x \in \mathbb{R}^4_+ : 0 \leq x < \bar{X}_1\}$. *The basin of attraction of* $\bar{X}_1$ *contains the set* $\{x \in \mathbb{R}^4_+ : x \geq \bar{X}_1, E \leq K_C\}$.
(iii) if $0 < F_p < \bar{F}_p^{**}$, *and* $\mathcal{R}_M > 1$, *then system (14) has three equilibria:* $\mathbf{0}$ *and two positive equilibria* $\bar{X}_1$ *and* $\bar{X}_2$ *such that* $\bar{X}_1 < \bar{X}_2$. *The basin of attraction of* $\mathbf{0}$ *contains the set* $\{x \in \mathbb{R}^4_+ : 0 \leq x < \bar{X}_1\}$. *The basin of attraction of* $\bar{X}_2$ *contains the set* $\{x \in \mathbb{R}^4_+ : x \geq \bar{X}_2, E \leq K_C\}$.

Proof. See Appendix D. □

Using the previous results, and assuming $\mathcal{R} > 1$ and $\mathcal{R}_M > 1$, we can deduce the following results for the delayed system (12).

Theorem 3.5. *There exists a threshold value* $\overline{F}_p^{**}$ *such that*

(i) if $F_p > \overline{F}_p^{**}$, $\mathbf{0}$ *is the only equilibrium for the system (12)*
(ii) if $0 < F_p < \overline{F}_p^{**}$, $\mathcal{R} > 1$, *and* $\mathcal{R} > \dfrac{\mu_M r}{(1-r)(\nu_F + \mu_F)\gamma}$, *we have* $\bar{E}_1, \bar{E}_2 \in [0, K]$. *The system has three equilibria: trivial equilibrium* $\mathbf{0}$ *and two positive equilibria* $\bar{X}_1$ *and* $\bar{X}_2$ *such that* $\bar{X}_1 < \bar{X}_2$.

Since model (12) is a delayed cooperative model, we can deduce from [4] the following result about the stability of equilibria:

Theorem 3.6. *Let* $F_p > 0$. *Then, the following holds for the model (12):*

- *If* $0 < F_p \leq \overline{F}_p^{**}$, *then the basin of attraction of the trivial equilibrium contains* $\{x \in \mathbb{R}^4_+ : x \leq \bar{X}_{1,F_p}\}$.
- *If* $F_p \geq \overline{F}_p^{**}$, *then trivial equilibrium is GAS on* $\mathbb{R}^4_+$.

Finally we can deduce the following GAS result for the PWS-DDE system (3) (or system (2)).

Theorem 3.7. *Let* $F_p > 0$ *then the following holds for the model (2):*

- *If* $0 < F_p \leq \overline{F}_p^{**}$, *then the basin of attraction of* $\mathbf{0}$ *contains* $\{x \in \mathbb{R}^4_+ : x \leq \bar{X}_{1,F_p}\}$.
- *If* $F_p \geq \overline{F}_p^{**}$, *then* $\mathbf{0}$ *is GAS on* $\mathbb{R}^4_+$.

In fact, the last theorem is very useful to derive a long term control strategy. Indeed, if the control stops, the system will automatically recover. In the other hand, using only long time massive releases of pheromones is not a sustainable option. However, we know that once the non-massive control starts, i.e. $0 < F_p < \overline{F}_p^{**}$, the system become bistable, such that locally, at least in $\{x \in \mathbb{R}^4_+ : x \leq \bar{X}_{1,F_p}\}$, $\mathbf{0}$ is stable and attractive, for a given (small) amount of pheromones, F_p.

3.3. On a long term control strategy related to the level of infestation of mirids

The previous theoretical results lead to two strategies for long term control

Table 2
Values used for simulations of model (2) with $\mathcal{R} > 1$ [1] and $\mathcal{R}_M > 1$.

b	r	K_C	$1/\nu_L$	$1/\nu_F$	μ_L	μ_A	μ_M	μ_F	μ_E
3.28	0.58	5000	25	10	0.01	0.08	0.08	0.08	0.001

α	γ	$1/\nu_E = \tau_1$	τ_2	τ_3
0.1	1	15	25	10

- When the mirid population is small or at an invading stage (not established in the field, but starting to settle), thanks to the size of the plot, a limited number of traps (releasing a small amount of pheromones) can be sufficient to control it. In other words, knowing the population size, it could be possible to estimate F_p, with $0 < F_p < \overline{F}_p^{**}$, such that the mirid population stays in $[\mathbf{0}, X_{1,F_p}[$, i.e. inside the basin of attraction of $\mathbf{0}$.
- When the population is large, at equilibrium for instance, then, to reduce sharply the population, we need to increase the number of traps in order to release enough pheromones/Fake females, using the GAS property of $\mathbf{0}$ when $F_p > \overline{F}_p^{**}$. This is what we called the "maximal treatment". Thus, according to the GAS of $\mathbf{0}$, there exists $t^* > 0$, such that for $t > t^*$, the mirid population becomes small enough that a small amount of pheromones is sufficient to maintain the population under a given threshold, here $X^{(1)}$, the lowest equilibrium for a given (small preferably) amount of pheromones $F_p \ll \overline{F}_p^{**}$. This is what we called the "minimal treatment". Altogether, when the population is large, the best way to control it is to first start the control with the "maximal treatment", followed by the "minimal treatment".
  To summarize the "maximal–minimal treatment" strategy: for a given large amount of pheromones, $F_p > \overline{F}_p^{**}$, it suffices to estimate the time, t^*, necessary to enter $[\mathbf{0}, X^{(1)}[$, where $X^{(1)}$ is estimated for a given small amount of pheromones, $F_p^{(1)} \ll \overline{F}_p^{**}$. Since $X^{(1)}$ cannot be estimated analytically, we can only estimate the minimum time, t^*, numerically. This is what is illustrated in the next subsection.

3.4. Applications — numerical simulations

In this section, we illustrate the previous results. The values used for the next simulations are given in Table 2, (taken from [1]), leading to the case $\mathcal{R} = 4.5547 > 1$ and $\mathcal{R}_M = 7.4211$.

According to the theoretical part and the parameters values, for a maximal control, we need to release more than $\overline{F}_p^{**} \approx 1162$ fake females (per ha), in other words for any value of F_p larger than $\overline{F}_p^{**}$, the system will converge to $\mathbf{0}$ for t sufficiently large. However, as explained above, we are not interested in a permanent maximal treatment, but we only want to reach (rapidly) a level of population where the damages can be acceptable and where the population can be controlled with a small amount of pheromones. That is why we choose $F_p^{(1)}$ to estimate $\mathbf{X}^{(1)}$ and thus target the box $[\mathbf{0}, \mathbf{X}^{(1)} - \epsilon]$, for a given $0 < \epsilon \ll 1$.

In the sequel, we initiate the simulations at the wild equilibrium. We choose $F_p = 100$ such that we estimate numerically $X^{(1)} = (95.1836, 35.8291, 4.4550, 13.5112)$ (the red dot in Fig. 6(b)). Hence, in the next simulations, for a given $F_p > \overline{F}_p^{**}$, we estimate the minimum time necessary to enter $[\mathbf{0}, X^{(1)} - \epsilon]$. In Figs. 5 and 6, we present an example of the control strategy described above: first, we consider a large amount of pheromones traps, such that $F_p = 2000$, to use the GAS property of $\mathbf{0}$, in order to reach the box $[\mathbf{0}, \mathbf{X}^{(1)}[$, where $X^{(1)}$ is estimated based on the targeted level of control, i.e. $F_p^{(1)} = 100$. Numerically, we estimate that 440 days of maximum treatment are necessary to enter the basin $[\mathbf{0}, \mathbf{X}^{(1)}[$. Then, for all $t > 440$ days, we remove some pheromones traps in order to reach the value $F_p^{(1)} = 100$: the system continues to converge to $\mathbf{0}$, thanks to the LAS property of $\mathbf{0}$ in $[\mathbf{0}, \mathbf{X}^{(1)}[$, when $F_p^{(1)} = 100$.

Note, that the previous results correspond to the case when male trapping occurs, $\alpha = 0.1$. If we assume that there is no trapping, i.e. $\alpha = 0$, then the $M_{T_1} \approx 3576$, and also the minimal time necessary to enter the basin $[\mathbf{0}, \mathbf{X}^{(1)}[$ increases to 536 days but we have to use the double amount of pheromones (fake females)

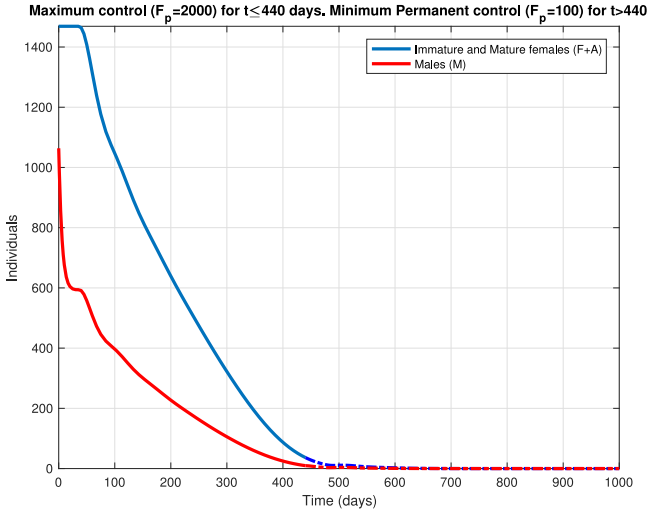

Fig. 5. Mating disruption and Trapping Control with, first $F_p = 2000$ (solid lines), then $F_p = 100$ (dotted lines) once the system has reach $[\mathbf{0}, \mathbf{X}^{(1)}[$.

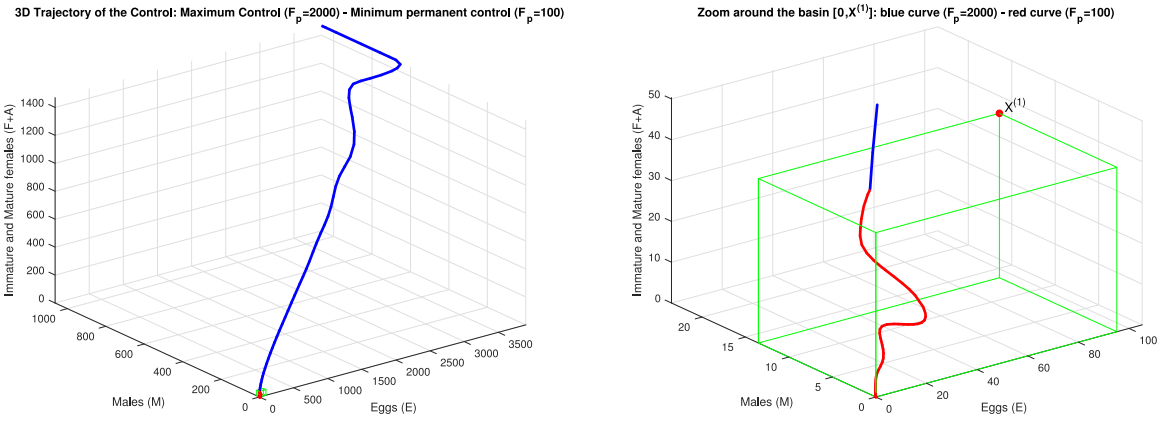

Fig. 6. Maximal Control with, first, $F_p = 2000$ (blue solid line), then, once the system has reached $[\mathbf{0}, \mathbf{X}^{(1)}[$, the minimal control starts with $F_p = 100$. The system continues to converge to $\mathbf{0}$ (red solid line), but slowly. (For interpretation of the references to color in this figure legend, the reader is referred to the web version of this article.)

$M_T = 4000$. That is why the combination of mating disruption and trapping is of utmost importance, not only to minimize the duration of the treatment but also to minimize the release of pheromones.

Fig. 6(a), shows different phase of the control: a first phase, where only the male population is reducing, then the eggs population, before the whole system $(E+F+A+M)$ starts to decay. This shows that in constant environmental conditions (constant parameters) the duration of the control is crucial. In Fig. 6(b), the green box represents the basin $[\mathbf{0}, \mathbf{X}^{(1)}]$: the red trajectory represents the trajectory when the control is defined by $F_p = 100$. Of course, in that case, since $\mathbf{0}$ is LAS in $[\mathbf{0}, \mathbf{X}^{(1)}]$, the system continues to decay (slowly) to $\mathbf{0}$. Of course, the time necessary to enter the basin $[\mathbf{0}, \mathbf{X}^{(1)}]$ depends on the initial maximum control, the larger, the shorter the time needed. However, as showed in Fig. 7, it seems that choosing F_p between 2000 and 4000 provides the more interesting results. However, the cost of pheromones need to be taken into account in order to derive the best strategies. The previous strategy is based on two given values for F_p. Other strategies based on the use of several values for F_p could be chosen in order to reduce progressively the amount of pheromones and to use the LAS of $\mathbf{0}$ in the box $[\mathbf{0}, \mathbf{X}^{(1)}_{F_p}]$, for a given F_p. However, from a practical

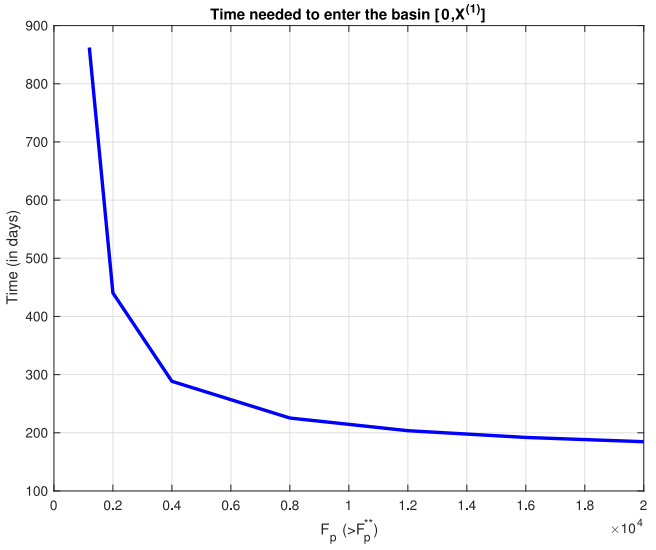

Fig. 7. Time needed to enter the basin $[\mathbf{0}, \mathbf{X}^{(1)}_{F_p}]$ for a given $F_p > F_p^{**}$.

point of view, reducing F_p, while convenient on the paper, seems to be more difficult from a practical point of view.

4. About mating disruption strategy when the pods carrying capacity is periodic

Like in [1], we have to consider that the mirid population dynamics is mainly related to the presence/absence of pods, but not only. Indeed, the cacao production in Cameroon is seasonal, which is not the case, for instance, in Central America. Thus, in Cameroon, the pods carrying capacity, K_C, is not constant but has to be approximated by a yearly periodic function. Last but not least, we know that, in the absence of pods, mirids can maintain in the area using secondary host plants, like *Cola nitida*, or *Ceiba pentandra* [1]. That is why we consider the following pods carrying capacity $K_C(t) = K(t) + C$, where $C > 0$ is a given constant, equal to 100 [1], and $K(t)$ is defined as in [1] (see Table E.3): see Fig. 8.

In that case, the control strategy is rather different than in the constant coefficients case. Here, knowing the inter-period (from March to June), when no cocoa pods are available, is rather crucial: it seems obvious to start the control at the beginning of this period , i.e. in March, in order to use the LAS property of model (3), when $K(t) \equiv 0$, to avoid the establishment of the mirid population within the cocoa plantation when $K(t)$ rises again (in July).

We thus consider the following non-autonomous periodic DDE-PWS system

$$\frac{dx}{dt} = f(x, x_\tau, t) := \begin{cases} f_1(x, x_{\tau_2}, x_{\tau_3}, t) & \text{if} \quad F + F_p \leq \gamma\, M \\ f_2(x, x_{\tau_2}, x_{\tau_3}, t) & \text{if} \quad F + F_p \geq \gamma\, M \end{cases} \tag{16}$$

where $x = (E, F, A, M)^t$,

$$f_{1,per}(x, x_\tau, t) = \begin{pmatrix} b\, e^{-\tau_3\, \mu_A}\, A(t-\tau_3) \left(1 - \dfrac{E(t)}{C + K(t)}\right) - (\nu_E + \mu_E)\, E(t) \\ r\, \nu_E\, e^{-\tau_2\, \mu_L}, E(t-\tau_2) - (\nu_F + \mu_F)\, F(t) \\ \nu_F\, F(t) - \mu_A\, A(t) \\ (1-r)\, \nu_E\, e^{-\tau_2\, \mu_L}\, E(t-\tau_2) - \left(\mu_M + \alpha \dfrac{F_p}{F(t) + F_p}\right) M(t) \end{pmatrix} \tag{17}$$

and

$$f_{2,per}(x,x_\tau,t)=\begin{pmatrix} b\,e^{-\tau_3\,\mu_A}\,A(t-\tau_3)\left(1-\dfrac{E(t)}{C+K(t)}\right)-(\nu_E+\mu_E)\,E(t)\\ r\,\nu_E\,e^{-\tau_2\,\mu_L}\,E(t-\tau_2)-\nu_F\gamma\dfrac{M(t)}{F(t)+F_p}\,F(t)-\mu_F\,F(t)\\ \nu_F\,\gamma\dfrac{F(t)}{F(t)+F_p}\,M(t)-\mu_A\,A(t)\\ (1-r)\,\nu_E\,e^{-\tau_2\,\mu_L}\,E(t-\tau_2)-\left(\mu_M+\alpha\dfrac{F_p}{F(t)+F_p}\right)M(t)\end{pmatrix} \tag{18}$$

The methodology to study the periodic PWS-DDE (16) follows the methodology of the previous sections, thanks to the fact that $0<C\le K(t)+C\le K_{\max}+C$. Indeed, for $i=1,2$, it is straightforward to check that

$$f_{i,C}(x,x_\tau)\le f_{i,per}(x,x_\tau,t)\le f_{i,C+K_{\max}}(x,x_\tau),\quad \text{for all } t>0. \tag{19}$$

1. In the male abundance case, $f_{1,C}$ and $f_{1,C+K_{\max}}$ are delayed system that verify the (QM) condition. Thus, using (19), and applying Theorem 5.1.1 [10], we deduce that

$$x_{1,C}(t)\le x_{1,per}(t)\le x_{1,C+K_{\max}}(t),\quad \text{for all } t>0.$$

where $x_{1,per}$ is the solution of the periodic male abundance equation, $x_{1,C}$ and $x_{1,C+K_{\max}}$ are respectively solutions of the autonomous male abundance system (6), with $K\equiv C$ and $K\equiv C+K_{\max}$ respectively. Thus, using Theorem 3.2, we can deduce

Theorem 4.1

- Assume $\mathcal{R}_0<1$, then $x_{1,per}$ converges to $\mathbf{0}$.
- Assume $\mathcal{R}_0>1$, then the male abundance system is permanent, i.e. $x_{1,per}>0$ for all $t>0$.

where $\mathcal{R}_0$ is defined in (8).

Remark 4.1 Following [1], when $\mathcal{R}_0>1$, it is possible to show that the male abundance system converges to a unique periodic solution, $x^*_{per}(t)$, defined as follows:

$$E^*_{per}(t)=\left(1-\frac{1}{\mathcal{R}}\right)(C+K(t)),\quad F^*_{per}(t)=\frac{r\,\nu_E\,e^{-\tau_2\,\mu_L}}{\mu_F+\nu_F}\,E^*_{per}(t),$$
$$A^*_{per}(t)=\frac{\nu_F}{\mu_A}\,F^*_{per}(t),\quad M^*_{per}(t)=\frac{(1-r)\,\nu_E\,e^{-\tau_2\,\mu_L}}{\mu_M+\alpha\,\dfrac{F_p}{F^*_{per}(t)+F_p}}\,E^*_{per}(t).$$

2. The male scarcity case is rather more difficult to study. However, we can use the second inequality in (19): $f_{2,per}(t,x,y)$ is nondecreasing in y; thus, according to Theorem 3.6 in [12], page 29, we deduce that $x_{2,per}\le x_{2,C+K_{\max}}$, such that the methodology developed in Section 3.2, can be applied to the system

$$\frac{dx}{dt}=f_{2,C+K_{\max}}(x,x_\tau).$$

Hence, we deduce that there exists $\overline{F}^{**}_{p,C+K_{\max}}>0$ such that $\mathbf{0}$ is GAS when $F_p>\overline{F}^{**}_{p,C+K_{\max}}>0$, i.e. $x_{2,C+K_{\max}}$ converges to $\mathbf{0}$ and so is $x_{2,per}$ as t goes to $+\infty$.
However, for a practical application, this result is not interesting since the amount of pheromones to release can be very large.
Another possibility is to focus on the case where $K\equiv 0$ from March to June, such that we know that periodic system reduces to the autonomous system with carrying capacity C, in other word: $f_{i,per}(x,x_\tau)=f_{i,C}(x,x_\tau)$. In that case, we are able to estimate $\overline{F}^{**}_{p,C}$. When $C=100$, then $\overline{F}^{**}_{p,C}\approx 23.23$.

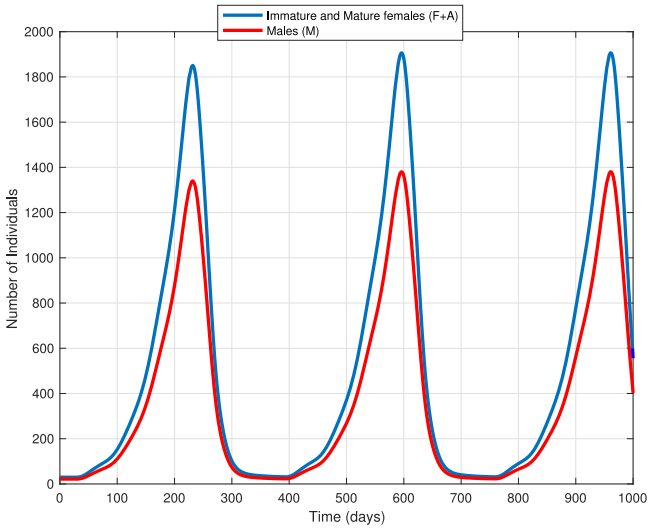

Fig. 8. Time evolution of the periodic system, without control.

4.1. Periodic case — simulations

As explained above we focus on the period from March to June, i.e, we adapt the starting time of our control: either at the end or at the beginning of that period.

Thus, we consider two starting times: $t = 390$ (beginning of July), see Fig. 9, and $t = 300$ (beginning of March), see Fig. 10. When choosing $F_p = 20$ as the targeted amount of pheromones, we are looking at the time t^* necessary to enter and also stay inside $[\mathbf{0}, \mathbf{X}^{(1)}[$, with $X^{(1)} = (27.11, 10.20, 1.70, 4.04)$ (the red dot in Fig. 9(b) and Fig. 10(b)).

As illustrated in Fig. 9, starting lately within the no-production period, at $t_{start} = 390$, will have an effect during the production period, with a population fourth times less than without control, and it is only after 470 days of $F_p = 100$ treatment that the trajectory enter the box $[\mathbf{0}, \mathbf{X}^{(1)}[$ and then continues to decay to zero with $F_p = 20$.

In contrary, starting the treatment early, at $t_{start} = 300$, within the no-production period, the population decreases rapidly, and in 217 days, the trajectory enter the box $[\mathbf{0}, \mathbf{X}^{(1)}[$ and then continues to decay to zero with $F_p = 20$. In addition, the population has become so small, that even when the pods are back, the mirid population stay within $[\mathbf{0}, \mathbf{X}^{(1)}[$, event with a small amount of pheromones, $F_p = 20$.

In fact, the periodic case, for mating disruption and trapping control, is the most favorable case, as we can use the no-production period, and thus when the mirid population is at its lowest, to be very efficient, especially if the treatment starts early (beginning of March, for instance).

5. Conclusion

We have considered a mating disruption and trapping model to study the opportunity of using sex-pheromones to control a mirid population. We obtain a PWS-DDE model, a kind of model that is not so common in Mathematical Biology. Thanks to the previous works done by some of the authors and a suitable use of the Monotone System theory, we were able to provide theoretical results that helped us to provide interesting strategies that could be used in the field for long term control.

Of course, this work provides only partial insight of this complex system. Using a temporal approach, we implicitly assume that mirids and pheromones are homogeneously distributed, which is not the case in the

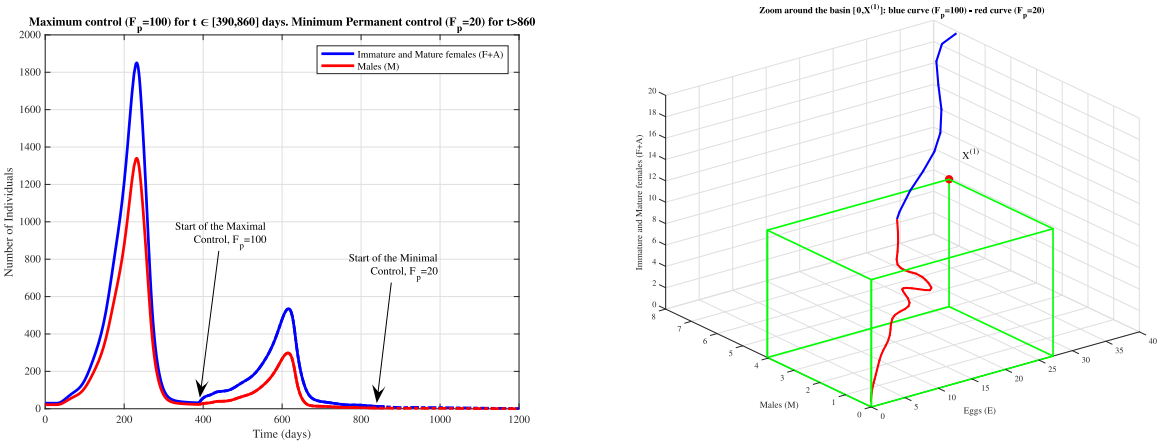

Fig. 9. Maximal Control, with $F_p = 100$, then, once the system has reached $[\mathbf{0}, \mathbf{X}^{(1)}[$ at time $t_{max} = 860$, the minimal control starts (dotted lines), with $F_p = 20$: (a) trajectories of the system (b) Zoom of the trajectory near $[\mathbf{0}, \mathbf{X}^{(1)}[$ (blue solid line: maximal control; red solid line: minimal control. (For interpretation of the references to color in this figure legend, the reader is referred to the web version of this article.)

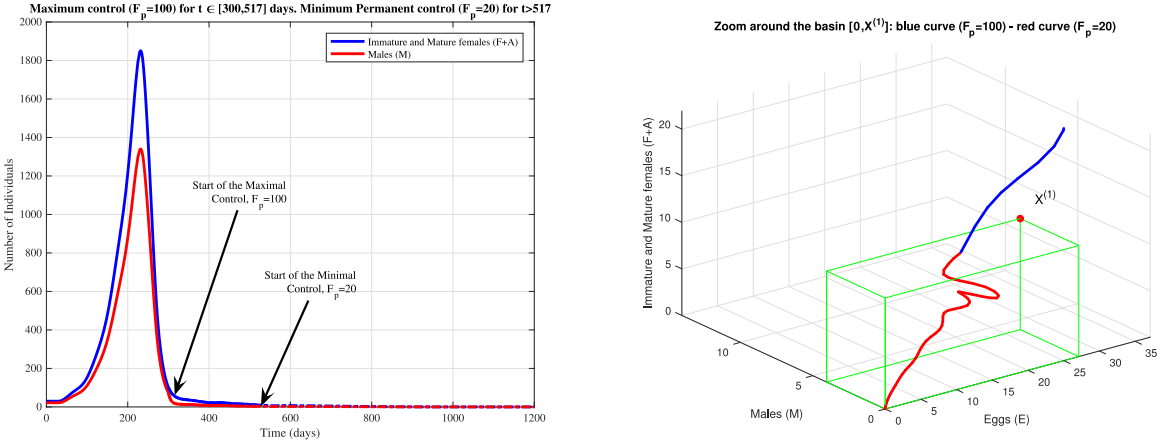

Fig. 10. Maximal Control, with $F_p = 100$, then, once the system has reached $[\mathbf{0}, \mathbf{X}^{(1)}[$ at time $t_{max} = 517$, the minimal control starts (dotted lines), with $F_p = 20$, : (a) trajectories of the system (b) Zoom of the trajectory near $[\mathbf{0}, \mathbf{X}^{(1)}[$ (blue solid line: maximal control; red solid line: minimal control. (For interpretation of the references to color in this figure legend, the reader is referred to the web version of this article.)

field. A next step would be to take into account the spatial component, like in [13]. Last, but not least, it is well known that mirids aggregate on some particular trees, such that aggregation and dispersion processes should be taken into account, and also the impact of these behaviors in terms of the distribution and the density of the pheromone traps. This may require another modeling approach, thanks to the fact that very few knowledge is available about pheromone spreading, mirid's sensitivity to pheromone, etc.

Acknowledgments

YD acknowledges the (partial) support of the DST/NRF SARChI Chair, South Africa M3B2 in Mathematical Models and Methods in Biosciences and Bioengineering at the University of Pretoria, South Africa (grant 82770).

The authors thank the anonymous reviewers for their fruitful comments that greatly improved the initial manuscript.

Appendix A. Piecewise smooth (PWS) dynamical systems

We just provide some definitions related to PWS dynamical systems, given in [14]. For a general presentation, the interested readers are referred to [15] or [4].

Definition A.1. A piecewise-smooth flow is given by a finite set of ODEs $\dot{x}_i(t) = F_i(x,\mu), x \in S_i$; where $\cup_i S_i = \mathcal{D}$ is a domain, each S_i has a non-empty interior.

The intersection $\sum_{ij} := S_i \cap S_j$ is either an $\mathbb{R}^{n-1}$-dimensional manifold included in the boundaries ∂S_j and ∂S_i, or is the empty set. Each vector field F_i is smooth in both state x and parameter μ, and defines a smooth flow $\phi_i(x,t)$ within any open set $U \supseteq S_i$.

A non-empty border between two regions $\sum_{ij}$ will be called a discontinuity set, discontinuity boundary, or a switching manifold.

Definition A.2 (*[14]*)**.** Let $\dot{x}(t) = f(x(t), x(t-\tau))$ be a delay dynamical system. A simple example of a PWS-DDE composed of two smooth vector fields is

$$\dot{x}(t) = \begin{cases} f_1(x(t), x(t-\tau)) & if \quad f(x(t), x(t-\tau)) \leq 0 \\ f_2(x(t), x(t-\tau)) & if \quad f(x(t), x(t-\tau)) \geq 0. \end{cases} \tag{A.1}$$

where $x(t) \in \mathbb{R}^n$, and f_1, f_2, f are sufficiently smooth functions. Transitions between the different vector fields occur on the switching surface defined by $f = 0$.

Definition A.3 (*[14]*)**.** We define a PWS-DDE to be a collection of smooth vector fields

$$\dot{x}(t) = f_m(x^t) \tag{A.2}$$

indexed by a mode variable $m \in \mathcal{M}$ where $x^t \in \mathcal{C}([-\tau, 0], \mathbb{R}^n)$ is the solution segment $x(t+s)$ for $-\tau \leq s \leq 0$ and $\mathcal{M}$ is a finite set. (Eq. (A.2) encompasses distributed delays as well as discrete delays; however, we deal here with discrete delays only.) Associated with this is a collection of events $e \in \mathcal{E}$ where $\mathcal{E}$ is a finite set and e consists of a pair $\pi_e = (m_{in}, m_{out})$, a smooth event function $h_e(x^t) : \mathcal{C}([-\tau, 0], \mathbb{R}^n) \longleftrightarrow \mathbb{R}$ and a smooth jump function $g_e(x^t) : \mathcal{C}([-\tau, 0], \mathbb{R}^n) \longleftrightarrow \mathcal{C}([-\tau, 0], \mathbb{R}^n)$.

The event function $h_e = 0$ implicitly defines a switching manifold marking the transition point between the (potentially) different vector fields $(f_{m_{in}}, f_{m_{out}})$ and the jump function g_e determines the instantaneous change of state that occurs upon impact with the switching manifold. The minimal state needed to uniquely identify a particular trajectory of the system starting at time t_0 is thus x^{t^0} along with the mode m at time t_0.

Definition A.4. Following [15], the degree of smoothness at a point x_0 in a switching set $\sum_{ij}$ of a piecewise-smooth ODE is the highest order r such the Taylor series expansions of $\phi_i(x_0, t)$ and $\phi_j(x_0, t)$ with respect to t, evaluated at $t = 0$, agree up to terms of $\mathcal{O}(t^{r-1})$. That is, the first non-zero partial derivative with respect to t of the difference $[\phi_i(x_0, t) - \phi_j(x_0, t)]|_{t=0}$ is of order r.

Appendix B. Proof of Proposition 3.1

Setting the left-hand side of system (10) to zero, and after some straightforward calculations, we get the following equation in E to solve:

$$\psi(E) := E\,\xi(E)\,\phi(E) = \eta(F_p, E). \tag{B.1}$$

where

$$\xi(E) = \gamma\,(1-r)\,e^{-\tau_2\,\mu_L}\nu_E\,\nu_F\,e^{-\tau_3\,\mu_A}\,b\,\left(1-\frac{E}{K_C}\right) - \mu_A\,(\alpha+\mu_M)\,(\nu_E+\mu_E), \tag{B.2}$$

$$\eta(F_p, E) = \mu_A\,\mu_F\,\mu_M\,(\nu_E+\mu_E)\,be^{-\tau_3\,\mu_A}\,\left(1-\frac{E}{K_C}\right)\,F_p. \tag{B.3}$$

and

$$\phi(E) = b\,e^{-\tau_3\,\mu_A}\,r\,\nu_E\,e^{-\tau_2\,\mu_L}\,\left(1-\frac{E}{K_C}\right) - \mu_A\,(\nu_E+\mu_E).$$

Therefore, assuming that E_{eq} is a positive root of (B.1), the other components of the non trivial equilibria of (10) are:

$$F_{eq} = \frac{\phi(E_{eq})}{\mu_F be^{-\mu_A\tau_3}\left(1-\dfrac{E_{eq}}{K_C}\right)}E_{eq}, \tag{B.4}$$

$$A_{eq} = \frac{(\nu_E+\mu_E)}{e^{-\tau_3\,\mu_A}b\,\left(1-\dfrac{E_{eq}}{K_C}\right)}\,E_{eq}, \tag{B.5}$$

$$M_{eq} = \frac{(1-r)\,\nu_E\,e^{-\tau_2\,\mu_L}}{\mu_M+\alpha\,\dfrac{F_p}{F_{eq}+F_p}}\,E_{eq}. \tag{B.6}$$

Further, to ensure $F_{eq} > 0$, we need to have $\phi(E_{eq}) > 0$, that is E_{eq} must satisfy the condition:

$$E_{eq} < K_C\,\left(1-\frac{\mu_A\,(\nu_E+\mu_E)}{r\,b\,\nu_E\,e^{-\tau_2\,\mu_L}\,e^{-\tau_3\,\mu_F}}\right) \tag{B.7}$$

In fact, according to the definition of $\psi(E)$, it is straightforward to check that ψ admits two real positive roots in $[0, K]$,

$$E_1 = \left(1-\frac{\mu_A\,(\nu_E+\mu_E)}{b\,e^{-\tau_3\,\mu_A}\,r\,\nu_E\,e^{-\tau_2\,\mu_L}}\right)K_C, \quad \text{and } E_2 = \left(1-\frac{\mu_A\,(\alpha+\mu_M)\,(\nu_E+\mu_E)}{\gamma\,(1-r)\,e^{-\tau_2\,\mu_L}\nu_E\,\nu_F\,e^{-\tau_3\,\mu_A}b}\right)K_C,$$

provided that $\dfrac{\mu_A\,(\nu_E+\mu_E)}{b\,e^{-\tau_3\,\mu_A}\,r\,\nu_E\,e^{-\tau_2\,\mu_L}} < 1$ and $\dfrac{\mu_A\,(\alpha+\mu_M)\,(\nu_E+\mu_E)}{\gamma\,(1-r)\,e^{-\tau_2\,\mu_L}\nu_E\,\nu_F\,e^{-\tau_3\,\mu_A}b} < 1$.

Thus, only the points of intersection between the straight line $\eta(F_p, E)$ and the cubic $\psi(E)$ that belong to $[0, \min\{E_1, E_2\}]$ are of interest for us: see Fig. B.11. We denote by F_p^{**} the value of F_p such that the straight line $\eta(F_p, E)$ is tangent to the indicated section of the graph $\psi(E)$. Then, it is clear that for $F_p > F_p^{**}$ there is no intersection between $\eta(F_p, E)$ and Ψ (no positive equilibrium) while for $0 < F_p < F_p^{**}$, there are two points of intersection (2 positive equilibria).

Finally, straightforward computations show that $\mathbf{0}$ is an absolutely stable equilibrium of system (10).

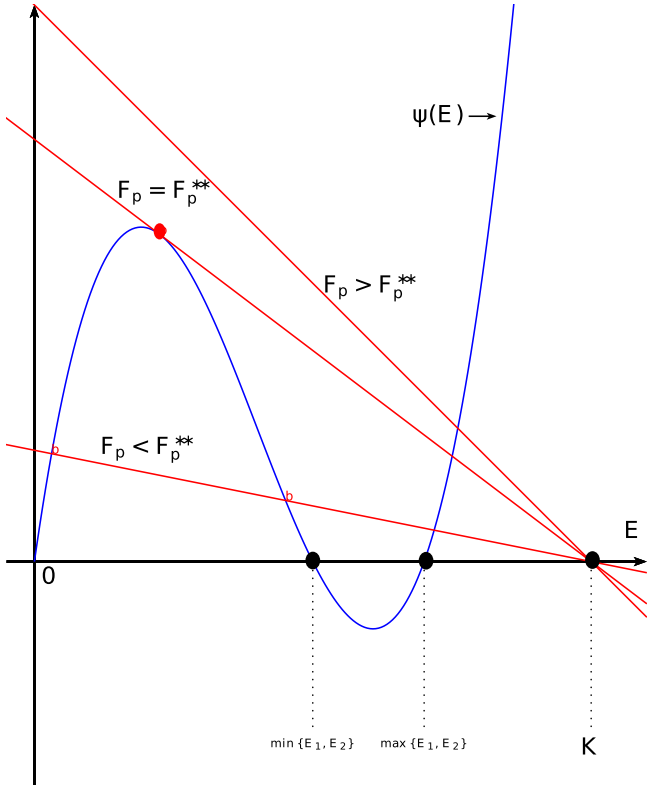

Fig. B.11. Intersection between $\psi(E)$ (in blue) and $\eta(F_p, E)$ (in red) for three values of F_p. (For interpretation of the references to color in this figure legend, the reader is referred to the web version of this article.)

Appendix C. Proof of Theorem 3.3

Assume $0 < F_p < F_p^{**}$. Then, let $E_{eq}^{(1)}$ and $E_{eq}^{(2)}$, $E_{eq}^{(1)} < E_{eq}^{(2)}$ be the roots of (B.1). We denote the respective equilibria by $X^{(1)}$ and $X^{(2)}$. To show that any equilibrium of (10) is a regular equilibrium of (2), we need to show that it belongs to the male scarcity region. Using the previous relationships, it suffices to study the sign of $F_{eq} + F_p - \gamma M_{eq}$. In fact, we can show that

$$F_{eq} + F_p - \gamma M_{eq} = \frac{1}{\mu_M + \alpha \dfrac{F_p}{F_{eq} + F_p}} \left(\mu_M \left(F_{eq} + F_p \right) + \alpha F_p - \gamma (1-r) \nu_E e^{-\tau_2 \mu_L} E_q \right)$$

Thus, studying the sign of $F_{eq} + F_p - \gamma M_{eq}$ is equivalent to study the sign of

$$\left(\mu_M F_{eq} - \gamma (1-r) \nu_E e^{-\tau_2 \mu_L} E_q \right) + \left(\alpha + \mu_M \right) F_p.$$

In fact we have

$$\left(\mu_M F_{eq} - \gamma (1-r) \nu_E e^{-\tau_2 \mu_L} E_q \right) + \left(\alpha + \mu_M \right) F_p = \tag{C.1}$$

$$= \left(\mu_M \frac{\phi(E_{eq})}{\mu_F b e^{-\mu_A \tau_3} \left(1 - \dfrac{E_{eq}}{K_C} \right)} - \gamma (1-r) \nu_E e^{-\tau_2 \mu_L} \right) E_q + \left(\alpha + \mu_M \right) F_p \tag{C.2}$$

$$= r\, \nu_E\, e^{-\tau_2\, \mu_L} \left(\frac{r \mu_M}{\mu_F} - \frac{\mu_M \mu_A \left(\nu_E + \mu_E \right)}{\mu_F b e^{-\mu_A \tau_3} \left(1 - \dfrac{E_{eq}}{K_C} \right)} - \gamma (1-r) \right) E_q + \left(\alpha + \mu_M \right) F_p \tag{C.3}$$

using the inequality $E_{eq}^{(1)} < E_{eq}^{(2)} < E^*$, we have:

$$\geq r\,\nu_E\,e^{-\tau_2\,\mu_L}\left(\frac{r\mu_M}{\mu_F}-\frac{\mu_M\mu_A\,(\nu_E+\mu_E)}{\mu_F b e^{-\mu_A\tau_3}\left(1-\frac{E^*}{K_C}\right)}-\gamma(1-r)\right)E_q+(\alpha+\mu_M)\,F_p$$
$$=\ r\,\nu_E\,e^{-\tau_2\,\mu_L}\left(\frac{r\mu_M}{\mu_F}-\frac{\mu_M\mu_A\,(\nu_E+\mu_E)\mathcal{R}}{\mu_F b e^{-\mu_A\tau_3}}-\gamma(1-r)\right)E_q+(\alpha+\mu_M)\,F_p$$

and after some simplifications

$$=\ r\,\nu_E\,e^{-\tau_2\,\mu_L}\left(\frac{r\mu_M}{\mu_F+\nu_F}-\gamma(1-r)\right)E_q+(\alpha+\mu_M)\,F_p.$$

Using (9), we deduce

$$\left(\mu_M F_{eq}-\gamma(1-r)\nu_E e^{-\tau_2\mu_L}E_q\right)+(\alpha+\mu_M)\,F_p=\frac{(\alpha+\mu_M)}{E^*}\left(F_pE^*-E_qF_p^*\right).$$

Since $E_{eq}^{(1)} < E_{eq}^{(2)} < E^*$, then $F_pE^* - E_qF_p^* > \left(F_p - F_p^*\right)E_q$. Using the fact that $F_p^* < F_p$, then $F_pE^* - E_qF_p^* > 0$, such that $F_{eq} + F_p - \gamma M_{eq} > 0$. Therefore, in this case, $X^{(1)}$ and $X^{(2)}$ are both in the male scarcity region. Hence, they are also equilibria of (2).

If $F_p < F_p^*$ and $E_{eq} > E^*$, considering the fact that for $0 < F_p < F_p^*$, we have $E_{eq}^{(1)} < E^* < E_{eq}^{(2)}$ and using the same method as previously, we obtain $F_p + F_{eq}^{(2)} - \gamma\,M_{eq}^{(2)} < 0$.

Therefore, $X^{(2)}$ is not in the male scarcity region. Hence, it is not an equilibrium of (2). Taking into consideration the previous results regarding $X^{(1)}$ and $X^{(2)}$, the theorem is proved.

Appendix D. Proof of Theorem 3.4

The first assertion is obvious. Setting the first, second, and fourth terms in (13) equal to zero, we derive

$$\bar{F}=\frac{r\,\nu_E\,e^{-\tau_2\mu_L}}{\mu_F}\bar{E},\quad \bar{A}=\frac{(\nu_E+\mu_E)}{b\,e^{-\tau_3\,\mu_A}\left(1-\frac{\bar{E}}{K_C}\right)}\bar{E},\quad \bar{M}=\frac{\left((1-r)\,\nu_E\,e^{-\tau_2\,\mu_L}\right)\left(\bar{F}+F_p\right)}{\mu_M\,\bar{F}+(\mu_M+\alpha)\,F_p}\bar{E}$$

Solving the third equation equal to zero and substituting the expressions for $\bar{F}$, $\bar{A}$ and $\bar{M}$ above, we obtain an equation for $\bar{E}$ in the form

$$E\phi(E)=\eta(F_p,E), \tag{D.1}$$

with

$$\begin{aligned}\eta(F_p,E)&=\mu_M r\nu_E e^{-\tau_2\mu_L}E+\mu_F\,(\alpha+\mu_M)\,F_P\\ \phi(E)&=(\mu_F+\nu_F)(1-r)\nu_E e^{-\tau_2\mu_L}\gamma\mathcal{R}\left(1-\frac{E}{K_C}\right)\end{aligned} \tag{D.2}$$

In other words, if (D.1) admits roots, they is intersection between a parabola and a straight line: see Fig. D.12.

In fact, solving (D.1) is equivalent to solve the following quadratic equation

$$\frac{\mathcal{R}(1-r)\nu_E e^{-\tau_2\mu_L}\,(\nu_F+\mu_F)\,\gamma}{K_C}E^2+\nu_E e^{-\tau_2\mu_L}\,(\mu_M r-\mathcal{R}(1-r)\,(\nu_F+\mu_F)\,\gamma)\,E+$$
$$+\mu_F\,(\alpha+\mu_M)\,F_p=0.$$

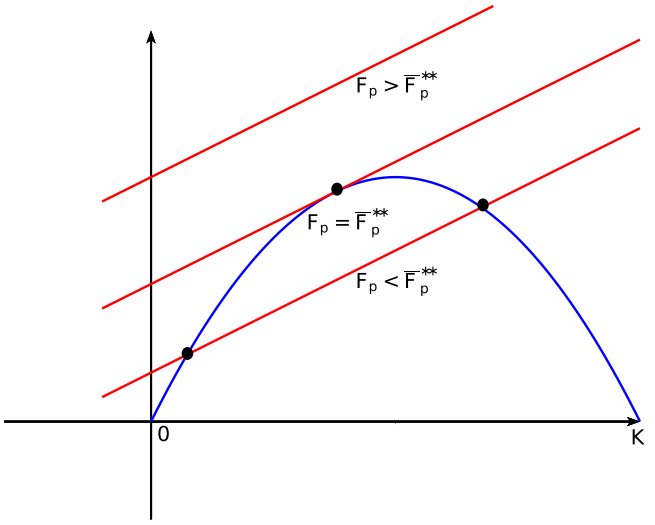

Fig. D.12. Intersections between the graphs of $E\phi(E)$ (in blue) and $\eta(F_p, E)$ (in red) for different values of F_p. The black dots represent the intersection points on the interval $[0, K]$ ($K = K_C$). (For interpretation of the references to color in this figure legend, the reader is referred to the web version of this article.)

Then, we estimate the discriminant

$$\Delta = \left(\nu_E e^{-\tau_2\mu_L}\left(\mu_M r - \mathcal{R}(1-r)\left(\nu_F+\mu_F\right)\gamma\right)\right)^2 - 4\frac{\mathcal{R}(1-r)\nu_E e^{-\tau_2\mu_L}\left(\nu_F+\mu_F\right)\gamma}{K_C}\mu_F\left(\alpha+\mu_M\right)F_p$$

or equivalently

$$\Delta = \left(\nu_E e^{-\tau_2\mu_L}\mu_M r\left(1-\mathcal{R}_M\right)\right)^2 - 4\frac{\mathcal{R}(1-r)\nu_E e^{-\tau_2\mu_L}\left(\nu_F+\mu_F\right)\gamma}{K_C}\mu_F\left(\alpha+\mu_M\right)F_p$$

Clearly, if $F_p > \overline{F}_p^{**}$, with

$$\overline{F}_p^{**} = \frac{\left(\nu_E e^{-\tau_2\mu_L}\mu_M r\left(1-\mathcal{R}_M\right)\right)^2}{4\mathcal{R}(1-r)\left(\nu_F+\mu_F\right)\gamma\mu_F\left(\alpha+\mu_M\right)}K_C,$$

then $\Delta < 0$, and no positive real roots exist. Otherwise, when $F < \overline{F}_p^{**}$, two real roots exist. If in addition, we assume that

$$\mathcal{R}_M > 1,$$

then, we obtain the following positive real roots $\bar{E}_1 < \bar{E}_2$:

$$\bar{E}_1 = \frac{1}{2}\left(\frac{\nu_E e^{-\tau_2\mu_L}\mathcal{R}(1-r)\left(\nu_F+\mu_F\right)\gamma - \mu_M r - \sqrt{\Delta}}{\mathcal{R}(1-r)\nu_E e^{-\tau_2\mu_L}\left(\nu_F+\mu_F\right)\gamma}\right)K_C$$

$$\bar{E}_2 = \frac{1}{2}\left(\frac{\nu_E e^{-\tau_2\mu_L}\mathcal{R}(1-r)\left(\nu_F+\mu_F\right)\gamma - \mu_M r + \sqrt{\Delta}}{\mathcal{R}(1-r)\nu_E e^{-\tau_2\mu_L}\left(\nu_F+\mu_F\right)\gamma}\right)K_C.$$

Using (D.1) and (D.2), it is straightforward to show that $\bar{E}_1 < \bar{E}_2 < K_C$. Assume $F_p > \overline{F}_p^{**}$, then setting

$$\bar{y}_q = \begin{pmatrix} K_C \\ \dfrac{r\,\nu_E\,e^{-\tau_2\mu_L}}{\mu_F}q \\ \dfrac{\gamma\nu_F(1-r)\,\nu_E\,e^{-\tau_2\,\mu_L}}{\mu_M} \\ \dfrac{(1-r)\,\nu_E\,e^{-\tau_2\,\mu_L}}{\mu_M} \end{pmatrix},$$

Table E.3
Daily mean number of cocoa pods.

Months	Jun	Jul	Aug	Sept	Oct	Nov	Dec	Jan	Feb	Mar	Apr	May	Jun
$K_C(t)$	0	$\frac{32000}{31}$	$\frac{160000}{31}$	$\frac{416000}{30}$	$\frac{544000}{31}$	$\frac{304000}{31}$	$\frac{416000}{31}$	$\frac{120000}{31}$	$\frac{8000}{28}$	0	0	0	0

where q is any real number, such that $q \geq K$. We check that $g_2(\bar{y}_q, \bar{y}_q) \leq 0$. Thus, by Theorem 7 [4], $\mathbf{0}$ is GAS on $\Omega_K = \bigcup_{q \geq K}[\mathbf{0}, \bar{y}_q]$, which implies that $\mathbf{0}$ is GAS on $\mathbb{R}^4_+$ since Ω_K is an absorbing set.

Appendix E. Biological data

Following [1], we consider the data issued from [16] for the time evolution of the pods carrying capacity along the year.

References

[1] M. Djoukwe Tapi, L. Bagny-Beilhe, S. Bowong, Y. Dumont, Models for miridae, a cocoa insect pest. Application in control strategies, Math. Methods Appl. Sci. 41 (2018) 8673–8696, http://dx.doi.org/10.1002/mma.5063.

[2] R. Mahob, R. Babin, G. ten Hoopen, L. Dibog, D. Hall, C. Bilong Bilong, Field evaluation of synthetic sex pheromone traps for the cocoa mirid *Sahlbergella singularis* (Hemiptera: Miridae), Pest Manag. Sci. 67 (6) (2011) 672–676, http://dx.doi.org/10.1002/ps.2107.

[3] J. Sarfo, C. Campbell, D. Hall, Optimal pheromone trap density for mass trapping cacao mirids, Entomol. Exp. Appl. 166 (7) (2018) 565–573, http://dx.doi.org/10.1111/eea.12699.

[4] R. Anguelov, C. Dufourd, Y. Dumont, Mathematical model for pest–insect control using mating disruption and trapping, Appl. Math. Model. 52 (2017) 437–457, http://dx.doi.org/10.1016/j.apm.2017.07.060.

[5] E. Joseph, Behavioural Responses of Cocoa Mirids, *Sahlbergella singularis* Hagl. and Distantiella Theobroma Dist. (Heteroptera: Miridae), to Sex Pheromones (Ph.D. thesis), University of Greenwich, 2013.

[6] Y. Dumont, J.-M. Tchuenche, Mathematical studies on the sterile insect technique for the Chikungunya disease and *Aedes albopictus*, J. Math. Biol. 65 (5) (2012) 809–855, http://dx.doi.org/10.1007/s00285-011-0477-6.

[7] M. Strugarek, H. Bossin, Y. Dumont, On the use of the sterile insect release technique to reduce or eliminate mosquito populations, Appl. Math. Model. 68 (2019) 443–470, http://dx.doi.org/10.1016/j.apm.2018.11.026.

[8] P. Bliman, D. Cardona-Salgado, Y. Dumont, O. Vasilieva, Implementation of control strategies for sterile insect techniques, Math. Biosci. 314 (2019) 43–60, http://dx.doi.org/10.1016/j.mbs.2019.06.002.

[9] J. Hale, Theory of Functional Differential Equations, in: Applied Mathematical Sciences, vol. 3, Springer, New York, 1977.

[10] H. Smith, Monotone dynamical systems: An introduction to the theory of competitive and cooperative systems, Ann. Math. Stat. 41 (2008).

[11] R. Anguelov, Y. Dumont, J.-S. Lubuma, Mathematical modeling of sterile insect technology for control of anopheles mosquito, Comput. Math. Appl. 64 (3) (2012) 374–389, http://dx.doi.org/10.1016/j.camwa.2012.02.068.

[12] H. Smith, An Introduction to Delay Differential Equations with Applications to the Life Sciences, in: Texts in Applied Mathematics, vol. 57, Springer, New York Dordrecht Heidelberg London, 2011.

[13] R. Anguelov, C. Dufourd, Y. Dumont, Simulations and parameter estimation of a trap-insect model using a finite element approach, Math. Comput. Simulation 133 (2017) 47–75, http://dx.doi.org/10.1016/j.matcom.2015.06.014.

[14] D. Barton, Stability calculations for piecewise-smooth delay equations, Int. J. Bifurcation Chaos 19 (2009) 639–650, http://dx.doi.org/10.1142/S0218127409023263.

[15] M. Bernardo, C. Budd, A. Champneys, P. Kowalczyk, Piecewise-Smooth Dynamical Systems: Theory and Applications, Vol. 163, Springer Science & Business Media, 2008.

[16] D. Bisselua, Yede, S. Vidal, Dispersion models and sampling of cacao mirid bug *Sahlbergella singularis* (Hemiptera: Miridae) on *Theobroma cacao* in Southern Cameroon, Environ. Entomol. 40 (1) (2011) 111–119, http://dx.doi.org/10.1603/EN09101.